Eren Billur *Editor*

Hot Stamping of Ultra High-Strength Steels

From a Technological and Business Perspective

Springer

Hot Stamping of Ultra High-Strength Steels

Eren Billur
Editor

Hot Stamping of Ultra High-Strength Steels

From a Technological and Business Perspective

Springer

Editor
Eren Billur
Billur Makine Ltd.
Ankara, Turkey

ISBN 978-3-319-98868-9 ISBN 978-3-319-98870-2 (eBook)
https://doi.org/10.1007/978-3-319-98870-2

Library of Congress Control Number: 2018950941

This Springer imprint is published by the registered company Springer Nature Switzerland AG
The registered company address is: Gewerbestrasse 11, 6330 Cham, Switzerland

Dedicated to my family.

Foreword

The use of ultrahigh-strength steel (UHSS) in the automotive industry has increased in the last few years as manufacturers try to improve crash safety and reduce weight. Parts such as B-pillars, side impact reinforcement beams, and bumpers are increasingly manufactured from UHSS by hot stamping.

In hot stamping, the blanks from a special boron-alloyed steel are heated in a furnace to its austenitization temperature (about 900 °C), formed in an internally cooled die set, and quenched under pressure at a minimum cooling rate of 27 °C per second. This minimum cooling rate ensures the formation of martensitic microstructure in the part, which gives it strength of about 1,500 MPa.

Finite element (FE) simulation of the hot stamping process can help manufacturers predict such final part properties as thickness, temperature, and hardness distribution. Mechanical deformation, heat transfer, and microstructure evolution occur simultaneously during hot stamping. This makes FE simulation of the process challenging. Most researchers use a combination of different FE codes to capture what occurs during hot stamping. When using FE simulation, making suitable assumptions while ignoring the effects of some of the less significant parameters can help shorten the time needed to obtain reasonably accurate results. Some parameters, however, are required as input to the FE codes. As input, the essential material properties include emissivity and flow stress as a function of temperature, strain and strain rate. Also required are Young's modulus, Poisson's ration, thermal conductivity, specific heat capacity, and coefficient of thermal expansion, each as a function of temperature. The essential process parameters are final austenitization temperature, blank transfer time, blank temperature as forming begins, die stroke versus time, contact heat transfer coefficient between the blank and tool as a function of pressure and distance between the tool and die surface, coefficient of friction as a function of pressure; initial tool temperature for non-isothermal simulation; average tool temperature for isothermal simulation; temperature of the cooling medium needed to cool dies; blank holder force; closing pressure of the tools; and time required for quenching and air cooling.

There are several publications on hot stamping, mostly in the form of review articles or proceedings of conferences on this topic. The present book gives an excellent summary of the latest state of the art and covers all the relevant aspects of hot stamping.

Chapter 1 gives an introduction to materials used in automotive industry, while Chap. 2 covers the metallurgy and microstructure of steels, with emphasis on boron-alloyed steels, widely used in hot stamping.

Chapter 3 gives an overall review of the technology development during the last several decades. Chapter 4 discusses blank materials and their coatings, used in hot stamping. Various heating furnaces and methods, as well as material handling systems and hot stamping presses are discussed in Chap. 5. Die design and manufacturing, especially the design of cooling channels for hot forming and rapid quenching to reduce cycle time, are covered in Chap. 6 that also includes novel quenching techniques. Post-forming operations that are significant for part quality and trimming/pressing issues that are critical in hot stamped parts, are discussed in Chap. 7.

Chapter 8 discusses hot stamping of parts with tailored properties that are increasingly used in industry. Tailored properties can be achieved by using tailor-welded, tailor-rolled, or tailored heated blanks. These issues are also discussed in this chapter.

Chapters 9 and 10, cover new and essential topics, namely hot tube hydroforming and computer modeling. Computer modeling, specifically, has been very influential in die design in reducing cycle time, thereby increasing the productivity of hot stamping. Considerable research has been conducted in determining the parameters that are essential for conducting reliable computer simulations of the process.

Chapter 11 discusses the overall state of the hot stamping industry. This chapter also reviews the technical and economic aspects of hot stamping specific parts, especially in comparison with cold forming of new generation UHSS, with tensile strengths up to 1,600 MPa and improved elongation and formability.

This book represents an up-to-date review of technology and will be very helpful to researchers as well as practicing engineers in the understanding and further development of hot stamping technology.

Columbus, OH, USA
August 2017

Prof. Taylan Altan

Acknowledgements

This book would never be possible without Prof. Taylan Altan's advising throughout my Ph.D. studies at The Ohio State University. I am grateful to have his supervision and support even after graduation. Special thanks to Dr. Blaine Lilly and Dipl.-Ing. Harald Porzner, who gave me the idea to extend my studies and publish as a book.

Most of the chapters are coauthored by well-known academics and experts from the industry. I would like to express my gratitude to Prof. Takehide Senuma, Dipl.-Ing. Frank Schieck, Dr. Hyun-Sung Son, and Mr. Barış Çetin for their long support. Special thanks to Mr. Rick Teague, Mr. Christian Kovacs, Mr. Vladimir Bošković, and Mr. Felix Quasniczka who have lately joined the effort but made a significant contribution.

This book has been a much longer than expected journey, and during this time, I met many new people who all agreed to help and send some input to this book. Although their names are listed in the contributors list, I cannot miss the opportunity to thank: Mr. David Jeanjean; Mr. Robert Veit (the best lecturer I have ever met), Prof. Marion Merklein.

Authors would like to offer special thanks to Prof. Ralf Kolleck, sadly who is no longer with us, but his legacy continues with his students and graduates.

A considerable amount of work has been carried out by my students. I would like to thank Türkay Muratoğlu, Ebru Kılcı, and Deniz Otlu for their valuable support in preparation of this book.

Last but not the least, I would like to thank my wife, Deniz Billur, and my parents Gülder and Ahmet Billur for their support in this long journey. Without Deniz's support, this book would never be completed.

Contents

Contributors

Göran Berglund Luleå, Sweden

Eren Billur Billur Makine Ltd., Ankara, Turkey; Atılım University, Ankara, Turkey

Vladimir Bošković Technische Universität Graz, Graz, Austria

Barış Çetin FNSS Defense Systems Co. Inc., R&D Center, Gölbaşı, Ankara, Turkey

Tord Gustafsson Blatraden AB, Öjebyn, Sweden

Jan Jonasson AP&T AB, Ulricehamn, Sweden

Halim Meço FNSS Defense Systems Co. Inc., R&D Center, Gölbaşı, Ankara, Turkey

Aitor Ormaetxea Fagor Arrasate S. Coop., Gipuzkoa, Spain

Harald Porzner ESI North America, Farmington Hills, MI, USA

Felix Quasniczka Associated Spring, Plymouth, MI, USA

Frank Schieck Fraunhofer IWU, Chemnitz, Germany

Takehide Senuma Okayama University, Okayama, Japan

Hyun-Sung Son POSCO Global R&D Center, Incheon, South Korea

Rick Teague Telos Global, Caryville, TN, USA

Acronyms

AHSS	Advanced High-Strength Steels
AISI	American Iron and Steel Institute
bcc	Body-centered cubic
bct	Body-centered tetragonal
BDC	Bottom Dead Center
BH	Bake Hardening effect or Bake Hardenable steels
BTU	British Thermal Unit
CCT	Continuous Cooling Transformation
CP	Complex Phase Steels
CVD	Chemical Vapor Deposition
DP	Dual Phase (Ferrite + Martensite)
fcc	Face-centered cubic
FE	Finite Element
FEA	Finite Element Analysis
FIR	Far Infrared
FLD	Forming Limit Diagram
GA	Galvannealed
GI	Galvanized
HAZ	Heat-Affected Zone
HPF	Hot Press Forming
HRC	Rockwell C Hardness
HSLA	High-Strength Low Alloy
HSS	High-Strength Steels
HV	Vickers Hardness
IF	Interstitial Free
LMAC	Liquid Metal Assisted Crack
MS	Mild Steels
NIR	Near Infrared
NVH	Noise, Vibration and Harshness
PAGS	Prior Austenite Grain Size

PHS	Press Hardened Steels
PVD	Physical Vapor Deposition
Q&P	Quenching and Partitioning, or the steel grades processed with this technique
RSW	Resistance Spot Welding
SEM	Scanning Electron Microscope
SOP	Start of Production
TDC	Top Dead Center
THF	Tube hydroforming
TRB	Tailor-Rolled Blanks
TRIP	Transformation Induced Plasticity effect, or the steel grades with retained austenite having this effect
TTT	Time Temperature Transformation
TWB	Tailor-Welded Blanks
TWIP	Twinning Induced Plasticity effect, or the steel grades having this effect
UHSS	Ultrahigh-strength steel
UTS	Ultimate Tensile Strength
YS	Yield Strength

Chapter 1
Introduction

Eren Billur

Abstract Vehicle manufacturers are under pressure of reducing fuel consumption and greenhouse gas emissions and still improving safety. One method to reduce the consumption and emissions is to make the vehicles lighter. Several approaches are employed to make cars lighter and yet stronger to ensure safety standards:

(1) to use high strength-to-weight ratio materials (higher strength steels, Aluminum, Magnesium, Carbon Fiber Reinforced Polymers, etc.) and
(2) to reduce the material use wherever possible.

This chapter discusses the material requirements in a car body, steel grades used in automotive industry and introduces the hot stamping process.

1.1 Material Requirements in a Car Body

A car body has to fulfill a number of performance criteria, such as, carrying the weight of passengers, useful loads, and car parts in a confined space. However, for material selection purposes, it is possible to reduce it to four different requirements [1–3]:

(1) High bending and torsional stiffness (Fig. 1.1) for better handling as well as damping "noise, vibration and harshness" (NVH),
(2) Esthetic outer panels with high dent resistance (Fig. 1.2a),
(3) Deformation/intrusion resistant safety cage to protect the passengers in the event of a crash (Fig. 1.2b),
(4) Crumple zones to absorb the energy of a crash (Fig. 1.2c),

E. Billur (✉)
Billur Makine Ltd., Ankara, Turkey
e-mail: eren@billur.com.tr

E. Billur
Atılım University, Ankara, Turkey

E. Billur (ed.), *Hot Stamping of Ultra High-Strength Steels*,
https://doi.org/10.1007/978-3-319-98870-2_1

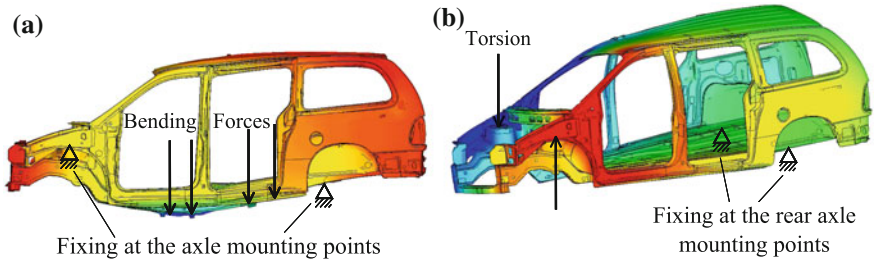

Fig. 1.1 Stiffness of a car body: **a** bending stiffness, **b** torsional stiffness [3]

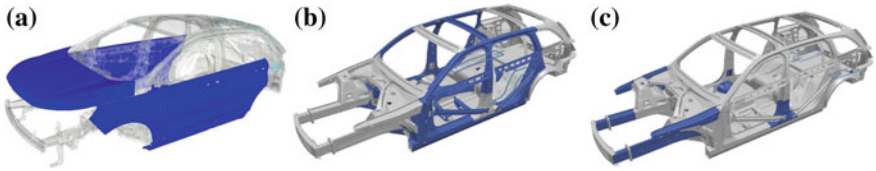

Fig. 1.2 In a car body, several different material properties, such as **a** dent resistance, **b** intrusion resistance, **c** energy absorption are required in different regions [4, 5]

Also, any component, whether crash relevant or not, has to withstand the loads induced during the component's lifetime, without fracturing due to fatigue. Several components, such as shock towers are subjected to repeated loads.

For bending stiffness, the only material parameter required is Young's modulus (E). According to [3], bending stiffness of 1.0-mm-thick steel is equivalent to 1.4-mm-thick aluminum as stiffness is proportional to Et^3. For bending stiffness purposes, aluminum could save 50% weight compared to steel. The yield or tensile strength of material has no effect on its bending stiffness.

For torsional stiffness, shear modulus (G) is critical, which is a function of Young's modulus and Poisson's ratio. Similar to bending stiffness, 1.0-mm-thick steel has equivalent torsional stiffness of 1.4-mm-thick aluminum. Thus, aluminum could save 50% weight [3].

Dent resistance is measured by the force required to form a permanent dent on the sheet metal. Dent resistance is important for outer panels, as hail, stones, or other objects (another car's door, shopping cart, etc.) may deform them. For higher dent resistance, yield strength is critical. A simple equation for equivalent dent resistance is shown in Fig. 1.3 [2]. A more detailed formula is given by [1], which takes anisotropy and work/bake hardening effects into account.

For intrusion resistant crash components, higher in-service yield strength is required (in-service = initial yield strength + work hardening + bake hardening).

For energy absorbing components, larger area under the stress–strain curve is required. Thus, elongation and strength are equally important.

Next section discusses different steel grades used in automotive industry.

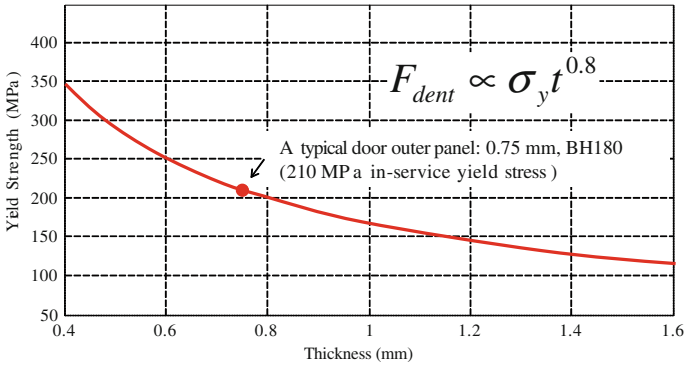

Fig. 1.3 Empirical relation between thickness and yield strength for constant dent resistance (re-created after [2]). See Fig. 1.5 for in-service yield stress of BH180

1.2 Steels in Automotive Industry

Higher strength steels may help reducing the weight by down-gaging (i.e., using thinner sheets), while keeping the crash performance constant or further improving it [6]. However, there are several problems associated with using thinner and stronger sheets:

(1) As the strength is increased, the formability is generally lowered (see Fig. 1.4), making it harder to design a component without splits in press shop;
(2) As the strength is increased, the sheet will tend to springback more and it is a challenge to make the part within the tolerances;
(3) Die wear problems are more common with higher strength steels, as the forming/cutting forces/stresses and contact pressures are much higher [7].

Figure 1.4 shows several steels used in automotive industry. As of today, automotive steels are classified into five main groups:

- **Mild Steels** (abbreviated as MS, not to be confused with Martensitic Steels)
- (Conventional) **High-Strength Steels** (abbreviated as HSS)
- First-generation **Advanced High-Strength Steels** (abbreviated as AHSS)
- **Second-generation Advanced High-Strength Steels**
- **Third-generation Advanced High-Strength Steels**

In the later subsections, all these classes are explained in detail.

1.2.1 Mild Steels

Mild steels are generally composed of ferrite only. These steels have a relatively low tensile strength, typically lower than 280 MPa (40 ksi). Their main advantage is their

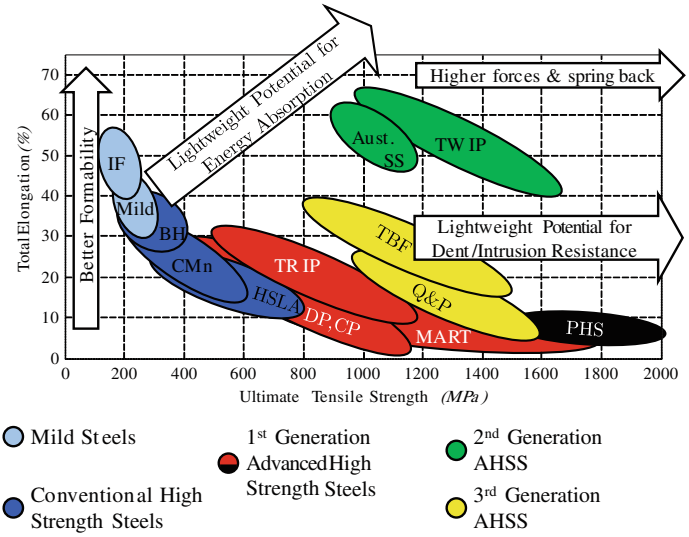

Fig. 1.4 "Banana Curve" shows that higher strength steels have lightweight potential, but limited formability and hard to control springback

ability to be formed to complex geometries. Total elongation (which is one of the indicators of formability) of these grades may vary from 25%, all the way up to 50%. Their r-values (Lankford parameters, an indicator of deep drawability) are over 1.0 and can be as high as 2.5. These steels are sometimes commercially named as Deep Draw Quality (DDQ) steels, as they can be drawn to deep shapes without fracture. Mild steels were the dominating material in the car bodies until 1990s [8], but now their uses are limited to (1) stiffness related components (i.e., floor panels that do not carry crash loads) and (2) cosmetic parts with complex bending and drawing (outer panels). This family has two classes:

(1) **Mild steels** (also called low-carbon or plain carbon steels) have very little alloying elements.
(2) **Interstitial Free (IF)** steels have ultra low-carbon resulting with even lower strength and even higher formability compared to mild steels. They are commercially known as Enhanced Deep Draw Quality (EDDQ). IF steels have r-values over 1.5, up to 3.0 and total elongation over 40% [9–13].

1.2.2 Conventional High-Strength Steels

Conventional **high-strength steels (HSS)** use "solid-solution hardening" mechanism to achieve higher strength levels. Although more types could be listed, in automotive industry, four classes of HSS are commonly used. These steels are typically named

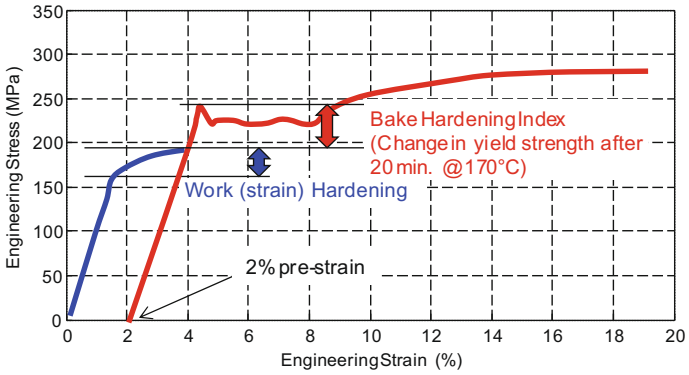

Fig. 1.5 Work (strain) and bake hardening of BH180 steel (re-created after [13, 15]). Note that both work and bake hardening are observed in most other steels as well

with their yield strength values. BH180 for example is a bake hardenable steel with minimum 180 MPa (26 ksi) yield strength.

(1) **Bake Hardenable (BH)** steels' chemistry and processing are designed to take carbon out of solution during the paint baking cycle. These steels are softer and more formable in the press shop. Parts with complicated geometry can be produced with less press force and lower springback. However, once it is welded to a car body and baked after the painting process (which is a standard process in car making), the yield strength is increased. BH steels are available from BH 180 level to BH 300 with respect to their yield strength as delivered (180–300 MPa, 26–44 ksi). Their tensile strength may be up to 450-480 MPa (65–70 ksi) level. Once they are formed, they are work hardened just like any other steel. However, after paint baking cycle, these steels gain an additional 25–45 MPa (3500–6500 psi) yield strength, as shown in Fig. 1.5. In recent years, BH steels are used dominantly in doors and closures, as they are very formable and their dent resistance is improved after paint baking [8, 12–14].

(2) **Carbon-Manganese steels (CMn)** are simply mild steels solid solution strengthened by adding 1.2–1.8% manganese alloying. Although most conventional HSS are named by their yield strength, CMn steels are named by their ultimate tensile strength. For example, CMn 440 is a carbon-manganese alloyed steel that has 440 MPa (65 ksi) ultimate tensile strength. These steels could be produced between 310 and 540 MPa (45–80 ksi) ultimate tensile strength levels. Honda has been using CMn 440 since 2001 in various body structures [16–19].

(3) **High-Strength Low-Alloy (HSLA)** steels are CMn steels strengthened by adding very little amount (micro-alloying) of Titanium, Vanadium or Niobium. HSLA grades are typically named by their yield strength values. However, sometimes steel makers guarantee the tensile strength value. These steels have yield strength from 220MPa to 850MPa (32–123), and ultimate tensile strength from 340 MPa to 1000 MPa (50–145 ksi). An HSLA grade with 850 MPa (123 ksi)

yield and 980 MPa (142 ksi) UTS can still have a total elongation in the order of 8%. HSLA has been used in automotive industry since 1980s, however they are being replaced with DP and TRIP grades [10, 13, 20, 21].

(4) **High-Strength Interstitial Free (HS-IF)** is an ultra low-carbon steel with $C \leq 30ppm$. To increase the strength level, P, Mn, and Si are added. Ti and/or Nb is also added for grain refinement and stabilizing. These steels are commercially available in Yield Strength levels of 160–300 MPa (23–44 ksi), and UTS levels of 340–500 MPa (50–73 ksi). r-values of HS-IF steels are between 1.5 and 2.5. Total elongation could be over 35% [9, 13, 19].

1.2.3 Advanced High-Strength Steels: The First Generation

First-generation Advanced High-Strength Steels (AHSS) has martensitic microstructure with at least one more phase. In automotive industry, five classes of AHSS are used. AHSS grades are typically named with their tensile strength level.

(1) **Dual Phase (DP)** steels contain ferrite in addition to 5–50 vol.% martensite, thus they are named as "dual phase". The amount of martensite determines the strength of the steel. DP steels typically have better formability compared to HSLA at similar strength levels. These grades are available from 450 MPa (65 ksi) tensile strength, all the way up to 1400 MPa (203 ksi). DP is currently the most common AHSS type in the automotive industry [7, 13, 22, 23].

(2) **Complex Phase (CP)** steels usually have higher formability than DP and contain bainite in addition to martensite and ferrite. Some retained austenite may also be present. Micro-alloying of Titanium, Vanadium, and/or Niobium is added to ensure grain refinement. These grades are commercially available between 600 and 1200 MPa (87 and 174 ksi) tensile strength level. CP steels have better hole expansion ratio compared to DP steels at same strength level [11–13].

(3) **Transformation Induced Plasticity (TRIP)** steels contain 10–15% retained austenite phase. Retained austenite transforms to the strong martensite phase when deformed, which helps distribution of the strain and increases elongation. This is called TRIP effect. These steels have higher formability than CP, DP, and HSLA. TRIP steels currently are available in tensile strengths from 590 to 1,180 MPa (85-171 ksi). These grades are sometimes named as "Retained Austenite" steels [5, 13, 22].

(4) **Martensitic (MART) Steels**, (also abbreviated as **MS**, not to be confused with mild steels) as the name suggests, are mostly martensitic, with trace amounts of ferrite and bainite. Martensitic steels are the strongest but least formable steel grades. Their strength levels can be altered by alloying with carbon (C), manganese (Mn), chromium (Cr), molybdenum (Mo), and boron (B). These steels are available from 900 to 1,900 MPa (130–275 ksi). Although lower strength versions could be stamped, these steels are typically roll formed [13, 19].

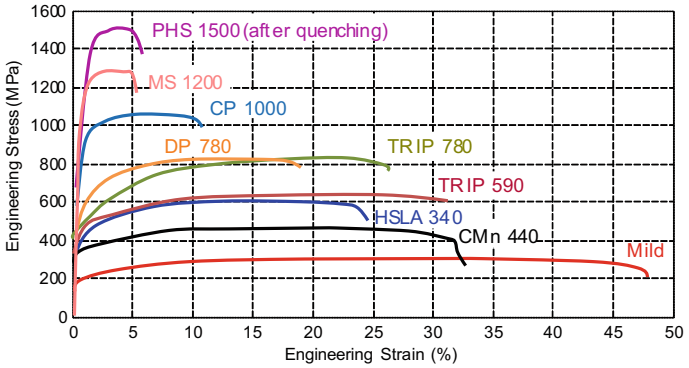

Fig. 1.6 Engineering stress–strain comparison of several AHSS, HSS, and mild steel grades. Note that HSLA 340 is named after its yield stress. The rest of this book is about PHS grades (re-created after [24])

(5) **Press hardened steels (PHS)** (also known as hot-formed steel or hot stamped steel) are considered as first-generation AHSS. Section 1.3 and the rest of this book discusses PHS grades.

A comparison of engineering stress–strain curves of mild steels with conventional HSS and first-generation AHSS is given in Fig. 1.6.

1.2.4 Second-Generation AHSS

Second-generation AHSS use TRIP (Transformation Induced Plasticity) and TWIP (Twinning Induced Plasticity) effects for enhanced formability. TRIP steels (which are classified as first-generation AHSS) have 10–15% retained austenite to increase formability, whereas second-generation AHSS consist of almost 100% austenitic microstructure at delivery. Since austenite is not stable at room temperature in low alloyed steels, to achieve 100% austenite, high alloying elements are required. Another strengthening mechanism is called Twinning Induced Plasticity (TWIP) effect which is found in high-Mn steels, commercially known as TWIP steels. Second-generation AHSS have very high formability and strength, but their use in the automotive industry is still limited. This can be attributed to two main factors:

(1) High alloying elements increase the cost of steel and makes it harder to weld.
(2) The material has a tendency for delayed cracking—the parts fracture after they are formed and stored for a while [22, 25].

There are two types of second-generation AHSS:

(1) **Austenitic Stainless Steels** have been commercially available since 1912, long before the introduction of AHSS [26]. However, due to their ~100% austenitic structure and high elongation, they are also classified as second-generation AHSS. In automotive industry, stainless steels are not commonly used in the car bodies. A few exceptions are: 1981–83 DeLorean DMC-12, several Porsche models and 2005–2012 Audi A6 (known as C6) [22, 27, 28].

(2) **TWIP steels** also are 100% austenite at room temperature. However, in these steels, high Mn alloying (typically over than 15%) causes formation of twins when the steel is deformed. The twin boundaries act like grain boundaries to strengthen the steel. These steels typically have more than 60% elongation at a about 1000MPa (145 ksi) tensile strength level [29]. TWIP steels are available at 900–980 MPa (130–142 ksi) levels, but studies published by several steel makers have shown the feasibility of TWIP 1180–1250 (170–180 ksi). One steel maker has shown that it may be possible to produce TWIP 1700 (247 ksi) steel. The density of TWIP steels is typically lower than other steels and thus could save some extra weight [13, 22, 30–33]. TWIP steels are already in use in several Fiat vehicles [34]. Renault's EOLAB prototype also had some TWIP Steels [35]. Although TWIP steels have not been used extensively in the automotive industry, according to a survey at the Materials in Car Body Engineering 2012 conference (May 2012, Bad Nauheim, Germany, sponsored by Automotive Circle Intl.), 87% of the participants from the automotive industry believed that TWIP steels could be applied in mass production in select applications with further improvements.

A comparison of engineering stress–strain curves of mild steels with conventional HSS and first-generation AHSS is given in Fig. 1.7.

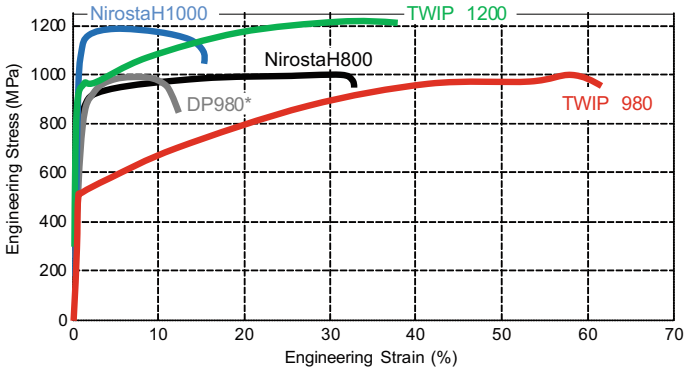

Fig. 1.7 Engineering stress–strain comparison of several second-generation AHSS with DP980. Note that Nirosta grades are named according to their yield stresses. *DP980 is a first generation AHSS shown only for comparison (re-created after [8])

Table 1.1 US/DOE targets for third-generation AHSS [39]

Target #	Yield strength	Tensile strength	Elongation (%)	
			Total	Uniform
1	≥800 MPa ≥115 ksi	≥1000 MPa ≥145 ksi	≥30	≥20
2	≥1200 MPa ≥175 ksi	≥1500 MPa ≥215 ksi	≥25	≥8

1.2.5 Third-Generation AHSS

First-generation Advanced High-Strength Steels (AHSS) have limited formability. Second-generation AHSS have high strength and are very formable, but they have high alloying elements. This has increased the cost and reduced the weldability. As a result, demand has grown for a new generation of steel that has higher formability compared to first generation, but have less alloying elements than second generation (see Figs. 1.4 and 1.8). Both EU and US are funding research on these new grades. US Department of Energy (DOE) had two targets for third-generation AHSS as summarized in Table 1.1 [36–39]

To achieve these goals, most steelmakers are following one of these three paths [39–41]:

(1) To improve formability properties of first-generation AHSS. Common ones are: Enhanced DP, Enhanced TRIP, Modified hot formed (see Chap. 4).
(2) To reduce the alloying elements in second-generation AHSS: Medium-Mn or low-Mn TRIP/TWIP steels, and tensilized stainless steels.
(3) To design a new steel class (chemistry, processing or both). Examples are Quenching and Partitioning (QP or Q&P) steels, TRIP-aided Bainitic Ferrite (TBF) steels and NanoSteel (NS).
Several third-generation AHSS have been proposed and developed in the last few years, but only two classes currently are in series production through several steelmakers: Q&P and TBF steels. Nanosteel has been only recently produced in coil-scale [42].

(1) **Q&P steels** contain carbon, manganese, silicon, nickel, and molybdenum alloying elements. Depending on the strength level, alloying elements can be as high as 4%, which is much lower than that of second-generation AHSS, as shown in Fig. 1.8. During heat treating of Q&P steel, quenching is interrupted before cooling down martensite finish temperature. Later, the steel is reheated for partitioning. During partitioning, martensite loses its carbon to austenite (see Fig. 1.9) which makes the austenite stable. After the heat treatment, the steel has 5–12% stable retained austenite, 20–40% ferrite, and 50–80% martensite [23, 39].

As of 2017, Q&P steels are commercially available between 980 MPa and 1,180 MPa (142–171 ksi) tensile strength levels. A steelmaker has demonstrated that a B-pillar reinforcement can be cold-formed using Q&P 1180. Auto/Steel Partnership

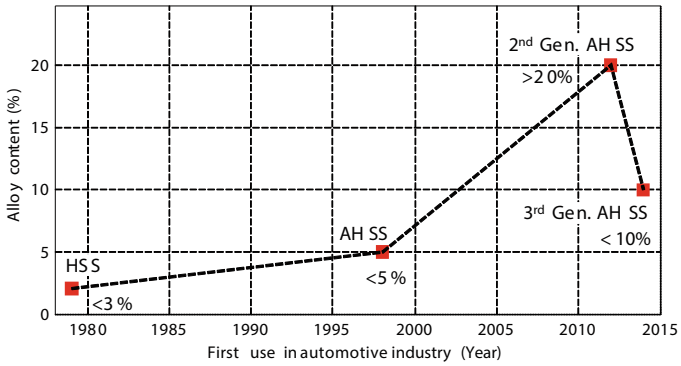

Fig. 1.8 Alloy content of several steel classes, plotted against the year they were first used in automotive applications (re-created after [8, 43])

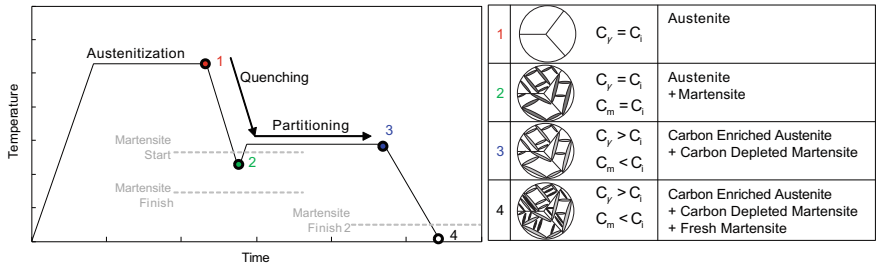

Fig. 1.9 Heat treatment cycle and the microstructural evolution during Q&P process (re-created after [39, 44])

(A/SP) has also tested Q&P 980 using GM's B-pillar die, proving that the steel is more formable and less prone to edge cracking compared to DP 980. Several automakers in China have adopted Q&P steels in A- and B-pillar reinforcements. At least one steelmaker is currently working towards commercialization of Q&P 1300 (190 ksi) grade. Researchers have developed steels up to 2,100 MPa (305 ksi) tensile strength with 9% uniform elongation and about 13% total elongation in lab scale. The elongation level of this steel is comparable to DP 980, which is a cold-formable grade [29, 39, 40, 45–48].

(2) **TBF** steels, a low-alloy steel class similar to Q&P, can be produced by existing heat treatment facilities. Again, for improved formability, "stable retained austenite" is its key component. These steels were first developed in Japan in 2000 [49]. These steels are also named as "Carbide Free Bainitic Steel" (CFB) by other researchers [50]. Kobe Steel was one of the first to develop and commercialize TBF steels. The initial studies showed that TBF steels were feasible from 980 MPa to 1,470 MPa (142–213 ksi) [51]. In 2012, Renault-Nissan group has announced its decision to use TBF steels in future vehicles [52]. In 2013, Infiniti Q50 was introduced, in which A and B-pillar reinforcements and cantrail were made of TBF 1180. This was 4% of

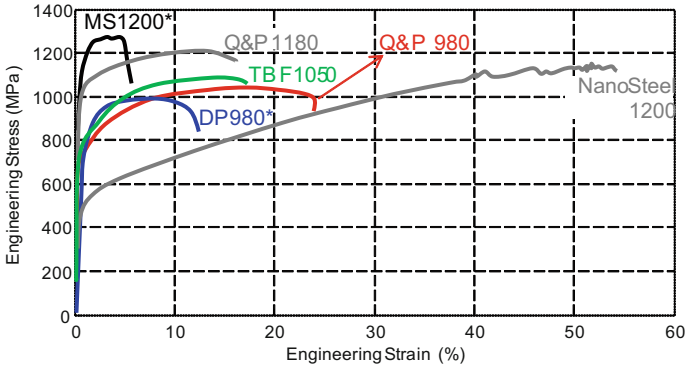

Fig. 1.10 Engineering stress–strain curves of several third-generation AHSS. *DP980 and MS1200 are first-generation AHSS shown only for comparison. (re-created after [8, 29, 42])

the mass of the body-in-white [53]. In 2015, Nissan Murano was introduced. This vehicle had 3% of its body-in-white, composed of TBF 1180 components. Nissan plans to increase the use of TBF steels to 25% in the future [54]. In September 2014, ArcelorMittal has introduced FortiForm steel family. Currently, FortiForm 1050 (152 ksi) is commercially available. ArcelorMittal is currently developing 980 and 1,180 MPa (142 and 171 ksi) versions [55] (Fig. 1.10).

1.3 Hot Stamping

Hot stamping (also known as press hardening or hot press forming) is a relatively new technology which allows ultra high-strength steels (typically 22MnB5) to be formed into complex shapes. The part is formed in soft condition. By this way, the material is more formable and requires less force. Thus, springback is reduced as well. After forming, the part is quenched to gain high strength. A typical hot stamped part (22MnB5 steel) has over 1,000 MPa (145 ksi) yield strength and approximately 1,500 MPa (218 ksi) tensile strength [56]. Recently, new steel grades are introduced to have strength level from 500MPa to 2,000MPa (73 to 290 ksi), as discussed in Chap. 4 in detail. There are four different methods of hot stamping [57]:

(1) **Indirect Process**: the blank is formed, trimmed, and pierced in cold condition (i.e., state ❶ in Fig. 1.11). It is later heated over its austenitization temperature (>880 °C, >1615 °F) and quenched in a die (Fig. 1.12a) to get high strength properties.

(2) **Direct Process**: the unformed blank is heated in a furnace, formed in hot condition (state ❷ in Fig. 1.11, and as shown in Fig. 1.12), and quenched in the die to achieve the required properties. For 22MnB5 steel, if the quenching rate is over 27 °C/s (49 °F/s), the part will transform to almost 100% martensite. Typical cycle times for a direct process is 10–20 s.

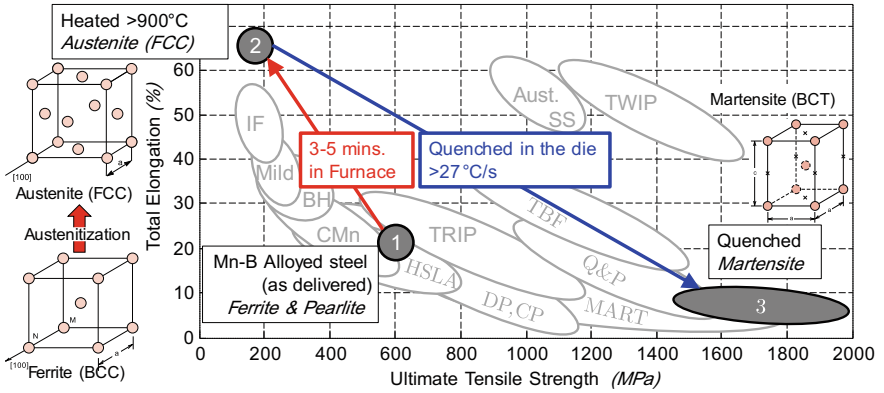

Fig. 1.11 A short summary of hot stamping process (re-created after [58, 59])

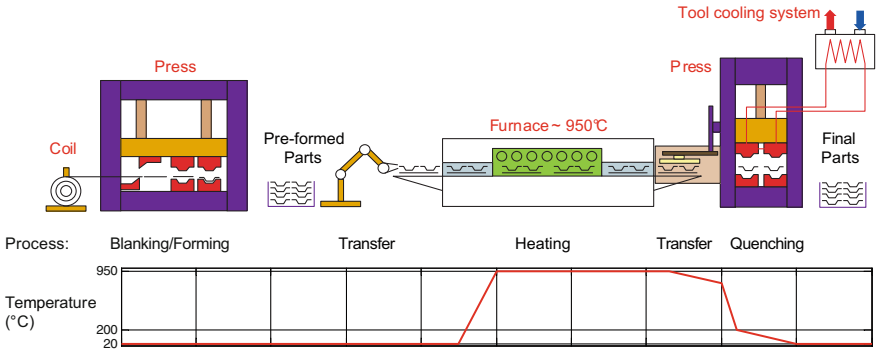

Fig. 1.12 Indirect hot stamping process. (re-created after [57])

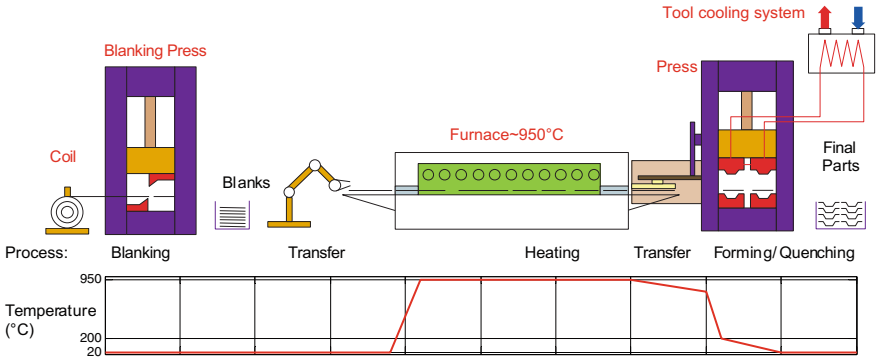

Fig. 1.13 Direct hot stamping process. (re-created after [57])

Table 1.2 A comparison of direct and indirect hot stamping processes [61]

	Direct process	Indirect process
Advantages	Cost efficient for simple geometries	Very complex components can be produced
	Reduced material usage	Undercuts and sharp radii
	Simpler furnace	Very large components can be produced
	Only one die set is required	Trimming/Piercing is done in soft condition
Disadvantages	High die wear	Cold forming dies are required
	Trimming/Piercing is done in hard condition	Furnace carriers are required (see Sect. 5.2)

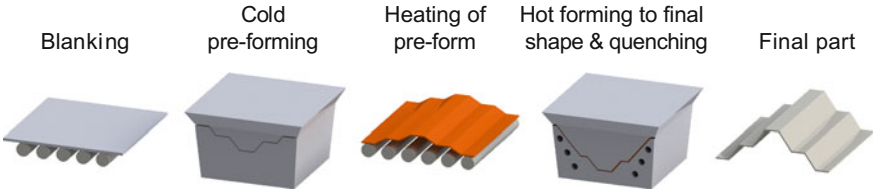

Fig. 1.14 Hybrid hot stamping: where the deformation is given in two steps (re-created after [63])

Selection of the process depends on part complexity and blank coating (Zn-based coatings typically require indirect process) (Fig. 1.13). In either method, the blank is formed in a much softer and formable state and is later hardened between the dies, which have integrated cooling channels. Table 1.2 summarizes the advantages and disadvantages of both methods [60–62].

(3) Although not listed in any publication as a separate hot stamping process, a "**hybrid hot stamping**" or "two-stage hot stamping" can be listed as well. In production of deep drawn parts, such as transmission tunnels, a two-stage hot stamping process may be required. The preforming is done at cold state, similar to indirect hot stamping. However, before quenching and hardening the part, it is deformed significantly in the second forming process. Figures 1.14 and 1.15 show an example transmission tunnel hot stamped in a two-stage process [63–65].

(4) Recently, a new hot stamping method is proposed for Zn coated blanks: **Multi-step hot stamping**. Here, a slightly modified steel is used (not 22MnB5 but 20MnB8) [61, 66]. With higher Mn content, the steel can be formed at lower temperatures, and thus it was possible to make transfer press dies—similar to cold forming. Dies are heated using electric heaters or hot liquid and maintained over 200 °C (∼400 °F). This new steel grade can be formed at around 570 °C (∼1060 °F) and hardens at air cooling rates. Gestamp is expected to commercialize this technique in 2017–18 [67, 68]. Details of this steel grade will be investigated in Chap. 4. A typical line is shown in Fig. 1.16.

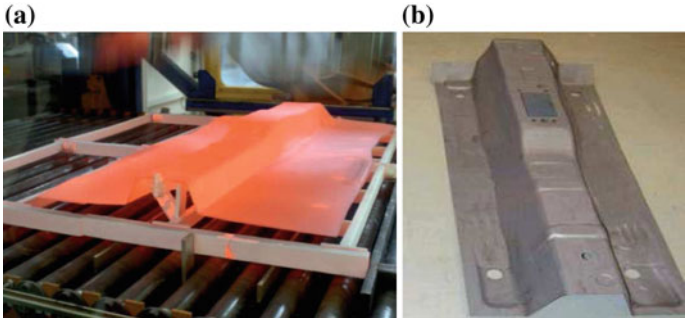

Fig. 1.15 A hybrid hot stamping example: transmission tunnel. **a** shows the heated preform, **b** is the final part [63]

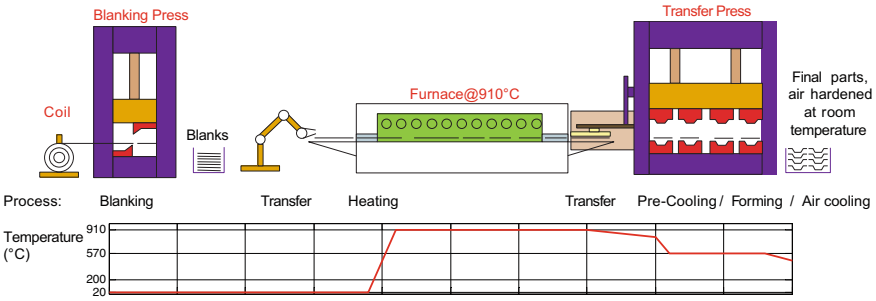

Fig. 1.16 Multistep hot stamping process (re-created after [57, 66, 67])

References

1. N. Asnafi, On strength, stiffness and dent resistance of car body panels. J. Mater. Process. Technol. **49**(1), 13–31 (1995)
2. L. Morello, L.R. Rossini, G. Pia, A. Tonoli, *The Automotive Body: Volume I: Components Design*. Mechanical Engineering Series (Springer, Netherlands, 2011)
3. R. Wohlecker, R. Henn, H. Wallentowitz, J. Leyers, Mass reduction. fka Report 56690, fka Aachen (2006)
4. J. Reed, Advanced High-Strength Steel Technologies in the 2015 Ford Edge. Presented at Great Designs in Steel 2015, May 13, Livonia, MI, USA (2015)
5. E. Hilfrich, D. Seidner, *Crash Safety with High Strength Steels*. Presented at International Automotive Congress, Shengyang (2008)
6. D. Smith, Grand Cherokee. Presented at Great Designs in Steel 2011, May 18, Livonia, MI, USA (2011)
7. E. Billur, T. Altan, Challenges in forming advanced high strength steels, in *Proceedings of New Developments in Sheet Metal Forming Conference, Stuttgart, Germany* (2010), pp. 285–304
8. E. Billur, B. Çetin, M. Gürleyik, New generation advanced high strength steels: developments, trends and constraints. Int. J. Sci. Technol. Res. **2**(1), 50–62 (2016)
9. R. Rana, W. Bleck, S.B. Singh, O.N. Mohanty, Development of high strength interstitial free steel by copper precipitation hardening. Mater. Lett. **61**(14–15), 2919–2922 (2007)

10. J. Dykeman, Advanced high strength steel - recent progress, ongoing challenges, and future opportunities, in *International Symposium on New Developments in Advanced High-Strength Sheet Steels*. AIST (2013), pp. 15–28
11. S. Keeler, M. Kimchi, Advanced high-strength steels application guidelines version 5.0. By WorldAutoSteel (2014)
12. ArcelorMittal, Extract from the product catalogue (2015). Accessed 10 June 2015
13. Posco, Automotive steel data book (2016)
14. voestalpine Stahl GmbH, Cold-rolled steel strip, technical terms of delivery. Product Catalogue (2012)
15. European Committee for Standardization, EN 10325:2006: Steel - Determination of yield strength increase by the effect of heat treatment [Bake-Hardening-Index] (2006)
16. Y. Okano, H. Shirasawa, Present state and future prospects of high tensile strength steel sheets. Res. Dev. - Kobe **47**, 38–41 (1997)
17. K. Osawa, Y. Suzuki, S. Tanaka, TS590 $\sim$ 980 MPal grade low-carbon equivalent type galvannealed sheet steels with superior spot-weldability. Kawasaki Steel Tech. Rep. **48**, 9–16 (2003)
18. R.Z. Mallen, S. Tarr, J. Dykeman, Recent applications of high strength steels in North American Honda production. Presented at Great Designs in Steel 2008, April 9, Livonia, MI, USA (2008)
19. ArcelorMittal North America, Driving advanced automotive steel solutions (2014)
20. M. Wilhelm, Materials used in automobile manufacture-current state and perspectives. Le Journal de Physique IV **3**(C7), 31–40 (1993)
21. K. Fredin, Future materials for body structure applications. Presented at Uddeholm Automotive Seminar, Sunne, Sweden (2005)
22. L. Samek, D. Krizan, Steel–material of choice for automotive lightweight applications. *Metal Review* (2012), pp. 1–6
23. W. Wang, X. Wei, The effect of martensite volume and distribution on shear fracture propagation of 600–1000 MPa dual phase sheet steels in the process of deep drawing. Int. J. Mech. Sci. **67**, 100–107 (2013)
24. E. Billur, T. Altan, Three generations of advanced high-strength steels for automotive applications, Part I. Stamp. J. 16–17 (2013)
25. D.K. Matlock, J.G. Speer, E. De Moor, P.J. Gibbs, Recent developments in advanced high strength sheet steels for automotive applications: an overview. Jestech **15**(1), 1–12 (2012)
26. H.M. Cobb, *The History of Stainless Steel* (ASM International, 2010)
27. H. Wilde, H. Hunger, R. Erbe, H. Fuest, Die karosserie des neuen Audi A6. Proc. EuroCarBody **2004**, 315–333 (2004)
28. Dr. Ing. h. c. F. Porsche AG Presse-Datenbank. http://presse.porsche.de
29. E. Billur, B. Çetin, M.M. Yılmaz, A.G. Oğuz, A. Atay, K. Ersoy, R.O. Uğuz, B. Kaftanoğlu, Forming of new generation AHSS using servo presses, in *5th International Conference on Accuracy in Forming Technologies, Chemnitz, Germany* (2015), pp. 175–191
30. D. Guo, Body light weight and cost control, in *Proceedings of the FISITA 2012 World Automotive Congress* (Springer, Berlin, 2013), pp. 977–985
31. J.B. Nam, Development of new auto steels and application technology, in *China Automotive Steel Conference, World Steel/CISA* (2013)
32. M. Schneider, M. Gramling, High strength and ductility - a new steel generation for future developments. Presented at Automotive Expo, June 5, Nürnberg, Germany (2013)
33. K. Lee, Introduction to development and application of automotive steels of Posco, in *Posco Gloval EVI Forum* (2014)
34. S. Maggi, C. Federici, F. D'Aiuto, TWIP Steel application on the Fiat Nuova Panda body, in *Materials in Car Body Engineering 2012* (2012)
35. Renault Media Services, http://media.renault.com
36. Z.C. Xia, AHSS Stamping Project –A/SP 050. Auto/Steel Partnership (2011)
37. J. Shaw, Development of complex, UHS steels to provide vehicle OEMs with a commercially viable option to meet fuel economy standards. Auto/Steel Partnership (2012)

38. J. Speer, D. Matlock, E. De Moor, D. Edmonds, Quenching and partitioning: science and technology. Powerpoint presentation (2013), p. 23
39. G. Thomas, D. Matlock, R. Rana, L. Hector, F. Abu-Farha, ICME 3G AHSS lab heat results supporting DOE targets. Presented at Great Designs in Steel 2015, May 13, Livonia, MI, USA (2015)
40. Y. Gao, Sustainable steel solutions for Chinese cars. Presented at Green Manufacturing – the Future of Steel and Automobile, November 21, Guangzhou, China (2013)
41. D. Branagan, Overview of a new category of 3rd generation AHSS. Presented at Great Designs in Steel 2013, May 1, Livonia, MI, USA (2013)
42. D. Branagan, Launch of a new class of 3rd generation cold formable AHSS. Presented at Great Designs in Steel 2016, May 16, Livonia, MI, USA (2016)
43. Y. Kang, Synthetic properties and potentialities of future automobile steel. Presented at Green Manufacturing – the Future of Steel and Automobile, November 21, Guangzhou, China (2013)
44. J.G. Speer, F.C.R. Assunção, D.K. Matlock, D.V. Edmonds, The "quenching and partitioning" process: background and recent progress. Mater. Res. **8**(4), 417–423 (2005)
45. L. Wang, W. Feng, *Development and Application of Q&P Sheet Steels* (Springer, Berlin, 2011), pp. 255–258
46. G.A. Thomas, E. De Moor, J.G. Speer, Advanced high strength steel - recent progress, ongoing challenges, and future opportunities. Presented at AIST Symposium, Vail, CO, USA (2013)
47. G. Hsiung, Advanced high-strength steel stamping – A/SP 050. Auto/Steel Partnership (2012)
48. H. Du, Y. Li, H. Jie, K. Bai, The automobile steel of the third generation in b-pillar reinforced panel. Eng. Sci. **10**(6), 20–22 (2012)
49. K. Sugimoto, J. Sakaguchi, T. Iida, T. Kashima, Stretch-flangeability of a high-strength TRIP type bainitic sheet steel. ISIJ Int. **40**(9), 920–926 (2000)
50. N. Fonstein, *Advanced High Strength Sheet Steels* (Springer, Berlin, 2015)
51. T. Kimura, Formability of trip type banitic ferrite steel sheet. Kobelco Technol. Rev. **30**, 85–89 (2011)
52. S. Jacque, K. Obayashi, Renault and Nissan light weight body engineering strategy. Presented at Strategies in Car Body Engineering 2012, March 21–22, Bad Nauheim, Germany (2012)
53. T. Kondo, K. Ishiuchi, 1.2GPa advanced high strength steel with high formability, in *SAE Technical Paper*. (SAE International, 2014), p. 04
54. D. Coakley, Nissan Murano. Presented at Great Designs in Steel 2015, May 13, Livonia, MI, USA (2015)
55. ArcelorMittal, Steels for cold stamping -Fortiform> (2014). Accessed 10 June 2015
56. H. So, D. Faßmann, H. Hoffmann, R. Golle, M. Schaper, An investigation of the blanking process of the quenchable boron alloyed steel 22MnB5 before and after hot stamping process. J. Mater. Process. Technol. **212**(2), 437–449 (2012)
57. H. Engels, O. Schalmin, C. Müller-Bollenhagen, Controlling and monitoring of the hot-stamping process of boron-alloyed heat-treated steels, in *The International Conference on New Development in Sheet Metal Forming Technology, Stuttgart, Germany* (2006), pp. 135–150
58. W.D. Callister, D.G. Rethwisch, *Fundamentals of Materials Science and Engineering*, vol. 21 (Wiley, New York, 2013)
59. E. Billur, C. Wang, C. Bloor, M. Holecek, H. Porzner, T. Altan, Advancements in tailored hot stamping simulations: cooling channel and distortion analyses. AIP Conf. Proc. **1567**(1), 1079–1084 (2013)
60. T. Kurz, New developments in zinc coated steel for press hardening. Presented at Insight Edition Conference, September 20-21, Gothenburg, Sweden (2011)
61. T. Kurz, G. Luckeneder, T. Manzenreiter, H. Schwinghammer, A. Sommer, Zinc coated press-hardening steel - challenges and solutions, in *SAE Technical Paper*. SAE International (2015), p. 04
62. J. Watkins, Material development. Presented at AP&T Press Hardening, Next Step Seminar, Novi, MI (2011)
63. S. Sepeur, The company Nano-X GmbH: products for the automotive industry. Presentation at Deutsche Börse, July 10th, Frankfurt, Germany (2006)

64. ThyssenKrupp Steel Europe, *Warmumformung im Automobilbau*. Die Bibliothek der Technik (2012)
65. W. Runge, *Technology Entrepreneurship: A Treatise on Entrepreneurs and Entrepreneurship for and in Technology Ventures*, vol. 2. KIT Scientific Publishing, Karlsruhe (2014)
66. I. Martin, M. López, P. Raya, A. Sunden, D. Berglund, K. Isaksson, S. Isaksson, Press systems and methods, US Patent 9,492,859 (2016). Accessed 15 Nov 2016
67. P. Belanger, Steel innovations in hot stamping, in *Great Designs in Steel 2016* (2016)
68. I.M. Gonzalez, O. Straube, Development of zinc coated parts for hotstamping, in *Proceedings of New Developments in Sheet Metal Forming Conference, Stuttgart, Germany* (2016), pp. 265–276

Chapter 2
Metallurgy of Steels

Barış Çetin and Halim Meço

Abstract In hot stamping, typically, C-Mn-B alloyed steels are used and the process involves phase transformations. Thus, a clear understanding of the effects of alloying elements, different phases of steels, and their kinematics are critical for comprehensive understanding of the process.

2.1 Phases of Steels and Their Properties

Hot stamping involves a number of phase changes during the process. The as-received material contains a "Ferritic-Pearlitic" microstructure, and then during processing, it is heated over its "Austenitization" temperature (above A_3). For the required ultra high strength, it is then quenched to form "Martensite". As discussed in the next sections, there is also a recent trend to tailor the properties of the part by slowly quenching "soft zones" to have "Bainitic" structure which may have better elongation properties.

Based on this discussion, the properties of the five microstructures/phases involved in hot stamping process are explained in the following sections (Fig. 2.1).

Austenite

Austenite, also known as γ-iron, is the face-centered cubic (*fcc*) phase of steel, see Fig. 2.3a. This phase is typically not stable at low temperatures, although special alloying elements may stabilize austenite as in TWIP (Twinning-Induced Plasticity) steels and austenitic stainless steels. Most heat treatment operations start with austenite phase [2, 3].

B. Çetin (✉) · H. Meço
FNSS Defense Systems Co. Inc., R&D Center, Gölbaşi, Ankara, Turkey
e-mail: cetin.baris@fnss.com.tr

H. Meço
e-mail: halim.meco@fnss.com.tr

E. Billur (ed.), *Hot Stamping of Ultra High-Strength Steels*,
https://doi.org/10.1007/978-3-319-98870-2_2

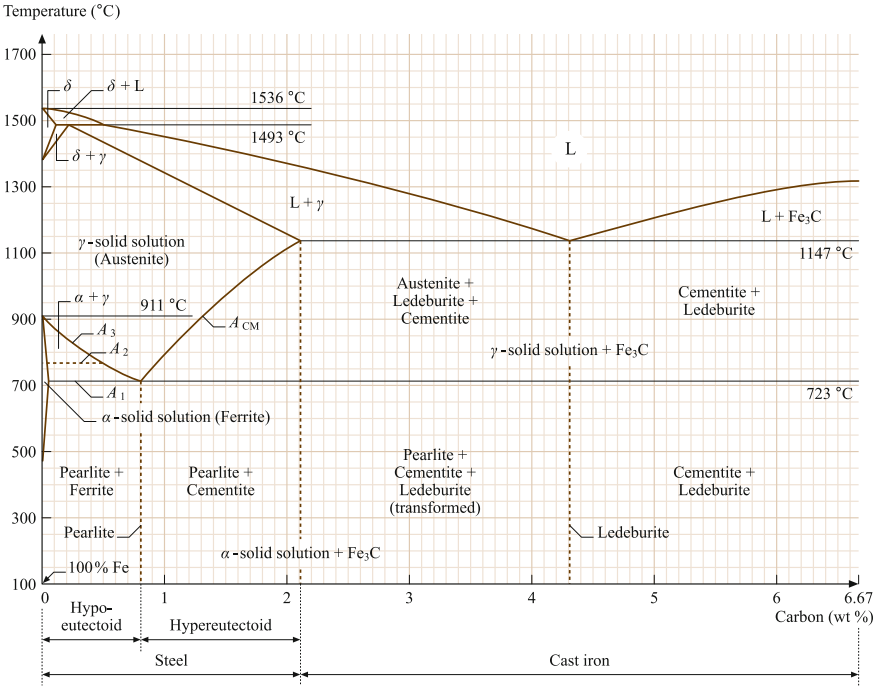

Fig. 2.1 Fe-C phase diagram [1]

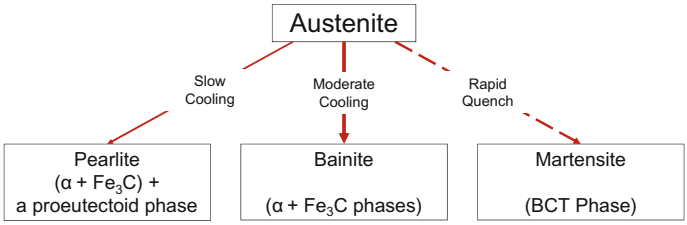

Fig. 2.2 Possible transformations of austenite: solid lines show transformation with diffusion, dashed line shows diffusionless transformation (re-created after [2])

Bainite

As shown in Fig. 2.2, if austenite is cooled at a moderate rate, bainite is produced. Bainite is not a phase, but a microstructure composed of cementite (Fe_3C) and ferrite [1, 2], which is explained in the next section.

Ferrite

Ferrite, also known as α-iron, is the body-centered cubic phase of steel, Fig. 2.3b. Low-carbon steels are mostly ferrite, whereas medium-carbon and high-carbon steels are mostly ferrite with some pearlite [2, 4].

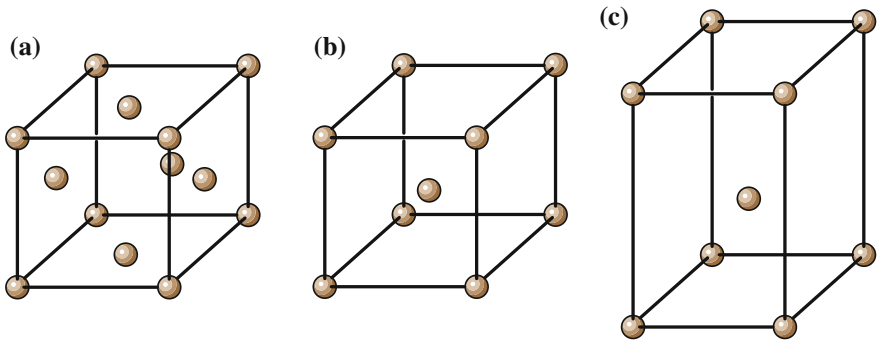

Fig. 2.3 **a** Austenite is face-centered cubic, **b** Ferrite is body-centered cubic (bcc) and **c** Martensite is body-centered tetragonal [1]

Martensite

Martensite is the hardest form of steel. This microstructure is formed by rapid cooling of Austenite, so rapid that carbon diffusion cannot take place. Because of carbon supersaturation, martensite has a larger and slightly expanded crystal structure compared to *bcc* (body-centered cubic) ferrite. The resultant martensite crystal structure is *bct* (body-centered tetragonal) as shown in Fig. 2.3c. The martensitic transformation is a diffusionless solid-state shear deformation. In steels, martensite is formed from austenite containing relatively higher amounts of carbon atoms and in view of the diffusionless nature of its formation, martensite ideally inherits the carbon atoms of the parent austenite. The carbon atoms are trapped in octahedral interstitial sites between iron atoms. In addition to the fact that the chemical composition of the austenite is directly inherited by the martensite, the martensitic shear deformation is accomplished by a plane strain shape change parallel to a set of crystallographic planes of the parent austenite. Therefore, when the martensite is formed, the volume of metal is increased, and the transformation plasticity is also produced, which directly affects the distortion and residual stress state of the final part [5, 6].

Pearlite

Pearlite microstructure is a lamellar mixture of ferrite and cementite (Fe_3C). These exist as grains, called as "pearlite colonies". In each colony, the layers of Cementite points in the same direction, as shown in Fig. 2.4 [2].

2.2 The Effect of Alloying Elements

In plain carbon steels, the nose of the TTT (Time-Temperature- Transformation) and CCT (Continuous Cooling Transformation) curves are located at very short times; hence, very fast cooling rates are required to produce an all-martensite microstructure.

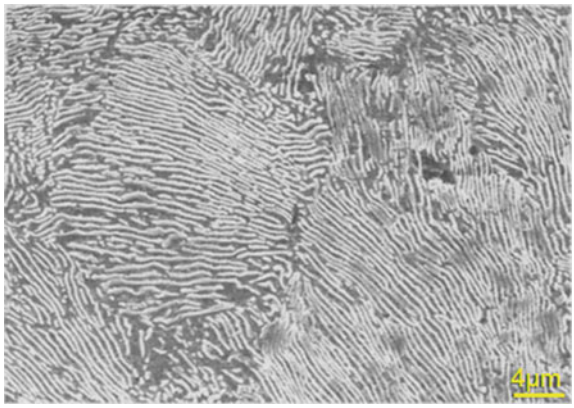

Fig. 2.4 SEM image of pearlite: white areas show ferrite and black areas show cementite [7]

In the thin sections of steel, the rapid quench produces distortion and cracking. In thick sections, it is not possible to produce fully martensitic microstructures. All common alloying elements in steel shift the TTT and CCT diagrams to longer times, permitting us to obtain all-martensite even in thick sections at slow cooling rates [8]. As alloying elements influence CCT and TTT curves, they may also alter the Martensite-start (M_s) and Martensite-finish temperatures (M_f). All alloying elements apart from Cobalt and Aluminum lower the M_s and M_f temperature [9]. For high- carbon steels, the M_f temperature generally lies below the room temperature, which means that there always exists some amount of retained austenite in the final product.

In hot stamping, typically manganese-boron alloyed steels are used. Typical hot stamping steel (22MnB5) has about 0.22% C, 1.18% Mn and 0.002% B [10].The alloying is designed in such a way that:

(1) the parts have high yield and ultimate tensile strength after quenching [11],
(2) martensitic transformation can be completed in a water cooled die [11],
(3) phase transformations are avoided during blank transfer from the furnace to the press [12],
(4) the final parts are weldable in automotive body shops (which requires low C and Mn) [13].

In the next subsections, the effects of common alloying elements are explained individually.

Carbon (C)

As carbon content increases, steel's strength and hardness increases as displayed in Fig. 2.5, but weldability and ductility decrease. In hot stamping applications, Carbon content in the most common steel 22MnB5 is 0.22%. Steels with higher strength (i.e., 1800–2000 MPa) have even higher carbon contents up to 0.37%. Recently, energy absorbing grades for hot stamping are also introduced with carbon content between 0.10–0.12% and strength levels between 450–1000 MPa. Carbon also has an effect in phase transformations such as lowering the Martensite-start temperature, as shown in Fig. 2.6 [4, 10, 14–17].

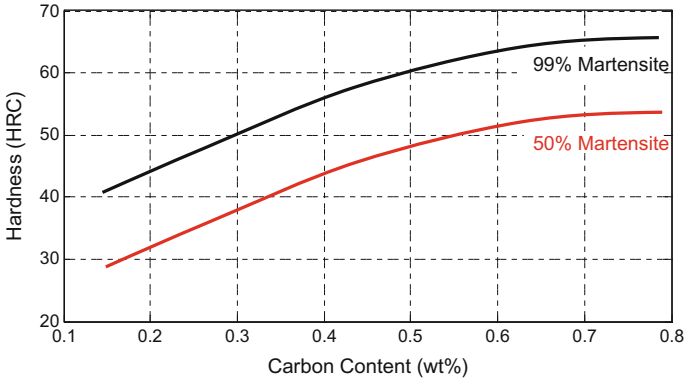

Fig. 2.5 Dependence of carbon content on hardness and martensite phase fraction (re-created after [17])

Manganese (Mn)

Manganese is found in almost all steels, at least by ∼0.3%. It is used as a deoxidizer and also reduces susceptibility to hot shortness during hot working. It also increases the hardness and hence results in a reduction in ductility as well as weldability. There is also a concurrent increase in hardenability with Mn addition. Large quantities of Mn (>2%) cause cracking and distortion problems after quenching. However, after 5 %, a complex microstructure with austenite at room temperature may be present. The so-called Medium-Mn (typically 5–12% Mn) and High-Mn (TWIP steels, >15 % Mn) steels have both high strength and elongation for cold stamping applications. Medium-Mn steels have also been studied for hot stamping as explained in Sect. 4.4. Mn lowers the austenitization temperature, which could reduce the furnace temperature in hot stamping and thus save energy and reduce the carbon emissions during heating [4, 9, 18, 19]. In low-carbon steels, Mn retards bainite formation, which is useful for hot stamping where the final microstructure is expected to have ∼100% martensite. Mn also reduces martensite-start temperature, but is not as effective as carbon (Fig. 2.6) [16, 20].

The steels used in hot stamping contain 0.8 to 1.3% Mn, the typical amount is around 1.2% [10, 14].

Boron (B)

Certain elements such as Ti, Al, V, Zi, and B improve the hardening properties of steel by forming carbides. Boron is the most effective of these elements. Hardenability of steels with carbon level up to 0.5 % increases with even a very small amount of boron (0.001–0.003 %) [1, 4, 17]. According to Zhu et al., this can be explained by segregation of free B atoms and/or borocarbide ($Fe_{23}(CB)_6$) at the austenite grain boundaries and delaying the ferrite and pearlite formation [21]. This can be seen in Fig. 2.6. Naderi et al. studied a total of nine different C-Mn alloys, five with B addition, and found out that without B-alloying, it was not possible to get 100% martensitic structure with water-cooled dies [22].

Chromium (Cr)

Chromium is used as an alloying element mainly to increase the hardenability and corrosion resistance, and also to improve the high-temperature properties such as strength and oxidation resistance. It also provides abrasion resistance in high-carbon compositions as it is a strong carbide former. Chromium is one of the major hardening elements and superior mechanical properties can be attained when used together with a toughness increasing element such as nickel. It is generally used with molybdenum when high-temperature strength is required. Hot stamping steels typically contain up to 0.30 % Cr [23–26].

Niobium (Nb)

Niobium is known to inhibit grain growth during austenitizing [9]. It is well known that for low-carbon steels "Prior Austenite Grain Size" (PAGS) improves the strength and toughness [27]. For higher strength hot stamping steels, Nb is recommended for improved toughness [28]. Another advantage of Nb is reducing the hydrogen diffusivity. This is important to reduce Hydrogen-Induced Delayed Fracture [29, 30]. The effects of Nb are also investigated in Sects. 4.2 and 6.5.

Silicon (Si)

Silicon is used as a deoxidizer in steelmaking process. Its amount depends on the steelmaking process employed and can reach to the levels of 0.15–0.30 % in fully killed steels. Silicon has a slight hardening effect on the ferrite phase and is usually detrimental to surface quality for low-carbon steels. Typically, hot stamping steels contain 0.20–0.35 % Si [23–25].

Phosporus (P)

Phosphorus results in increased strength and hardness, however, this comes at a cost of decreased ductility and toughness. It also causes temper embrittlement in medium-carbon steels. It can be used as a deliberate alloying addition in order to increase the machinability and corrosion resistance. However, its amount should be restricted typically to 0.030 % in hot stamping steels [23–26].

Sulfur (S)

Transverse ductility and notch impact toughness characteristics suffer with increased sulfur content. Moreover, weldability also decreases with increased sulfur content. It is very detrimental to surface quality, particularly in steels containing low-carbon and low-manganese. Except for free machining steels, sulfur is considered as a detrimental element and therefore its amount is restricted typically to 0.015 % in hot stamping steels. Sulfur also has a great segregation tendency in steels and usually occurs in the form of sulfides, the most common form of which is MnS (manganese sulfide) [23–26].

Aluminum (Al)

Aluminum's main function in steelmaking process is to deoxidize and control the grain size. It is added to steel mainly to inhibit the growth of austenite grains during heating prior to quenching. Besides aluminium, other elements such as titanium, vanadium, and zirconium are used for controlling austenite grain size, however, aluminum is the most effective element used for this purpose. Conversely, it also has adverse effects on the hardenability for heat-treatable grades as aluminum form stable carbides which are difficult to dissolve during heat treatment. Hot stamping steels contain a restricted amount of aluminum which is typically limited to 0.08% [23–26].

Nitrogen (N)

Nitrogen additions to steel results in increased strength, hardness and machinability. However, these come at the expense of decreased ductility and toughness. By forming aluminum nitrides, it acts as a grain size controlling agent in aluminum-killed steels, hence increasing both ductility and toughness. Nitrogen can reduce the effect of boron on the hardenability of steels and therefore its amount is restricted typically to 0.01 % for hot stamping steels [23–26].

2.3 Phase Transformations

To achieve ultra high strength steel at the end of hot stamping process, the transformation of austenite to martensite is required. Phase transformations take place either

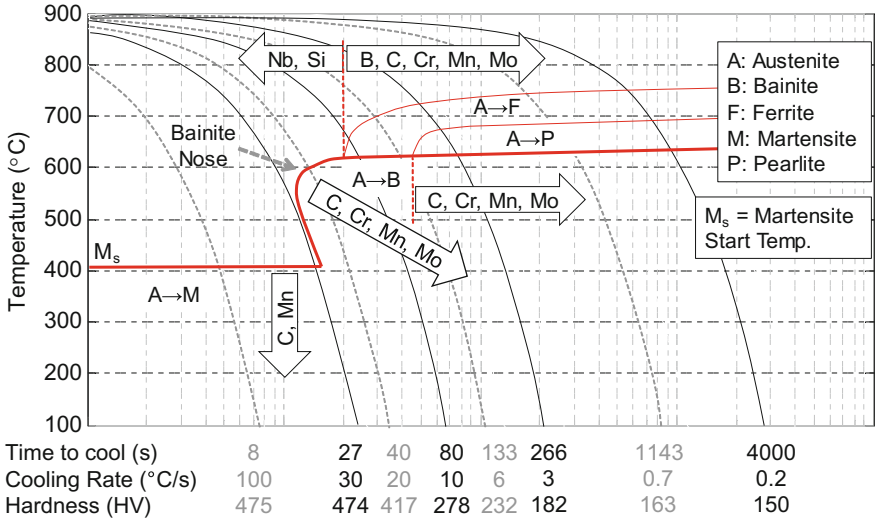

Fig. 2.6 CCT diagram for 22MnB5 steel and the effects of alloying elements (re-created from [16, 31])

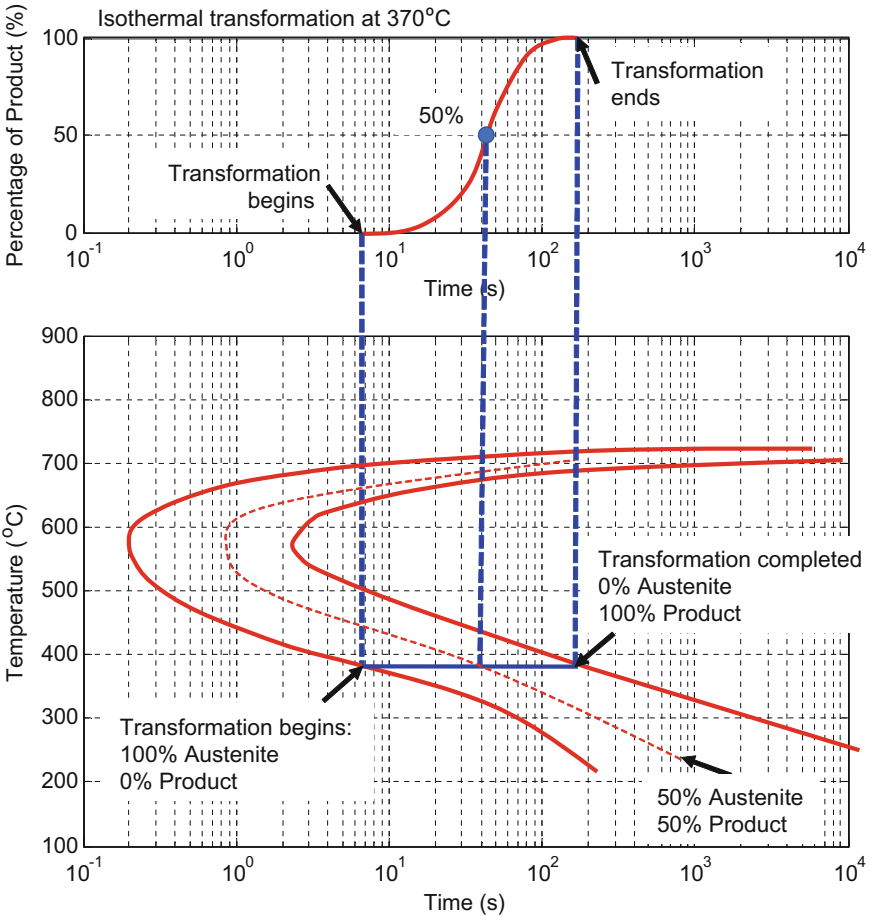

Fig. 2.7 Approximation of phase transformation by using Avrami equation (re-created after [2, 32])

during heating the steel (i.e., ferrite and pearlite transforms to austenite) or during cooling (from austenite to others).

During cooling, austenite transforms to ferrite and pearlite if cooled slowly, bainite forms at a moderate cooling rate and at high cooling rate martensite forms. As shown in Fig. 2.6, the final microstructure can be predicted by using CCT curves [2, 4, 25].

In finite element models, Avrami (also known as Johnson–Mehl–Avrami–Kolmogorov) equation Eq. (2.1) is used to model phase transformations. Coefficients of Avrami equation are b and n, for each phase, and these can be calculated by using TTT diagrams, as shown in Fig. 2.7.

$$P, B, F = 1 - exp\left(-b * \left(\frac{t}{t_0}\right)^n\right) \tag{2.1}$$

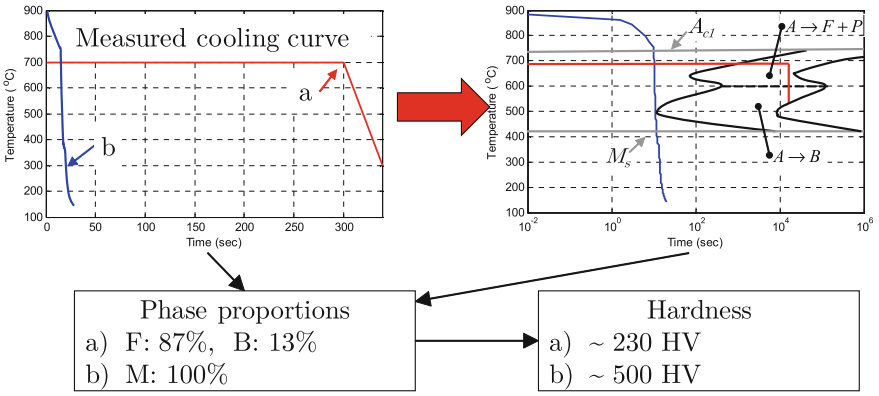

Fig. 2.8 Prediction of microstructure evolution in finite element analysis (re-created after [4, 34–36])

where, P, B, and F stand for pearlite, bainite and ferrite percentages, respectively. For each phase and at given temperature levels, b and n can be calculated using TTT curves. For martensite transformation, the equation slightly changes into Eq. (2.2):

$$M = 1 - exp[-c * (M_s - T)^m] \tag{2.2}$$

In the literature, there are some equations which are specifically dedicated to determine the martensitic transformation such as Koistinen-Marburger equation. By this formulation, the volume fraction of transformed martensite as a function of temperature could also be computed [33].

The main factor that determines the rate in a phase transformation, such as austenite-to-pearlite transformation, is temperature. The sigmoidal-shaped curve shown in the upper portion of Fig. 2.7 gives the percentage transformation versus the logarithm of time at a specific temperature (i.e. 370 °C (700 °F)) for an iron–carbon alloy of eutectoid composition. Depending on the temperature relative to the tip of the TTT curve (approx. 580 C), varying the temperature shifts the sigmoidal curve, for example increasing temperature shifts it to the right if above the tip of TTT curve or to the left if below the tip of TTT curve. For each such curve, data is collected after rapidly quenching a specimen composed of 100% austenite to a specific temperature of interest; after which temperature is maintained constant throughout the course of the reaction.

The bottom portion of Fig. 2.7 represents another suitable way of depicting time and temperature dependence of this transformation. In this graph, two solid curves represent the time required for the start of the transformation and the finish of the transformation, respectively at a specific temperature of interest. The dashed curve that is located in the middle of start and finish curves correspond to 50% of transformation completion. These curves are typically generated from a series of plots of the percentage transformation versus the logarithm of time taken over a range of temperatures, an example of such curves is the sigmoidal-shaped curve given in

Fig. 2.7. Upper portion of Fig. 2.7 illustrates how the data transfer is made at a specific isothermal hold temperature, in this case 370 °C (700 °F) [2, 32].

FE model can use the coefficients of Avrami equation to estimate the final microstructure distribution. For example, for two different cooling conditions *a* and *b*, as shown in Fig. 2.8, it is possible to calculate the expected phase fractions upon cooling to room temperature using TTT or CCT curves. These phase fractions can then be taken into account for calculating the expected mechanical properties, in this case, hardness for cooling conditions *a* and *b*.

References

1. K.H. Grote, E.K. Antonsson, *Springer Handbook of Mechanical Engineering* (Springer, Würzburg, 2009)
2. W.D. Callister, D.G. Rethwisch, *Fundamentals of Materials Science and Engineering*, vol. 21 (Wiley, New York, 2013)
3. B.C. De Cooman, O. Kwon, K.G. Chin, State-of-the-knowledge on TWIP steel. Mater. Sci. Technol. **28**(5), 513–527 (2012)
4. G.E. Totten, *Steel Heat Treatment: Metallurgy and Technologies* (CRC Press, Boca Raton, 2006)
5. G. Krauss, Deformation and fracture in martensitic carbon steels tempered at low temperatures. Metall. Mater. Trans. B **32**(2), 205–221 (2001)
6. D. Deng, FEM prediction of welding residual stress and distortion in carbon steel considering phase transformation effects. Mater. Des. **30**(2), 359–366 (2009)
7. D.C. Madeleine, *The Pearlite Transformation* (Springer, Berlin, 2004), pp. 195–208
8. D.R. Askeland, W.J. Wright, *Essentials of Materials Science & Engineering* (Cengage Learning, Boston, 2013)
9. M. Maalekian, The effects of alloying elements on steels (i). Christ. Doppler Lab. Early Stages Precip. **23**, 221–230 (2007)
10. H. Karbasian, A.E. Tekkaya, A review on hot stamping. J. Mater. Process. Technol. **210**(15), 2103–2118 (2010)
11. M. Naderi, *Hot Stamping of Ultra High Strength Steels*
12. S. Bruschi, G. Liu, *Hot Stamping-Comprehensive Materials Processing* (Elsevier, Amsterdam, 2014)
13. American Society of Metals, *ASM Handbook of "Welding and Brazing"*, vol. 06, , 2nd edn. (ASM International, 1993)
14. S. Graff, T. Gerber, F.J. Lenze, S. Sikora, About the simulation of microstructure evolution in hot sheet stamping process and the correlation of resulting mechanical properties and crash-performance, in *3rd International Conference on Hot Sheet Metal Forming of High Performance Steel, CHS2, Kassel, Germany* (2011), pp. 323–330
15. ArcelorMittal Flat Carbon Europe S.A. ArcelorMittal Automotive Product Offer Europe, Android App, V1.0 (2015)
16. H. Mohrbacher, Martensitic automotive steel sheet - fundamentals and metallurgical optimization strategies, in *Innovative Research in Hot Stamping Technology*, vol. 1063. Advanced Materials Research (Trans Tech Publications, 2015), pp. 130–142
17. American Society of Metals, *ASM Handbook of "Heat Treating, 3rd printing"*, vol. 4 (ASM International, 1995)
18. H. Aydin, E. Essadiqi, I.H. Jung, S. Yue, Development of 3rd generation AHSS with medium Mn content alloying compositions. Mater. Sci. Eng.: A **564**, 501–508 (2013)

19. Q. Han, W. Bi, X. Jin, W. Xu, L. Wang, X. Xiong, J. Wang, P. Belanger, Low temperature hot forming of medium-Mn steel, in *5th International Conference on Hot Sheet Metal Forming of High Performance Steel, CHS2, Toronto, ON, Canada* (2015), pp. 381–389
20. W. Alqhadafi, Laser welding of boron and bainitic steels (2012)
21. Kangying Zhu, Carla Oberbillig, Céline Musik, Didier Loison, Thierry Iung, Effect of b and b+nb on the bainitic transformation in low carbon steels. Mater. Sci. Eng.: A **528**(12), 4222–4231 (2011)
22. M. Naderi, M. Ketabchi, Abbasi M., Bleck W., Analysis of microstructure and mechanical properties of different boron and non-boron alloyed steels after being hot stamped. Procedia Eng. **10**, 460–465 (2011)
23. ArcelorMittal. Extract from the product catalogue (2015). Accessed 10 June 2015
24. SSAB, Docol 22MnB5 - cold rolled boron steel for hardening in water or oil. Product Catalogue (2011)
25. J.R. Davis, *Carbon and Alloy Steels* (ASM International, 1996)
26. Salzgitter Flachstahl, 22MnB5 boron alloyed quenched and tempered steel. Product catalogue (2014)
27. C. Wang, M. Wang, J. Shi, W. Hui and H. Dong, Effect of microstructure refinement on the strength and toughness of low alloy martensitic steel. J. Mater. Sci. Technol. **23**(05), 659 (2007)
28. J. Wang, C. Enloe, J. Singh, C. Horvath, Effect of prior austenite grain size on impact toughness of press hardened steel. SAE Int. J. Manuf. **9**, 488–493, 04 (2016)
29. H. Mohrbacher, Influence of alloy modifications and microstructure on properties and crash performance of press hardened steel components, in *6th International Conference on Hot Sheet Metal Forming of High Performance Steel, CHS2, Atlanta, GA, USA* (2017), pp. 213–222
30. S. Tateyama, R. Ishio, K. Hayashi, T. Sue, Y. Takemoto, T. Senuma, Microstructures and mechanical properties of V and/or Nb bearing ultrahigh strength hot stamped steel components. Tetsu-to-Hagane **100**(9), 1114–1122 (2014)
31. L. Vaissiere, J.P. Laurent, A. Reinhardt, Development of pre-coated boron steel for applications on PSA Peugeot Citroën and Renault bodies in white, in *SAE Technical Paper*, vol. 7. (SAE International, 2002)
32. American Society for Metals. Ohio. *Atlas of Isothermal Transformation and Cooling Transformation Diagrams* (Metals Park, Ohio, 1977)
33. C. Şimşir, C.H. Gür, An FEM based framework for simulation of thermal treatments: application to steel quenching. Comput. Mater. Sci. **44**(2), 588–600 (2008)
34. F.F. Li, M.W. Fu, J.P. Lin, Effect of cooling path on the phase transformation of boron steel 22MnB5 in hot stamping process. Int. J. Adv. Manuf. Technol. **81**(5), 1391–1402 (2015)
35. G.-Z. Quan, T. Wang, L. Zhang, Research on the influence of hot stamping process parameters on phase field evolution by thermal-mechanical phase coupling finite element. Int. J. Adv. Manuf. Technol. **89**(1), 145–161 (2017)
36. C. Koroschetz, K. Eriksson, O. Kragt, A. Ademaj, Production method for locally, graded presshardened components through process integration of a heating technology in combination with appropriate process control, in *IDDRG 2016, Linz, Austria* (2016), pp. 356–362

Chapter 3
History and Future Outlook of Hot Stamping

Eren Billur, Göran Berglund and Tord Gustafsson

Abstract Hot stamping can be traced back to traditional Japanese sword making techniques of thirteenth–fourteenth centuries [1]. The earliest patent about "Preßhärten" (Press hardening) was granted in 1914 in Switzerland. The technique described in this patent has been used in agricultural products since 1930s [2]. Hot stamping, as we know it today differs from these applications since the quenching is done at the press die to reduce distortion. Although hot stamping has been commonly used since early to mid-2000s, the beginning was in 1970s.

3.1 Early Developments: 1973–1990

Hot stamping was developed in Luleå, Sweden by Norrbottens Järnverks AB (Norrbotten Iron Works), in 1970s. The first patent application was completed in 1973 and was issued on November 2nd, 1977 [3]. In 1975, Swedish National Board for Technical Development (STU) funded a 6-year project at Luleå University of Technology (LTU) together with Volvo Trucks and Norrbottens Järnverks [4].

The group headed by Prof. Krister Källström built a number of research tools. These included several simple dies such as the flat hardening die, deep drawing die, and channel forming die as shown in Fig. 3.1. The next step was to produce a real part, and for research purpose, a hinge geometry was selected, Fig. 3.2.

E. Billur (✉)
Billur Makine Ltd., Ankara, Turkey
e-mail: eren@billur.com.tr

E. Billur
Atılım University, Ankara, Turkey

G. Berglund
Luleå, Sweden
e-mail: 0920.251947@telia.com

T. Gustafsson
Blatraden AB, Öjebyn, Sweden
e-mail: tord.gustafsson@blatraden.se

E. Billur (ed.), *Hot Stamping of Ultra High-Strength Steels*,
https://doi.org/10.1007/978-3-319-98870-2_3

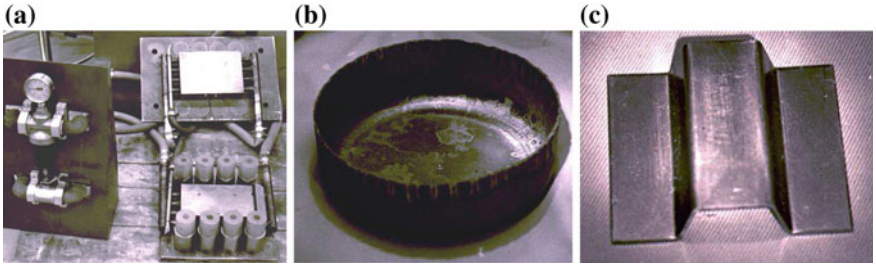

Fig. 3.1 Several research tools at LTU: **a** Flat hardening die, **b** deep drawing and **c** channel forming [4]

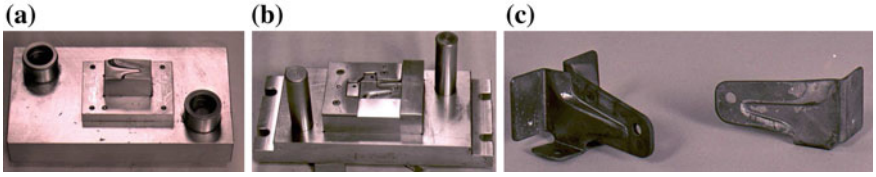

Fig. 3.2 Hinge halves: **a** upper and **b** lower die, **c** sample parts [4]

Fig. 3.3 Various geometries to study formability: **a** Stretch flanging, **b** Curved flange, **c** Stretching [4]

Together with Volvo Trucks, additional 6 dies were produced. These included several flanging dies emulating different geometries as shown in Fig. 3.3. Later, real parts such as gas tank brackets, bumper beams and cross member pieces were also produced, see Fig. 3.4. Some of these components were further tested for performance (load test, fatigue test, etc.) [4].

In 1978, while the studies were still continuing at Luleå University of Technology (LTU), Norrbottens Järnverk was merged with Domnarvets Järnverk and Oxelösunds Järnverk to form SSAB (Svenskt Stål AB, Swedish Steel) [5].

The first mass production hot stamping die—shown in Fig. 3.5—was made for Norbergs Spad- och Redskapsfabriker AB (Norberg Spades and Tools Plant). The cast iron die was designed for forming and quenching 1.5 mm thick spade. The cycle time was 20 s. This first mass production die was used for producing at least 20.000 parts.

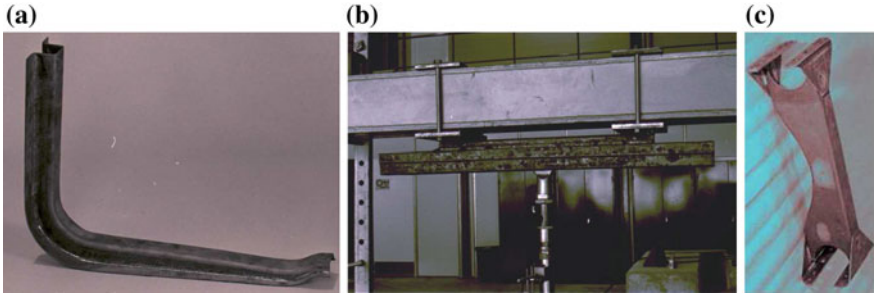

Fig. 3.4 Volvo Trucks prototype parts: **a** gas tank bracket, **b** bumper beam under load test, and **c** cross member piece [4]

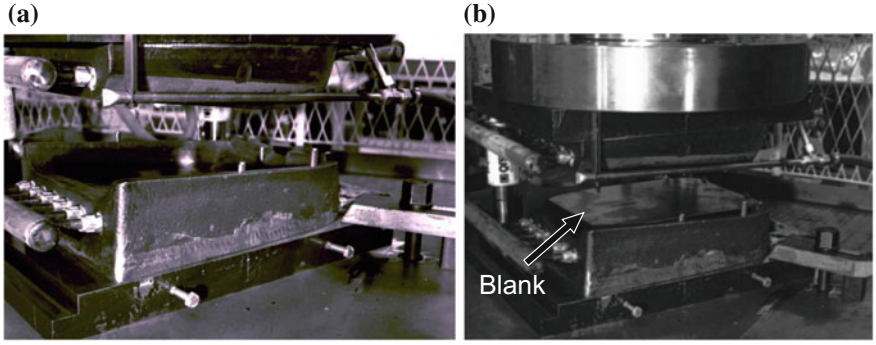

Fig. 3.5 First production tool for Norberg spade company [4]

Fig. 3.6 1984 Saab 9000 was the first automobile to have hot stamped side impact door beams [image from http://wikipedia.org]

Table 3.1 Advantages and disadvantages of AlSi-coated boron steels [17]

Advantages	Disadvantages
No scale formation (reducing one manufacturing step)	High material cost, compared to uncoated blank
Atmosphere controlled furnace is not needed	Cold-forming (indirect hot stamping) is impossible
Some corrosion protection	Heating system has to be accordingly (longer furnaces)

In 1982, the rights for hot stamping were sold to Plannja AB. The first application in automotive industry was in 1984, when Saab started buying hot stamped side impact door beams for Saab 9000, Fig. 3.6. In 1986, Jaguar also started using hot stamped door beams in its XJ model [6–10].

3.2 Further Developments 1990s

In 1991, Ford decided to use hot stamped door beams in its new middle class sedan, which was produced both in North America (Ford Contour/Mercury Mystique) and Europe (Ford Mondeo). The production for this car has started in 1993. Until 1995, Plannja AB was the only manufacturer of hot stamped products. However, as the patent rights expired in 1995, the competition started and many other companies started investing in hot stamping [6, 10].

Until the mid-90s, the hot stamped automobile components were only limited to side impact beams. In 1996, Renault facelifted its flagship model Safrane. The Phase II Safrane had a hot stamped bumper beam [11, 12]. In 1997, SSAB HardTech (the new name of the Plannja HardTech AB), together with Saab, applied for a patent to manufacture B-pillar reinforcements by hot stamping [13, 14].

In 1998, Volvo introduced the S80, equipped with a hot stamped rear bumper reinforcement [15]. Ford Focus I also introduced in 1998 had a hot stamped front bumper beam [8, 14]. In the same year, SSAB HardTech opened its first hot stamping line in the US (Mason, MI) [6].

3.3 Coated Blanks and Increased Usage: 2000s

In 1998, the French steel supplier Usinor (later merged to Arcelor) developed the aluminum-silicon-coated 22MnB5 steel, USIBOR 1500 ® [11, 16]. According to [17], the advantages and disadvantages of coated boron steels are given in Table 3.1. Figure 3.7 shows how uncoated blanks had scaling on their surfaces [18].

Fig. 3.7 VW Passat transmission tunnel stamped using: **a** uncoated blank causes scales; **b** coated blank has no scale problems [18]

In 2000, another French company, Sofedit started manufacturing hot stamped parts for the automotive industry. The same year (2000), BMW started using 3 mm thick A-pillar reinforcements in the new 3 series convertible. The parts were supplied by Benteler and were uncoated (Fig. 3.9). This was the first application of hot stamped steel at BMW [19–21].

In March 2001, Renault Laguna II (SOP 2001) was introduced which was the first car to receive 5 stars from EuroNCAP tests and had several components hot stamped. Figure 3.8a–c shows the manufacturing steps of the bumper beam of Laguna [16, 22] (Fig. 3.9).

In the same month, the new Citroën C5 was rolled out which had hot stamped A-pillar reinforcements from Sofedit. It is important to note that two A-pillars were produced from one blank and later laser trimmed, as shown in Fig. 3.8d–f. According to [23], this was the first use of hot stamped components in PSA (Peugeot-Citroën) Group. Parts of Citroën C5 and bumper beam of Renault Laguna II were also the first AlSi-coated hot-formed steels used in a car body [16, 24].

In April 2001, Peugeot 307 was introduced. This vehicle had hot stamped A and B-pillar reinforcements and rear bumper beam, accounted for 3.4% of the mass of the body in white. Contrary to PSA group's Citroën C5, all the hot stamped components in this vehicle were uncoated. One reason behind this selection could be the relatively higher production volume of 307 (2700 vehicles/day) compared to C5 (950 vehicles/day) [22–24].

In 2002, Volvo introduced its first SUV, XC90. This was a breakthrough, as 7% of the body-in-white was hot stamped, see Fig. 3.16. A total of 10 parts were hot stamped: 2 B-pillars (left and right), 4 door beams, roof rail, rear bumper beam, back panel, and rear seat frame [26, 27].

In 2003, Gestamp started prototype hot stamping work. The same year, Sofedit was acquired by ThyssenKrupp. By 2004, there were 4 big players in the market: Benteler, ThyssenKrupp Sofedit, Gestamp, and SSAB HardTech. In late 2004, VW became the first OEM to have an in-house hot stamping line, around the same time, SSAB

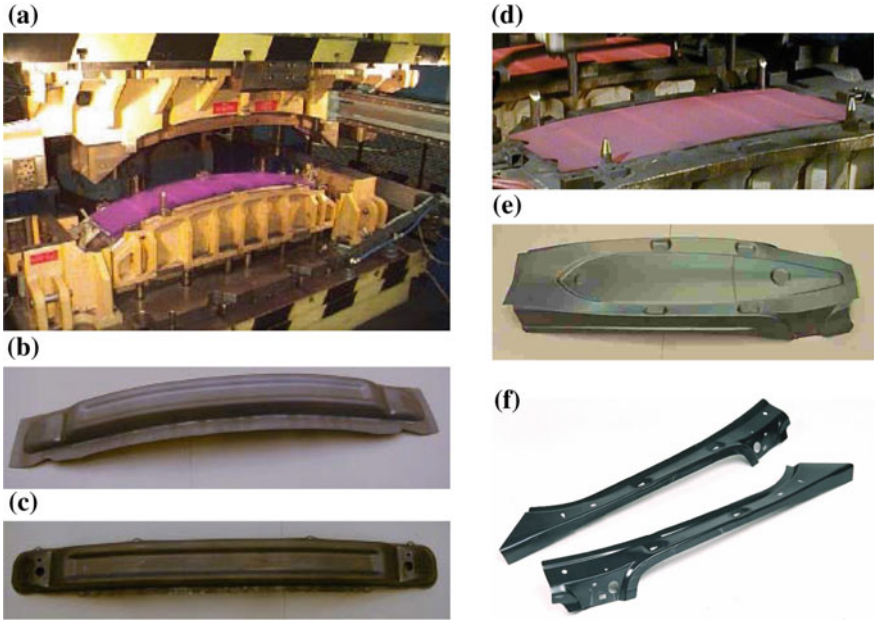

Fig. 3.8 Parts produced by Sofedit: **a–c** bumper reinforcement for Renault Laguna II (SOP 2000), **d–f** A-pillars for Citroën C5 (SOP 2001) [16, 25]

Fig. 3.9 One of the earliest examples of A-pillar reinforcement in BMW 3 Convertible (E46, SOP 2000) (Image re-created from [19])

Fig. 3.10 Hot stamped boron steel components in Passat B6 (SOP 2005) [30]

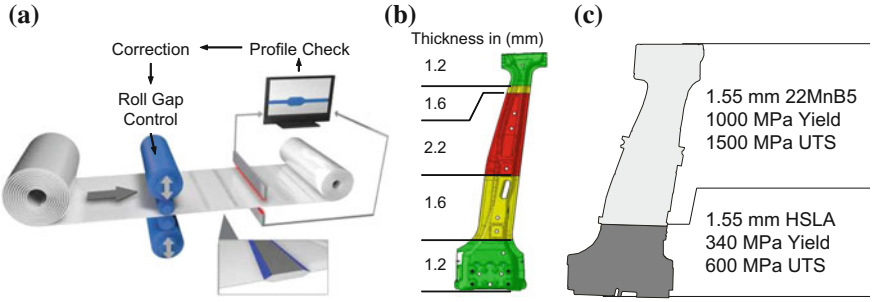

Fig. 3.11 **a** Tailor Rolling process [image courtesy of Mubea Tailor Rolled Blanks GmbH], **b** BMW X5 (SOP 2006) was the first car to have a tailor-rolled + hot stamped component [34], **c** Audi A5 (SOP 2007) had a tailor-welded b-pillar (re-created after [33, 35])

HardTech was acquired by Gestamp. In 2005, Magna Cosma started hot stamping [7, 21, 28, 29]. In 2005, VW rolled out the new Passat (B6) which had 19% hot stamped components in body-in-white. As shown in Fig. 3.10, the transmission tunnel and subplate were also hot stamped, which were both first time in the industry [9, 18, 30].

In 2006, Dodge Caliber and BMW X5 became the first cars to have tailor-rolled, hot stamped B-pillars [31]. According to [32] the tailor-rolled blank (Fig. 3.11a, b) saved 4 kg (9 lbs.)/vehicle in BMW X5. The tailor-rolled blank was supplied by Mubea and hot stamped at Benteler. In 2007, Audi A5 was built using tailor-welded transmission tunnel, B-pillars (Fig. 3.11c), and rear rails, all blanks were supplied by ThyssenKrupp Tailored Blanks [33].

3.4 Further Uses of Hot Stamping: 2010s

Beginning with 2010, most carmakers—including but not limited to: Alfa Romeo, Audi, Bentley, BMW, Chevrolet, Chrysler, Citroën, Dodge, Fiat, Ford, Honda, Jaguar, Jeep, Land Rover, Mazda, Mercedes, Nissan, Opel, Peugeot, Porsche, Renault, Rolls-Royce, Saab, Seat, Škoda, Toyota, Volkswagen, Volvo—had already started using

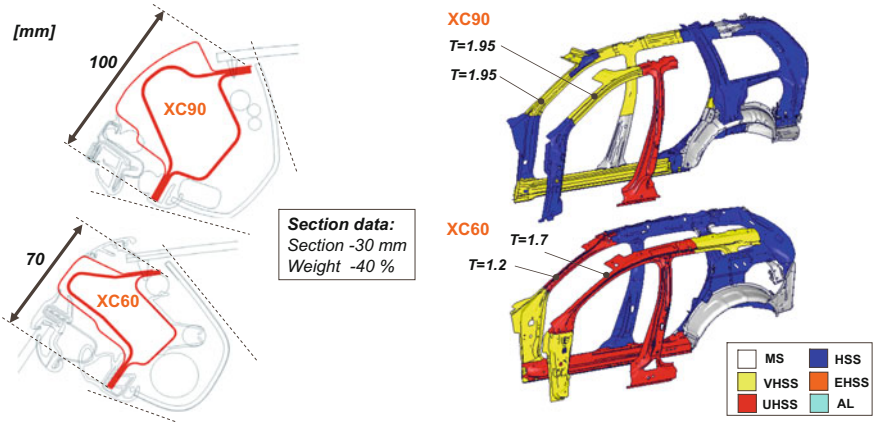

Fig. 3.12 Hot stamping not only saves weight (by decreasing the sheet thickness) but also improves visibility [41]

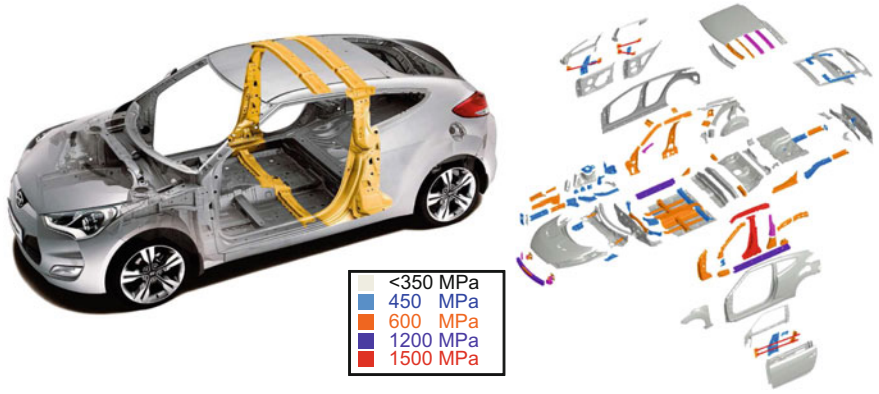

Fig. 3.13 2011 Hyundai Veloster's B-pillars are not in the same plane. This design was possible with use of hot stamped steels [51, 52]

hot stamped components in bodies-in-white or hang-on parts [8, 19, 20, 23, 33, 36–39].

As the technology advanced, hot stamping was not only used to reduce the weight of components, but new uses were found. The first was to make thinner pillars for improved visibility. Currently Ford Fiesta (SOP 2008), Jaguar XF (SOP 2008), Volvo XC60 (SOP 2008), BMW 5-series (SOP 2010), Opel Meriva (SOP 2010), Audi A6 (SOP 2011), and Subaru Impreza (SOP 2014) use hot stamped A-pillars specifically to reduce the width of the A-pillars to further improve the driver's vision. Figure 3.12 shows how hot stamped A-pillars improved the visibility in XC60 compared to 1st generation XC90 (SOP 2002). The new design also saved 5 kg (11 lbs.)/vehicle [40–46].

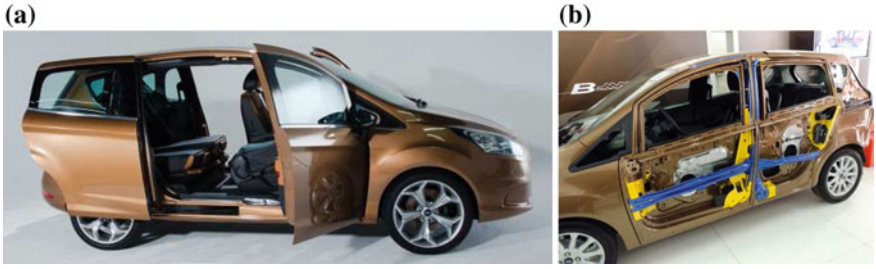

Fig. 3.14 2012 Ford B-Max: **a** showing the pillarless entry, **b** showing the hot stamped reinforcements (blue color) in both front and rear doors [54]

Many convertible vehicles (e.g., VW Golf Cabrio), even including high-end mostly aluminum ones (e.g., Ferrari California, Mercedes SLS-AMG and SL) have ultra high-strength steel reinforcements in their A-pillars to confirm with the rollover requirements [47–50]. As discussed, the first application of a hot stamped A-pillar was also a convertible BMW (Fig. 3.9).

Hot stamped boron steels allowed vehicle manufacturers to design unusual vehicles. One example to this was 2011 Hyundai Veloster. The vehicle was a 3-door coupe where the B-pillars are not one the same plane. This is because in the passenger side, there is a rear door whereas in the driver side there is not, Fig. 3.13 [51].

Another unusual design is seen in Ford B-Max (SOP 2012), a small van for European market. The car has a sliding rear door, but what makes it unique is that the car does not have a B-pillar (Fig. 3.14). The B-pillar was integrated in front and rear doors by using hot stamped boron steel reinforcements [53, 54].

Hot stamped steel is also used in hybrid and/or electric vehicles to protect the battery. The new "Range Rover" (SOP 2012) has an Aluminum intensive body-in-white but the hybrid version has boron steel battery protection which will allow it to "balance on a rock" without risk of battery damage [55]. Nissan Leaf (Electric Vehicle) on the other hand has AHSS battery cover [56]. The city car shown in Fig. 3.15, Chevrolet Spark (SOP 2009), had no martensitic or hot stamped (press hardened) steel in its body-in-white. The electric version of this vehicle is introduced in 2013 and had 14% hot stamped components by mass to protect the batteries [57].

3.5 Summary of the 40 Years

Figure 3.16 shows the mass percentage of hot stamped boron steel usage in several vehicles in the last decade. In this figure, only the highest usage of boron steel up to that year is listed. As explained earlier, Volvo XC90 and VW Passat were the first two breakthroughs in using hot stamped components.

Since 2012, several vehicles have surpassed 20% (by mass) barrier of hot formed body components. The first one was Volvo V40 (SOP 2012) with 20% hot stamped

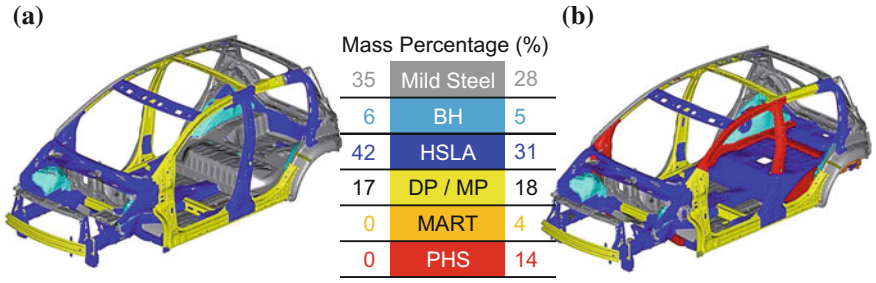

Fig. 3.15 Chevrolet Spark: **a** standard version does not have any hot stamped component, **b** electric version's body has 14% by mass hot stamped components (re-created after [57])

parts by mass [58]. Later on several Volkswagen Group vehicles on MQB platform were introduced; these vehicles typically had 24–28% of hot formed body by mass. These vehicles include, but are not limited to, Audi A3 (3rd generation), VW Golf 7, VW Passat B8, Seat Leon Mk3 and Škoda Octavia Mk3 [59]. However, since 2014, the highest usage of hot formed steels is in Volvo XC90 (2nd generation, production started in 2014), which accounts for 38% of the body mass [58].

As hot stamped parts found more applications in auto-body, more vehicle manufacturers adopted the technology. Figure 3.17 shows the increasing demand and future forecast of hot stamping industry. Note that, initially the technology was only used for simple parts, such as side impact door beams. With improvements in the

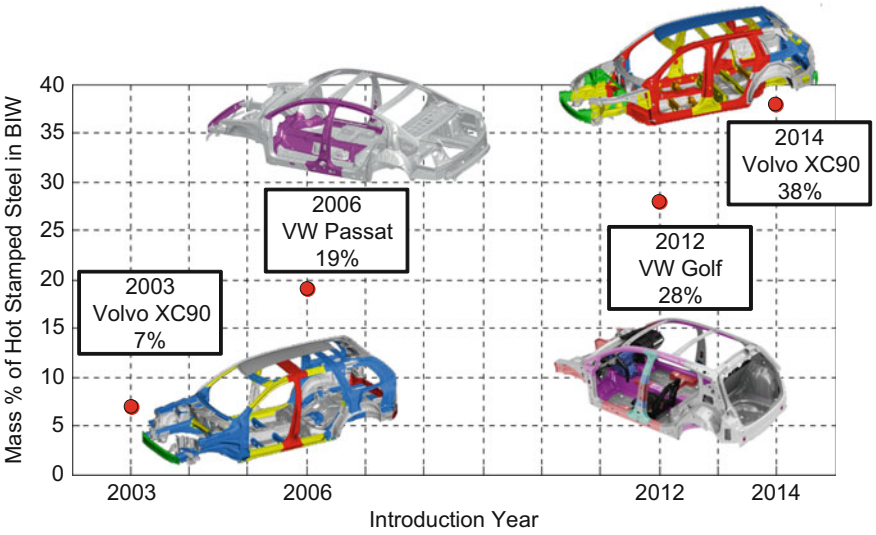

Fig. 3.16 Highest mass percentage of boron steels in automobiles by years (re-created after [9, 59–63])

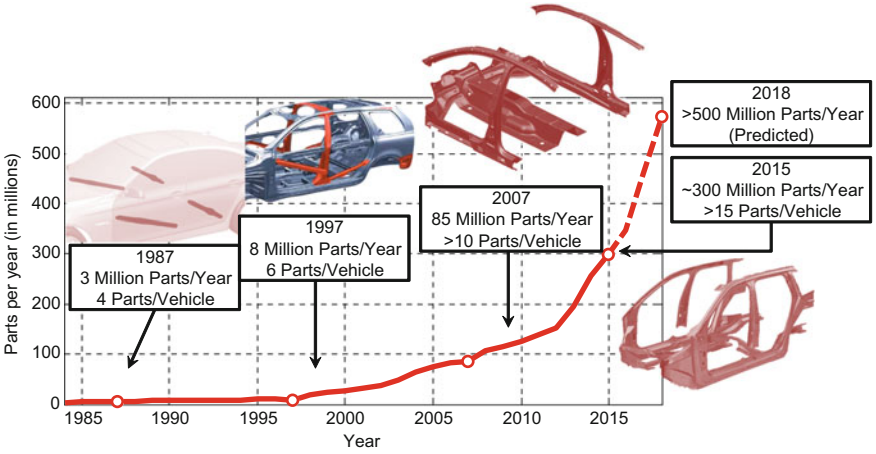

Fig. 3.17 Since its inception, both the complexity and production volume of hot stamped parts have been increasing (re-created after: [6, 44, 64–66])

technology, it has been used for transmission tunnels and subplates using tailored technologies. Currently, door rings and parts that are longer than 2 m (78 inches) can be hot formed [58, 67].

References

1. A. Shapiro, Finite element modeling of hot stamping. Steel Res. Int. **80**(9), 658–664 (2009)
2. R. Kolleck, Press hardening - materials and coatings. Presented at Schuler Hot Stamping Workshop, May 14, Dearborn, MI, USA (2013)
3. A.B. Norrbottens Jaernverk, Manufacturing a hardened steel article. Great Britain Patent, GB1490535 (1977)
4. G. Berglund, Boron steel history (2014)
5. SSAB, Corporate presentation (2014)
6. P. Fahlblöm, Analys för val av emballage system : en studie gjord för att underlätta valet av emballagesystem. Master's Thesis, Luleå University of Technology, Sweden (1997)
7. A. Ullberg, Address to SSAB's 2005 general meeting (2005)
8. H. Lanzerath, A. Bach, G. Oberhofer, H. Gese, Failure prediction of boron steels in crash, in *SAE Technical Paper* (SAE International, 2007), p. 4
9. H. Karbasian, A.E. Tekkaya, A review on hot stamping. J. Mater. Process. Technol. **210**(15), 2103–2118 (2010)
10. B.A. Behrens, Hot stamping, *CIRP Encyclopedia of Production Engineering* (Springer, Berlin, 2013)
11. X. Bano, J. P. Laurent, Heat treated boron steels in the automotive industry, in *39 th Mechanical Working and Steel Processing Conference* (1997), pp. 673–677
12. B. Fossati, A. Machado-Baglietto, M. Cappelaere, Hot stamping industrialization at Renault. Presented at Forming in Car Body Engineering 2014, September 24–25, Bad Nauheim, Germany (2014)

13. P.O. Marklund, L. Nilsson, S. Rahmn, M. Jonsson, T. Svantesson, L.O. Hellgren, Optimization of a press hardened B-pillar by use of the response surface method, in *SAE Technical Paper* (SAE International, 1999), p. 9
14. M. Jonsson, Pillar for a vehicle body, June 3 2003. US Patent 6,572,181 (2003)
15. J.K. Larsson, L. Hanicke, Multi-material approach with integrated joining technologies in the new Volvo S80, in *SAE Technical Paper* (SAE International, 1999), p. 9
16. L. Vaissiere, J.P. Laurent, A. Reinhardt, Development of pre-coated boron steel for applications on PSA Peugeot Citroën and Renault bodies in white, in *SAE Technical Paper* (SAE International, 2002), p. 7
17. H. Lehmann, Furnaces for press hardening. Presented at AP&T Press Hardening, Next Step Seminar, March 24, Shanghai, China (2010)
18. S. Sepeur, The company Nano-X GmbH: Products for the automotive industry. Presentation at Deutsche Börse, July 10th, Frankfurt, Germany (2006)
19. J. Staeves, Höherfeste stähle für die karosserie (high strength steels for car body - in German). Presented at Technical University of Munich, June 28th, Munich, Germany (2004)
20. P. Süß, M. Pfestorf, Press hardening at BMW. Presented at Insight Edition Conference, September 20–21, Gothenburg, Sweden (2011)
21. M. Kahl, Some like it hot. *Automotive Manufacturing Solutions* (2004), pp. 49–52
22. C. Cazes, F. Ronin, Use of HSS, VHSS and UHSS steels in the body in white: a panorama of the latest European vehicles, state of art and perspectives, in *SAE Technical Paper* (SAE International, 2002), p. 7
23. G. Plassart, G. Philip, Materials criteria selection and certification process for the body in white in PSA Peugeot Citroën, in *SAE Technical Paper* (SAE International, 2002), p. 7
24. A. Reinhardt, Development of hot stamped ultra high strength steel parts on the Peugeot 307 and the Citroën C5. Presented at EuroCarBody 2001 - 3rd Global Car Body Benchmarking Conference, Bad Nauheim, Germany (2001)
25. ThyssenKrupp, ThyssenKrupp Sofedit Le Theil (2006), https://www.thyssenkrupp.com/en/. Accessed 17 Feb 2012
26. M. Jonsson, Products in hot stamped boron steel, in Presented at Great Design in Steel 2005, March 3, Livonia, MI, USA (2005)
27. J. Bernquist, Safety cage design in the Volvo XC90. Presented at Great Design in Steel 2004, February 18, Livonia, MI, USA (2004)
28. U. Ekström, Gestamp acquires ssab hardtech. Presented at Press Release by SSAB Public Affairs, November 12, 2004 (2004)
29. Gestamp Corporacion, Cold forming & UHSS for lightweight steel applications. Presented at Uddeholm Automotive Tooling Seminar, February 5, Sunne, Sweden (2004)
30. D. Holzkamp, Recent developments on uhss welding and its simulation for prevention of heat distortion. Presented at Insight Edition Conference, September 20–21, Gothenburg, Sweden (2011)
31. M. Rehse, Flexible rolling of tailor rolled blanks. Presented at Great Designs in Steel, Livonia, MI, March 8th, 2006 (2006)
32. M. Pfestorf, The mixed material concept of the new BMW X5. Presented at Great Designs in Steel 2007, March 7, Livonia, MI, USA (2007)
33. E. Hilfrich, D. Seidner, Crash safety with high strength steels. Presented at International Automotive Congress, Oct. 30, Shengyang, China (2008)
34. M. Pfestorf, J. Rensburg, Functional properties of high strength steel in body in white. Presented at Great Designs in Steel, Livonia, MI, March 8th (2006)
35. A. Breuer, Optimizing parameters for hotformed tailored-blank applications. Presented at Great Designs in Steel 2015, May 13, Livonia, MI, USA (2015)
36. L. Brooke, H. Evans, Lighten up! *Automotive Engineering International* (2009), pp. 16–22
37. S. Hortlund, Accra, Linde+Wiemann. Presented at CHS 2015, Seminarium, October 7th, Luleå, Sweden (2010)
38. S. Maggi, C. Federici, F. D'Aiuto, TWIP Steel application on the Fiat Nuova Panda body. Presented at Materials in Car Body Engineering 2012, May 10–11, Bad Nauheim, Germany (2012)

39. T. Shiga, Challenge for light weight. Presented at CAR Management Briefing Seminars, August 4–7, Traverse City, MI, USA (2014)
40. B. Liesenfelder, The new Ford Fiesta. Presented at EuroCarBody 2008, October 21-23, Bad Nauheim, Germany (2008)
41. S. Nedic, H. Ljungquist, E. Hollander, The New Volvo XC60 Car Body. Presented at EuroCarBody 2008, October 21–23, Bad Nauheim, Germany (2008)
42. M. White, The new Jaguar XF car body. Presented at EuroCarBody 2008, October 18, Bad Neuheim, Germany (2008)
43. G. Heim, J.L. Perez-Freije, T. Jahn, The new Opel Meriva. Presented at EuroCarBody 2010, October 18–20, Bad Nauheim, Germany (2010)
44. B. Kandlbinder, The doors of the new BMW 5 Series sedan. Presented at Doors and Closures in Car Body Engineering 2010, November 16–17, Bad Nauheim, Germany (2010)
45. F. Martin, K. Latzel, Das Aluminumtürsystem des neuen A6 (the aluminum door system of the new A6 - in german). Presented at Doors and Closures in Car Body Engineering 2011, November 16–17, Bad Nauheim, Germany (2011)
46. K. Uejima, C. Beku, T. Onoe, The 2015 WRX STI. Presented at EuroCarBody 2014, October 21-23, Bad Nauheim, Germany (2014)
47. Daimler Global Media Site, http://media.daimler.com
48. Ferrari California (2008)
49. F. Wegert, A. Wanning, The best place on earth - the new vw golf cabriolet. Presented at EuroCarBody 2011, October 18, Bad Neuheim, Germany (2011)
50. G. Ast, M. Trabner, The New Mercedes-Benz SL 231. Presented at EuroCarBody 2012, October 16–18, Bad Nauheim Germany (2012)
51. A. Marsh, Hyundai Veloster bodyshell – what a challenge, http://www.autoindustryinsider.com/?p=3752. Accessed 21 Feb 2012
52. B. Ramirez, Media Launch: 2013 Veloster Turbo. Hyundai Motor North America Newsroom (2012)
53. T. Benderoth, E. Ignatiadis, Ford B-Max: easy access door system with integrated B-pillar. Presented at Doors and Closures in Car Body Engineering 2012, November 14–15, Bad Nauheim, Germany (2012)
54. D. Ludlow, Ford B-Max preview, http://www.expertreviews.co.uk/cars/51585/ford-b-max-preview. Accessed 23 Feb 2012
55. S. Birch, Aluminum range rover slims down by 420 kg. Automot. Eng. Int. **3**(9), 10–15 (2012)
56. Y. Terashima, Y. Takeshi, Nissan LEAF. Presented at EuroCarBody 2011, October 18–20, Bad Nauheim, Germany (2011)
57. I. Han, Chevrolet Spark & Spark EV. Presented at Great Designs in Steel, Livonia, MI, May 14th 2014 (2014)
58. H. Ljungqvist, K. Amundsson, O. Lindblad, The all-new Volvo XC90 car body. Presented at EuroCarBody 2014, October 21–23, Bad Nauheim, Germany (2014)
59. Volkswagen Media Services, http://www.volkswagen-media-services.com
60. H. Lindh, Strategic role of UHSS in the automotive industry and at Volvo Cars. Presented at Insight Edition Conference, September 20–21, Gothenburg, Sweden (2011)
61. C. Bielz, S. Heis, The new audi a3. Presented at EuroCarBody 2012, October 16–18, Bad Nauheim, Germany (2012)
62. R. Mattsson, Volvo car's press hardening strategy. Presented at AP&T Press Hardening, Next Step Seminar, September 19th, Dearborn, MI, USA (2012)
63. Volvo Car Group Global Media Newsroom, http://www.media.volvocars.com/
64. M. Oldenburg, Simulation methods for press hardening applications. Tutorial presented at 5th Intl. Conference on Hot Sheet Metal Forming of High Performance Steel, CHS2, June 2nd, Toronto, ON, Canada (2015)
65. R. Hund, M. Braun, Continuous improvement of hot forming technology, in *3rd International Conference on Hot Sheet Metal Forming of High Performance Steel, CHS2, Kassel, Germany* (2011), pp. 189–200

66. Schuler Pressen GmbH, Press hardening with PCH Flex – fast, flexible, cost-effective. Product/Service Brochure (2014)
67. A. Madsen, 2015 Acura TLX body structure review. Presented at Great Designs in Steel 2015, May 13, Livonia, MI, USA (2015)

Chapter 4
Blank Materials

Eren Billur and Hyun-Sung Son

Abstract All sheet metal forming operations start with the blank material. The final part properties are dependent on the incoming material properties and how they could be changed during the process. To engineer the final part, it is essential to understand the incoming blank material. This chapter discusses the most common 22MnB5 steel, and other steel grades already in use or proposed to be used in hot stamping processes. Incoming blank could be uncoated or coated. Coatings can affect the final properties due to scale formation, decarburization and by the presence of microcracks. In the last decade, tailored blanks have been used in a number of automotive applications. The last section of this chapter summarizes Tailor Rolled, Patchwork, Tailor Welded blanks, and their combinations.

4.1 22MnB5

Currently, most of the production and research is being done using 22MnB5 grade (Material number 1.5528). This is a low-carbon steel, with manganese and boron alloying. The chemical composition of 22MnB5 is given in Table 4.1. As delivered, the steel has a yield strength of approximately 400 MPa, UTS around 600 MPa and approximately 22% total elongation. After quenching, the material's yield strength exceeds 1000 MPa and UTS reaches 1500 MPa. The total elongation of the final part is typically over 5% [1–3] (Fig. 4.1).

E. Billur (✉)
Billur Makine Ltd., Ankara, Turkey
e-mail: eren@billur.com.tr

E. Billur
Atılım University, Ankara, Turkey

H.-S. Son
POSCO Global R&D Center, Incheon, South Korea
e-mail: hsson@posco.com

E. Billur (ed.), *Hot Stamping of Ultra High-Strength Steels*,
https://doi.org/10.1007/978-3-319-98870-2_4

Table 4.1 Chemical composition of 22MnB5 [4–6]

	C	Mn	B	Cr	Si	Al	Ti	N
Minimum	0.19	1.10	0.0008	0.10	0.00	0.02	0.015	0.000
Nominal	0.22	1.18	0.0020	0.16	0.22	0.03	0.040	0.005
Maximum	0.25	1.40	0.0050	0.35	0.40	0.08	0.050	0.010

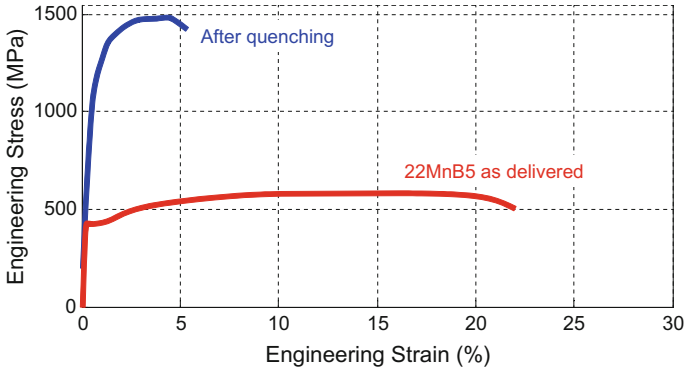

Fig. 4.1 Engineering stress–strain curves of 22MnB5, in as-delivered conditions and after quenching (re-created after [2])

This alloy has been commercialized by several names, including but not limited to:

- Ultralume by AK Steel, available as uncoated or Al/Si coated [7].
- USIBOR 1500 by ArcelorMittal, typically AlSi-coated steel produced and patented by ArcelorMittal. Zn-coated versions are also available by the name USIBOR 1500 GI or GA [8, 9].
- BR 1500 HS: by BaoSteel [10],
- BTR 165: uncoated steel by Benteler [11],
- SQ 1500: (Sumi-quench) by Nippon-Sumitomo [12],
- Hot Press Forming (HPF) 1470 by posco, available uncoated, AlSi coated or Zn (GI) coated [13, 14]
- Docol 1500 PHS: uncoated steel by SSAB, earlier named as Docol 1500 Bor [15, 16]
- MBW1500: Mangan-Bor-Stähl zum Warmumformung, literally meaning manganese-boron steel for hot form hardening, produced by ThyssenKrupp. Available uncoated or AlSi coated (MBW1500+AS) [17]. There was a ZnNi-coated version [18] which was later discontinued [19, 20].
- phs-ultraform 1500: Zn-coated steel by voestalpine [21]
- WHT1500HF: uncoated steel by Wisco [22].[1]

[1] Steel companies are listed alphabetically.

4.2 Higher Strength Steels (>1700 MPa)

Mn-B alloyed steels have been long available in hot-rolled (i.e., thick blanks) and uncoated conditions for agriculture and construction machinery industries [23]. Chemical compositions of several standard Mn-B and Mn-B-Cr alloyed steels that have higher carbon than 22MnB5 are tabulated in Table 4.2 [1, 6].

Mn-B alloyed steels are typically delivered in soft, ferritic-pearlitic condition. First, they have to be austenitized in an atmosphere controlled furnace. Once quenched, their strength levels are at least doubled, as listed in Table 4.3. Steels with higher carbon level than the most common 22MnB5 typically have higher strength. These grades may save even more weight, with equivalent intrusion resistance [12, 24, 25]. For hot stamping applications, some of the steels listed in Tables 4.2 and 4.3 are slightly modified and commercialized under different names.

Table 4.2 Chemical compositions (wt-%) of higher strength Mn-B and Mn-B-Cr steels (trace amounts of other elements, balance Fe) [1, 4, 6]

Steel	(Mat'l number)	C	Mn	B	Cr
27MnCrB5	(1.7182)	0.25	1.24	0.002	0.34
28MnB5		0.28	1.30	0.005	–
30MnB5	(1.5531)	0.30	1.30	0.005	–
33MnCrB5	(1.7185)	0.33	1.35	0.005	0.45
34MnB5		0.34	1.30	0.005	–
37MnB4	(1.5537)	0.33	0.81	0.001	0.19

Table 4.3 Yield and Ultimate Tensile Strength of several quenchable steels before and after quenching [1, 4, 6]

Steel	As delivered		Quenched	
	Yield stress MPa (ksi)	UTS MPa (ksi)	Yield stress MPa (ksi)	UTS MPa (ksi)
27MnCrB5 (1.7182)	478 (69)	638 (93)	1097 (159)	1611 (234)
28MnB5	420 (61)	620 (90)	1135 (165)	1740 (252)
30MnB5 (1.5531)	510 (61)	700 (90)	1230 (165)	1740 (252)
33MnCrB5 (1.7185)	420 (61)	620 (90)	1290 (187)	1850 (268)
34MnB5	600 (87)	820 (119)	1225 (178)	1919 (278)
37MnB4 (1.5524)	580 (84)	810 (117)	1378 (200)	2040 (296)

For example, ArcelorMittal has been developing a steel grade similar to 34MnB5, commercially named as USIBOR® 2000P, which is currently under customer trials. This grade will be available with AlSi coating [8, 31]. Baosteel is also preparing a 1800 MPa steel [13].

Mazda has become the first vehicle manufacturer to use higher strength boron steels. The CX-5 (SOP 2011) has 1,800 MPa (~260ksi) tensile strength reinforcements in front and rear bumpers, Fig. 4.3. According to Mazda, the new material saved 4.8 kg (~10.6lbs.) per vehicle. The material was supplied by Sumitomo Metals (SumiQuench 1800, SQ1800 as shown in Fig. 4.2, modified 30MnB5) and hot stamped at a facility of Aisin Takaoka, both in Japan [12, 32]. Figure 4.4 shows the comparison of bumper beams with SQ1500 and SQ1800. With the higher strength material, it was possible to save 12.5% weight with equal performance [12].

Posco has already demonstrated HPF 2000 steel in a number of component-based examples, and also in the Renault EOLAB concept car [28, 33]. Since 2016, Posco has also been developing a 1800 MPa grade [14]. SSAB has already commercial-

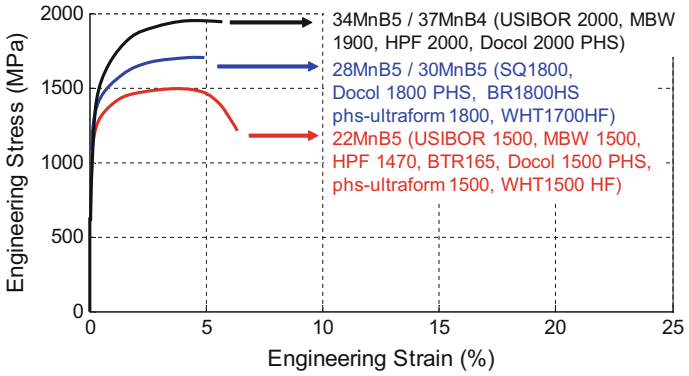

Fig. 4.2 Engineering strain–stress diagram for 22MnB5 and higher strength boron steels (re-created after: [12, 24, 26–30]. Note that some of these grades may not be commercially available

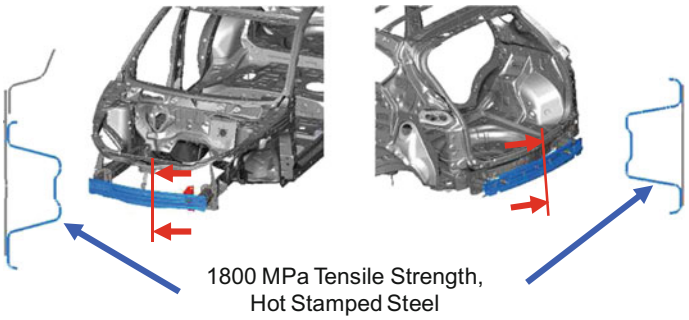

Fig. 4.3 Bumper beam reinforcements of Mazda CX-5 (SOP 2011) are the first automotive applications of higher strength boron steels [32]

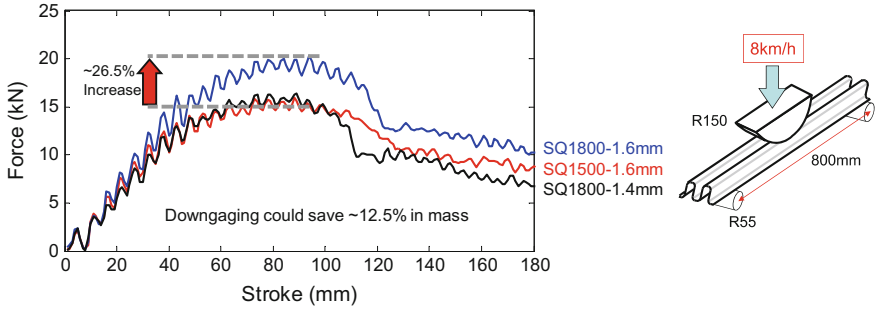

Fig. 4.4 Comparison of bumper beams with SQ1500 and SQ1800 (re-created after [12])

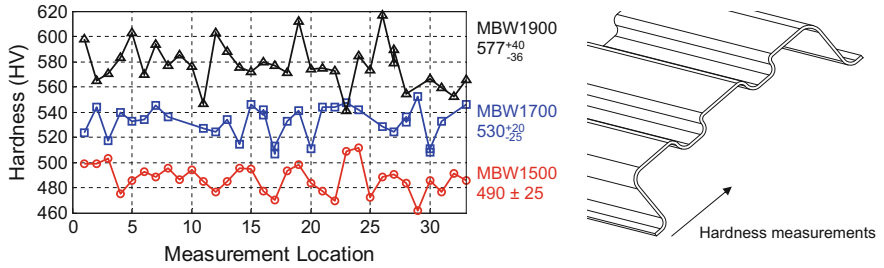

Fig. 4.5 Hardness distribution of an impact beam using ThyssenKrupp Mn-B steels (re-created after [18, 26])

ized uncoated Docol PHS 1800 (∼30MnB5) and is preparing Docol PHS 2000 [34]. ThyssenKrupp has demonstrated that an MBW® 1900 B-pillar with correct properties can save 22% weight compared to DP600 and yet costs 9% less than the original dual-phase design [35]. Ford had also demonstrated that by using MBW1900 instead of 22MnB5, a further 15% weight could be saved [24]. Another grade in development by ThyssenKrupp was MBW® 1700 (28MnB5). Figure 4.2 shows MBW® 1900 (34MnB5) tensile data, compared with MBW® 1700 (28MnB5) and MBW® 1500 (22MnB5), with commercial names from other suppliers as well [27]. Voestalpine has already commercialized phs-ultraform 2000 [36].

Table 4.4 summarizes commercially available and under development steel grades, designed for hot stamping applications.

Vickers Hardness (HV) values for conventional 22MnB5 steel are in the order of 450–500 HV after quenching. 37MnB4, on the other hand, has a Vickers Hardness of 600–610 HV [4]. Similarly, Overrath et al. [26] found ∼490 HV for MBW® 1500, ∼530 HV for MBW® 1700 and ∼580 HV for MBW® 1900, as shown in Fig. 4.5. ThyssenKrupp has commercialized MBW® 1900 in 2013 [42]. MBW 1700 has not been commercialized yet [43].

Problems with higher strength materials are (1) their low toughness/energy absorption (i.e., typically even lower elongation than 22MnB5, see Fig. 4.2), (2) delayed

Table 4.4 Chemical compositions, final properties, and commercial availability of >1700 MPa steels specifically designed for hot stamping applications [12, 14, 27, 31, 34, 36–41]

Steel[a]	Chemical Composition (%wt)				Yield	Tensile	Elongation	Bending	Availability		
	C	Mn	B	Nb	(MPa)	(MPa)	(%)	Angle	U/C	AlSi	Zn
USIBOR 2000	0.37	1.4	0.005	–	≥1400	≥1800	≥3	≥45°	–	+	–
BR1800 HS	–	–	–	–	≥1200	≤1800	≥5	–	–	–	–
SQ 1800	0.30	1.8	0.002	0.08	1267	1882	7.6	–	–	+	–
HPF 1800					≥1200	≥1750	≥6	–	*	+	–
HPF 2000					≥1300	≥1900	≥5.5	–	*	–	–
Docol 1800 PHS	0.27–0.33	1–1.35	≤0.005	–	1300	1800	6	–	+	–	–
Docol 2000 PHS	0.36–0.42	1.15–1.45	≤0.005	–	1700	2000	3.7	–	*	–	–
MBW 1700	0.26–0.30	1.15–1.45	≤0.005	–	~1150	≥1700	≥4	–	–	–	–
MBW 1900	0.32–0.38	1.0–1.4	≤0.005	–	≥1200	≥1900	≥4	55–65°	+	–	–
phs-ultraform 2000	0.20–0.36	≤2.0	≤0.005	≤0.01 (incl. Ti)	≥1100	≥1800	≥5	≥45°	–	–	+

*Under development

[a]Steel companies are listed alphabetically

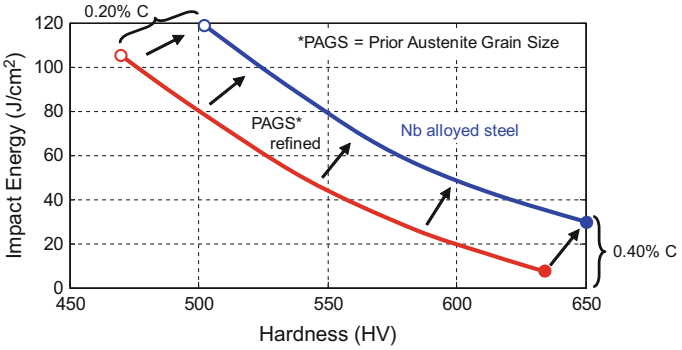

Fig. 4.6 Energy absorbing capacity decreases with increased hardness. If "Prior Austenite Grain Size" (PAGS) can be refined, significant improvements can be achieved [re-created after [41, 42]]

cracking and (3) weldability [12]. Delayed cracking is investigated in Sect. 6.19 and weldability in Chap. 7.

Naderi [4] noted that, during tensile test of 37MnB4 (UTS = 2040 MPa, 296 ksi), all of the hardened tensile samples were cracked out of the gage length. One possible way to improve the toughness (energy absorbing capacity) of higher strength steels is grain refinement. Wang et al. had shown that as the "prior austenite grain size" (PAGS) of a high-strength steel is reduced, both the strength and elongation values are improved. Thus, the toughness is improved [44]. Figure 4.6 shows energy absorption of martensitic steels with hardness between 450–650 HV - in the range of most hot stamping grades. When Nb alloying is introduced, the toughness is increased through PAGS refinement [41].

4.3 Higher Elongation/Energy Absorbing Materials

Since hot-stamped parts are extremely strong, but do not absorb much energy, they are mostly used where intrusion resistance is required. However, lately, there are new materials for hot stamping which have higher elongation (ductility) compared to 22MnB5. Thus, these materials can save weight where energy absorption is required.

These new grades can be investigated in two different strength levels:

(1) 450–600 MPa tensile strength level and >15% total elongation and
(2) 1000–1300 MPa tensile strength level and >5% total elongation.

ArcelorMittal has been developing 4 new materials, as shown in Table 4.5. Figure 4.7 shows the approximate engineering strain–stress diagrams of USIBOR 1500 (22MnB5), DUCTIBOR 1300 and 500. There is also research going on laser welding DUCTIBOR grades to USIBOR grade material to combine intrusion resis-

Table 4.5 Higher elongation hot stamping materials, developed by ArcelorMittal [8, 31, 47]

Product name	Yield strength MPa (ksi)	Tensile strength MPa (ksi)	Elongation (%)	Status
DUCTIBOR 450	340–460 (50–65)	460–610 (65–90)	≥16	Industrial
DUCTIBOR 500	370–470 (55–70)	550–700 (55–100)	≥16	Industrial
DUCTIBOR 1000	≥800 (≥115)	≥1000 (≥145)	≥6	Customer testing
DUCTIBOR 1300	≥950 (≥135)	≥1300 (≥190)	≥5	n/a

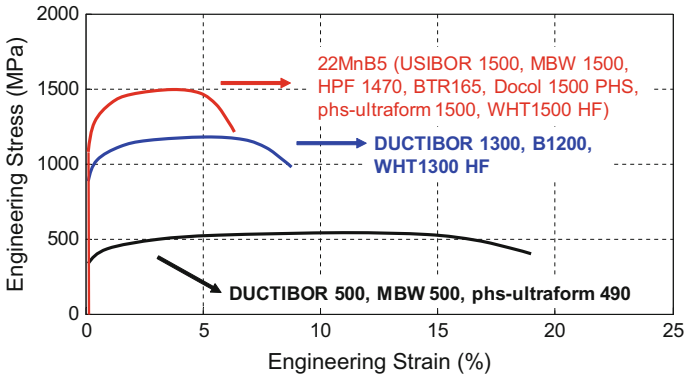

Fig. 4.7 Comparison of 22MnB5 with high elongation grades [8, 10, 43, 49, 52]

tance and energy absorption properties. For details of these studies, see Sect. 8.2.1 [8, 45]. Since 2015, several Fiat models have a rear rail with Ductibor 450 [46].

ThyssenKrupp and voestalpine have also developed 500 MPa (~75 ksi) grades with the commercial names MBW® 500 and phs-ultraform 490, respectively. Production of MBW® 500 started in January 2012. Since 2014, Volvo is using MBW500 steel in the new XC90 in energy absorbing areas [48]. Since then, ThyssenKrupp also developed MBW® 600 [43], voestalpine rolled phs-ultraform 490, which is available with Zn coating, in February 2013 [49].

For crashworthiness, bending angle may be a more important indicator compared to total elongation [50]. Thus, bending angles are also reported in the summary of 450–600 MPa steels is given in Table 4.6.

In 1000–1300 MPa tensile strength grades, BaoSteel has commercialized B1200 steel since 2013. This steel has minimum 900 MPa yield, 1200 MPa tensile strength when quenched properly and can still have 7% uniform elongation [10]. WISCO has also commercially available 1300 MPa grade, WHT 1300 HF [22, 53]. As of 2017, Ductibor 1000 is under customer testing, and there are no updates about Ductibor 1300 [31] (Table 4.7).

Table 4.6 Chemical compositions, final properties, and commercial availability of 450–600 MPa steels [31, 43, 49, 51]

Steel[a]	Chemical Composition (%wt)				Yield (MPa)	Tensile (MPa)	Elongation (%)	Bending Angle	Availability		
	C	Mn	B	Si					U/C	AlSi	Zn
Ductibor 450	≤0.11	≤1.1	≤0.001	≤0.06	≥350	≥460	≥16	≥120°	–	+	*
Ductibor 500	≤0.1	≤1.3	≤0.001	≤0.5	≥400	≥550	≥16	≥120°	–	+	–
MBW® 500	≤0.10	≤1.0	≤0.005	≤0.35	≥400	≥550	≥17	≥140°	–	+	–
MBW® 600	≤0.10	≤2.0	≤0.005	≤0.5	≥450	≥650	≥16	–	–	+	–
phs-ultraform 490	≤0.11	≤1.4	–	≤0.5	≥340	≥460	≥12	≥120°	–	–	+

[a]Steel companies are listed alphabetically

Table 4.7 Chemical compositions, final properties and commercial availability of 1000–1300 MPa steels [22, 31, 54, 55]

Steel[a]	Chemical Composition (%wt)				Yield	Tensile	Elongation	Bending	Availability		
	C	Mn	B	Si	(MPa)	(MPa)	(%)	Angle	U/C	AlSi	Zn
Ductibor 1000	≤0.12	≤2.0	≤0.005	≤0.06	≥800	≥1000	≥6	≥80°	–	+	–
BR1200 HS	0.16–0.20	1.0–1.5	≤0.0030	≤0.40	≥900	≥1200	≥8	–	+	–	–
WHT1300 HF	0.2	1.15	≤0.005	0.24	≥950	≥1300	≥8	–	+	–	–

[a]Steel companies are listed alphabetically

4.4 Other Steels for Hot Stamping

In the last few years, new steels are also considered for hot stamping process. Although these are not in mass production yet, research and development were done on hot stamping of:

(1) Stainless steels,
(2) Medium-Mn steels (including steels with higher Mn content compared to 22MnB5),
(3) Sandwich materials.

4.4.1 Stainless Steels

Aperam and Outokumpu have already demonstrated stainless steel grades that can be formed in the current hot stamping lines. Aperam's method is to get almost 100% martensitic structure, whereas Outokumpu recommends duplex (Austenite + Martensite) microstructure after hot forming and quenching [56, 57]. Stainless steels are corrosion resistant by their nature in service conditions. They also do not require a special coating or controlled atmosphere at hot conditions [58].

Aperam has already developed three different steels for hot stamping, one for intrusion resistance applications and two for energy absorbing areas. The chemical compositions and mechanical properties are tabulated in Table 4.8. According to Herbelin, almost 100% martensite can be formed at very low cooling rates (as low as 1 °C/s, as shown in Fig. 4.8), thus parts produced with this steel could be air hardened [58]. The low critical cooling rate allows the part to be formed in a multistep operation (Fig. 4.22) [59].

Outokumpu has shown that Nirosta 1200 PH grade can be hot formed, which would have 1100–1300 MPa yield and 1700–1850 MPa tensile strength, combined with 12–16% total elongation after quenching (see Table 4.8) [56]. The material can save weight both in intrusion resistance components and energy absorbing components, since it can absorb three times the energy 22MnB5 can absorb. Figure 4.9 shows the comparison of Nirosta 1200 PH and 22MnB5. This material is classified as duplex stainless steel, as it contains austenite and martensite.

4.4.2 Medium-Mn Steels

Medium-Mn steels are being developed both for cold and hot stamping applications. There are several advantages of medium-Mn steels over 22MnB5 in hot stamping:

(1) Austenitization temperature is typically lower than 22MnB5 and decreases with increasing Mn content. This could reduce the energy requirement of the furnaces and save energy and cost (see Fig. 4.11) [62, 63].

Table 4.8 Chemical compositions and final properties (after hot stamping and quenching) of stainless steels designed for hot stamping [56–58, 60, 61]

Steel[a]	Chemical Composition (%wt)					Yield	Tensile	Elongation	Bending
	C	Mn	Cr	Ni	Others	(MPa)	(MPa)	(%)	Angle
MaX 1.2	0.10	0.4	12	0	Nb	>800	~1200	>10	>65°
MaX 1.2 HY	0.06	+	11	0.5	Nb	>800	~1200	~10	>95°
MaX 2	0.2–0.25	>0.3	13	0–2	Nb	>1000	~1800	~10	–
H1200 PH	0.43–0.5	<1.0	13.5±1	0	–	1100–1300	1700–1850	12–16	–

[a]Steel companies are listed alphabetically

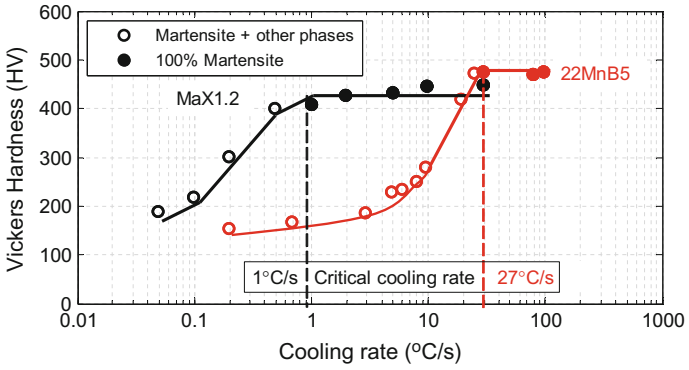

Fig. 4.8 Critical cooling rate comparison of MaX 1.2 and 22MnB5 (re-created after: [58])

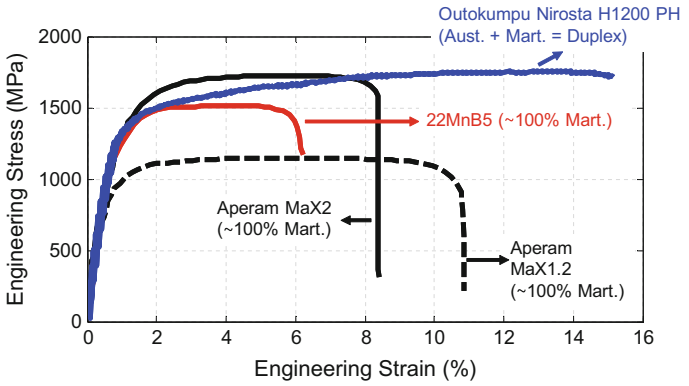

Fig. 4.9 Comparison of 22MnB5 with potential new hot stamping stainless steel grades. All curves shown here are after hot stamping and quenching (re-created after: [56, 58])

(2) Martensitic transformation can occur at very low cooling rates and thus simple dies could be built for hot forming of these grades, as they could be air hardened. They can also be formed in multistep operations. Martensite start/finish temperatures are also lower than 22MnB5 [64, 65].

(3) Some retained austenite may be present in the final part. Medium-Mn steels, when properly hot stamped, may have high strength and high elongation. For example, tensile strength of 1800 MPa could be achieved with 10% total elongation, similar to the high yield strength medium-Mn steel shown in Fig. 4.10 [62]. Yi et al. achieved 1880 MPa tensile strength with 16% total elongation [66]. Rana et al. studied a number of heat treatment conditions with a 10 wt.% Mn steel and achieved 1330-1450 MPa tensile strength with 16–25% total elongation [67].

Recently, BaoSteel has shown two medium-Mn grades for hot stamping applications. One of these steels was designed for intrusion resistance applications and have high yield strength, in the order of 1000–1050 MPa (~145–150 ksi). As shown in

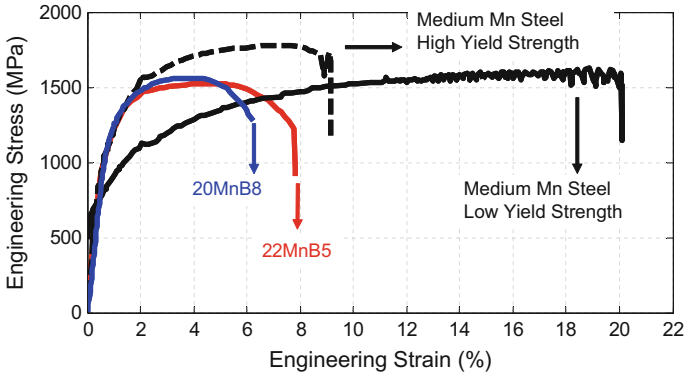

Fig. 4.10 Engineering stress–strain curves of 20MnB8, 22MnB5, and medium-Mn steels (re-created after: [20, 30, 62])

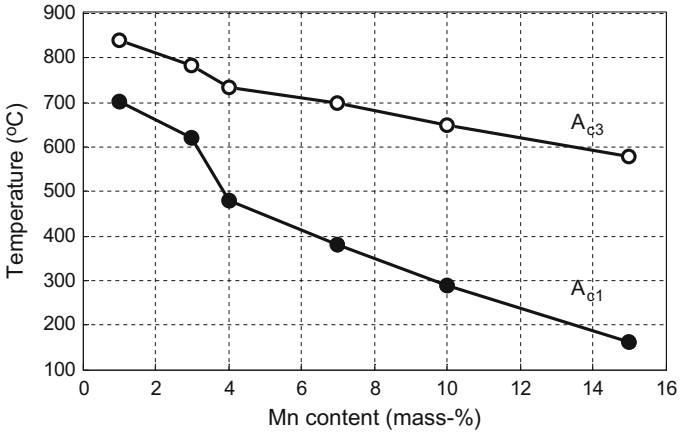

Fig. 4.11 Effect of Mn content on equilibrium transformation temperatures (re-created after: [62])

Fig. 4.10, the low yield strength version has 20% total elongation and approximately 1500 MPa (215 ksi) tensile strength. The chemical compositions were not published yet, but the austenitization temperatures were listed as 750–850 °C (~1350–1600 °F) [30].

Han et al. have calculated the austenitization temperatures using ThermoCalc software [62]. As shown in Fig. 4.11, the furnace temperature can be reduced with increased Mn content. A study funded by the EU for energy efficient hot stamping has shown that a typical industrial furnace consumes 32 m^3/h gas for mass production 22MnB5 at furnace temperature of 930 °C. When the furnace temperature was reduced to 808 °C the consumption went down to 19 m^3/h and at 785 °C it was as low as 17 m^3/h [63]. Thus, a medium-Mn steel may save energy in the life cycle assessment (Table 4.9).

Table 4.9 Chemical compositions and final properties (after hot stamping and quenching) of medium-Mn steels designed for hot stamping [56–58, 60, 61]

Reference	Chemical Composition (%wt)				Yield (MPa)	Tensile (MPa)	Elongation (%)
	C	Mn	B	Others			
20MnB8 [68]	0.195	1.98	0.003	Ti, Cr,…	>1000	~1500	>8
BaoSteel [30] Low Yield Strength	n/a	n/a	n/a	n/a	690	1620	20.0
BaoSteel [30] High Yield Strength	n/a	n/a	n/a	n/a	1045	1770	9.2
BaoSteel [30] Medium-Mn [62]	0.1–0.2	5–12	0	Ti+V	>900	~1800	~10
Medium-Mn [64]	0.22	4–7	0.0024	Ti	1220	1519	>11.8

Manganese alloying reduces martensite start–finish temperatures (M_s and M_f) and also retards bainite formation. For 20MnB8 (2.0%-wt. Mn), the critical cooling rate is around 20 °C/s (36 °F/s) [68]. In medium-Mn steels (4–7%-wt. Mn), even 10 °C/s (18 °F/s) could be sufficient for 100% martensitic transformation [64].

4.4.3 Steel Composites

ThyssenKrupp has been developing a family steel composites, called TriBond ®, since 2006 [69]. Here, three slabs (one core material and two cladding layers) are surface prepared, stacked on top of each other, and welded around the edges. Initially, TriBond ® was designed for wear-resistant cladding and ductile core materials [69].

In 2014, the original composite was modified for hot stamping. The core material was 22MnB5 and the thinner cladding layers were ductile material (MBW 1500 and MBW 500 respectively), as shown in Fig. 4.12. Coilmaking process was also slightly modified: after hot rolling, the slabs were then cold rolled, annealed, and aluminum coated [70]. As tabulated in Table 4.10, there are currently two planned versions of Tribond with approximately 1200 and 1400 MPa tensile strength (~175 and 205 ksi respectively). Both grades have higher bending angles compared with 22MnB5 after quenching [71].

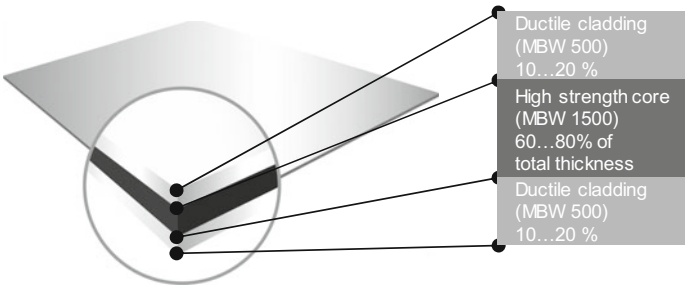

Fig. 4.12 Schematic view of Tribond®grades (re-created after [72])

Table 4.10 Through thickness compositions and final properties of ThyssenKrupp hot forming composites [17, 51, 71]

Steel	Through thickness composition	Yield (MPa)	Tensile (MPa)	Elongation (%)	Bending Angle
MBW 500+AS	100% MBW500	≥400	≥550	≥17	140–155°
MBW 1500+AS	100% MBW1500	≥1000	≥1400	>5	≥55°
TRIBOND®1200+AS	20% MBW500 60% MBW1500 20% MBW500	≥730	≥1100	>5	≥135°
TRIBOND®1400+AS	10% MBW500 80% MBW1500 10% MBW500	≥890	>1300	>5	≥75°

4.5 Coatings

As discussed in Chap. 3, uncoated boron steels suffer from scaling, which adds up another manufacturing step of descaling. Coating the blank does not only solve the scaling problem, but also improves protection against corrosion and reduces the risk of decarburization [21, 73].

If the steel's surface is not coated and exposed to high-temperature atmosphere, oxygen and other oxidizing gases react with the steel. Thus, scale forms on the surface—an oxide layer, typically composed of Fe_3O_4 [74]. The scale must be cleaned by sandblasting after hot forming process [1].

Another phenomenon happening during high-temperature heating is "surface decarburization". If the conditions are favorable for iron (Fe) to oxidize, it may also be possible for carbon (C) to be oxidized as well. If the carbon is oxidized to produce gaseous carbon monoxide and/or carbon dioxide (CO and/or CO_2), a layer close to the surface would lose their carbon content [76]. As discussed in earlier sections, carbon is one of the most important alloying element affecting the final hardness. Choi and De Cooman studied the effects of decarburization of uncoated 22MnB5 steel. They found that the depth of decarburization layer increases with time, until the oxide layer forms a barrier between the steel and atmosphere. As the carbon is depleted in near-surface regions, the hardness is lowered (Fig. 4.13a) [50]. Decarburization is usually undesirable since it lowers the strength/hardness and may affect fatigue life [77]. However, in the case of 22MnB5, lower carbon layers close to the surface creates a composite with high-strength core and ductile layers, similar to the one explained in previous subsection. As a result, bendability may improve with decarburized layers, as shown in Fig. 4.13 [50].

Belanger [78] estimated that only 38% of hot stamped components in auto-body will be in dry areas. Therefore, high cathodic protection is required in 62% of hot-stamped components. Currently, most coated boron steels sold are AlSi coated, which only offer barrier corrosion protection. Zn-based coatings are favored for their cathodic protection, but may require indirect hot stamping followed by an additional surface cleaning process, such as sandblasting [79]. Table 4.11 is a summary of coatings available in the market and/or proposed for hot stamping.

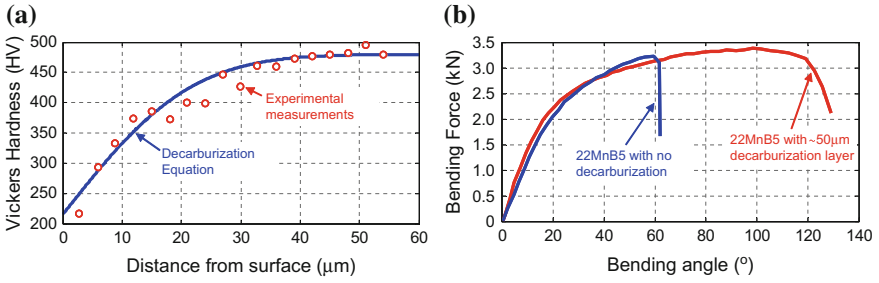

Fig. 4.13 **a** As the surface layers lose carbon (Decarburization), their hardness is lowered, **b** bendability may be improved by decarburized layers (re-created after [50, 75])

Table 4.11 Coatings available for hot stamping blanks [1, 3, 8, 21, 74, 80–85]

Coating type (commercial name)	Thickness and chemistry (before/after quenching)	Advantages	Disadvantages
Uncoated (22MnB5, BTR165)	N/A	• Cost	• No corrosion protection, • Scale formation, • Decarburization
AlSi (ArcelorMittal USIBOR, ThyssenKrupp MBW + AS)	AS 150 (150 g/m^2) 25 μm AlSi / 40 μm AlSiFe	• No scale formation, • Barrier corrosion protection	• No cathodic protection, • Only applicable for direct hot stamping
	AS 80 (80 g/m^2) 13 μm AlSi / 20 μm AlSiFe	• Shorter time in furnace	
Zn (voestalpine phs-ultraform GI)	10 μm Zn / 20 μm ZnFe	• Cathodic protection, • Applicable to both direct and indirect hot stamping.	• Surface conditioning may be required, • Risk of LMAC
ZnNi (ThyssenKrupp GammaProtect)	~10 μm ZnNi / 20–25 μm ZnNiFe	• Fast heating possible, • Low friction coefficient (Fig. 4.14a), • Applicable to both direct and indirect processes	• Risk of LMAC.
Al-Zn (Galvalume)	Not a Standard Coating	• Weldable and has good paint adhesion, • Better corrosion protection than GA	• May require a preheating to 550–730 °C, • May result in microcracks.
Zn-Al-Mg	Not a Standard Coating	• Best corrosion protection, • Can be applied as a postprocess coating.	• Risk of LMAC
(Henkel Bonderite S-FN 7500 PH) Coil Coating	2–3 μm	• Fast heating possible, • Weldable without sandblasting	• Coil Application
Al particles, graphite and wax in inorganic–organic matrix (Nano-X x-tec CO 4020 coil coating)	7 μm Al	• Fast heating possible, • Low friction coefficient (Fig. 4.14b) • Easy to apply (Fig. 4.23) • Room Temp. curing	• Has to be removed before painting/welding, • Coil Application
Al in inorganic matrix (Nano-X Alsi 4001 coil coating)	2–3 μm	• Spot weldable, • Suitable for e-coat	• No cathodic protection, • Coil Application, • High temp. curing

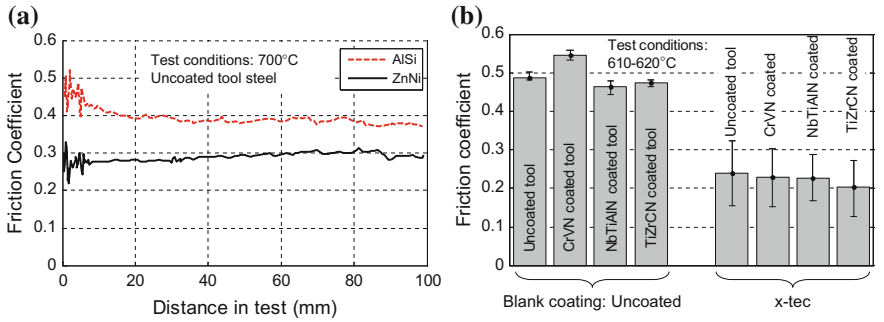

Fig. 4.14 Friction coefficients of: **a** AlSi and ZnNi at 700 °C (~1300 °F), **b** uncoated and x-tec coated blanks versus several tool coatings tested at 620 °C (~1150 °F) (re-created after [86, 87])

Blank coatings and the way they are heat treated have great influence on friction during stamping and the final part quality. Friction coefficient of several coatings and uncoated steels are given in Fig. 4.14 [86, 87]. Other important expectations from the coating are:

(1) weldability,
(2) compatibility with e-coating and paint baking cycles, and
(3) corrosion protection [85].

Although uncoated blanks are still used in automotive applications, there are different coatings available on the market, which could be classified under three main types [82]:

(1) Al-based coatings.
(2) Zn-based coatings.
(3) Varnish coatings.

4.5.1 Aluminum-Based Coatings

Aluminum-based hot stamping coating was first developed by Usinor, a French steel-maker that was later merged to Arcelor, and then to ArcelorMittal. The first pre-coated steel parts were used in Citroën C5 in 2001 [88–90].

The most common coating used in the recent years is 150 g/m^2 AlSi coating. This is equivalent to 25 μm coating thickness before heating. The typical composition is 7–11% Si (nominal 10%) and balance Al. Si is added to form ductile layers in the coating. In the absence of Si, the coating would be very hard but also brittle. Once the pre-coated blank is heated, iron diffusion takes place and forms a 40 μm thick AlSiFe of 5 layers, as shown in Fig. 4.15 [8, 82, 85, 91, 92].

The iron diffusion is a time-dependent process. If the diffusion is not completed (short heating time) the layers would not form as shown in Fig. 4.16a. In a typical process, the blank is kept in the furnace for 5–6 min.s (300–360 s). Layers of coating

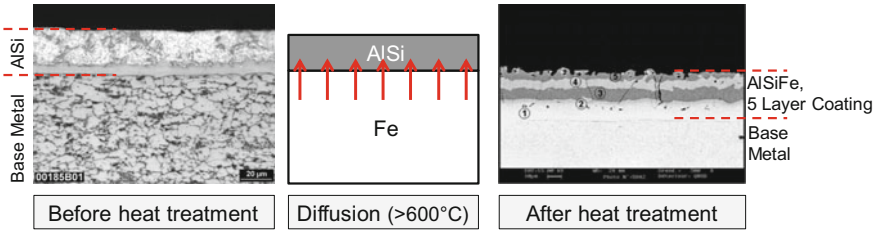

Fig. 4.15 During heat treatment, Fe diffuses from the base steel to the coating and forms AlSiFe coating (re-created after [95])

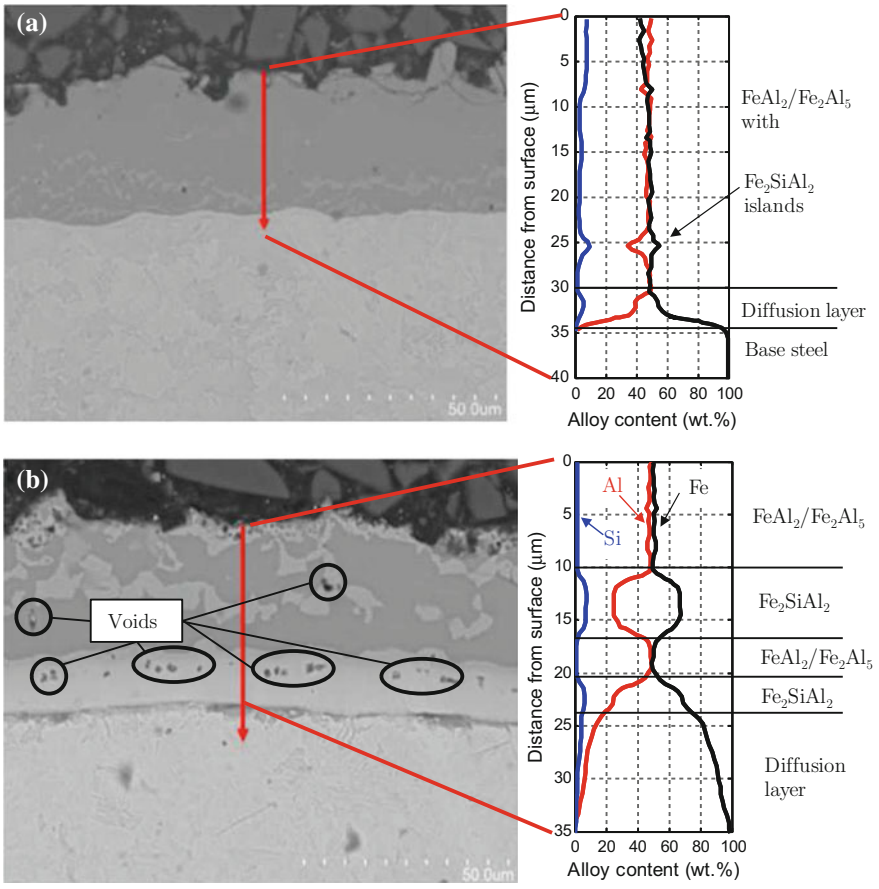

Fig. 4.16 Coating diffusion after: **a** 2 min, and **b** 6 min, in roller hearth furnace set at 930 °C (1700 °F) (re-created after [82, 93, 96])

after 6 min in the furnace can be seen in Fig. 4.16b, for a 1.2 mm thick AS150-coated steel [93]. If the blank is heated for longer durations, (1) more voids may occur which increases the porosity of the coating, (2) the total thickness of the coating increases and (3) Fe_2Al_5, $FeAl_2$, and Fe_2SiAl_2 layers disappear and the coating becomes a single layer of α-iron with Al and Si in solid solution [8, 82, 94]. The coating diffusion is extremely important for most applications as it will affect:

(1) weldability of the final part and
(2) surface properties for painting [91].

AlSi coatings successfully prevent scale formation and decarburization even without an atmosphere controlled furnace. The coating provides barrier corrosion protection. As a disadvantage, these coatings cost more compared to uncoated blanks and require a longer time in the furnace. The total time in furnace is equal to the sum of heating and dwell times, and depends on three variables [21, 95, 97]:

(1) The initial blank thickness: heating time to ensure austenitization.
(2) The type of coating: AlSi coating requires a maximum 12 °C/s, as it will melt over this rate.
(3) The initial coating thickness: dwell time to ensure coating diffusion.

AlSi-coated steels cannot be cold formed (as in indirect hot stamping) as the Fe–Al intermetallic coating is very hard (>600 HV) and brittle during cold deformation. The brittleness of the coating is also critical for the parts produced as their coatings could be damaged in service. Fan and De Cooman showed that the coating could crack easily but the cracks would not propagate to the diffusion layer [82]. For this reason, the thickness of the diffusion layer is critical and has to be controlled. This can be done by controlling the furnace temperature and dwell time [97].

The typical AlSi coating weighs 150 g/m^2. In 2013, ArcelorMittal developed USIBOR 1500 P AS80 with 80 g/m^2 AlSi coating. There were two rationales behind this development [98]:

(1) Lower cost, to be more competitive.
(2) Reduced coating weight would reduce the heating/dwell time in furnace.

Alden [99] has shown that the furnace dwell time could in practice be halved with AS80. Windmann et al. found that the dwell time required to form a single layer coating (which has to be avoided) was 20 min for AS80 and 40 min for AS150 [94]. Both studies prove that the dwell time could be reduced. On the other hand, Fujita [100] has shown that hot-formed steel with AS80 coating had approximately twice the blister width after cyclic corrosion test. Thus, the corrosion resistance is also halved with AS80 coating.

4.5.2 Zinc-Based Coatings

AlSi coating provides limited corrosion protection—"barrier protection"—as AlSi coating forms a barrier between the oxidizing environment and the bare steel. How-

ever, most of the car body components are already zinc coated. Thus, a similar level of corrosion protection may also be required in hot-stamped components [101].

Most Zn-based coatings have problems associated with "Liquid Metal Assisted Cracking (LMAC)". This phenomenon occurs when the coating is in liquid phase (melting point of zinc is around 420 °C ∼ 790 °F which is much lower than the forming temperatures in hot stamping) and stress is applied to the base metal, which cannot be avoided during metal forming. When both conditions are met, the liquid coating may penetrate into the base metal, causing cracks on the surface, as seen in Fig. 4.19.

To avoid LMAC, Zn-based coated steels were typically indirect hot stamped—where Zn is in solid phase. Indirect hot stamping could be through two different methods [1, 101]:

1. Cold deformation (most of the deformation is done in cold state) followed by hot calibration (very little deformation in hot state).
2. 100% of deformation, cutting, and piercing done at cold forming followed by a "form hardening" (where no deformation is done at hot state).

BMW 7 Series (F01, SOP 2008) was the first car to have Zn-coated hot stamped steel in its body-in-white [102]. Figure 4.17 shows the use of uncoated and Zn-coated boron steels in BMW 5 Series GT, (F07, SOP 2009) [103, 104].

For LMAC to happen there are three prerequisites as shown in Fig. 4.18 [79, 105]:

(1) Stress level: during hot stamping stress can be reduced by die design or by improving lubricity (i.e., ZnNi coating has low friction coefficient),

(2) Presence of liquid metal: Pure Zn melts at 420 °C (790 °F), which is far lower than the temperatures in hot stamping process. Therefore, even during heating the blank (i.e., in the furnace) Zn coating on the blank may melt. Thus, liquid

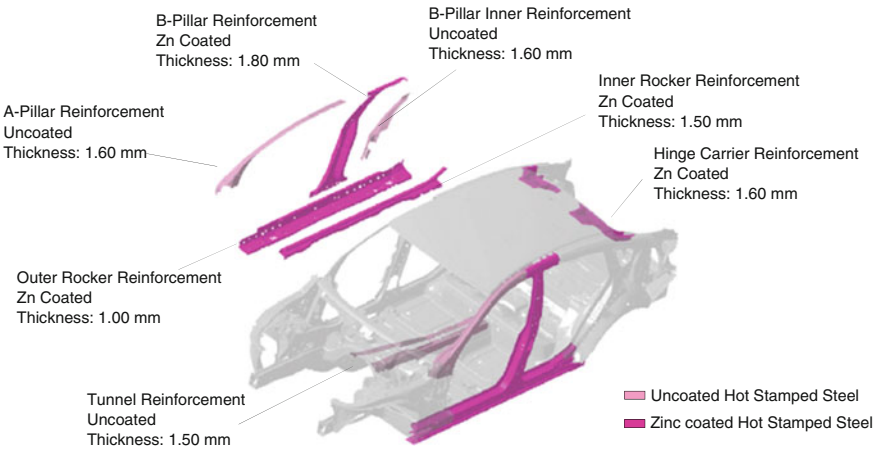

Fig. 4.17 Usage of hot-stamped steels in BMW 5 Gran Turismo (F07, SOP 2009) (re-created after [104])

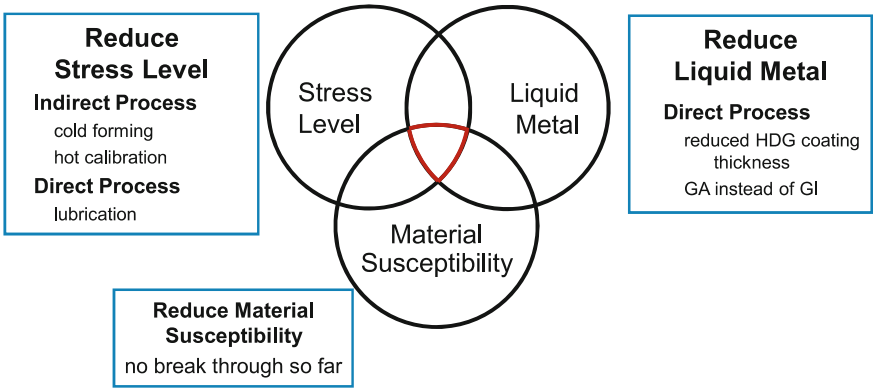

Fig. 4.18 Factors leading to LMAC (Liquid Metal Assisted Cracking) [21]

metal cannot be avoided if the blank is Zn coated. However, the amount of liquid Zn can be adjusted by the weight of coating (typically given by g/m^2) and the coating technology. Reducing coating weight would sacrifice from cathodic protection and decrease the time required in furnace for coating to diffuse [21]. If the coating is galvannealed, iron would diffuse into the coating and increases the melting temperature. Another possibility is to use alloying elements in the coating to increase the melting temperature. One such design was ZnNi coatings [20, 106] (Fig. 4.19).

(3) Reducing material susceptibility: covers a number of properties of the steel, including but not limited to (1) chemical composition and carbon equivalence, (2) yield strength/hardness, and (3) residual stresses [105]. In hot stamping grades, no practical method was found to lower material susceptibility [68].

The presence of microcracks could reduce the fatigue life of the components. Kurz has studied the crack depth and fatigue stress. As seen in Fig. 4.20, microcracks up to 10 μm in the base metal do not affect the fatigue stress. However, if the crack size exceeds 10 μm, fatigue stress reduces drastically [21].

As the coating weight increases, the time in furnace has to be longer. It was also found that as the depth of microcracks is also affected by the coating weight. To avoid microcracks deeper than 10 μm in the base metal, GI coating weight is limited to 70 g/m^2 per side (140 g/m^2 total, abbreviated as Z140) [21].

Hot dip galvanized (GI) steels have an iron diffusion during heating, similar to AlSi coating. In GI coatings, 0.2–2.5 wt.% Al is added to form an Al-enriched layer between the steel and Zn coating [82, 108, 109]. After iron diffusion, there has to be three layers, as shown in Fig. 4.21a [110]. The outermost layer is an oxide layer, consisting of aluminum and zinc oxides. This layer is functional during hot stamping as it suppresses evaporation of Zn but has to be removed before welding/painting by sandblasting [82, 98, 109]. Below the oxide layer, Zn-rich Γ phase is found. This layer plays significant role in the corrosion resistance. For adequate cathodic protection, this layer should have at least 70 wt.% Zn. The Fe-rich α phase determines

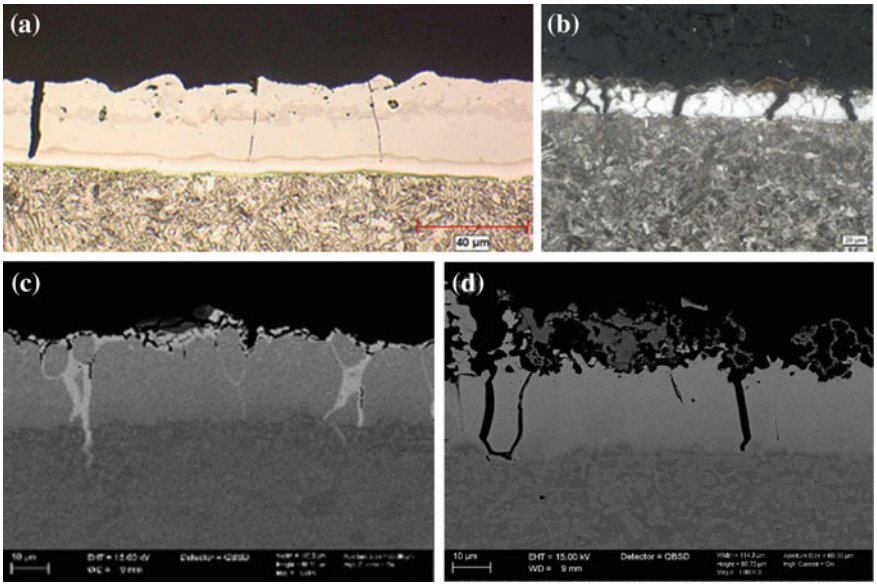

Fig. 4.19 Coatings after hot stamping: **a** microcracks in AlSi coating do not penetrate into steel substrate [8], **b** GI coating melts and Zn may penetrate into base material depending on coating thickness [21]. In **c** GA and **d** ZnAlMg coatings, LMAC problem is reduced but still microcracks may be formed, predominantly not in the base metal [107]

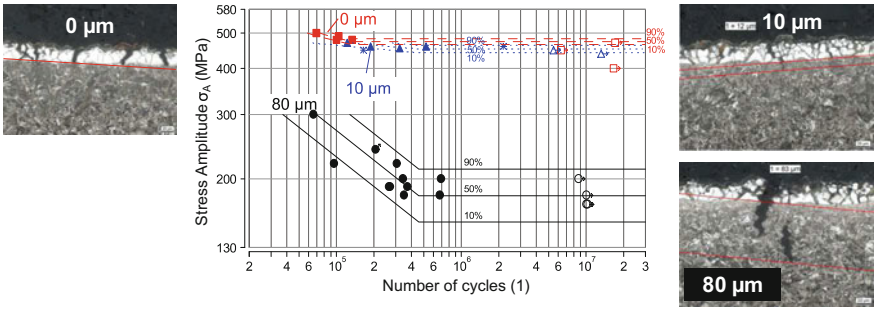

Fig. 4.20 Effect of microcrack depth in base material on fatigue life of Zn-coated 22MnB5 steel. Micrographs showing the cracks are also shown [21]

the adhesion of coating to the base metal. It should contain at least 10 wt.% Zn, preferably in the range of 17–44 wt.% [82, 109].

Zn coating has relatively narrow process window for hot stamping compared to uncoated and/or AlSi-coated blanks. As pure zinc's boiling point (907 °C ≃ 1665 °F) is very close to the austenitization temperature of 22MnB5 (880 °C ≃ 1615 °F). If furnace dwell time is too short, the coating diffusion would not be completed. If the time is too long, deep microcracks may occur in the base metal [21, 111, 112].

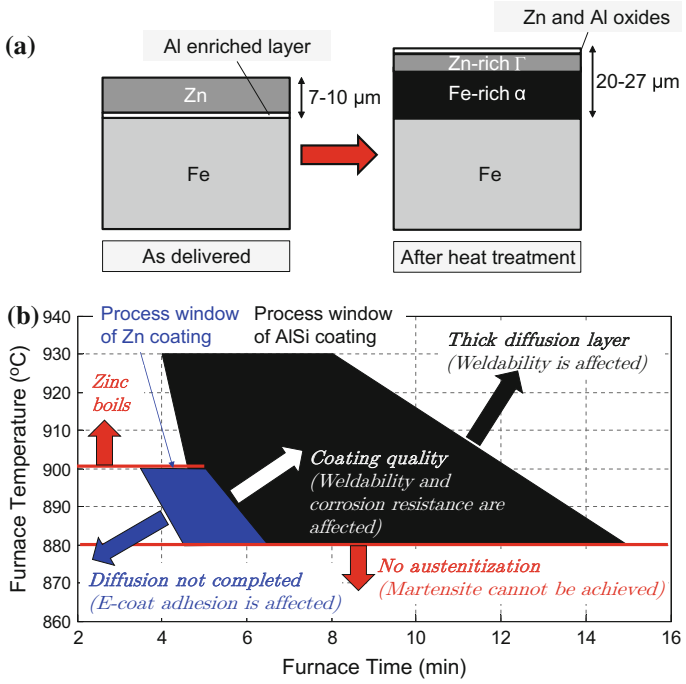

Fig. 4.21 **a** Diffusion of Zn (GI) coating (re-created after [82, 110]), **b** process windows of Zn and AlSi coatings (re-created after [111–114])

To reduce LMAC and/or the need for surface conditioning, alloying elements increasing the melting point of Zn could be added into coating. ZnNi coating was once commercialized by ThyssenKrupp with the name GammaProtect. There were two mass-produced automotive parts using this coating. However, the coating has been discontinued and production was switched to AlSi-coated blanks [20, 111, 115]. Other Zn-alloyed coatings could be ZnFe (Galvannealed coating, abbreviated as GA) and ZnAlMg [92, 108]. Galvannealing (GA) is a process where the galvanized steel is heated to 480–520 °C (~900–970 °F). During this process, iron diffuses into coating and the final coating may have 10–15 wt.% Fe and 85–90 wt.% Zn [116]. GA coatings may be welded and painted without removing the oxide layer [82, 98].

Another recent solution to LMAC is precooling before plastic deformation. Ghanbari [117] found that microcrack formation occurs if forming is done over 782 °C (1440 °F). Kurz et al. [101] developed a precooling stage where the cooling rate is over 50 °C/s (90 °F/s) but the cooling is interrupted before the martensite start temperature, Fig. 4.22a. By this method, forming is still done at austenitic phase [101]. Faderl and Kelsch have shown that if the precooling temperature is lowered, microcrack depth is reduced [118]. At around 550–570 °C (1020–1060 °F), Zn coating is solidified and microcracks are reduced [119, 120]. Typical 22MnB5 could be held at 550 °C (1020 °F) for only 2 s before bainite transformation starts. The newly

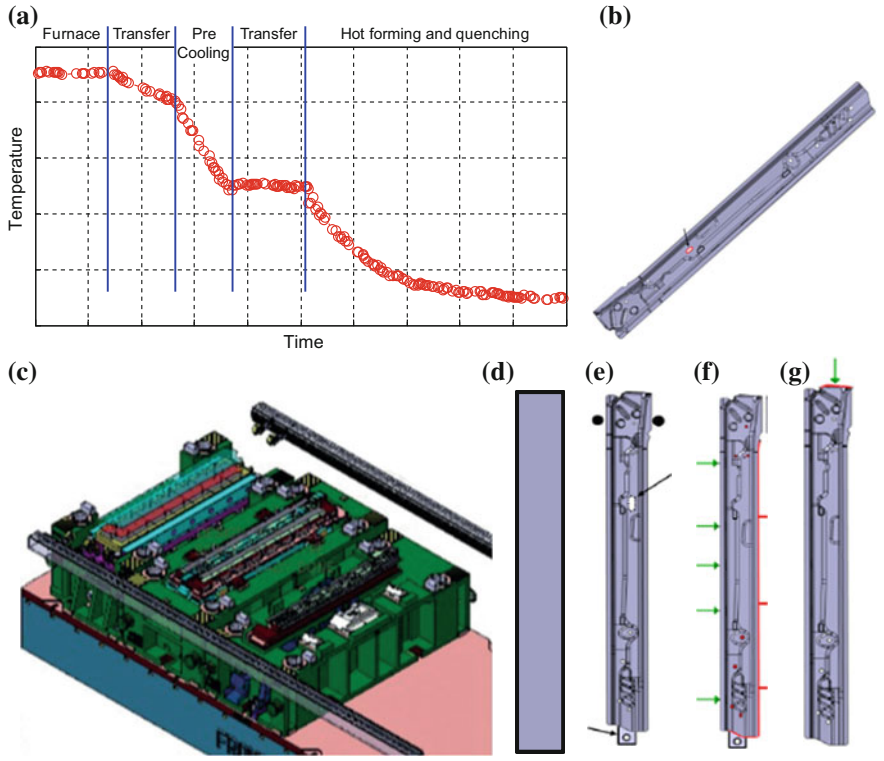

Fig. 4.22 Multistep hot stamping: **a** the temperature-time profile, including the "precooling" stage, **b** The final part geometry, **c** thermal controlled transfer die set, **d** OP10: Precooling, **e** OP20: Forming, **f** OP30: Cutting/Piercing, and **g** OP40: Cam Trimming (re-created after [20, 101, 121])

designed 20MnB8 alloy can be held at this temperature level for more than 20 s before the transformation [68]. By using precooling system 20MnB8 GA 90/90 (ZF180) can be formed in a multistep operation in a transfer press, as shown in Fig. 4.22b–f.

Currently ArcelorMittal, POSCO, and voestalpine offer Zn GI coatings. ArcelorMittal and voestalpine also offer GA coating. Tata Steel is developing MagiZinc (ZnAlMg) coating for press hardening, but this product is currently not in the market [9, 14, 101, 122]. According to Dormegny [123], 76% of the hot stamping steel in EU27+Turkey is AlSi coated. In these markets, 18% of hot stamping steel is uncoated and only 6% is Zn coated.

4.5.3 Varnish Coatings

Another method to avoid scaling and decarburization is to apply varnish coatings. In this method, uncoated blanks are either coil coated or roll coated with the paint-like

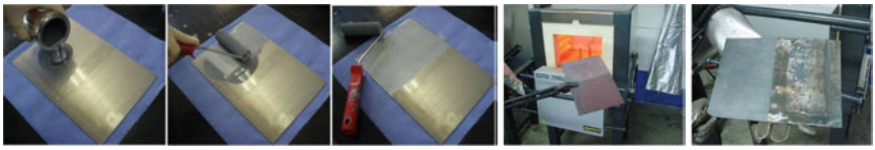

Fig. 4.23 x-tec coating can be applied simply by a paint roll or spray gun [74]

varnish coatings. The first such application for hot stamping process was developed by Nano-X company in 2005. By then, AlSi coating was already in production. However, in several components of the (then) new Passat, part shapes were extremely complex. A two-step forming process was needed where some deformation would be done by cold forming and more in hot forming, as shown in Fig. 1.15, in Chap. 1 [124, 125].

The first-generation x-tec (see CO 4020 in Table 4.11) had Al particles, graphite and wax in inorganic–organic matrix. This coating should be applied 6–7 μm thick on the uncoated base steel. It can be applied simply by paint rollers (Fig. 4.23) or could be coil coated. cures in room temperature. x-tec coating has lower friction compared to uncoated and AlSi-coated blanks, and was on a par with ZnNi coatings, see Fig. 10.7. This coating had to be removed (by sandblasting) before e-coating and/or welding [74].

Second-generation x-tec, AlSi 4001 as shown in Table 4.11, was developed to be weldable without sandblasting. The coating has high heat absorption and since extra time for diffusion is not required, the total furnace time could be lowered significantly. It can also handle inductive, conductive, and near infrared heating and could be applied as thin as 2–3 μm [74].

In 2015, Henkel has introduced a varnish coating for hot stamping, called Bonderite S-FN 7500 PH. The coating is suitable for fast heating and provides barrier corrosion protection. Although its friction coefficient is not published yet, it helps lubricating the blank. The coating is not required to be removed/sandblasted before e-coating or spot welding [85].

References

1. H. Karbasian, A.E. Tekkaya, A review on hot stamping. J. Mater. Process. Technol. **210**(15), 2103–2118 (2010)
2. T.K. Eller, L. Greve, M.T. Andres, M. Medricky, A. Hatscher, V.T. Meinders, A.H. van den Boogaard, Plasticity and fracture modeling of quench-hardenable boron steel with tailored properties. J. Mater. Process. Technol. **214**(6), 1211–1227 (2014)
3. C.W. Lee, W.S. Choi, Y.R. Cho, B.C.D. Cooman, Microstructure evolution of a 55 wt. hardening steel during rapid heating. Surf. Coat. Technol. **281**, 35–43 (2015)
4. M. Naderi, Hot stamping of ultra high strength steels. PhD Dissertation, RWTH Aachen, Germany (2007)
5. M. Spittel, T. Spittel, *Steel Symbol/Number: 22MnB5/1.5528* (Springer, Berlin, 2009), pp. 930–935

6. S. Flachstahl, 22MnB5 boron alloyed quenched and tempered steel. Product catalogue (2014)
7. A.K. Steel, ULTRALUME Aluminized Type 1 Press Hardenable Boron Steel. Product catalogue (2016)
8. T. Vietoris, New developments in PHS: materials, coatings, production methods. Presented at AP&T Press Hardening, Next Step Seminar, Novi, MI (2011)
9. ArcelorMittal, Extract from the product catalogue (2015). Accessed 10- June 2015
10. BaoSteel, Automotive advanced high strength steels. Product catalogue (2013)
11. B. Macek, Optimization side crash performance using a hot-stamped B-pillar. Presented at Great Designs in Steel Seminar (2006)
12. K. Hikita, Properties of new TS1800 MPa grade hot staming steel and components. Presented at Materials in Car Body Engineering 2012, May 10–11, Bad Nauheim, Germany (2012)
13. J.B. Nam, Development of new auto steels and application technology, in *China Automotive Steel Conference, World Steel/CISA* (2013)
14. Posco, Automotive steel data book (2016)
15. SSAB, Docol 1500 Bor. Product catalogue (2013)
16. SSAB, DOCOL PHS 1500. Product catalogue (2015)
17. ThyssenKrupp Steel Europe, *Warmumformung im Automobilbau*. Die Bibliothek der Technik (2012)
18. E. Hilfrich, Trends and potentials of new hotforming steels. Presented at Insight Edition Conference, September 19th, Neckarsulm, Germany (2012)
19. ThyssenKrupp Steel Europe, Mangan-bor-stähle für die warmumformung. Product catalogue (2014)
20. I.M. Gonzalez, O. Straube, Development of zinc coated parts for hotstamping, in *Proceedings of New Developments in Sheet Metal Forming Conference, Stuttgart, Germany* (2016), pp. 265–276
21. T. Kurz, New developments in zinc coated steel for press hardening. Presented at Insight Edition Conference, September 20–21, Gothenburg, Sweden (2011)
22. Y. Bi, Development of advanced automotive materials at WISCO. Presented at the State Key Lab of Rolling and Automation (RAL), Northeastern University (2014)
23. J. Komenda, R. Sandström, M. Tukiainen, Multiple regression analysis of jominy hardenability data for boron treated steels. Steel Res. **68**(3), 132–137 (1997)
24. H. Lanzerath, Simulation: enabler for the efficient design of lightweight boron intensive body structures. Presented at Insight Edition Conference, September 20–21, Gothenburg, Sweden (2011)
25. D. Wenk, Global capability: hot stamping. Presented at Global Automotive Lightweight Materials Asia 2014, Shanghai, China, March 26–27 (2014)
26. J. Overrath, F.J. Lenze, S. Sikora, Aktuelle entwicklung der warmumformung im automobilen fahrzeugbau. Bauteile der Zukunft–Methoden und Prozesse, Tagungsband zum 30 (2010)
27. S. Graff, T. Gerber, F.J. Lenze, S. Sikora, About the simulation of microstructure evolution in hot sheet stamping process and the correlation of resulting mechanical properties and crash-performance. In *3rd International Conference on Hot Sheet Metal Forming of High Performance Steel, CHS2, Kassel, Germany* (2011), pp. 323–330
28. H.W. Lee, K.-H. Chung, A new body concept for electric vehicle. Presented at Materials in Car Body Engineering 2012, May 11, Bad Nauheim, Germany (2012)
29. M. Garcia, Remote laser welding. Presented at European Automotive Laser Applications (EALA) 2013, February 19-20, Bad Nauheim, Germany (2013)
30. Y. Zhong, Recently Progress of AHSS in BAOSTEEL, in *Presented at Driving Steel 2016, December 5–7, Kuala Lumpur, Malaysia* (2016)
31. ArcelorMittal Flat Carbon Europe S.A. ArcelorMittal Automotive Product Offer Europe, Android App, V1.0 (2015)
32. H. Matsuoka, K. Fujihara, Mazda cx-5. Presented at EuroCarBody 2011, October 18–20, Bad Nauheim, Germany (2011)
33. Renault Media Services, http://media.renault.com
34. SSAB, Data sheet 2115, Docol PHS 1800 (2017)

35. O. Hoffmann, Lightweight steel design in the modern vehicle body. In Werkstoff-Forum Intelligenter Leichtbau. Hannover, Germany (2011)
36. voestalpine Steel Division. phs-ultraform®data sheet • 03/2017 (2017)
37. H. Mohrbacher, M. Maikranz-Valentin, Recent progress in the metallurgical development of press hardening steel with improved application properties. Presented at Materials in Car Body Engineering 2014, May 13–14, Bad Nauheim, Germany (2014)
38. J. Mura, T. Gerber, S. Sikora, F.-J. Lenze, MBW1900 mit mikrolegierung zur optimierung der technologischen eigenschaften nach dem presshärten, in *Tagungsband zum 7. Erlanger Workshop Warmblechumformung 2012* (2012), pp. 1–10
39. K. Lee, J.-H. Kim, S.-Y. Kwak, Y.-R. Cho, S. Choo, K.-G. Chin, Recent developments of automotive sheet steels. Presented at Materials in Car Body Engineering 2014, May 13–14, Bad Nauheim, Germany (2014)
40. SSAB, Let's talk about boron steel. Product catalogue (2015)
41. J. Bian, H. Mohrbacher, Novel alloying design for press hardening steels with better crash performance. Presented at AIST Symposium, Vail, Colorado, USA (2013)
42. K. Fahlström, Laser welding of boron steels for light-weight vehicle applications. Licentiate Thesis, Högskolan Väst, Sweden (2015)
43. ThyssenKrupp Steel Europe. Product information for manganese-boron steel for hot forming (2016)
44. C. Wang, M. Maoqiu Wang, J. Shi, W. Hui, H. Dong, Effect of microstructure refinement on the strength and toughness of low alloy martensitic steel. J. Mater. Sci. Technol. **23**(05), 659 (2007)
45. D.D. Múnera, A. Pic, D. Abou-Khalil, F. Shmit, F. Pinard, Innovative press hardened steel based laser welded blanks solutions for weight savings and crash safety improvements. SAE Int. J. Mater. Manf. **1**, 472–479, 04 (2008)
46. F. D'Aiuto, M.M. Tedesco, Development of new structural components with innovative materials and technological solutions. Presented at Materials in Car Body Engineering 2015, April 22–23, Bad Nauheim, Germany (2015)
47. ArcelorMittal Media Services, http://www.arcelormittal.com/corp/news-and-media
48. H. Ljungqvist, K. Amundsson, O. Lindblad, The all-new Volvo XC90 car body. Presented at EuroCarBody 2014, October 21–23, Bad Nauheim, Germany (2014)
49. voestalpine Media services, http://www.voestalpine.com/group/en/press
50. W.S. Choi, B.C. De Cooman, Characterization of the bendability of press-hardened 22MnB5 steel. Steel Res. Int. **85**(5), 824–835 (2014)
51. D. Pireronek, L. Kessler, H. Richter, S. Myslowicki, Virtuelle produktentwicklung und crashauslegung von stahl-werkstoffverbundsystemen, in *14. German LS-Dyna Forum, 10–12.10.2016, Bamberg* (2016)
52. H. Ferkel, J.N. Hoffmann, L. Keßler, Resource gentle light weight construction for today's and oncoming mobility, in *The International Conference on New Development in Sheet Metal Forming Technology, Stuttgart, Germany* (2012), pp. 1–16
53. K.H. Hu, G.W. Feng, X.D. Liu, R.D. Han, The effect of heating process on strength and the original austenite grain size of hot forming parts, in *Innovative Research in Hot Stamping Technology*. Advanced Materials Research, vol. 1063 (Trans Tech Publications, Switzerland, 2015), pp. 28–31
54. K. Liu, B. Chi, Y. Zhang, J. Li, Constitutive analysis on thermal-mechanical properties of WHT1300HF high strength steel, in *Proceedings of SAE-China Congress 2015: Selected Papers* (Springer, Singapore, 2016), pp. 309–316
55. BaoSteel, Hot-rolled pickled automotive steel sheets. Product catalogue (2010)
56. T. Fröhlich, Maximum safety and lightweight potential due to use of new high strength steels. Presented at Outokumpu Experience 2013, May 22–23, London, UK (2013)
57. P.-O. Santacreu, G. Badinier, J.-B. Moreau, J.-M. Herbelin, Fatigue properties of a new martensitic stainless steel for hot stamped chassis parts, in *SAE Technical Paper* (SAE International, 2015), p. 4

58. J.M. Herbelin, 1000–2000 MPa Martensitic stainless steels for flexible hot forming processes. Presented at Materials in Car Body Engineering 2014, May 13–14, Bad Nauheim, Germany (2014)
59. J.M. Herbelin, MaX: martensitic stainless steel for hot stamping. Product catalogue (2015)
60. G. Badinier, J.-D. Mithieux, P.-O. Santacreu, J.-M. Herbelin, Development of a 1.8 GPa martensitic stainless steel for hot stamping application, in *5th International Conference on Hot Sheet Metal Forming of High Performance Steel, CHS2, Toronto, ON, Canada* (2015), pp. 715–723
61. G. Badinier, J.-B. Moreau, B. Petit, C. Boissy, J.-D. Mithieux, S. Saedlou, J. Paegle, Development of press hardening stainless steels for body-in-white application, in *6th International Conference on Hot Sheet Metal Forming of High Performance Steel, CHS2, Atlanta, GA, USA* (2017), pp. 77–84
62. Q. Han, W. Bi, X. Jin, W. Xu, L. Wang, X. Xiong, J. Wang, P. Belanger, Low temperature hot forming of medium-Mn steel, in *5th International Conference on Hot Sheet Metal Forming of High Performance Steel, CHS2, Toronto, ON, Canada* (2015), pp. 381–389
63. I.A. Mendieta, M.A. Telleria, J.P. Drillet, J.D. Puerta Velasquez, M. Alsmann, J. Clobes, S. Bruschi, A. Ghiotti, European commission. directorate-general for research, and innovation. *Green Press Hardening Steel Grades (GPHS): Final Report*. EUR (Luxembourg. Online). Publications Office (2015)
64. Y. Chang, C.Y. Wang, K.M. Zhao, H. Dong, J.W. Yan, An introduction to medium-Mn steel: metallurgy, mechanical properties and warm stamping process. Mater. Design **94**, 424–432 (2016)
65. Y.-K. Lee, J. Han, Current opinion in medium manganese steel. Mater. Sci. Technol. **31**(7), 843–856 (2015)
66. H.L. Yi, P.J. Du, B.G. Wang, A new invention of press-hardened steel achiving 1880 MPa tensile strength combined with 16% elongation in hot-stamped, in *5th International Conference on Hot Sheet Metal Forming of High Performance Steel, CHS2, Toronto, ON, Canada* (2015), pp. 725–734
67. R. Rana, C.H. Carson, J.G. Speer, Hot forming response of medium manganese transformation induced plasticity steels, in *5th International Conference on Hot Sheet Metal Forming of High Performance Steel, CHS2, Toronto, ON, Canada* (2015), pp. 391–400,
68. T. Kurz, P. Larour, J. Lackner, T. Steck, G. Jesner, Press-hardening of zinc coated steel - characterization of a new material for a new process. IOP Conf. Ser.: Mater. Sci. Eng. **159**(1), 012025 (2016)
69. H.W. Tamler, J.-U. Becker, R. Wunderlich, K.E. Friedrich, P. Rademacher, TriBond®-: hot-rolled clad strip, customized steel composite material from coil. ThyssenKrupp techforum **1**, 18–23 (2006)
70. ThyssenKrupp Steel Europe. Multi-layer composite for weight reduction: TriBond. Press Release, 2014
71. ThyssenKrupp Steel Europe. TRIBOND ®- high strength and high ductility. Product catalogue (2016)
72. ATZ/MTZ (Wiesbaden), *The Project ThyssenKrupp InCar Plus: Solutions for Automotive Efficiency*. ATZ/MTZ extra (Springer Vieweg, Berlin, 2014)
73. J. Wang, R.W. Hyland Jr, Zinc coated steel with inorganic overlay for hot forming, May 17 2012. US Patent App. 13/317,819
74. G. Frenzer, Nano-x gmbh x-tec®and alsi®coat products against scale formation on steel. Presentation at Nano-X (2015)
75. R.G. Baggerly, R.A. Drollinger, Determination of decarburization in steel. J. Mater. Eng. Perform. **2**(1), 47–50 (1993)
76. G.E. Totten, *Steel Heat Treatment: Metallurgy and Technologies* (CRC Press, Boca Raton, 2006)
77. S. Kalpakjian, S.R. Schmid, *Manufacturing Engineering and Technology* (Prentice Hall, Englewood Cliffs, 2010)

78. P. Belanger, The future for press hardening in the automotive industry. Presented at AP&T Press Hardening, Next Step Seminar, Novi, MI, October (2011), p. 2011
79. M. Van Genderen, W. Verloop, J. Loiseaux et al., Zinc-coated boron steel, ZnX®: Direct hot forming for automotive applications, in *3rd International Conference on Hot Sheet Metal Forming of High Performance Steel, CHS2, Kassel, Germany* (2011), pp. 145–152
80. K. Lamprecht, G. Deinzer, A. Stich, J. Lechler, T. Stöhr, M. Merklein, Thermo-mechanical properties of tailor welded blanks in hot sheet metal forming processes, in *IDDRG, Graz, Austria* (2010), pp. 37–48
81. J. Banik, Hot forming state-of-the-art and trends. Presented at Insight Edition Conference, September 20–21, Gothenburg, Sweden (2011)
82. D.W. Fan, B.C. De Cooman, State of the knowledge on coating systems for hot stamped parts. Steel Res. Int. **83**(5), 412–433 (2012)
83. O. Hoffmann, *Environment oriented light weight design in steel*, in *Ökologischer Leichtbau in Stahl, Hannovermesse Werkstoff-Forum, Hannover, Germany* (2012)
84. Henkel Corporation. BONDERITE®S-FN 7500 PH. Product catalogue (2014)
85. W. Fristad, New coil-applied coating for press-hardening steel. Proc. Galvatech **2015**, 892–898 (2015)
86. J. Kondratiuk, P. Kuhn, Tribological investigation on friction and wear behaviour of coatings for hot sheet metal forming. Wear **270**(11–12), 839–849 (2011)
87. R. Neugebauer, F. Schieck, S. Polster, A. Mosel, A. Rautenstrauch, J. Schönherr, N. Pierschel, Press hardening – an innovative and challenging technology. Arch. Civil Mech. Eng. **12**(2), 113–118 (2012)
88. X. Bano, J.P. Laurent, Heat treated boron steels in the automotive industry, in *39th Mechanical Working and Steel Processing Conference* (1997), pp. 673–677
89. L. Vaissiere, J.P. Laurent, A. Reinhardt, Development of pre-coated boron steel for applications on PSA Peugeot Citroën and Renault bodies in white, in *SAE Technical Paper* (SAE International, 2002), p. 7
90. A. Reinhardt, Development of hot stamped ultra high strength steel parts on the Peugeot 307 and the Citroën C5. Presented at EuroCarBody 2001 - 3rd Global Car Body Benchmarking Conference, Bad Nauheim, Germany (2001)
91. P. Siebert, M. Alsmann, H.J. Watermeier, Influence of different heating technologies on the coating properties of hot-dip aluminized 22MnB5, in *3rd International Conference on Hot Sheet Metal Forming of High Performance Steel, CHS2, Kassel, Germany* (2011), pp. 457–464
92. K.S. Jhajj, Heat transfer modeling of roller hearth and muffle furnace. Master's Thesis, University of Waterloo, Waterloo, ON, Canada (2015)
93. M. Jönsson, The problem with melted Al-Si in the hot stamping furnace, in *Advanced High Strength Steel and Press Hardening: Proceedings of the 3rd International Conference on Advanced High Strength Steel and Press Hardening (ICHSU2016)* (World Scientific, Singapore, 2017), pp. 479–485
94. M. Windmann, A. Röttger, W. Theisen, Formation of intermetallic phases in Al-coated hot-stamped 22MnB5 sheets in terms of coating thickness and Si content. Surf. Coat. Technol. **246**, 17–25 (2014)
95. T. Vietoris, Hot stamping with USIBOR1500®. Presented at AP&T Press Hardening, Next Step Seminar, Novi, MI, September 15th (2010)
96. D.W. Fan, H.S. Kim, J.-K. Oh, K.-G. Chin, B.C. De Cooman, Coating degradation in hot press forming. ISIJ Int. **50**(4), 561–568 (2010)
97. K. Takagi, E. Nakanishi, T. Yoshida, Aluminum-coated structural member and production method, November 9 2004. US Patent 6,815,087
98. E.J. Watkins, Hot stamping market, materials, coatings, and developments. Presented at Schuler Hot Stamping Workshop, May 14, Dearborn, MI, USA (2013)
99. R. Aldén, Metallurgical investigation in weldability of aluminium silicon coated boron steel with different coating thickness. Bahcelor Degree Thesis, KTH Royal Institute of Technology, Stockholm, Sweden (2015)

100. S. Fujita, S.J. Maki, H.I. Yamanaka, M. Kurosak, Corrosion resistance after hot stamping of 22MnB5 steels aluminized with 80g/m2 c.w. and ZnO coating, in *5th International Conference on Hot Sheet Metal Forming of High Performance Steel, CHS2, Toronto, ON, Canada*, pp. 681–690 (2015)
101. T. Kurz, G. Luckeneder, T. Manzenreiter, H. Schwinghammer, A. Sommer, Zinc coated press-hardening steel - challenges and solutions, in *SAE Technical Paper* (SAE International, 2015), p. 4
102. M. Pfestorf, T. Laumann, Potenziale verzinkter warm umgeformter stähle, in *Tagungsband zum 3. Erlanger Workshop Warmblechumformung* (2008)
103. BMW PressClub Global, http://www.press.bmwgroup.com
104. D. Copeland, M. Pfestorf, The body in white of the new BMW 5 Series Gran Turismo. Presented at Great Designs in Steel, Livonia, MI, May 5th (2010)
105. The British Constuctional Steelwork Association, Ltd. Galvanizing structural steelwork: an approach to the management of liquid metal assisted cracking (2005)
106. P. Nash, Y.Y. Pan, The Ni Zn (Nickel Zinc) system. Journal of Phase Equilibria **8**(5), 422 (1987)
107. W.C. Verloop, Development of Zn-coated boron steel ZnX at Tata Steel, in *Insight Edition Conference* (2011)
108. C.W. Lee, D.W. Fan, I.R. Sohn, S.-J. Lee, B.C. De Cooman, Liquid-metal-induced embrittlement of Zn-coated hot stamping steel. Metall. Mater. Trans. A **43**(13), 5122–5127 (2012)
109. M. Fleischanderl, S. Kolnberger, J. Faderl, G. Landl, A.E. Raab, W. Brandstätter, Method for producing a hardened steel part, US Patent 8,021,497, 20 Sept 2011
110. G. Kim, Quality evlauation of Zn coated hot press forming steel. Presented at Materials in Car Body Engineering 2013, May 7–8, Bad Nauheim, Germany (2013)
111. J. Banik, M. Köyer, J. Mura, GammaProtect ® - always well protected. Presented at Materials in Car Body Engineering 2013, May 7–8, Bad Nauheim, Germany (2013)
112. C. Allely, J. Petitjean, T. Vietoris, Corrosion resistance of zinc based and aluminized coatings on press-hardened steels for automotive, in *3rd International Conference on Hot Sheet Metal Forming of High Performance Steel, CHS2, Kassel, Germany* (2011), pp. 153–160
113. K. Teshima, Challenges of high-efficiency hot forming processes at Honda. Presented at Forming in Car Body Engineering 2012, September 26–27, Bad Nauheim, Germany (2012)
114. S.P. Bhat, Steel grades and coatings for hot stamping, in *4th PHS Suppliers Forum* (2016)
115. J.N. Belanger, P.J. Hall, J.J. Coryell, J.P. Singh, Automotive body press-hardened steel trends, in *International Symposium on New Developments in Advanced High-Strength Sheet Steels* (2013), pp. 239–250
116. American Society of Metals, *ASM Handbook of* "*Corrosion*", vol. 13 (ASM International, 1992)
117. Z. Ghanbari, Zinc coated sheet steel for press hardening. Master's Thesis, Colorado School of Mines, Golden, CO, USA (2014)
118. J. Faderl, R. Kelsch, Galvanized press-hardening steels. Presented at Insight Edition Conference, June 24, Bremen (2015)
119. I. Martin, M. López, P. Raya, A. Sunden, D. Berglund, K. Isaksson, S. Isaksson, Press systems and methods, US Patent 9,492,859, 15 Nov 2016
120. C. Hofer, T. Kurz, H. Clemens, R. Schnitzer, Atom probe study of prior austenite grain boundaries of zinc-coated press hardened steel, in *6th International Conference on Hot Sheet Metal Forming of High Performance Steel, CHS2, Atlanta, GA, USA* (2017), pp. 383–390
121. P. Belanger, New Zn multistep hot stamping innovation. Presented at Great Designs in Steel 2017 (2017)
122. Tata Steel, Magizinc®auto. Product Catalogue (2015)
123. L. Dormegny, Efficient lightweighting with new press hardenable steels. AMS Webinar (2017)
124. S. Sepeur, The company Nano-X GmbH: products for the automotive industry. Presentation at Deutsche Börse, July 10th, Frankfurt, Germany (2006)
125. W. Runge, *Technology Entrepreneurship: A Treatise on Entrepreneurs and Entrepreneurship for and in Technology Ventures*, vol. 2 (KIT Scientific Publishing, 2014)

Chapter 5
A Hot Stamping Line

Jan Jonasson, Eren Billur and Aitor Ormaetxea

Abstract Hot stamping requires a special production line, similar to but different than cold stamping operations. A typical hot stamping line consists of (1) a furnace/heating system, (2) a material handling system, (3) a press, and (4) an exit line. Sometimes trimming/piercing systems could also be included in the definition of "a line". In this chapter, the first three items are explained in detail.

5.1 Furnaces and Heating Systems

5.1.1 Conventional Roller Hearth Furnaces

The hot stamping process begins with heating the blank over its austenitizing temperature (depending on the raw material, generally for 22MnB5, 950 °C (1750 °F). Although it is possible to heat the material using inductive and conductive methods, the most common method in application is to use the so-called roller hearth furnaces. The energy for heating can be supplied by gas or electric [1, 2].

One problem with the roller hearth furnaces is the total space they require. As seen in Fig. 5.1, the length of a furnace is a function of heating time ($t_{heating}$), cycle time (t_{cycle}) and the length of the batch (L_{batch}) and can be calculated by the Eq. 5.1. An example calculation for a B-pillar production is given in as well [1].

J. Jonasson
AP&T AB, Ulricehamn, Sweden
e-mail: jan.jonasson@aptgroup.com

E. Billur (✉)
Billur Makine Ltd., Ankara, Turkey
e-mail: eren@billur.com.tr

E. Billur
Atılım University, Ankara, Turkey

A. Ormaetxea
Fagor Arrasate S. Coop., Gipuzkoa, Spain
e-mail: a.ormaetxea@fagorarrasate.com

E. Billur (ed.), *Hot Stamping of Ultra High-Strength Steels*,
https://doi.org/10.1007/978-3-319-98870-2_5

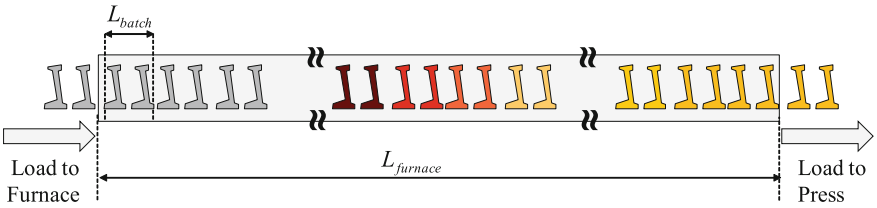

Fig. 5.1 Determination of furnace length (recreated after [1])

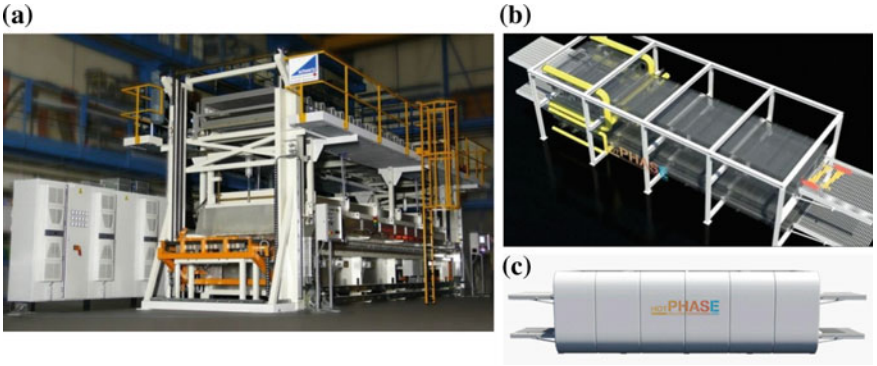

Fig. 5.2 **a** Photo [1] and **b**, **c** schematics of a double-decker furnace [6]

$$L_{furnace} = \frac{t_{heating}}{t_{cycle}} L_{batch} \rightarrow \text{e.g.: } L_{furnace} = \frac{330\,\text{s}}{15\,\text{s}} 1.6\,\text{m} = 35.2\,\text{m} = 115.5\,\text{ft} \quad (5.1)$$

Several new furnaces have been introduced to save space and conserve energy. Some new furnaces are also capable to tailor the austenitizing process (i.e., keep some portions of the blank in Ferritic/Pearlitic phase) in order to tailor the final properties of the workpiece (as discussed in Chap. 8). In addition, it has to be noted that if the productivity is to be increased (i.e., cycle time t_{cycle} is reduced), a longer furnace would be required [3, 4].

One of the designs to reduce the length of roller hearth furnace is a double-decker configuration, as shown in Fig. 5.2. The design can theoretically reduce the space requirement by half for the same production rate. A double-decker design, described by [5] reduced the furnace length from 57 m (187 ft) to 34 m (111 ft) for a process with cycle time of $t_{cycle} = 13\,\text{s}$.

Ebner Furnaces (Austria) has come up with the new furnace line called HotPHASE (Fig. 5.2b, c) which has two independent heating systems: (1) with natural gas and (2) electric. The furnace is capable of two heating modes:

(1) Rapid heating up with gas-fired furnace (Fig. 5.3a). The entrance zone of the furnace is heated to 1050 °C (~1920 °F). This set temperature is over the austenitizing temperature of 22MnB5, the typical hot stamping material ($A_{c3} = 950\,°\text{C}$). Thus, a

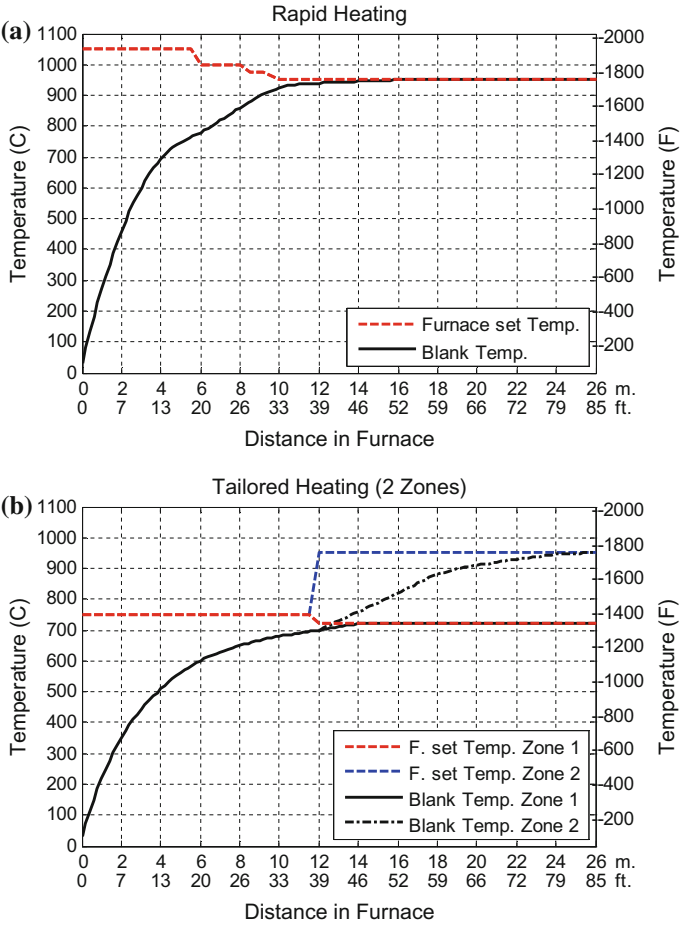

Fig. 5.3 Ebner HotPHASE heating modes: **a** Uniform heating, **b** Tailored heating with two zones [recreated after [6]]

rapid heating can be obtained at the beginning of heating. Later, electric heating is used to sustain a more uniform distribution of temperature.

(2) Tailored heating is possible up to five different temperature zones (Fig. 5.3b). The furnace is heated by gas in the first section up to 750 °C (∼1380°F). Later sections are separately controlled. It is possible to keep some portions of the blank at around 725 °C (∼1350°F) in order to ensure that the sections of interest are not austenitized. The rest of the blank can be heated by local electric heaters up to 950 °C (∼1750 °F), and thus are austenitized [6].

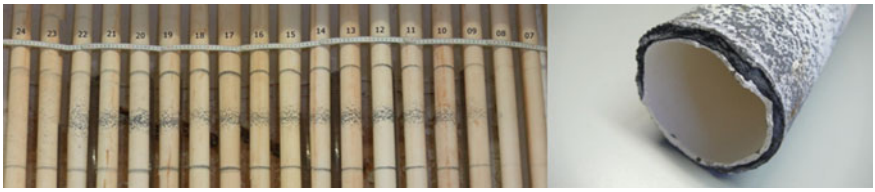

Fig. 5.4 AlSi coating builds up on ceramic rollers, if the blank is directly in contact with the rollers [7]

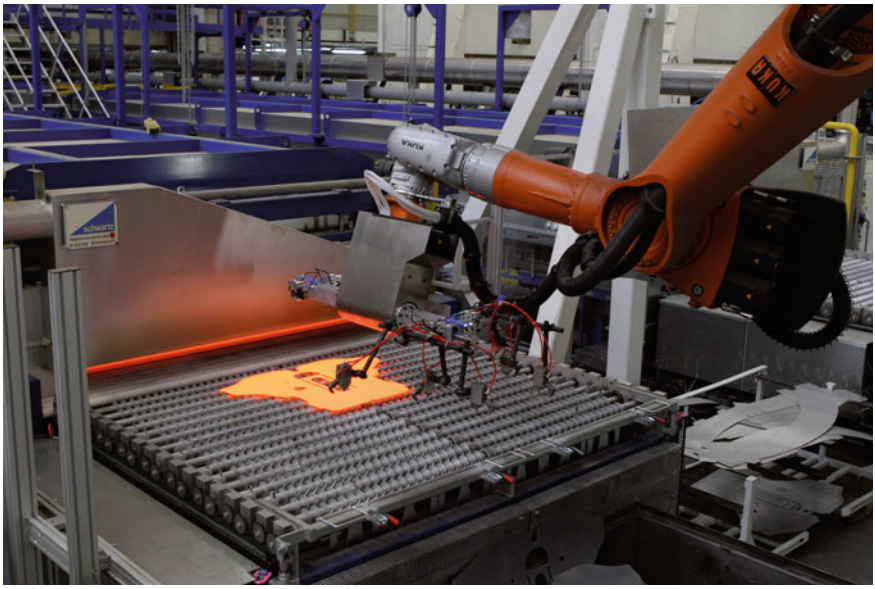

Fig. 5.5 Exit area with blank centering [7, 9]

5.1.2 Roller Hearth Furnaces with Tray

In typical roller hearth furnaces, the blanks may be placed on the ceramic rollers directly. In this case, the blank is only heated from the upper surface, which is suitable for thin blanks used in hot stamping process. The disadvantages of blank sitting on ceramic surfaces include the following:

(1) AlSi coating builds up on ceramic rollers, as shown in Fig. 5.4, causing them to be repaired or replaced frequently,
(2) Additional exit area with centering systems are needed (Fig. 5.5) which increase the space required and cycle time, as an additional centering operation has to be done [7, 8].

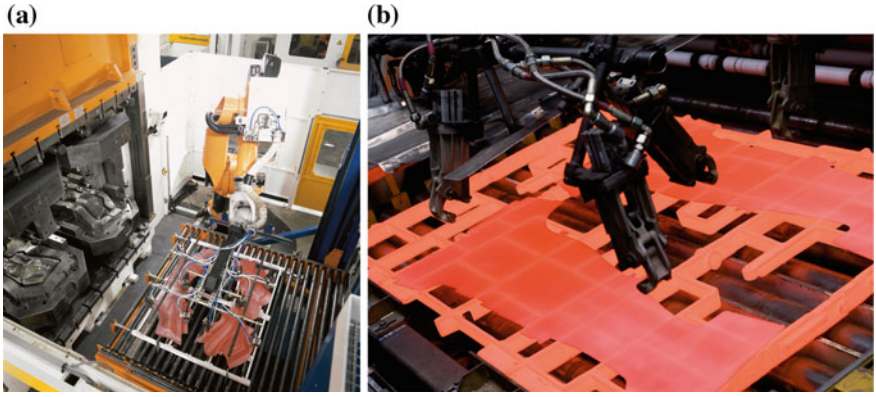

Fig. 5.6 Use of trays with roller hearth furnaces in: **a** indirect hot stamping [11] and **b** direct hot stamping [12]

One solution to both these problems is to use a "tray" in the roller hearth furnace. The cold blanks can be placed over the trays, and thus the blank will not be in contact with the rollers. It is also easier to center at the exit. Trays can also be preferred in indirect hot stamping where the blanks are already preformed (Fig. 5.6a). Two disadvantages of using tray are [5]:
(1) A secondary conveyor is required to bring the trays back into the furnace entrance,
(2) The blank may lose some heat where it touches the tray (this is visible in Fig. 5.6b).

More importantly, preformed components (either indirect or hybrid hot stamping) cannot be heated in the furnace without a support, Fig. 5.6a. For this reason, furnaces with tray are used in all plants which hot stamp preformed parts [8, 10].

If the trays are not allowed to cool down during their way back, the temperature gradient between the tray and the blank would be reduced. By optimizing this temperature gradient, in a particular process, a reduction of 570 kW in installed power was realized [5].

5.1.3 Multi-chamber Furnaces

Another furnace technique described by Eriksson, Multi-Chamber Furnace, reduces the space requirement and improves the control over the temperature. Here, each and every blank is placed in small furnaces and is heated for a predefined time. In a typical line, as illustrated in Fig. 5.7a, three fully automated robots are used [1, 5]:

(1) the first robot will take the blank from stack and place it in a buffer area,
(2) the second robot will take the blank from buffer area and put it in one of the furnace chambers,

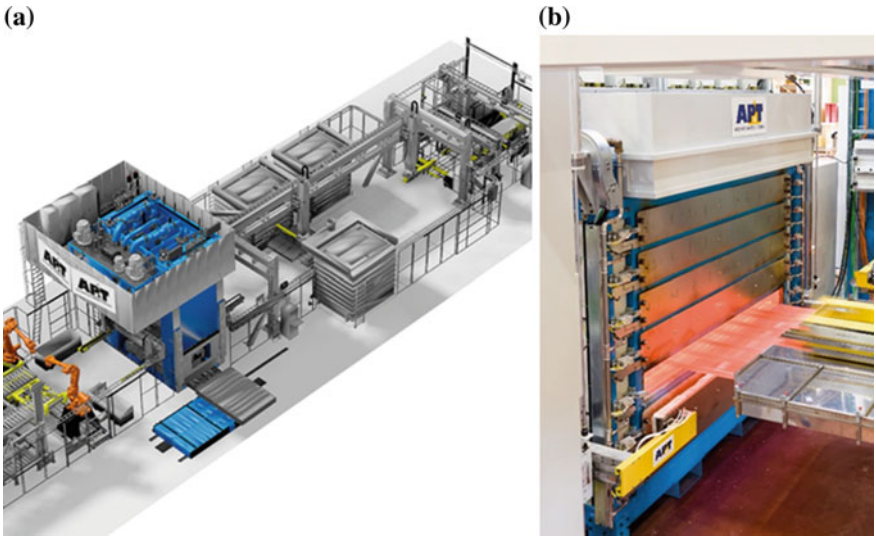

Fig. 5.7 **a** an overall schematic of a hot stamping line with multi-chamber furnaces, **b** unloading a heated blank from the furnace

(3) the third one will pick the heated blank from the furnace and put it in the press (Fig. 5.7b).

According to Kahl, this technique has been used in Gestamp plants at least since 2004, if not earlier [13]. The number of chambers depends on the cycle time of the process (t_{cycle}) and the heating time of the blanks ($t_{heating}$) and can be calculated by Eq. 5.2:

$$n_{chamber} = \frac{t_{heating}}{t_{cycle}} \rightarrow \text{e.g.: } \frac{330s}{15s} = 22 \tag{5.2}$$

According to Eriksson for this particular case, the roller hearth furnace would require ~35 m (115 ft) length (Eq. 5.1). However, a multi-chamber furnace would require 4–10 m (~13–33 ft) length and 6–10 m (~20–33 ft) width, depending on the layout [1].

5.1.4 Other Heating System Designs

According to Behrens [14], heating systems can be classified into two groups: (1) external or indirect heating, and (2) internal or direct heating. The typical furnaces explained until this section are all classified as external heating. Internal or direct heating techniques include conductive (Figs. 5.8b and 5.9c) and inductive (Figs. 5.8c and 5.9d) heating methods.

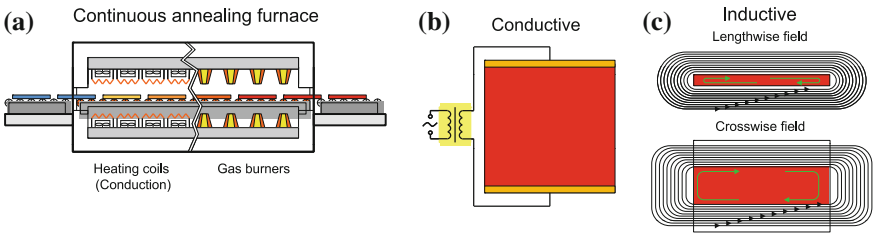

Fig. 5.8 **a** External heating, using heating coils or gas burners in a roller hearth furnace; internal heating using **b** electric current, **c** induction [14]

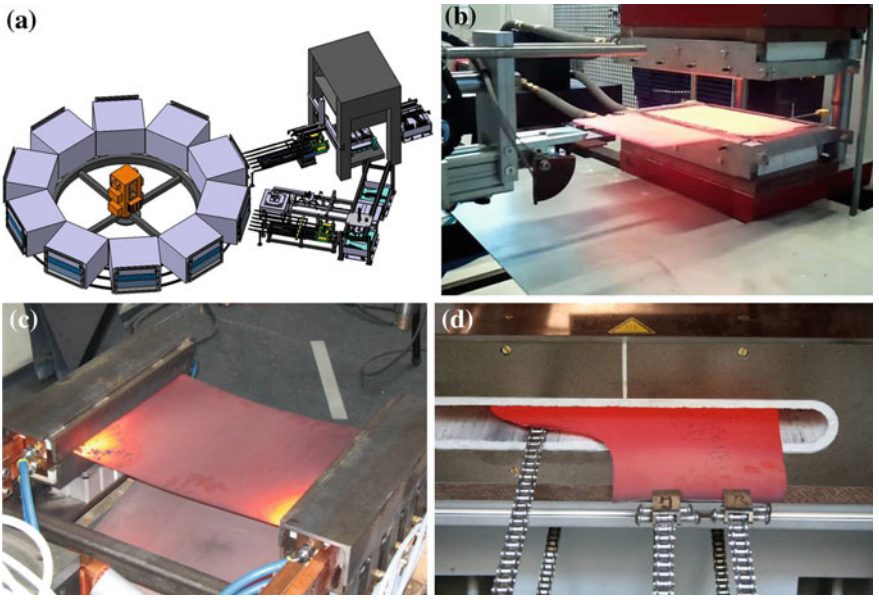

Fig. 5.9 Heating methods under development and/or for use in prototyping: **a** rotary furnaces [16], **b** hot plate/contact heating technique [18], **c** conductive heating [14] and **d** inductive heating [22]

Currently, several types of furnaces are used in the industry such as a double-decker or multi-chamber furnaces as discussed in the earlier sections. Another method, that is being developed for mass production is called “rotary roof furnaces”. One prototype of this type of furnace was set in Europe and being further tested, by Schuler [15]. Dalian University of Technology, in China, has also developed a rotary furnace as shown in Fig. 5.9a [16].

For prototyping purposes, hot plate heating or contact heating systems have been long used (Fig. 5.9b). In this heating technique, the blank sits on a flat heated die and is compressed with a second heated die. Using this method, it is possible to reduce the heating time. The heating cycle time is dependent on: (1) blank thickness, (2) temperature of the heated plates, (3) surface conditions and thermal contact

conductance (h_c) (Sect. 10.2.4) of the blank and heated plates, and (4) heat capacitance of the heated plates [17]. According to Ploshikhin [18], austenitization time of 15 s was feasible with contact heating (no information about blank thickness). A more recent study by Holzweißig showed that 3 s heating time was not enough to austenite the 1.5 mm thick blanks, but 6 s was possible. They also found that quick heating strengthens the part: after 10 s contact heating and rapid quenching, the steel was found to have 1850 MPa UTS. Thus, the strength of the steel is increased approximately 20% compared to furnace heating. In this study, uncoated blanks were used so coating diffusion was not studied [17]. Rasera used AlSi-coated blanks with contact heating. For the coating diffusion to be complete, their design required 21 s heating time [19]. Recently, Fraunhofer IWU has developed a contact heating device that can tailor the heating. For tailoring final part properties (see Chap. 8), several portions could be held at approximately 650 °C (~1200 °F). The system can heat 1.8 mm thick blanks in 15 s. Comparison of heating time of this technique with furnaces is given in Fig. 5.12a. As summarized in Table 5.1, contact heating does not have any geometric limitation and can heat the blanks to uniform temperatures [20]. Although it is a warm forming operation, in BMW i8 door beam production line, a similar heating system is used in production. Here the material was Aluminum 7075 alloy, and forming took place at 230 °C (~450 °F) [21].

Conductive heating (also known as, resistance heating or Joule heating) is known to work well with constant cross section parts [14, 23]. However, when the blank's cross section is not constant and only two electrodes are used, local hot spots may occur as shown in Fig. 5.10a. Behrens developed a new method with multi-electrodes to control the heating in nonuniform sections, Fig. 5.10b. By controlling different sections, it was also possible to get a tailored heating for soft zones [14].

Mori showed that it was possible to heat 1.2 mm thick steels from room temperature to 800 °C (~1500 °F) in only 2 s. Behrens showed that heating to 850 °C (~1550 °F) took 16 s, and heating to 950 °C (~1750 °F) took 20 s [14]. Both Mori and Behrens showed that rapid heating of uncoated blanks cause less scale formation compared to slow heating processes [14, 24]. Lee showed that heating rate of 100 °C/s (180°F/s) was possible, but caused AlSi coating to melt as shown in Fig. 5.11 [25].

One of the major drawbacks of conductive heating is that it cannot heat the area close to the conductors. Figure 5.12b shows that depending on the selected electrode geometry, areas close to the conductors were not fully hardened. Thus, the soft area could be trimmed and scrapped [26]. Liang showed that with a poorly designed conductor, the length of the unheated area may go up to 100 mm [27]. According to another study by the same group, thermal camera measurements show temperature at the contact point of electrodes were as low as ~300 °C(~570 °F) while 50 mm away the temperature of the blank was well over austenitization temperature (A_{c3}) [28].

Fast heating results in smaller grain sizes in martensitic structure and thus increases the strength and elongation at the same time [14, 30]. Liang showed that the tensile strength was increased ~7% and total elongation was increased by ~23% [28]. Senuma et al. used a slightly modified boron steel with higher Mn alloying

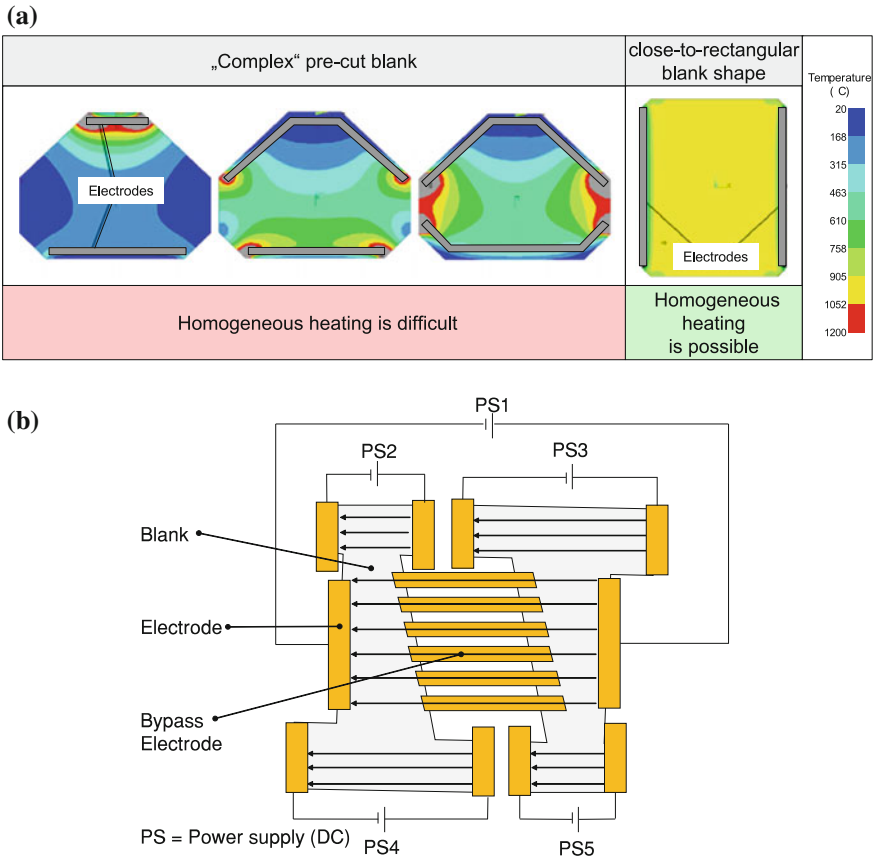

Fig. 5.10 In conduction heating: **a** with only two electrodes, it is not possible to get homogeneous heat distribution on complex shapes [14], **b** using bypass electrodes and separate power supplies for different five regions, homogeneous heating may be possible (recreated after [20])

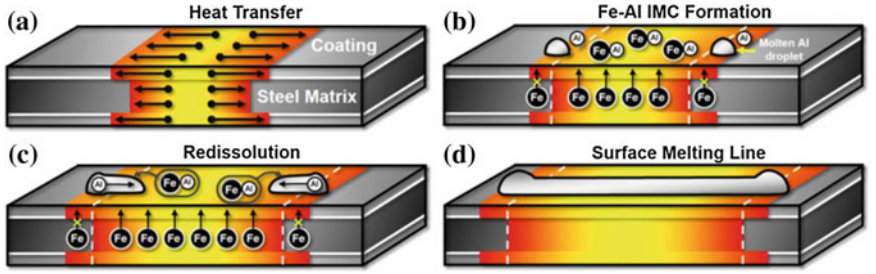

Fig. 5.11 Formation of surface melting line of AlSi coating [25]

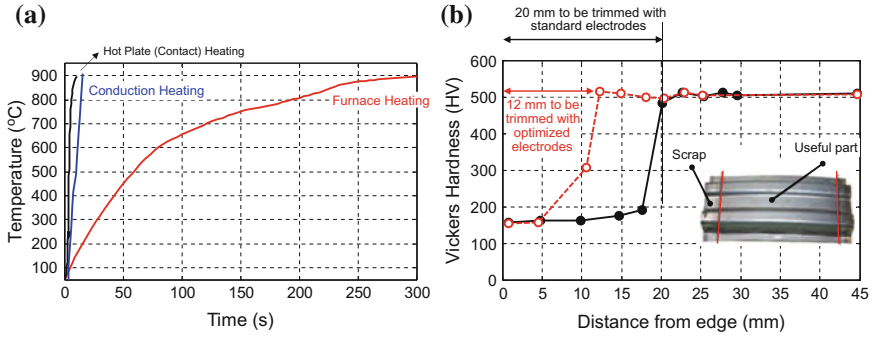

Fig. 5.12 **a** Comparison of heating times of different heating techniques (recreated after [19, 26, 29]), **b** when conduction heating is used, depending on the geometry some portions have to be trimmed off (recreated after [26])

Table 5.1 Summary of heating techniques [20]

	Roller hearth furnace	Infrared	Induction	Resistance	Contact
Time to A_3 (s)	300–360	50–70	20–30	5–10	15–30
Temperature distribution	Uniform	Uniform	Depends on coil geometry	No heating at the ends (Fig. 5.12b)	Uniform
Blank shape	No limitation	No limitation	Close to rectangle	Only rectangle (unless special measures are taken)	No limitation
Space requirement (m^2)	100–200	100–200	5–10	5–10	5–10
Energy efficiency	Low	Low	Medium	High	Low

(3 wt.% instead of 1.2 wt.% in 22MnB5), and found out that conduction heating increased the Charpy impact energy by threefold [31].

Conduction heating for press-hardening purposes had been patented many times [32, 33]. Currently, the technology is in mass production in Japan used in Lexus IS, since 2013. The parts produced are upper B-pillar reinforcement and cantrail, which have almost rectangular blank shapes. The process is used with Zn-coated blanks and surface conditioning (sandblasting, etc.) is not required [34].

5.1.5 Heating Time Reduction

There is also research going on how to reduce the heating time ($t_{heating}$). As of now, most of the production (with the typical material 22MnB5 and typical coating of 150 g/m^2 AlSi) require typically 5–6 min (300–360 s) in the furnace for the part to austenitize and the coating to diffuse. As shown in previous section, it is possible to austenitize the part in shorter time. However, homogeneous heating and the coating diffusion may require more time in the furnace. The coating diffusion is extremely important for most applications as it will affect: (1) weldability of the final part and (2) surface properties for painting [4]. Typically 30–420 s extra holding time is recommended for iron diffusion into AlSi coating [29].

If the time for heating could be shortened the initial investment and energy requirement for the furnace could be reduced drastically. Several alternative heating methods to reduce the time for heating ($t_{heating}$) include:

1. **Induction heating**: Induction heating is efficient and can heat the blank at a high rate ($\sim$ 70–100 °C/s, 125–180 °F/s) until Curie Temperature (T_{Curie}) which is around 740–760 °C ($\sim$1360–1400 °F) for 22MnB5. Both [35, 36] showed that heating up to Curie temperature would take 8–10 s. However, heating over T_{Curie} to A_{c3} has much lower efficiency. A possible solution was to use a more powerful face inductor to heat from T_{Curie} to A_{c3}, but the total time would be still around 70 s and the temperature distribution would not be uniform [22]. Heating the blank by using only induction heating is not suitable for hot stamping applications, unless these issues could be addressed: (1) the AlSi coating would be liquidized and the coating thickness would not be constant [4, 35, 37], (2) the uniform temperature distribution cannot be established over Curie temperature [22, 36]. Coryell and Belanger came up with the idea of "pre-diffused" blanks. In this technique, the AlSi coating on the steel is first diffused in a furnace. Pre-diffused coated blanks are later used with induction heating in the hot stamping line [38].
2. **Induction heating + furnace**: Induction heating cannot be used to keep the temperature constant. One solution to obtain uniform temperature distribution with inductive heating is to use induction as a quick preheating (i.e., heat up to Curie Temperature in 8–10 s), and then to use conventional furnaces for further heating the blank to its austenitization temperature [36, 37]. According to [36], a total time of 70 s was enough to homogeneously heat a blank with induction preheating. The paper did not discuss about coating diffusion.
3. **Infrared Heating**: uses infrared rays to heat the blank and can be classified into two: (1) Near Infrared (NIR) heating uses 0.7–2.5 μm wavelength created by halogen lamps at 2000–2800 °C ($\sim$3600–5000 °F), whereas (2) Far Infrared (FIR) uses 4–1000 μm wavelength [20]. Siebert et al., showed that it is possible to austenitize AlSi coated blanks in 30 s using NIR. However, the parts had a three-layer coating instead of five-layers, to have a five-layer coating higher cycle time was required [4]. Recently, FIR heating has been studied in Japan. The efficiency of this system is lower compared to NIR, but achieving uniform temperature distribution is easier. The austenitization times for 1.6 mm thick blanks were

measured to be 50*s* for uncoated blanks and 70 s for AlSi coated blanks [20]. Recently, a multi-chamber furnace based on FIR technique has been patented [39].

4. **Fluidized Bed/Immersing Heating**: A fluidized bed heater uses fine solid particles (powders) which are made to behave like fluid by pumping air inside the bed. Uniform heating can be achieved at high heating rates [40]. In a 2011 study, uncoated 22MnB5 materials were heated using a fluidized bed filled with Aluminum oxide powder and heated to 900 °C (∼1830 °F). Experiments with uncoated 22MnB5 steels showed that the method may reduce ($t_{heating}$) from 160 s to 40 s for 1.2 mm thick steels, and from 240 to 80 s for 2.4 mm thick steels. If the fluidized bed is heated to 1000 °C (1832 °F) the time required to heat a 2.4 mm thick blank would be reduced to 26 s. It was also possible to tailor the final hardness by partial austenitizing. This was done by immersing the workpiece partly into the fluidized bed [41]. A similar concept of immersing the blank into liquid zinc was proposed to both austenitize and coat the blanks in one step [42]. Neither concepts are in mass production.
5. **Use of Thinner Coatings**: As the weight or thickness of the coating on the blank is increased, the time the coating takes to diffuse increases. Thus, the time needed in furnace can be reduced by the penalty of corrosion resistance [43]. The most common AlSi coating today is applied at 150 g/m^2 (abbreviated as AS150). Since the last few years an 80 g/m^2 coating is also available as an option [44] (abbreviated as AS80). Studies have shown that the dwell time of AS80 in the furnace can be 2–4 min, which is almost halved compared to 6 minutes of AS150 coating [45, 46]. In cyclic corrosion tests, samples with AS80 coated blanks had twice the blister width compared to AS150 coated ones. On the other hand, AS80 with an additional 1 g/m^2 ZnO coating was found to outperform AS150 [47].

5.2 Material Handling Systems

Once the blank is heated, it is very important to start the forming process as soon as possible to reduce the heat loss. Depending on the production rate and the initial investment, material handling may be done manually, by a robot or by a linear feeding mechanism, as seen in Fig. 5.13. Typically blanks are carried by suction cups to the furnace and once they are heated and taken out from the furnace, they are carried with "grip fingers" [18, 48, 49].

As soon as the blank leaves the furnace, it loses its heat to environment both by radiation and convection. It is well known that the blank loses more heat by radiation than by convection when its temperature is over 100 °C (212 °F), as shown in Fig. 5.14a. The earlier material handling systems did not have a heat shield, and thus the blank would lose more heat, Fig. 5.14b [52]. This was not a problem when the material was thick. However, recently thinner gage materials were also employed, and the temperature drop in thin blanks without heat shield is much higher than thin blanks [29].

Fig. 5.13 Material handling systems: **a** manual handling [50], and **b** simple robot [18] are used for low volume production or tryouts; **c** industrial robot [51], and **d** linear feeders are used in mass production

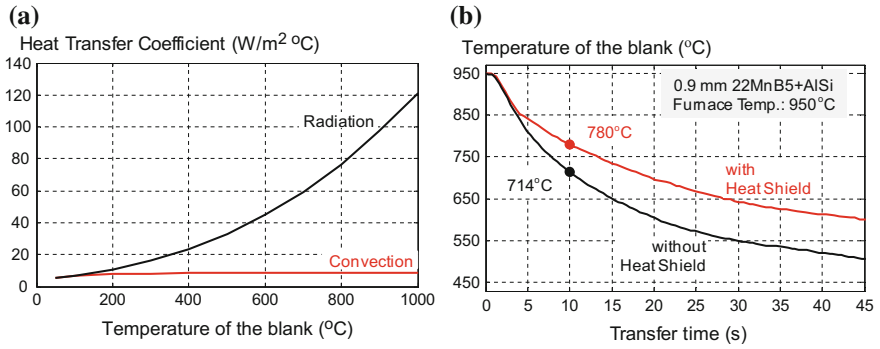

Fig. 5.14 **a** Radiation versus convection of steel with respect to its temperature (recreated using the data from [53]), **b** a comparison of heat loss during blank transfer (recreated after [52]), **c** earlier material handling systems lacked the heat shield [49], **d** recent systems have heat shield to reduce heat loss due to radiation [12]

To reduce heat loss during transfer from furnace to the die, it is essential to reduce radiation by reflective heat shields. However, the last step of transfer (i.e, right before leaving the blank on lower die) cannot be done with a heat shield. To reduce the heat loss, heat shield is brought as close to the die as the transfer system allows, the final transfer is done by a fast double-bar system to reduce the time in air, Fig. 5.15.

One other method to increase the production in the press is to use more than one dies in the press. Hot stamping dies do not require high force/energy compared to cold

Fig. 5.15 Material handling inside a heat shield as far as possible followed by handling with transfer feeder with two blanks at a time. The double-bar transfer system minimizes the time in open air

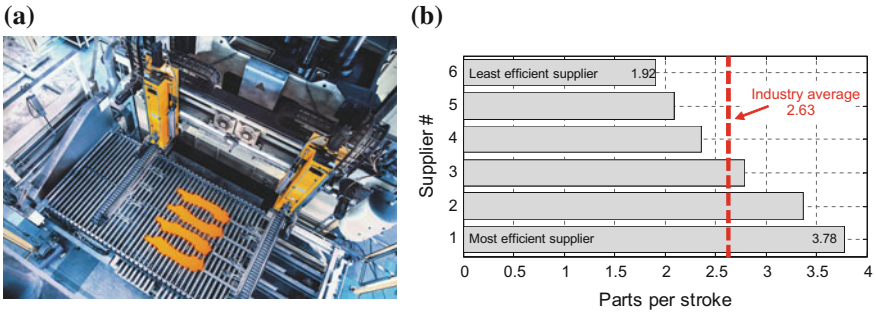

Fig. 5.16 **a** Material handling system modified to have 4 parts per stroke [58], **b** Comparison of major hot stamping suppliers efficiency in 2011, measured by parts produced per stroke [57]

stamping of high strength steels. Therefore a typical 800 ton (8000 kN) press can form and quench more than one part. Material handling systems have to be updated to have the ability of transferring more than one blank at a time. Schuler has developed "PCH 4-out" where four blanks can be transferred and formed at one stroke, Fig. 5.16a. It is even possible to produce 8 parts per stroke using double-attached blanks (i.e., four blanks, but eight parts) [15]. Similarly, Amino and AP&T have designed automated lines with up to 8 parts per stroke (4 double-attached blanks) [54–56]. According to a study in 2011, global suppliers with over 10 million parts per year capacity had on average 2.63 parts per stroke, Fig. 5.16b [57]. It is important to notice that the difference between the so-called the "least efficient supplier" and the "most efficient supplier" is almost two-fold.

5.3 Hot Stamping Presses

In hot stamping applications, the press has to operate at five different conditions [37, 59]:

(1) Fast approach: almost no force, at high speed,
(2) Forming: relatively low force requirement, at high speed,
(3) Quenching: highest force requirement for a long dwell at the bottom dead center (BDC),
(4) Fast return: almost no force, high speed,
(5) Dwell at top: for material handling to remove the formed part and leave the next cycle's blank.

Since there is a dwell at the (BDC), mechanical presses cannot be used. Typically, a conventional double-action hydraulic press or a single action hydraulic press with or without die cushion is used for hot stamping operations. The majority of the presses in hot stamping production worldwide are of the conventional hydraulic press with more or less developed technological solutions. In the next subsections, several types of presses that are already in mass production and those which are under R&D phase are examined in detail.

5.3.1 Direct Drive Hydraulic Press

A direct drive hydraulic press uses pump(s) to deliver a certain volume flow ($\dot{Q}$), depending on the pump type and motor rpm (ω). To speed up the press motion (V), more volume flow ($\dot{Q}$) is required. The press would generate force (F) only when there is a reaction force on the slide, such as forming load. Since hydraulic oil is compressible, to build up force, the oil column has to be compressed first. Thus, it takes some time to build up the force required. The power (P) required is the multiplication of force (F) and slide velocity (v) plus the mechanical and electrical losses [56, 60].

During fast approach, there is almost no force generated ($F = 0 \rightarrow P = Fv = 0$), so very low power is required. To reduce the cooling of the blank, the forming has to be done as fast as possible. Thus, during forming stage, high slide velocities in the order of 350–1000 mm/s (~800–2400 IPM) are desirable. Although forming forces are lower compared to cold forming, due to high slide velocity, forming is the most power requiring stage. During quenching—the longest portion of the cycle—the force is at maximum but the slide velocity is zero, resulting in almost no power consumption ($v = 0 \rightarrow P = Fv = 0$). While returning the slide to top dead center (TDC), the press has to carry the load of the slide and the upper die. To shorten the cycle time, return speed has to be as high as possible as well. The press would consume almost no power while waiting for the automation. An example power–time curve is shown in Fig. 5.17 [37, 56, 59–62].

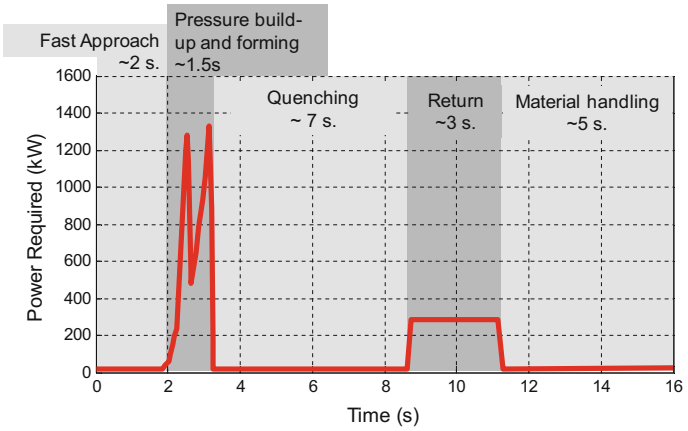

Fig. 5.17 Power requirement of a 1,600 tons direct drive hydraulic press during an example hot stamping cycle (recreated after [37])

Direct drive hydraulic presses do not have an energy storage, so the power required during forming has to be pulled from the grid. As seen in Fig. 5.17, if a direct drive hydraulic press is to be used in hot stamping, very high installed power may be required. However, the press will only use the maximum power for a short portion of the cycle. To reduce the requirement of installed power, a smaller pump can be used with a hydraulic accumulator. When the press is idle, the pump fills the accumulator, and when high flow rate is required, the fluid is provided by the accumulator [59, 60].

5.3.2 Accumulator Drive Hydraulic Press

A hydraulic accumulator has to be charged to its maximum pressure to ensure the availability of nominal press force during quenching at the bottom dead center [60]. At the beginning of the cycle, the pressure of the accumulator is applied to the piston, generating very high force, Fig. 5.18a [59]. Since there is no reaction on the slide, the slide accelerates quickly. An accumulator driven press is faster than a direct drive press. In a selected deep hot stamped part, Fig. 5.18b, the quenching time was 11 s, and depending on the hydraulic press drive the forming cycle was either 1 or 3 s. Considering the total time (12 s instead of 14 s) a ∼16% increase in output could be achieved by using an accumulator drive press [48]. The differences between the available force from the hydraulic accumulator system and the actual force required during forming the blank are waste of energy. Accumulator driven presses also have high maintenance costs due to complicated valve systems and additional hydraulic components [59, 60].

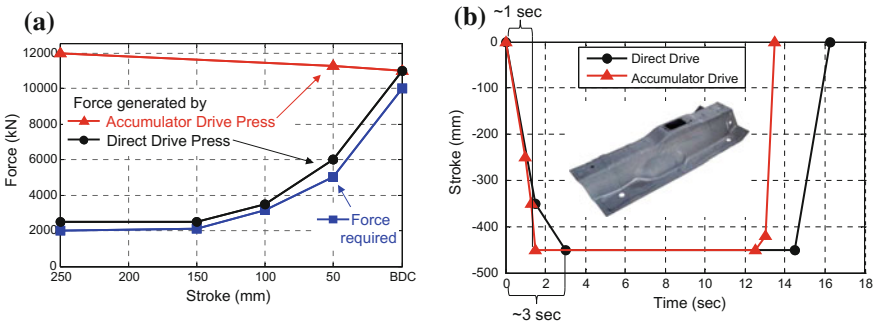

Fig. 5.18 Comparison of direct drive and accumulator drive presses in terms of: **a** force generation in 1200 ton press (recreated after [59]), **b** cycle time of an actual product requiring high force over a long drawing distance (recreated after [48])

Fig. 5.19 Hydraulic "gearbox" activating the five cylinders in steps following the actual need of press force

5.3.3 Multi-cylinder Hydraulic Press

One method to save and utilize the energy in an efficient way is using multiple cylinders and activating them separately when needed, Fig. 5.19. For "low force–high speed", such as fast approach and return, only one cylinder is activated. When the force needed increases, the system activates other cylinders, at the expense of slide velocity. During quenching, all cylinders are activated to increase the contact pressure between the die and the formed part. Since all cylinders could be controlled separately, the system can compensate for some off-center load as well. The drive system could be direct or accumulator type [48].

5.3.4 Flywheel Hydraulic Press

As discussed earlier, hydraulic accumulators are not energy efficient when they are not used at the maximum pressure. This also means that the efficiency of the press

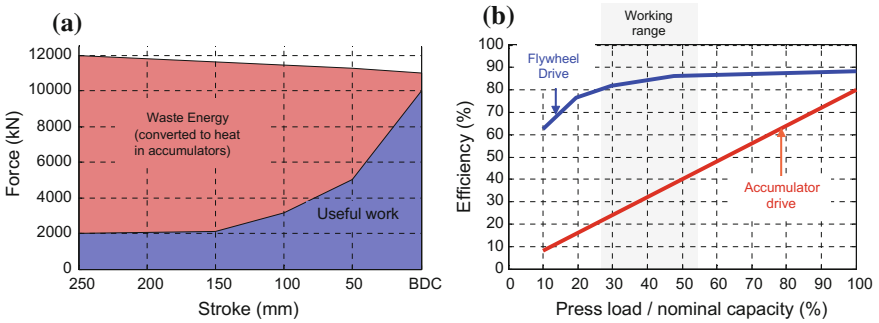

Fig. 5.20 **a** Efficiency calculation for an accumulator drive press (modified from Fig. 5.18a), and **b** Energy efficiency of flywheel hydraulic presses compared with accumulator drive press (recreated after [49])

is lowered when it is used at lower forces than the nominal capacity. [59]. As shown in Fig. 5.20a, for this given example the total efficiency was approximately 30%. Storing energy in a flywheel, rather than a hydraulic accumulator has been proposed by Schnupp [37, 63] and Schuler [64] as an efficient way of reducing the installed power.

The presses from Schnupp are available from 600 to 1,600 tons capacity. The flywheel is directly mounted between the electric motor and the pump. A press may have up to three flywheel pump units and can be driven by one, two or three of them depending on the force/energy demand. The system is claimed to reduce the energy consumption and installed electric power. It has to be noted that, when the power required by the press is higher than the installed power (in case of preforming and forming), the flywheel will slow down and supply the energy. When the power required is less than the input (i.e., in quenching), the flywheels would speed up and store the excess energy [37, 63].

Schuler has also patented a similar flywheel driven hydraulic press design, specifically for hot stamping purposes. In this design, there is only one flywheel to which three pumps are mounted. Another (fourth) hydraulic pump is mounted on an electric motor and can charge the flywheel from return line, when needed. The system is said to be more efficient than a comparable accumulator drive especially at 30–50% of the nominal load, where most hot stamping "forming operations" are done, Fig. 5.20b. Schuler has named this system as "HED" High Efficiency Drive [59, 64].

Multi-point Cushion System

In hot stamping dies, as explained in more detail in Chap. 6, blankholders and pads are typically used. These could be actuated by springs, gas cylinders or hydraulic cylinders installed in the die set. Another method of actuating (moving the die components and/or applying force on them) these die components is to use a cushion system which is a part of the press [65].

Cushion systems were originally developed for cold deep drawing operations. In a typical deep draw press, the blankholder sits on a number of cushion pins,

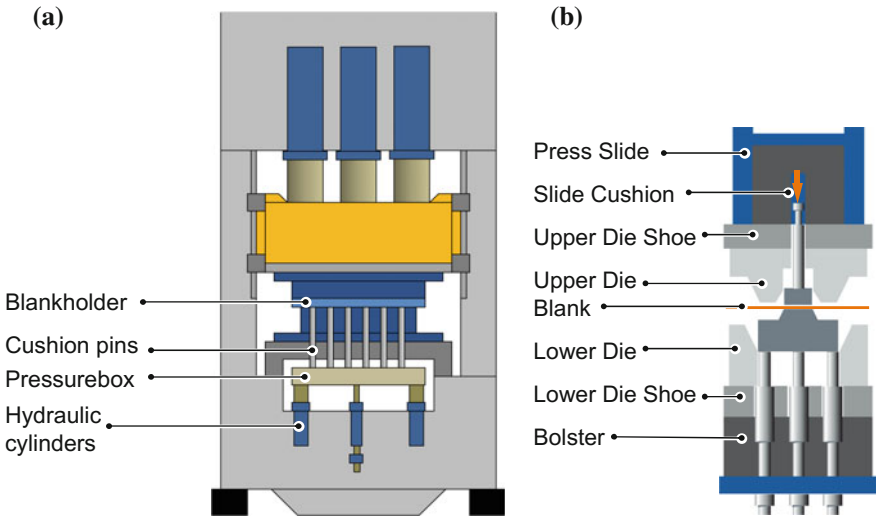

Fig. 5.21 Cushion systems in hot stamping hydraulic presses: **a** hydraulic cushion with pressure box (recreated after [66]), **b** multi-point cushion system for hot stamping purposes [70]

which are actuated by the pressure box below the bolster plate. A conventional cushion system is shown in Fig. 5.21a. Due to elastic deflection in pressure box and possible variations in cushion pins' height, uniform blankholder pressure may not be sustained. In practice, die spotting and/or shimming is done to improve the uniformity of blankholder pressure [61, 66].

To control the blankholder pressure instead of a pressure box and cushion pins, a series of hydraulic cylinders may be used to apply force directly on the blankholder. According to Altan and Penter, multi-point cushion systems have already been developed as early as 1991 [67].

Schuler has developed a series of hydraulic presses with multi-point cushions in the slide and in the bed to maintain a uniform contact pressure. The presses equipped with this cushion systems are commercially named as PCH, Pressure Controlled Hardening [65, 68].

According to Aspacher [69], these presses have been around since 1990's. One of the earliest designs had four separate bed cushions and four separate cushions on the slide, each generating up to 300 ton force [65]. This design was replaced by a 23 pins in the bed and 10 pins in the slide [68]. The latest design now has 105 separate cushion pins, each can apply up to 315 kN force [70].

By using a number of cushion pins, each controlled separately, it is possible to compensate for: (1) thickness variation of the blank, (2) slide tilting, (3) die wear.

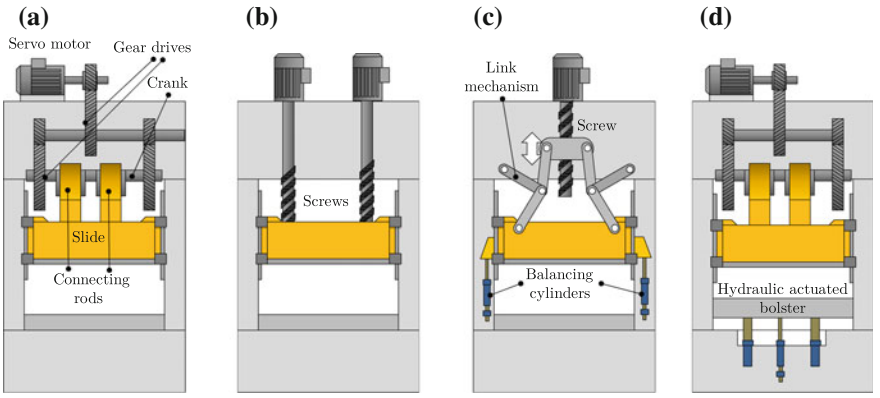

Fig. 5.22 Servo presses for hot stamping: **a** Mechanical (crank-type) servo press, **b** spindle press (screw-type servo press), **c** mechanical link servo press, and **d** hybrid press with hydraulic actuated bolster (recreated after [56, 73–75])

5.3.5 Servo-Mechanical Press

A servo-mechanical press is a press with crank, eccentric gear (Fig. 5.22a) or linkage drives (with or without ball screw, Fig. 5.22c) powered by a servo motor [71]. Theoretically, servo presses may have unlimited motion control and could be faster than hydraulic presses. Thus, they can complete a fast forming stage and can dwell at the bottom during quenching time. In practice however, servo-mechanical presses had two drawbacks for hot stamping processes [3, 56, 72, 73]:

(1) A servo-mechanical press is typically position (and speed) controlled, but not force. Unless a secondary control system is added, the force during quenching may not be constant due to dilatation/contraction of the tool and thinning of the blank due to forming.
(2) Restarting the press under load at BDC could damage the guides and bushings in crank or eccentric gear servo presses. A redesign in these components is advised for using servo-mechanical presses for long term in hot stamping.

Recently, several inventors and press makers have designed special servo mechanical hot stamping presses to address these problems.

Wood [74], for example, designed a hybrid hydraulic and servo-mechanical press, Fig. 5.22d. In this press, forming is done by the crank-slider mechanism of the top drive. Forming is completed when the slide is at the BDC. At this point the press may apply up to 200 tons force. During quenching, the bolster is actuated by hydraulic cylinders and may apply up to 1700 tons force. Although similar presses are known to be manufactured for cold stamping/coining operations [61], there is no information if such a press is being used in mass production hot stamping.

Japanese press maker Amino has already commercialized a servo press for hot stamping applications. A schematic (not exact representation) of this press is shown

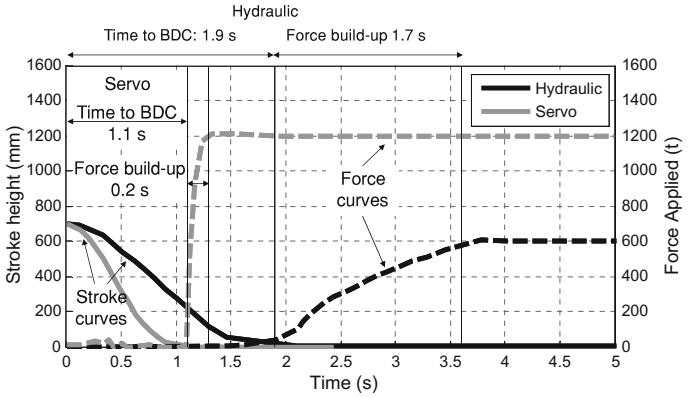

Fig. 5.23 Comparison of hydraulic and servo-mechanic presses in stroke-time and force-time (recreated after [56])

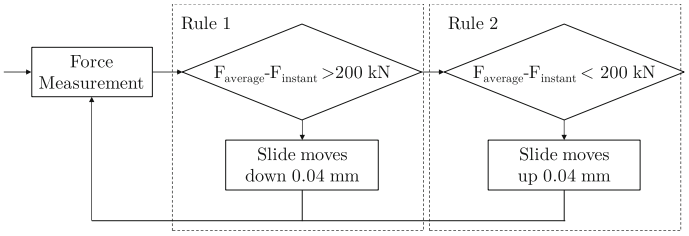

Fig. 5.24 Block diagram of servo-press force control system (recreated after [72])

in Fig. 5.22c. The press is equipped with a force control system. If the instant load on the slide is ±7.5% out of the set value, the screw mechanism would adjust the position of the slide [56]. Maki et al., studied a 1200 ton servo press and found that it could generate the maximum force in almost 0.2 s. In comparison, a 600 ton hydraulic press took 1.7 s to build up its maximum force. This is because, in a hydraulic press, the oil column has to be compressed first. Servo press, as expected, also had an advantage in die close time (i.e., time to BDC). Details can be seen in Fig. 5.23 [56].

Wang et al. [72], at Huazhong University of Science and Technology, have designed a responsive control system for a 600 ton (6000 kN) servo-mechanical press [76]. A simple logic control with only two rules were applied, Fig. 5.24. The system allowed the servo press to apply a stable quenching force at the BDC.

Researchers at the Fraunhofer IWU, Chemnitz, used a spindle (screw-type servo) press as shown in Fig. 5.22b. The machine also had a servo cushion with screw system [75]. By synchronizing cushion and ram in a patented pulsation mode, the gap between the blankholder and die is changed with time. During deep drawing phase, the gap is increased instantly to lower the thinning and the strain around the punch radius. The wrinkles caused by high gap are flattened with a “return” stroke of

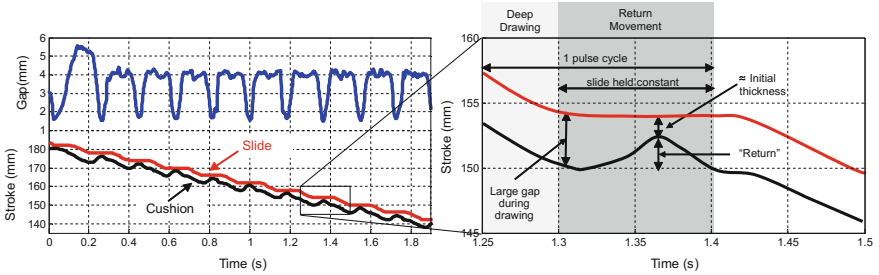

Fig. 5.25 Stroke–time curve of the slide (ram) and cushion. The gap is controlled with time to facilitate drawing and to reduce the wrinkles (recreated after [75])

Table 5.2 Maximum draw depth with cushion-ram pulsation [75]

Process type	Slide speed (mm/s)	Max. Draw Depth (mm) with		
		2 mm Gap	3 mm Gap	4 mm Gap
Conventional	10	22	24	26
Conventional	200	24	25	26
CRP	10	25	46	46
CRP	200	24	46	46

the cushion, while the slide is held stationary, Fig. 5.25. By using this "cushion-ram pulsation" (CRP) method, deeper parts could be manufactured. Table 5.2 shows the improvement in draw depth with this system. Although a hydraulic press could also be programmed any stroke–time profile, a servo press can stop and move the cushion up and down much faster than a hydraulic press. Note that, in the particular example shown in Fig. 5.25, a total of 10 pulses are realized in less than 2.0 s.

Fagor has been developing servo presses for hot stamping since 2013. The first installation was done in 2015. Fagor chose to use the mechanical (eccentric gear-type) servo press for hot stamping (similar to Fig. 5.22a). To make the press capable of hot stamping, a number of modifications were done. These include a force control system, similar to the one described earlier in Fig. 5.24. In addition, since these presses were designed for long-term mass production, the connecting rod and bushing systems were modified to withstand the damages that may be caused by dwell at the BDC, Fig. 5.26. Another modification was a new system that would start the press at the BDC under load [73].

In a servo-mechanical press, as there is no hydraulic oil and risk of leakage, fire risks are reduced [3]. By using energy recovery mode, a servo press can generate electricity while it is slowing down. For comparison purposes, an example hot stamping cycle was run in a hydraulic press and a servo press. As seen in Fig. 5.27, servo press not only improves the cycle time by almost 1 s, but also saves ~35% energy [73].

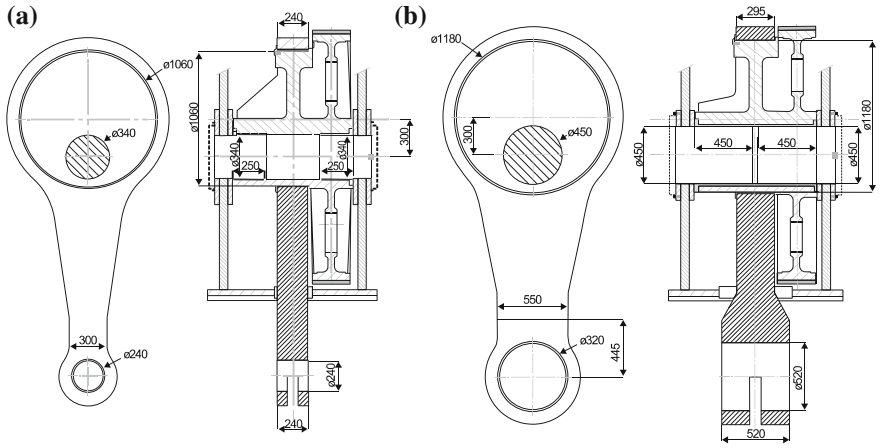

Fig. 5.26 Connecting rod and bushing design of **a** typical servo-mechanical press, **b** servo-mechanical press designed for hot stamping [73]

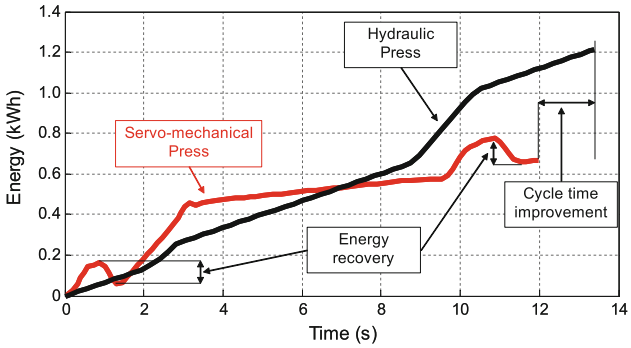

Hot stamping cycle	
Total Stroke	950 mm
Drawing Stroke	300 mm
Drawing Force	4,000 kN
Quenching Force	10,000 kN
Quenching Time	6 sec.

Fig. 5.27 Comparison of cycle time and energy consumptions of servo-mechanical and hydraulic presses (re-created after [73] with additional information from A. Ormaetxea)

5.4 Hot Stamping Lines by Capacity

The automotive industry has to offer more variants of cars, in much shorter development times and for shorter production periods, compared to a few decades ago. For example, BMW had only five different models in 1980 (3, 5, 6, 7 series and M1), whereas in 2015, there were 22 different BMW series [77]. Although car makers are taking advantage of part and platform commonality to reduce the number of different parts to be produced, still in the upper body a number of "exclusive to variant" parts have to be produced [78]. For these reasons, there is a demand for at least two types of lines: (1) small volume production lines for model exclusive parts, and (2) mass production lines for platform parts and/or high volume cars [52].

The Spanish press maker Loire Safe (later acquired by Gestamp and renamed as Loire Gestamp), introduced three tailored lines in 2011: Large, Medium and Small lines. In the small line a low die height 630 ton press was used, whereas the medium and large lines have larger presses and longer furnaces. The large line is also offered with a moving bolster to speed-up die changing [79, 80].

Similarly, German press maker Schuler also offers at least two different press hardening lines. In the PCH Hardline, a 600 ton press with 3.0 m × 1.2 m table is offered. The press has 23 cushion pins in the bolster, generating a total of 300 ton force. Additional 10 pins are installed in the slide to apply 250 ton force. The furnace length is limited to 20 m (65 ft). The line is optimized for 8–15 s cycle time and may be offered with a tandem die change cart system. The standard version is optimized for 1–2 parts/stroke. For higher production volume, Hardline Pro is offered. In this version, the press is a 1200 ton, with an array of 105 cushion pins. This version has a T-track bolster system for quick die change, and is offered with a 25 m (82 ft) long furnace and can produce up to four parts per stroke. Last, there is a Hardline twin, very similar to Hardline Pro in terms of dimensions but has two separate slides, each can apply 600 ton force. The slides could be synchronized or used separately. This version is offered with 60 m (197 ft) long furnace [59, 64, 70].

A recent development by Schnupp presses in collaboration with Neue Materialen Bayreuth is a vertical hot stamping line for small parts production. In this line, a contact-type heater is installed over a horizontal hydraulic press with 50 ton capacity, as shown in Fig. 5.28. Once the blank is austenitized the contact plates open, and the heated blank is moved very quickly to the hydraulic press with the help of gravity. The system can form thin materials (0.5–0.8 mm) and requires only 4–5 m^2 (~43–54 sq.ft) floor space. A working prototype has been introduced in EuroBlech 2016 [81–83].

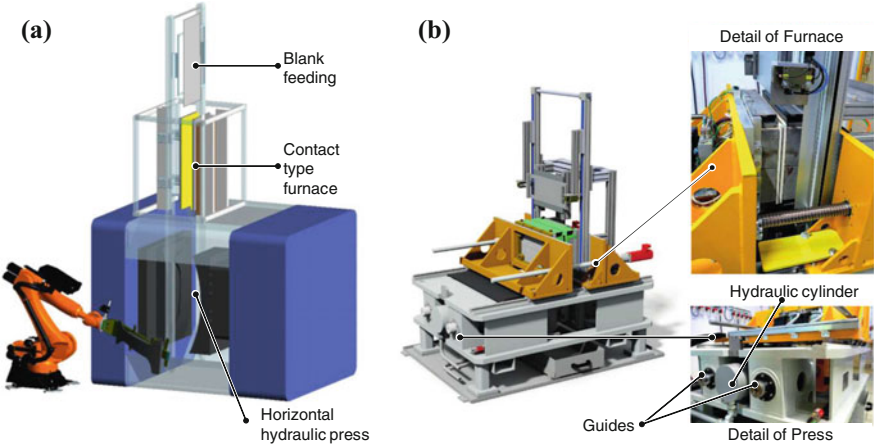

Fig. 5.28 Vertical press hardening line, "VertPress": **a** concept (recreated after [81]), and **b** photo of the system with details [82])

References

1. K. Eriksson, Bringing it together. Presented at AP&T Press Hardening, Next Step Seminar, Novi, MI (2010). Accessed 15 Sep 2010
2. H. Karbasian, A.E. Tekkaya, A review on hot stamping. J. Mater. Process. Technol. **210**(15), 2103–2118 (2010)
3. E. Gamboa, X. Agirretxe, J.M. Martin, K. Gorostiza, Compact line conception for hot forming lines, in *3rd International Conference on Hot Sheet Metal Forming of High Performance Steel, CHS2, Kassel, Germany* (2011), pp. 181–187
4. P. Siebert, M. Alsmann, H.J. Watermeier, Influence of different heating technologies on the coating properties of hot-dip aluminized 22MnB5, in *3rd International Conference on Hot Sheet Metal Forming of High Performance Steel, CHS2, Kassel, Germany* (2011), pp. 457–464
5. H. Lehmann, Developments in the field of schwartz heat treatment furnaces for press hardening industry, in *3rd International Conference on Hot Sheet Metal Forming of High Performance Steel, CHS2, Kassel, Germany* (2011), pp. 171–179
6. F.J. Ebner, Hotphase - press hardening automotive solutions by EBNER, in *3rd International Conference on Hot Sheet Metal Forming of High Performance Steel, CHS2, Kassel, Germany* (2011), pp. 247–253
7. H. Lehmann, Furnaces for press hardening. Presented at AP&T Press Hardening, Next Step Seminar, March 24, Shanghai, China (2010)
8. H. Lehmann, Roller hearth furnaces for hot-form hardening. IDDRG Graz Austria **2010**, 131–140 (2010)
9. Volkswagen Media Services, http://www.volkswagen-media-services.com
10. V. Uthaisangsuk, Hot stamping of ultra high strength steel: a key technology for lightweight automotive design. Presented Automotive Summit 2014, June 19–20, Bangkok, Thailand (2014)
11. Schuler. Hot forming systems: light-weight in volume production. Product catalogue (2006)
12. Audi Media Services, http://www.audi-mediaservices.com
13. M. Kahl, Some like it hot. *Automotive Manufacturing Solutions* (2004), pp. 49–52
14. B.A. Behrens, S. Hübner, Conductive heating in press-hardening process. Presented at Doors and Closures in Car Body Engineering 2011, November 16–17, Bad Nauheim, Germany (2011)
15. Schuler. Private communication (2013)
16. P. Hu, L. Ying, B. He, *Hot Stamping Technology and the Main Equipment* (Springer, Singapore, 2017), pp. 19–44
17. M.J. Holzweissig, J. Lackmann, S. Konrad, M. Schaper, T. Niendorf, Influence of short austenitization treatments on the mechanical properties of low-alloy steels for hot forming applications. Metall. Mater. Trans. A **46**(7), 3199–3207 (2015). Jul
18. V. Ploshikhin, A. Prihodovsky, J. Kaiser, R. Bisping, H. Lindner, C. Lengsdorf, K. Roll, New heating technology for the furnace-free press hardening process, in *Proceedings of TTP 2011* (2011)
19. J.N. Rasera, Development of a novel technology for rapidly austenitizing usibor 1500p steel (2015)
20. K. Mori, P.F. Bariani, B.A. Behrens, A. Brosius, S. Bruschi, T. Maeno, M. Merklein, J. Yanagimoto, Hot stamping of ultra-high strength steel parts. *CIRP Annals - Manufacturing Technology* (2017)
21. M. Reinstettel, The door sidecrash beam ın the new BMW i8: application of a press hardened 7xxx aluminium alloy panel, in *Proceedings of 5th International Conference on Accuracy in Forming Technology (ICAFT 2015)* (2015), pp. 349–356
22. R. Kolleck, R. Veit, M. Merklein, J. Lechler, M. Geiger, Investigation on induction heating for hot stamping of boron alloyed steels. CIRP Ann. - Manuf. Technol. **58**(1), 275–278 (2009)
23. M. Uslu, Docol 22mnb5 Çeliğinin balistik Özelliklerinin İncelenmesi (investigation of ballistic proerties of docol 22mnb5 steel - in turkish) (2007)
24. K. Mori, S. Maki, Y. Tanaka, Warm and hot stamping of ultra high tensile strength steel sheets using resistance heating. CIRP Ann. - Manuf. Technol. **54**(1), 209–212 (2005)

25. C.W. Lee, W.S. Choi, Y.R. Cho, B.C.D. Cooman, Microstructure evolution of a 55 wt. hardening steel during rapid heating. Surf. Coat. Technol. **281**, 35–43 (2015)
26. B.A. Behrens, S. Hübner, S. Schrödter, J. Uhe, Conductive heating opens up various new opportunitites in hot stamping, in *Proceedings of 5th International Conference on Accuracy in Forming Technology (ICAFT 2015)* (2015), pp. 157–174
27. W. Liang, L. Wang, Y. Liu, Y. Wang, Y. Zhang, Hot stamping parts with tailored properties by local resistance heating. Procedia Eng. **81**, 1731–1736 (2014); 11th International Conference on Technology of Plasticity, ICTP 2014, 19-24 October 2014, Nagoya Congress Center, Nagoya, Japan
28. W. Liang, Y. Liu, B. Zhu, M. Zhou, Y. Zhang, Conduction heating of boron alloyed steel in application for hot stamping. Int. J. Precis. Eng. Manuf. **16**(9), 1983–1992 (2015). Aug
29. K. Steinhoff, Retaining control of complexity - the real challenge in contemporary hot stamping, in *4th International Seminar on Hot Sheet Metal Forming Technology* (2016), pp. 9–40
30. C. Lobbe, O. Hering, L. Hiegemann, A.E. Tekkaya, Setting mechanical properties of high strength steels for rapid hot forming processes. Materials **9**(4), 25 (2016)
31. T. Senuma, Y. Takemoto, Effect of rapid heating on evolution of microstructures and coating layers in hot stamping processes, in *3rd International Conference on Hot Sheet Metal Forming of High Performance Steel, CHS2, Kassel, Germany* (2011), pp. 465–472
32. M. Terziakın, Instant heating process with electric current application to the workpiece for high strength metal forming, US Patent 6,463,779 (2002)
33. K. Ishiguro, M. Furuhashi, Hot press forming apparatus and hot press forming method, US Patent 9,206,488 (2015)
34. A. Mikuni, T. Sagisaka, T. Shiga, The new lexus is. Presented at EuroCarBody 2013, September 25–26, Bad Nauheim, Germany (2013)
35. R. Kolleck, W. Weiß, P. Mikoleizik, Cooling of tools for hot stamping applications. IDDRG Graz Austria **2010**, 111–119 (2010)
36. H. Schülbe, M. Jestremski, B. Nacke, Induction heat treatment for press hardening process, in *3rd International Conference on Hot Sheet Metal Forming of High Performance Steel, CHS2, Kassel, Germany* (2011), pp. 481–488
37. R. Hund, M. Braun, Continuous improvement of hot forming technology, in *3rd International Conference on Hot Sheet Metal Forming of High Performance Steel, CHS2, Kassel, Germany* (2011), pp. 189–200
38. J.J. Coryell, P.J. Belanger, Pre-diffused Al-Si coatings for use in rapid induction heating of press-hardened steel, US Patent 9,677,145 (2017). Accessed 13 June 2017
39. S. Aikawa, Far infrared heating furnace for steel plate for hot pressing, US Patent 9,677,145 (2017)
40. S.K. Chaudhury, D. Apelian, Fluidized-bed: high efficiency heat treatment of aluminum castings. Heat Treat. Prog. **7**(6), 29 (2007)
41. T. Marten, T. Troster, S. Adelbert, A. Kadim, Fluidized bed heating of blanks for the hot forming process, in *3rd International Conference on Hot Sheet Metal Forming of High Performance Steel, CHS2, Kassel, Germany* (2011), pp. 473–480
42. R. Neugebauer, R. Müller, A. Bester, Innovative concept for combining the austinitization and surface coating of steel into one step. Proc. Inst. Mech. Eng. Part B: J. Eng. Manuf. **226**(7), 1281–1284 (2012)
43. T. Kurz, New developments in zinc coated steel for press hardening. Presented at Insight Edition Conference, September 20–21, Gothenburg, Sweden (2011)
44. J. Watkins, Material development. Presented at AP&T Press Hardening, Next Step Seminar, Novi, MI (2011)
45. R. Aldén, Metallurgical investigation in weldability of aluminium silicon coated boron steel with different coating thickness. *Bahcelor Degree Thesis, KTH Royal Institute of Technology, Stockholm, Sweden* (2015)
46. M. Windmann, A. Röttger, W. Theisen, Formation of intermetallic phases in Al-coated hot-stamped 22MnB5 sheets in terms of coating thickness and Si content. Surf. Coat. Technol. **246**, 17–25 (2014)

47. S. Fujita, S.J. Maki, H.I. Yamanaka, M. Kurosak, Corrosion resistance after hot stamping of 22MnB5 steels aluminized with 80g/m2 c.w. and ZnO coating, in *5th International Conference on Hot Sheet Metal Forming of High Performance Steel, CHS2, Toronto, ON, Canada* (2015), pp. 681–690
48. J. Karlsson, Press requirements. Presented at AP&T Press Hardening, Next Step Seminar, Novi, MI (2010). Accessed 15 Sept 2010
49. Schuler Inc. Press hardening with pch (2008)
50. voestalpine Media services, http://www.voestalpine.com/group/en/press
51. L.A. Kren, Specialty hydraulic press. Metal Forming Magazine (2015), pp. 20–23
52. M. Skrikerud, Next generation of compact hot forming lines for optimised throughput with different materials. Presented at Forming in Car Body Engineering 2014, September 24–25, Bad Nauheim, Germany (2014)
53. A. Shapiro, Finite element modeling of hot stamping. Steel Res. Int. **80**(9), 658–664 (2009)
54. Schuler. PCH 4-out. *Newsletter Special Edition - PCH Technology* (2010)
55. P. Josefsson, General outlook - the future for press hardening in the automotive industry. Presented at AP&T Press Hardening, Next Step Seminar, September 19th, Dearborn, MI, USA (2012)
56. T. Maki, M. Amino, K. Hirano, H. Murai, Mechanical link servo press for hotforming, in *5th International Conference on Hot Sheet Metal Forming of High Performance Steel, CHS2, Toronto, ON, Canada* (2015), pp. 179–187
57. P. Belanger, *The Future for Press Hardening in the Automotive Industry*. Presented at AP&T Press Hardening, Next Step Seminar, Novi, MI (2011), p. 2011
58. P. Thom, From first draft to serial production: increase ROI with turnkey hot stamping solutions. Presented at Grundig-Akademie 4th PHS Suppliers Forum (2016). Accessed 22 Sept 2016
59. E. Lundström, Hot stamping press technology. Presented at Schuler Hot Stamping Workshop, May 14, Dearborn, MI, USA (2013)
60. E. Billur, Hydraulic presses, in *Sheet Metal Forming - Fundamentals*, ed. by T. Altan, A.E. Tekkaya (ASM International, 2012), pp. 181–201
61. Schuler GmbH, *Metal Forming Handbook* (Springer Science & Business Media, 1998)
62. A. Kirk, J. Neil, Selecting a hydraulic hot-stamping press. Stamp. J. 22–27 (2014)
63. ThyssenKrupp Steel Europe. Private communication (2013)
64. Schuler Pressen GmbH. Press hardening with PCH Flex –fast, flexible, cost-effective. Product/Service Brochure (2014)
65. J. Aspacher, Press hardening - "dead end" or "take off". Presented at 25th European Car Body Conference, March 13–14, Bad Nauheim, Germany (2007)
66. T. Altan, A. Erman Tekkaya, *Sheet Metal Forming: Processes and Applications* (ASM International, 2012)
67. T. Altan, L. Penter, Application of modern cushion systems to improve quality and productivity in sheet metal forming, in *Proceedings of the CIRP Conference Machine-Process Interactions, Vancouver* (2010)
68. J. Aspacher, Hydraulic presses in use for light weight production in the automotive industry. Presented at Forming in Car Body Engineering 2011, September 27th, Bad Nauheim, Germany (2011)
69. J. Aspacher, D. Haller, Hot stamping part design and feasibility study with respect to functionality and optimization of production cost. Presented at Forming in Car Body Engineering 2014, September 24–25th, Bad Nauheim, Germany (2014)
70. R. Vollmer, C. Palm, Improving the quality of hot stamping parts with innovative press technology and inline process control, in *IDDRG 2017, Munich, Germany* (2017)
71. E. Billur, B. Çetin, M.M. Yılmaz, A. G. Oğuz, A. Atay, K. Ersoy, R.O. Uğuz, B. Kaftanoğlu, Forming of new generation AHSS using servo presses, in *5th International Conference on Accuracy in Forming Technologies, Chemnitz, Germany* (2015), pp. 175–191
72. L. Wang, B. Zhu, Y. Zhang, Y. Wang, X. An, Q. Wang, A smart process control strategy for press hardening production, in *6th International Conference on Hot Sheet Metal Forming of High Performance Steel, CHS2, Atlanta, GA, USA* (2017), pp. 515–524

73. A. Ormaetxea, G. Ibañez, Servomechanical press makes foray into hot stamping. Stamp. J. 18–21 (2015)
74. C. Wood, Hot forming press, U.S. Patent App. 14/240,174 (2012). Accessed 22 Aug 2012
75. Dirk Landgrebe, Anja Rautenstrauch, Andreas Kunke, Stefan Polster, Sebastian Kriechenbauer, Reinhard Mauermann, The effect of cushion-ram pulsation on hot stamping. AIP Conf. Proc. **1769**(1), 070014 (2016)
76. J. Meng, L. Wang, Q. Wang, Y. Sun, Y. Zhang, Research on the model of the production of hot forming process and the optimization method of production cycle, in *5th International Conference on Advanced Design and Manufacturing Engineering (ICADME 2015)* (2015), pp. 1949–1952
77. F. Schieck, Energy and resource-efficient process routes in hot sheet metal forming. Presented at Forming in Car Body Engineering 2015, September 29–30, Bad Nauheim, Germany (2015)
78. S. Behm, The Honda Ridgeline. Presented at Great Designs in Steel 2017 (2017)
79. J.M. Berasategi, C. Garbalena, B. Irazu, G. Gonzalez, Past and future for taylor-made hot stamping lines, in *3rd International Conference on Hot Sheet Metal Forming of High Performance Steel, CHS2, Kassel, Germany* (2011), pp. 255–261
80. B. Osburg, G. Lengfeld, O. Straube, Innovation and globalization as a factor of success for global hotstamping growth, in *New Developments in Sheet Metal Forming Conference, Stuttgart, Germany* (2012), pp. 79–92
81. Bundesministerium für Bildung und Forschung, (German Federal Ministry of Education and Research). KMU-innovativ Forschung für die Produktion von morgen (SME-innovative "Research for the production of tomorrow") (2014)
82. Schnupp Gmbh & Co. Hydraulik KG. Vertpress. kompaktpresse für die warmumformung. Product Catalogue (2016)
83. Neue Materialien Bayreuth GmbH, Warmumformung auf kleinstem Raum: NMB präsentiert neuen Anlagenprototypen (hot forming in the smallest space: NMB presents new plant prototypes). Press Release (2016)

Chapter 6
Die Design and Manufacturing

Eren Billur and Takehide Senuma

Abstract In typical (cold) stamping operations, the dies are only used to plastically deform the metal material. In hot stamping, on the other hand, the dies are used to form the material and extract the heat energy from the blank. All this has to be done as quickly as possible to improve the part quality (to ensure martensite formation is completed) and part productivity. This chapter discusses the requirements from a hot stamping die, how they are designed, and how they are manufactured.

6.1 Quenching Requirements

The final strength of the part can be achieved by martensitic transformation. To achieve (almost) 100% martensitic structure, a minimum of 27 °C/s (49 °F/s) cooling rate must be sustained from martensite start temperature, M_s, to martensite finish temperature M_f. These values are approximately 425 °C (800 °F), and 280 °C (535 °F) for 22MnB5 steel [1].

During hot stamping, forming stage must be completed before M_s temperature. Typically, for formability and production rate purposes, forming is completed much above this temperature and quenching starts around 750 °C (1400 °F) [2, 3]. The final properties of the material depends on the time-temperature history during cooling and can be predicted by using Continuous Cooling Transformation (CCT) diagram, as shown in Fig. 6.1.

To achieve high productivity, tool components (blankholder, punch, pads, die, etc.) must sustain their temperature, even under mass production loads. Tools would heat up while forming and quenching the blanks. To cool a blank from 800 °C to

E. Billur (✉)
Billur Makine Ltd., Ankara, Turkey
e-mail: eren@billur.com.tr

E. Billur
Atılım University, Ankara, Turkey

T. Senuma
Okayama University, Okayama, Japan
e-mail: senuma@mech.okayama-u.ac.jp

E. Billur (ed.), *Hot Stamping of Ultra High-Strength Steels*,
https://doi.org/10.1007/978-3-319-98870-2_6

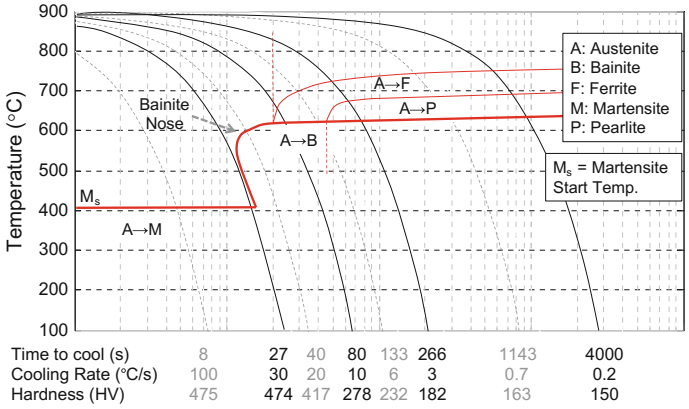

Fig. 6.1 CCT diagram for 22MnB5 steel (re-created from [4, 5])

Table 6.1 Cooling power requirement for some sample parts and cycle times (own work, example data are taken from [9–14])

Example application	Mass of blank (kg)	Heat to be extracted (kJ)	Cycle time (s)	Cooling power (kW)
Door beam	1.5	570	12	48
Bumper beam	3.7	1406	15	94
B-Pillar	5.4	2052	20	103
B-Pillar	5.4	2052	8	256
Tunnel	7.8	2964	18	165
Door ring	15.6	5928	20	296

180 °C (1470–360 °F), approximately 380 kJ/kg heat energy must be extracted by the tools (based on [6]). One can calculate the heat energy to be extracted by the die, by knowing the mass of the blank and the cycle time. An example study is presented in Table 6.1. If water cooled dies are not used, or the dies are undercooled in any local area, after a few cycles of hot stamping "hot-spots" would be observed. Blank in contact with this portion would not be hardened as expected. Figure 6.2 shows how water cooling could keep the die temperatures constant within a cycle [7, 8].

The industry standard is to use hot forming dies with integrated cooling channels. The next section explores how these dies could be manufactured. Recently, direct water quenching systems are also utilized, mostly in Japan. These are explained in detail in Sect. 6.4.

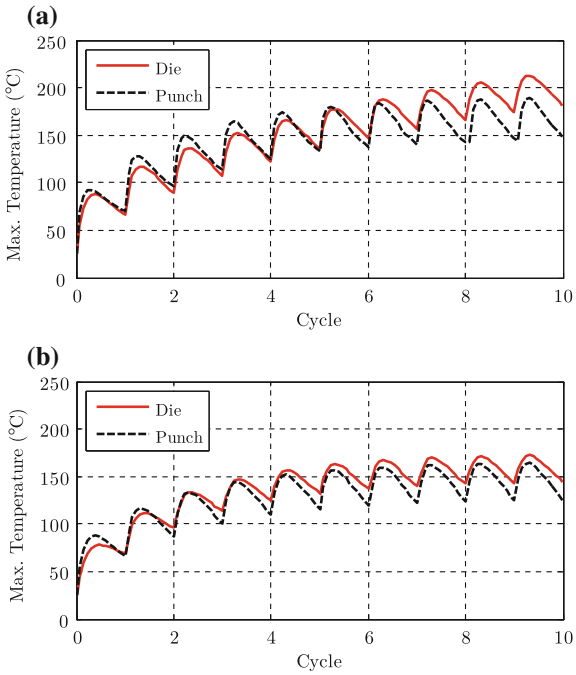

Fig. 6.2 Maximum tool temperature evolution in 10 cycles: **a** without cooling channels, **b** with cooling channels [7]

6.2 Designing and Manufacturing Dies with Cooling Channels

Currently, most of the hot stamping dies are built by drilling cooling channels to a number of die segments and assemble them together. Another method used is shell cooling, where the final part shape is machined on a shell die and cooling water is pumped between the shell and the core dies. Lastly, the die could be cast on cooling tubes. Figure 6.3 summarizes all three methods [15, 16]. All the methods will be explained in more detail.

To design cooling system of a die, it is essential to understand the heat transfer. As shown in Table 6.1, for shorter cycle times even higher cooling power is required. Figure 6.4 summarizes the heat transfer from the blank to the cooling system (i.e., the cooling fluid flowing in the cooling channels).

The heat energy that can be extracted from the blank in unit time, $\dot{Q}$ (W or BTU/h), can be calculated by Eq. 6.1. Here, A is the area of blank contacting the dies (m^2 or ft^2), ΔT is the temperature gradient between the blank and the tool (°C or °F); and h_c is the "thermal contact conductance" (W/m^2°K or $BTU/hr \cdot ft^2$°F). Thermal heat conductance is a function of surface conditions, and the contact. If there is no contact, the distance between the blank and the die determines the thermal contact conductance; if contact is present then the pressure level determines

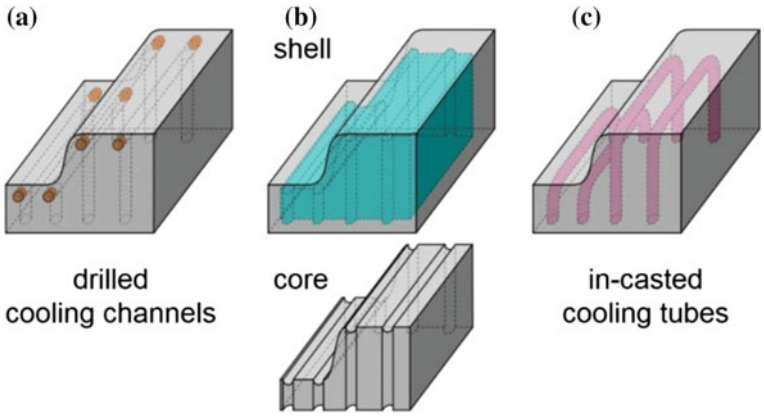

Fig. 6.3 Die making strategies for hot stamping dies with cooling channels [16]

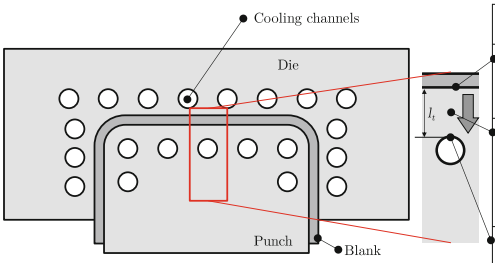

Heat transfer type	Factors affecting the heat transfer
From blank to the tool	- Minimizing gap, - Maximizing pressure, - Minimizing/preventing scale formation,
Heat conductivity within the tool	- Higher heat conductivity tool steels, - Distance between the tool surface and cooling channel - Surface quality
From tool to the cooling fluid	- Temperature of the fluid - Convection heat transfer coefficient.

Fig. 6.4 Factors affecting heat transfer (re-created after [7, 17])

it. Figure 6.5 shows the thermal contact conductance between AlSi-coated 22MnB5 and tool steels [18–21].

$$\dot{Q} = h_c A \Delta T \tag{6.1}$$

Once the heat energy is transferred from the blank to the dies, heat conduction of the tool steel becomes dominant (as seen in Fig. 6.4). The heat flux (heat energy per area and per time, W/m^2 or $BTU/hr \cdot ft^2$) that can be conducted is a function of the tool steel's thermal conductivity (k in $W/m\,°C$ or $BTU/hr \cdot ft \cdot °F$) and the distance between the cooling channel and the tool surface. Thermal conductivity of commercially available tool steels will be investigated in the next section.

The distance between the tool surface and the cooling channel (shown as l_t in Fig. 6.4), depends on how the dies are designed and built. Most hot stamped parts are not flat, but have a 3D surface. However, when cooling channels are drilled, they have to be straight lines. And thus, if the part contour is not a straight line, l_t cannot be constant, as seen in Fig. 6.6a. Whereas, with shell and core design or cast-in cooling channels, a relatively constant l_t can be achieved [15, 22].

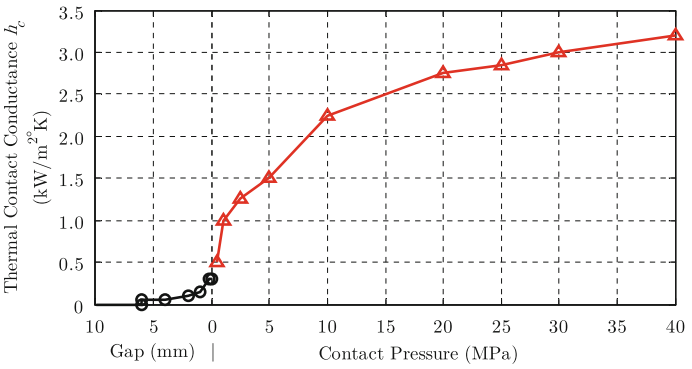

Fig. 6.5 Thermal contact conductance as a function of pressure and gap. (created using the data from [19–21])

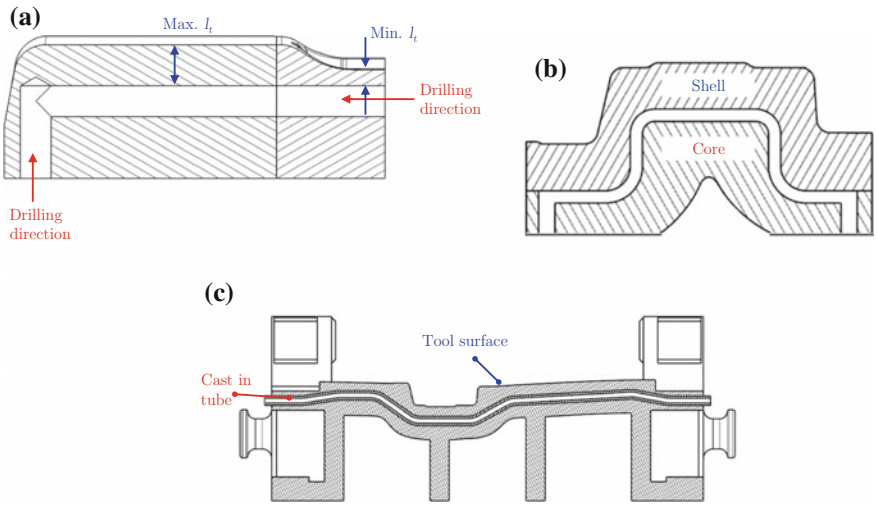

Fig. 6.6 Distance between the tool surface and cooling channel: **a** cannot kept constant when drilled cooling channels are used, whereas with **b** shell and core design or **c** cast-in cooling channels, l_t can be kept relatively constant (re-created after [22])

Number of cooling channels, the distance between the channels (l_x in Fig. 6.7) and the diameter of the cooling channels (d), all affect the heat transfer from the tool to the cooling medium, Fig. 6.7. For best performance, all three parameters must be minimized. However, in practice; (1) increased number of cooling channels would increase the cost of the tooling; (2) as the diameter is reduced the maximum drilling depth would be limited and may require more die segments (see Fig. 6.9); (3) shorter distance between the tool surface and cooling channel increases the stress concentration around the channel [22–24].

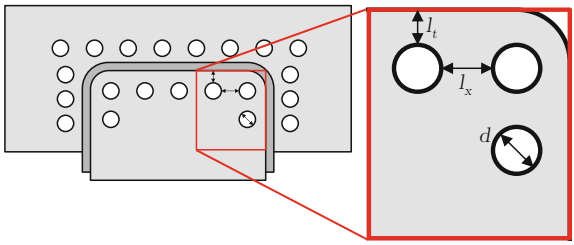

Fig. 6.7 Cooling channels parameters for optimization (note, l_x affects the total number of cooling channels)

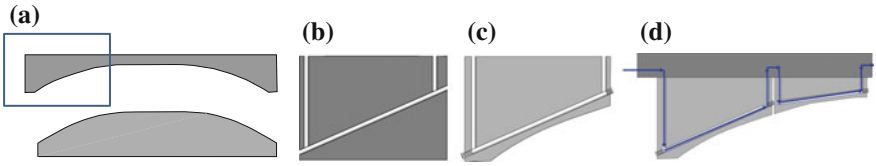

Fig. 6.8 A bumper beam tool manufacturing: **a** General outlook of a bumper beam tool, **b** deep drilling of cooling channels, **c** sealing of channels and machining of die surface, **d** coolant flow in the assembly

6.2.1 Drilled Cooling Channels

In this method, once the part contour is known, it is divided into smaller segments and each segment is made of flat bar tool steel. Figure 6.8 summarizes the process for a bumper beam geometry. Before machining the surface of the tool, cooling channels are drilled by deep drilling, Fig. 6.8b. Then the tool surface is rough machined. The tool is then hardened and tempered. Lastly finish machining is completed. The unused section of the cooling channels are sealed by using sealing bolts, Fig. 6.8c. Then, the segments are assembled into the toolset, Fig. 6.8d [25].

The number of segments depend on (1) the part complexity, (2) production rate, (3) cooling channel diameter, as there is a limit to the depth to diameter in drilling operations, and (4) total part length. As the number of segments are increased, more complex shapes can be cooled with relatively constant l_t. If higher production rates are planned, a better cooling system (i.e., constant and low l_t) would be required. Figure 6.9 shows how a four-segmented die could halve the l_t, compared to a two-segmented die.

The old generation dies had an assembly similar to Fig. 6.8d. In this design, the cooling water flows from the die shoe to the segment 1; flows in segment 1 and goes back to the die shoe, before flowing into segment 2. In this design, some hot spots may be present in the areas, where two segments are next to each other, Fig. 6.10a. An alternative to this design is to flow the coolant from one segment to the next without moving it through the die shoe, Fig. 6.10b. In this design, special care has to be taken for sealing.

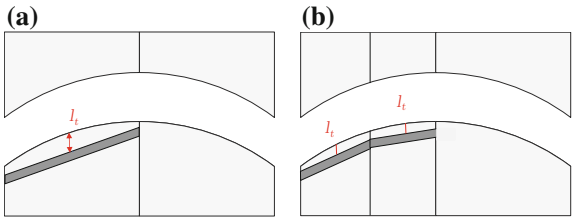

Fig. 6.9 Effects of segmenting: **a** two-segmented die, **b** four-segmented die (re-created after [24])

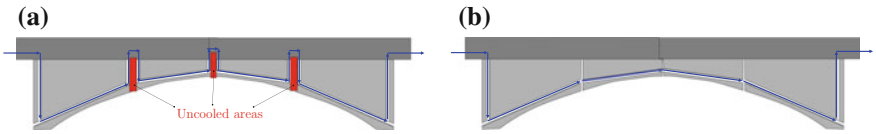

Fig. 6.10 Coolant flow between the segments: **a** over the die shoe, **b** direct: from one segment to the next (re-created after [25])

Advantages of making dies with drilled cooling channels are [22, 23, 25]:

1. Tested and proven method for many years,
2. Easy to repair,
3. Segments can be built with any die material without any limitation.

Disadvantages can be listed as:

1. For complicated and long parts, l_t cannot be kept constant,
2. Due to drilling and sealing with bolts, sharp corners may be present. Dead spots may occur where the flow is blocked at the sharp corner. This can be avoided by a fluid flow analysis in the design phase.
3. High cost of manufacturing and sealing.
4. Corrosion, and corrosion-induced cracks may limit the tool life.

6.2.2 Shell and Core Design

In the so-called shell and core design, the die face is machined on the "shell". Shell must be as thin as possible to ensure the shortest "tool surface to cooling channel distance", l_t. On the other hand must be strong enough to carry the load of hot stamping. The cooling channels are milled on the inner part of the die, named as the "core". A simple schematic is shown in Fig. 6.11.

As this method requires more efforts in sealing the shell and the core, researchers at TU Graz have come up with a similar method called "near-surface cooling channels". In this method, a forming die is built, similar to cold stamping tools. Cooling channels are then milled on the surface. An inlay sheet is inserted and coated (laser cladding, or

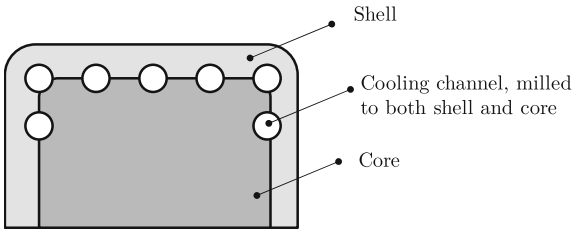

Fig. 6.11 Schematic of a shell and core design

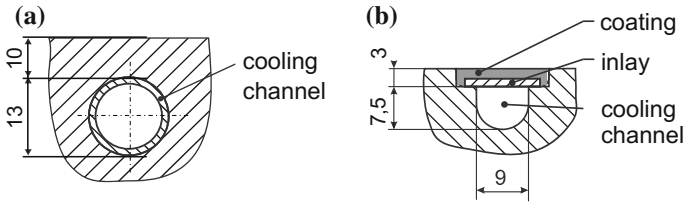

Fig. 6.12 Cross section comparison of: **a** conventional cooling channel and **b** near-surface cooling channel (similar to shell and core design) [15]

similar). Comparison of a drilled cooling channel and near-surface cooling channels is shown in Fig. 6.12 [15].

The shell and core design, in theory has many advantages [22, 25]:

1. l_t can be kept constant, even for complicated and long parts,
2. Very high cooling capability,
3. No sharp corners and dead spots.

However, the method is not favored, due to:

1. High cost of manufacturing and sealing,
2. Stiffness of the tool is inversely proportional with the shortest l_t,
3. Corrosion, and corrosion-induced cracks limiting the tool life.

6.2.3 Cast-in Cooling Channels

In this method, the cooling channels are made of high-grade steel tubes. The tube network is cut to length and bent to shape required, Fig. 6.13a. They are then embedded into the sand mold, Fig. 6.13b. It is important to make sure that the casting temperature should be less than the melting temperature of the tubes. When the molten tool material solidifies, it bonds with the tubes [26, 27].

With this method, segmented dies are not required. The cooling performance is a direct result of number of cooling tubes, their distance to the surface (l_t) and their orientation. Figure 6.14 shows the possible orientations for a B-pillar die [15].

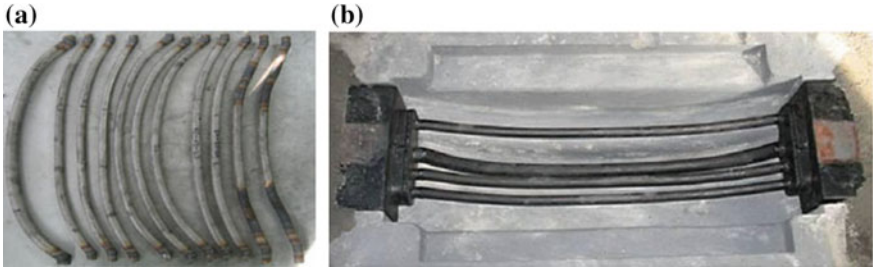

Fig. 6.13 **a** Tubes are cut and bent, **b** and replaced into the sand mold before casting [27]

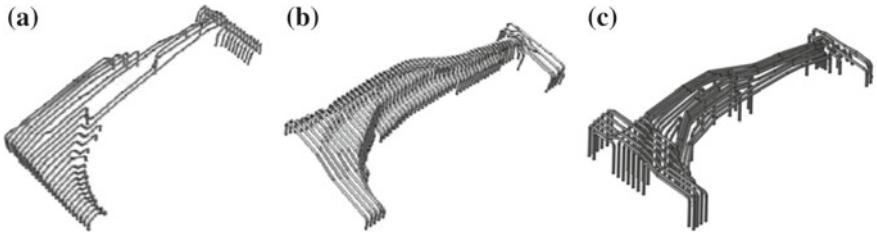

Fig. 6.14 Cooling tube orientations for a B-pillar die: **a** longitudinal, **b** transversal and **c** mixed [15]

The method has advantages such as [22, 26]:

1. Cost-effective,
2. l_t can be kept constant, even for complicated and long parts,
3. Corrosion resistance, as the tubes could be high-grade stainless steels,
4. No sealing problems.

Disadvantages are:

1. Limited die material options (melting temperature of the die material must be lower than that of the tubes),
2. Late modifications are expensive,
3. Minimum bending radii of the tube itself may limit the l_t,
4. Lower cooling performance as there is a secondary contact thermal conductance (tool to tube, tube to coolant).

6.3 Die Materials and Treatments

In hot stamping, the dies are expected to form the part and quench it. In order to achieve both goals, tool material of hot stamping dies must have [23, 28]:

Table 6.2 Hardness and heat conductivity values of several tool materials

Tool Steel	Hardness		Thermal Conductivity		References
	Delivery	Maximum	W/m °K	BTU/hr· ft · °F	
CR7V	240 HB (250 HV)	57 HRC (633 HV)	27	15.6	[30]
H13	185 HB (195 HV)	56 HRC (615 HV)	28	16.2	[31]
W360	57 HRC (633 HV)	185 HB (195 HV)	31	17.9	[32]
Dievar	160 HB (168 HV)	57 HRC (633 HV)	32	18.5	[33]
CP2M	225 HB (235HV)	65 HRC (846 HV)	40	23	[34]
HTCS 150	260 HB (275 HV)	55 HRC (600 HV)	53	30.6	[35]
HTCS 170	246 HB (260 HV)	65 HRC (846 HV)	66	38.1	[35]
Glidcop ®	–	86 HB (85 HV)	322	186	[36]

1. high compression strength—to avoid plastic deformation,
2. high hardness at elevated temperatures—to reduce die wear,
3. toughness—to prevent chipping,
4. good weldability—for repair and design modifications,
5. high thermal conductivity—to quickly quench the parts and thus improve the production rate.

All these requirements could be satisfied by hot work tool steels such H11 (1.2343), H13 (1.2344) and their modified versions. Table 6.2 summarizes commercially available hot stamping tool materials. Only Glidcop ® is a copper alloy and has been used for experimental hot stamping tools for its extra high heat conductivity [29]. Others are tool steels.

Since there are cooling channels inside the die, corrosion is an important issue for hot stamping dies. Most of the hot work tool steels do not have high Cr content, and therefore are susceptible to corrosion. One method to improve the tool life is to smooth out the cooling channels' surface roughness. However, this may not be sufficient. Typical precautions are to use closed-loop cooling systems, where the water is decontaminated. Additional corrosion inhibitors are also advised [23].

6.3.1 Treatments/Coatings for Tool Materials

Tool life for stamping tools are determined by five failure modes, Fig. 6.15. It is essential to understand these modes and the reasons behind them to properly design tools. The tool material must have some toughness and hardness in the core, but higher stresses are observed near the surface. In addition, sliding contact happens at the surface. Tools are typically through hardened to some extent (i.e., not to the maximum possible hardness) , case hardened (only a certain depth from the surface

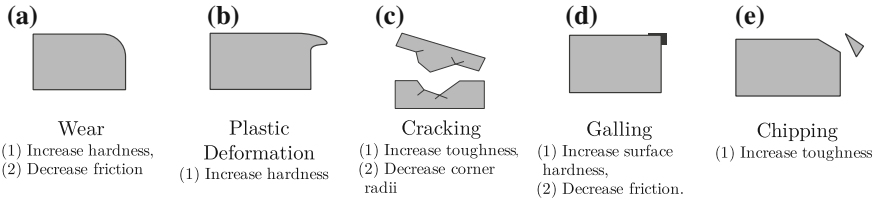

Fig. 6.15 Tool failure modes and changes to improve the tool life [28, 39]

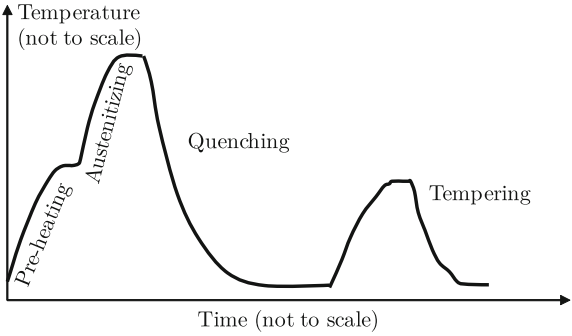

Fig. 6.16 Steps of heat treatment processes (re-created from [40])

is hardened to a higher degree than the core), and later coated. Coatings are typically at very high hardness and slows down wear [28, 37, 38].

Once the tools are rough machined, they are typically hardened and tempered. This is a heat treatment process. Basically, a four steps process is applied, as shown in Fig. 6.16 [28, 40]:

1. Preheating below austenitization temperature and soaking, to ensure the surface and the core have low-temperature gradient,
2. Austenitizing and soaking, to ensure even the core is austenitized,
3. Quenching, to ensure martensitic transformation,
4. Tempering, to temper the martensite and increase the toughness.

For tool steels, another commonly used treatment technique is Nitriding. Nitriding is a case hardening process. This is achieved by introducing (diffusing) nitrogen (N) atoms into the surface of a metal. This method is not a coating, but a diffusion process, see Fig. 6.18b. Based on the process, there are three different nitriding techniques [28, 41]:

1. Gas nitriding,
2. Liquid (salt bath) nitriding, and
3. Plasma nitriding.

Depending on the tool steel, hardness before nitriding process, and nitriding process parameters; a case depth of 5...10 μm (200...400 μin), and a surface hardness of 1000–1300 HV can be achieved [28, 42].

Table 6.3 PVD coatings and their properties [28, 47]

Coating	Thickness (μm)	Hardness (HV)
TiAlN	2–5	2600–3400
AlCrN	2–4	~3000
CrWN	5–8	3000–3200

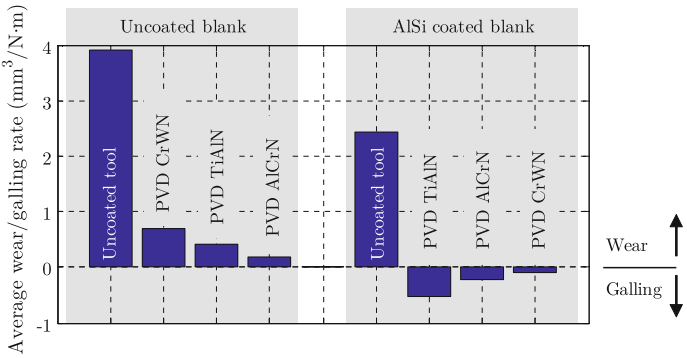

Fig. 6.17 Wear and galling rates of several PVD coatings in hot stamping of uncoated and AlSi coated blanks (re-created after [45])

To improve the wear resistance of tools, it is common to coat them with thin but very hard coatings [43]. There are different coating and plating techniques for cold stamping tools, but for hot stamping, tools are typically coated with Physical Vapor Deposition (PVD) method. This is because plating techniques cannot withstand high temperatures, and Chemical Vapor Deposition (CVD) has a high process temperature which may temper the dies [28].

PVD coatings refer to a family of relative low-temperature (compared to CVD) atomistic deposition processes. There are different types of PVD processes and coating chemistries [44]. For hot stamping purposes, AlCrN and TiAlN are the most common coatings [45, 46]. Table 6.3 lists some of the common PVD chemistries' mechanical properties.

It is essential to note the blank coating is the most important criterion to select the tool coatings. If the blank is uncoated, scale formation would cause abrasive wear. In hot stamping of AlSi- coated blanks, the tools may fail due to galling (i.e.,sticking of AlSi on the tools) [46, 48]. Figure 6.17 shows the wear and galling rates of several PVD coatings in hot stamping of uncoated and AlSi-coated blanks [45].

In a tool selection guide published by a tool steelmaker, for production volume less than 250,000 per year hardened and nitrided tool steels were recommended. If the production volume is more than 800,000 per year then hardening + plasma nitriding + PVD coatings were recommended [49]. Nitriding + PVD coating is called "Duplex coating", Fig. 6.18. This is required, as the PVD coating hardness may be as high as 3,000 HV (Table 6.3). A typical hot stamping tool steel may be hardened

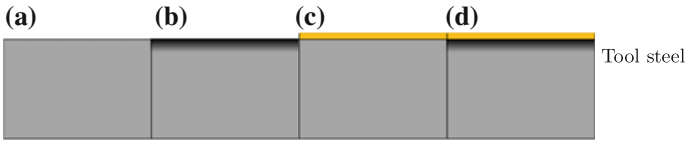

Fig. 6.18 Tool coatings and treatments in hot stamping: **a** fully hardened/uncoated, **b** fully hardened and nitrided, **c** fully hardened and PVD coated, **d** Duplex: hardened and nitrided+PVD coated

Table 6.4 Hot stamping tool lives, with different tool coatings [16, 48]

Sheet Steel	Tool Steel	Treatment/coating	Hardness (HV)	Tool life
1.2 mm 22MnB5 + x-tec	CR7V 54 ± 2 HRC	Plasma Nitriding	1100	20,000
1.2 mm 22MnB5 + x-tec	CR7V 54 ± 2 HRC	Duplex TiAlN	2600–3400	100,000
AlSi coated Bumper beam	1.2367 52–54 HRC	Plasma Nitriding	1100–1300*	120,000
AlSi coated Bumper beam	CP2M 58–60 HRC	Plasma Nitriding	1100–1300*	200,000

*Estimated

to 50–56 HRC, approximately equivalent to 513–613 HV [16, 48, 50]. Thus, when PVD is applied directly on the tool steel, there would be a very abrupt drop in the hardness. The very hard coating may easily crack due to plastic deformation of the tool steel below it. If nitriding is applied there would be another layer of 1000–1300 HV close to the surface and can support the load [51].

Tool life of a hot stamping die is a very confidential commercial secret. Thus, it is not found in literature; nor it is permitted to publish. In literature, there were a few examples of hot stamping tool lives. Here, tool life refers to the number of hits before a major rework/repair. Table 6.4 summarizes some of the publicly available information.

6.4 Novel Quenching Methods

The conventional design for hot stamping is the quenching in dies (die quenching) during press forming. Quenching with water cooled dies, requires approximately 10 s time to quench a part, which may be a bottleneck of productivity of hot stamping. Besides, the contact pressure between the die and sample is not homogeneous which results in different cooling rate and in fluctuation of the strength from part to part.

Figure 6.1 shows a CCT of the conventional 1500 MPa class steel, namely 22MnB5 [52]. This figure shows that a cooling rate of 30 °C/s is necessary to obtain full martensite microstructure. Figure 6.19 shows a relationship between contact pressure and average cooling rate in a temperature range from 800 °C to 500 °C [53].

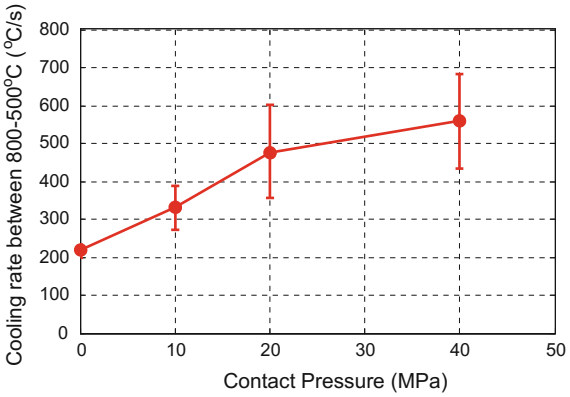

Fig. 6.19 Influence of contact pressure on the average cooling rate between 800 °C and 500 °C (re-created from [53])

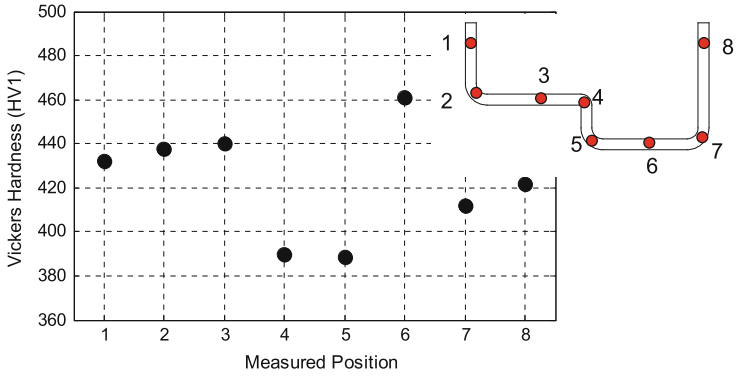

Fig. 6.20 Hardness distribution in a hot stamped hat shaped part (re-created from [38])

These cooling rates are far above the critical cooling rate of 30 °C/s. Figure 6.20 is the result of hardness measurement in a hot stamped hat shape part [38]. It is clearly seen that the edge corners where the contact pressure is low results in lower hardness. It is a contradictory result because the cooling rate is expected to be above the critical cooling rate of 30 °C/s even at the corners according to the result given in Fig. 6.19. It is noteworthy that the hardness difference was within 80 HV. This indicates that the hardness drops was not due to the occurrence of ferrite or pearlite transformations.

Nishibata et al. [54] conducted an investigation in which the cooling rate below 450 °C was changed and showed the influence of cooling rate on the hardness in Fig. 6.21. Although the microstructure is full martensite, the hardness decreased with decreasing cooling rate. This decrease in hardness was provided by formation of cementite in the martensite during cooling. This phenomenon called auto-tempering was quantitatively investigated by Hidaka et al. [55] with a metallurgical model developed.

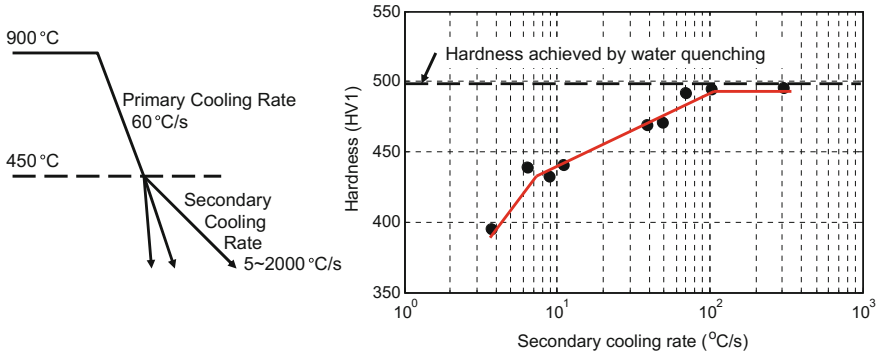

Fig. 6.21 Influence of the cooling rate below 450 °C on the hardness of samples heated at 900 °C and cooled to 450 °C at a cooling rate of 60 ° C/s (re-created from [54])

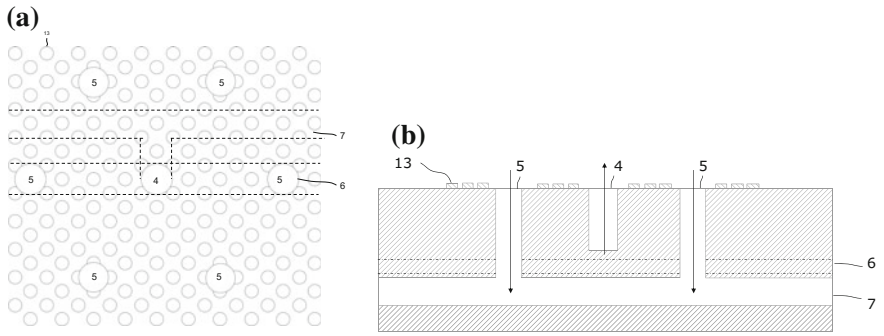

Fig. 6.22 Schematic depiction of a direct water injection cooling device (re-created after [56])

In the conventional die quenching, the cooling rate in a lower temperature range becomes slow and therefore, the sample is usually removed from the die around 200 °C and air cooled to avoid long holding of the sample in the dies. This second cooling causes the decrease and fluctuation of strength. A solution to overcome this problem is a direct water injection cooling. As seen in Fig. 6.22, there are in- and outlet of water and the entering water directly cools the sample and leaves die through outlet channel. Using this system, the die quenching time down to 100 °C is reduced less than 2 s and as a consequence, the productivity is drastically improved [56]. If auto-tempering can be suppressed by the quick cooling, 22MnB5 steel shows a tensile strength of around 1650 MPa. The direct water injection cooling increases the tensile strength by about 100 MPa in comparison of the conventional die quenching.

Nomura et al [57] showed that the shape fixability was affected by the position and number of water inlet. They achieved better shape fixability by homogeneous quenching through an increase on water inlets. They also showed better shape fixability by controlling the injection of water in two stages as seen in Fig. 6.23. It is also reported the water injection cooling is partially applied to the part where the contact

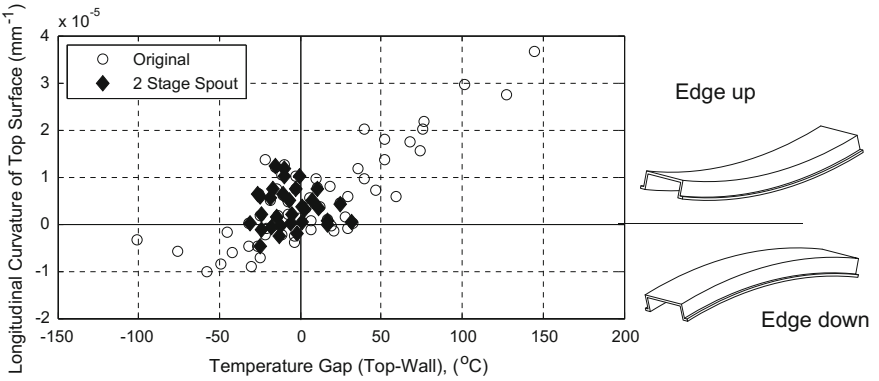

Fig. 6.23 Influence of cooling method on shape distortion (re-created from [57])

pressure is low and the cooling rate sufficient for necessary hardness is not achieved by die quenching.

Although an optimized direct water cooling leads to the homogenization of quality and realizes high productivity of the cooling process, there are two major drawbacks. One of them is the high production cost of dies with many spouts and the other is that this method is only applicable to coated sheets because the oxide scales of uncoated sheets block the outlet.

To overcome these drawbacks, quenching outside the dies has been proposed. Senuma et al. [58] measured the gage deviation of a hut profile sample stamped by a mechanical press and quenched outside the dies with and without a fixing jig from the die profile. Figure 6.24 shows the jig. Although the jig is simple, shape fixability was drastically improved using the jig as shown in Fig. 6.25. The samples of a high hardenable steel were heated to 900 °C and air cooled to the forming temperature. Immediately after stamping, the samples were quenched with and without fixing jig shown in Fig. 6.24. The deviation of the flange angle of the hut profile sample not fixed by jig is large and increases with decreasing forming temperature. On the other hand, the samples fixed by the jig reveal good shape fixability regardless of the forming temperatures if the temperature is above M_s. An additional experiment with big size hut shape samples showed that water spray quenching and oil quenching deliver better shape fixability than quenching by immersing into water.

The quenching outside the dies not only improves productivity and reduces the die production cost but also avoids a drop of strength due to auto-tempering. This avoidance of strength decrease can decrease the C content, which improves weldability.

As another novel cooling method, precooling before hot stamping has been reported. The precooling brings some advantages. Figure 6.26 shows the influence of forming temperature on stretch formability of dome cup formation. The limiting dome height (LDH) increases with decreasing forming temperature above M_s. It is because that the difference of temperature at the contact portion with die from

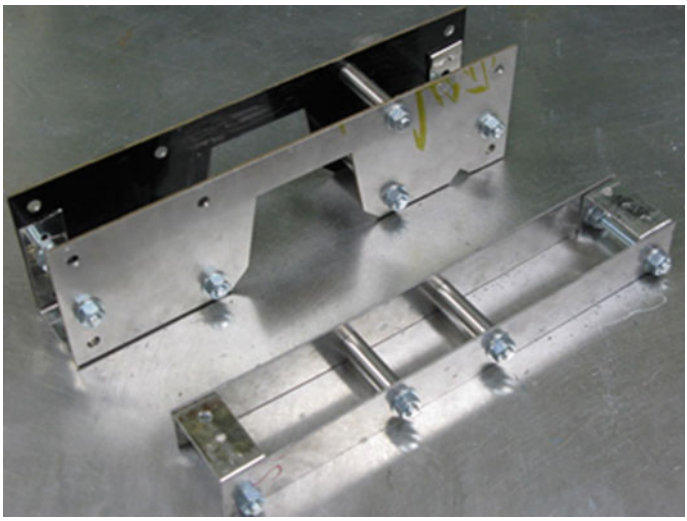

Fig. 6.24 Device for improving shape fixability of the sample cooled outside the die [58]

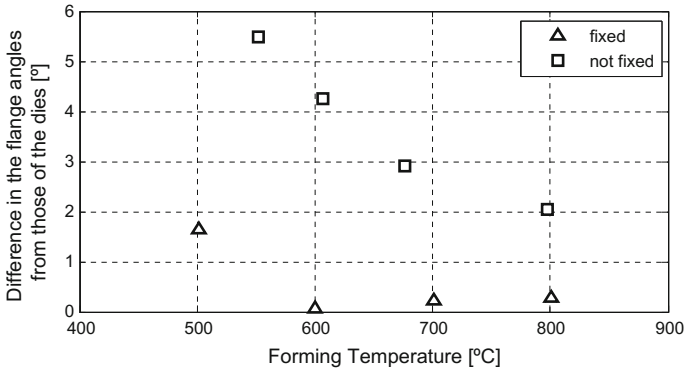

Fig. 6.25 Influence of forming temperature and effect of jig on the shape fixability. (Specimens were heated at 950 °C for 5 min. Specimens were taken out from die immediately after forming and quenched (re-created after [58])

that at noncontact portion is reduced with decreasing forming temperature, and the concentration of the thickness change in the high temperature, noncontact portion is reduced. The data marked with squares were the data from the samples which were formed by the metal punch insulated with paper. The paper covering metal punch suppresses the cooling of contact portion and reduces the difference of temperature at the contact portion with die from that at noncontact portion. Therefore, the "insulated" case shows the higher LDH [59].

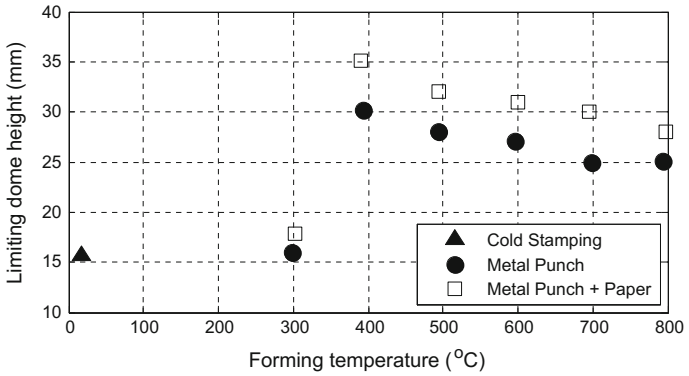

Fig. 6.26 Influence of forming temperature on the limiting dome height using metal punch and metal punch covered by paper. (Specimens were heated to 950 °C for 5 min, cold stamping is for reference) (re-created after [59])

Fig. 6.27 Comparison of the partial cooling technique with conventional hot stamping technique [60]

Ota et al. [60, 61] reported a novel cooling method for improving LDH. Figure 6.27 shows that the portion where a large thickness reduction is expected is cooled before stamping. The reduction of abovementioned temperature difference significantly increases LDH up to 80%. TRIP steels or TWIP steels strengthen the strain concentration portion by transformation-induced martensite or twin formation to achieve good formability. In hot stamping, a sophisticated cooling control obtains the same effect without use of high-grade steels. The possible fluctuation of material quality can be reduced by this partial cooling if the stamping is conducted before the precooled portion starts the $\gamma \rightarrow \alpha$ transformation. The sophisticated temperature control can achieve high formability which cannot be expected in cold stamping.

Precooling of the whole blank is reported to avoid liquid metal cracking of zinc-coated steel sheets [62]. The resultant low-temperature stamping also brings advantages in the improvement of formability, the reduction of die quenching time and the avoidance of the use of high-quality heat-resistant die material.

It is concerned that ferrite, pearlite or bainite transformation occur during the precooling. There is, however, the incubation time for these transformations. For example, if a 22MnB5 sample heated at 900 °C is immersed into a salt bath of 400 °C, the austenite state remains within 15 s. If the handling time after precooling is within this period, the hot stamping can be performed in austenite range. If a

longer handling time is needed, an increased addition of alloy elements improving hardenability such as Mn is an effective measure.

6.5 Hydrogen-Induced Delayed Fracture

The increase in strength is one of the most important targets of the R&D of the hot stamping technology. The conventional hot stamping steel sheet is 1500 MPa grade. A hot stamping steel sheet of 1800 MPa grade is partially employed to bumpers [63]. The next target is to develop hot stamping steel sheets of 1900–2200 MPa grades. To realize this target, the concerns of the occurrence of delayed fracture must be removed. The necessary condition for the occurrence of delayed fracture is the simultaneous existence of hydrogen and high tensile stress in high strength materials as shown in Fig. 6.28. The high tensile stress due to an external force can be avoided by proper design, but the residual tensile stress caused by welding and trimming requires attention. In particular, the tensile residual stress caused by mechanical trimming has a value close to the yield stress of the material. Therefore, the laser cutting is often employed to avoid high residual tensile stress at trimmed or pierced sections. In the case of 2000 MPa class hot stamping steel sheets, the damage of trimming tools is so serious that laser cutting or hot trimming are inevitable.

In the case of automotive steel components, hydrogen is mainly intruded by corrosion. Although coating can suppress the intrusion of hydrogen, attention should be paid that hydrogen intensively intrudes from the part at which coating is destroyed by scratching. It means that it cannot be said that coated hot stamping steel sheets have much higher resistance to delayed fracture than uncoated ones.

Many hypotheses on the mechanism of delayed fracture have been proposed. The mechanism of delayed fracture differs from case by case depending on the intruded

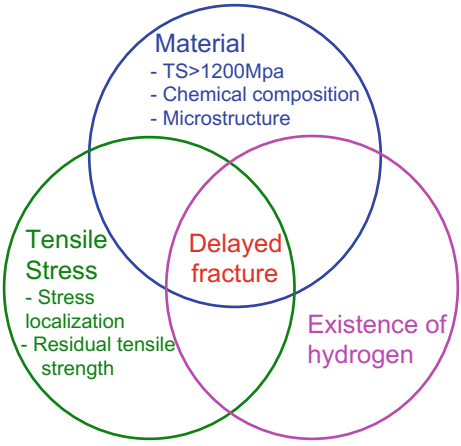

Fig. 6.28 Necessary conditions for occurring delayed fracture

hydrogen amount. If the amount of hydrogen is high, the intergranular cracking is the mechanism of the delayed fracture. In the case of low hydrogen content, the quasi-cleavage fracture which reveals the nature of ductile fracture occurs.

In the delayed fracture tests of ultra-high strength automotive steel sheets, the intergranular fracture hardly occurs and the quasi-cleavage fracture is overwhelmingly observed. In this case, the hydrogen-enhanced plasticity-induced vacancy theory proposed by Nagumo et al. [64] is a promising theory to describe the mechanism. According to their theory, the following phenomena are expected to occur: (1) Multiple slips occur by deformation in the vicinity of grain boundaries. (2) Excess vacancies are generated thereby cutting off dislocations each other. (3) Usually, the excess vacancies quickly disappear but if hydrogen is present, the diffusion of the vacancies is slowed down and their annihilation is suppressed. As a consequence, clusters of vacancies are formed near the grain boundaries and they grow to micro-voids. (4) Their linking finally leads to quasi-cleavage fracture.

The study on delayed fracture is advanced in quenched and tempered materials and it has been reported that grain refinement and presence of fine precipitates are effective for suppressing delayed fracture [65, 66]. It is not obvious if these findings are applicable to hot stamping steel sheets or not.

Figure 6.29 shows the influence of the martensite grain size on the time to delayed fracture of a hot stamped 1500 MPa grade steel sheet (22MnB5) [67]. The samples were quenched and BH treated (at 170 °C for 1200 s) . The delayed fracture tests were performed in the 20% ammonium thiocyanate solution by acting a stress of 1000 MPa at the notch of the sample. The grain size was varied by choosing various heating temperatures. It is clearly seen that the grain refinement increases the resistance to delayed fracture of the hot stamped steel sheet. The fracture mode was quasi-cleavage and not intergranular.

A further investigation revealed that the grain refinement leads to the decrease in the hydrogen content per unit area of the grain boundary. It was supposed that

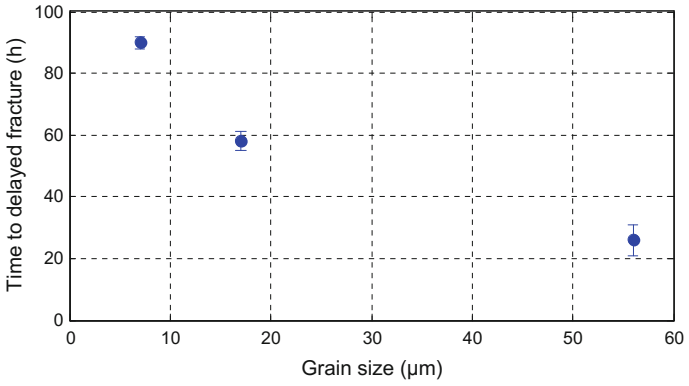

Fig. 6.29 Influence of martensite grain size on the time to delayed fracture of 1500 MPa class hot stamped steel sheets (re-created after [67])

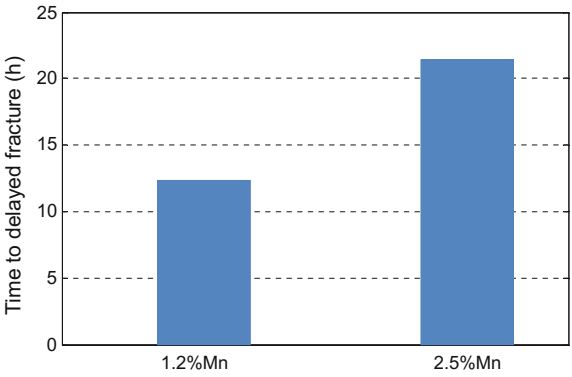

Fig. 6.30 Influence of Mn content on the time to delayed fracture of 1900 MPa class hot stamped steel sheets

the increasing amount of hydrogen in unit area decreased the strength of the grain boundary. However, it is not probable that this decrease in the grain boundary strength promotes grain boundary fracture because the fracture mode was not intergranular. Instead, the decrease in the grain boundary strength is supposed to accelerate the nucleation of dislocations at the grain boundary. The mutual cutting of dislocations creates supersaturated vacancies. According to Nagumo et al.'s hypothesis [64], these vacancies cluster to form micro-voids leading to fracture. They also suppose that the grain refinement suppresses the creation of dislocations and as a result, the creation of vacancies in the vicinity of grain boundaries.

Numerous studies on the effect of the chemical compositions on the resistance to delayed fracture of hot stamping steel have been already done. Grain boundary embrittlement elements such as P, S etc. are proposed to be lowered as much as possible [63]. The reduction of Mn content also increases the resistance to delayed fracture as seen in Fig. 6.30. The used samples contained 0.32% C and were quenched and BH treated. The delayed fracture tests were performed in the 20% ammonium thiocyanate solution by acting a stress of 1300 MPa at the notch of the sample.

On the other hand, the addition of micro-alloy elements improves the resistance to delayed fracture. Tokizawa et al. showed that the resistance to delayed fracture increased with increasing amount of Ti addition up to 0.1% [68]. Besides, Tateyama et al showed that the V addition and a combined addition with Nb also improve the resistance to delayed fracture [69]. Figure 6.31 shows the effect of Nb content on the time to delayed fracture using the 0.32% C-2.5% Mn-0.01% Ti-0.002% B steel as the base steel. The samples were quenched and BH treated. The tensile strength of the samples were around 2000 MPa. The delayed fracture tests were performed in the 20% ammonium thiocyanate solution by acting a stress of 1300 MPa at the notch of the sample. The resistance to delayed fracture was increased by increasing amount of Nb. This improvement of the resistance to delayed fracture cannot be explained merely by grain refinement, and therefore, other influential factors have been investigated. Because the samples were BH treated before the delayed fracture test, NbC was covered with ferrous carbide. Therefore, it is not probable that NbC were effective trap site of hydrogen and plays a significant role for suppressing the

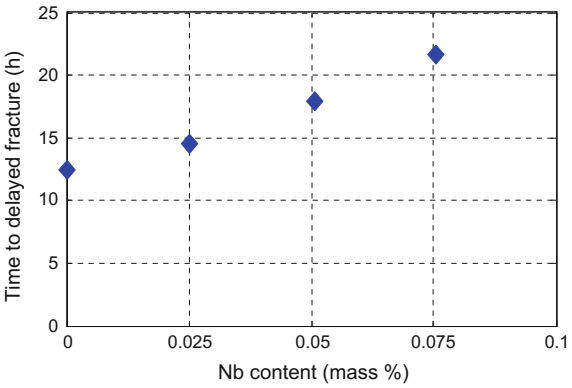

Fig. 6.31 Effect of Nb content on the time to delayed fracture

delayed fracture. Effects of the other phenomena such as the decrease in the mobility of the dislocations caused by Nb in solution and the increase in grain boundary strength due to grain boundary segregation of Nb on delayed fracture have also been discussed. The decrease in the mobility of dislocations initiated from the tip of a crack suppresses the propagation of the crack.

Yamamoto et al. [70] investigated the influence of microstructure on the resistance to delayed fracture. They conducted a delayed fracture test with two samples. One was heated to austenite region and quenched and had a full martensite microstructure. The other was heated to intercritical region and had a martensite matrix with about 10% ferrite. The existence of ferrite decreased the resistance to delayed fracture. They also investigated the influence of low-temperature annealing on the resistance to delayed fracture and showed that the BH treatment at 170 °C for 1200 s remarkably increases the resistance to delayed fracture. As its causes, annihilation of supersaturated vacancies, decrease in solution hardening of carbon and increase in hydrogen trap site at the interface of precipitated ferrous carbides have been considered. However, the quantitative analysis has not been still performed.

The above studies showed that the resistance to delayed fracture can be improved by grain refinement and decreasing alloy elements embrittling grain boundary, and adding micro-alloys. Considering these measures, 2000 MPa class hot stamping steel sheets with high resistance to delayed fracture will be produced in the near future.

References

1. H. Karbasian, A.E. Tekkaya, A review on hot stamping. J. Mater. Process. Technol. **210**(15), 2103–2118 (2010)
2. E.D. Schachinger, S. Kolnberger, J. Faderl, Evolution of phases and formation of oxides on different galvanized hot formed steel grades, in *5th International Conference on Hot Sheet Metal Forming of High Performance Steel, CHS2, Toronto, ON, Canada* (2015), pp. 111–119
3. P. Belanger, New Zn multistep hot stamping innovation, in *Presented at Great Designs in Steel 2017* (2017)

4. L. Vaissiere, J. P. Laurent, A. Reinhardt, Development of pre-coated boron steel for applications on PSA Peugeot Citroën and Renault bodies in white, in *SAE Technical Paper*. SAE International (2002)
5. H. Mohrbacher, Martensitic automotive steel sheet - fundamentals and metallurgical optimization strategies, in *Innovative Research in Hot Stamping Technology*, vol. 1063 of *Advanced Materials Research* (Trans Tech Publications, 2015), pp. 130–142
6. M. Spittel, T. Spittel, *Steel symbol/number: 22MnB5/1.5528* (Springer, Berlin 2009), pp. 930–935
7. E. Billur, Fundamentals and applications of hot stamping technology for producing crash-relevant automotive parts. Ph.D. Dissertation, The Ohio State University, Columbus, OH, USA (2013)
8. E. Billur, C. Wang, C. Bloor, M. Holecek, H. Porzner, T. Altan, Advancements in tailored hot stamping simulations: cooling channel and distortion analyses. AIP Conf. Proc. **1567**(1), 1079–1084 (2013)
9. P. Jonason, R. Johansson, J.K. Larsson, Challenges in process and design for multi material implementation in body and exterior parts at volvo cars, in *Presented at Insight Edition Conference, September 18-19th, Neckarsulm, Germany* (2012)
10. R. Wohlecker, R. Henn, H. Wallentowitz, J. Leyers. Mass reduction. fka Report 56690, fka Aachen (2006)
11. L. Sciarretta, Alfa romeo giulia. Presented at EuroCarBody 2016, October 17-20, Bad Nauheim, Germany (2016)
12. K. Teshima, Challenges of high-efficiency hot forming processes at Honda, in *Presented at Forming in Car Body Engineering 2012, September 26-27, Bad Nauheim, Germany* (2012)
13. P. Šimon, Škoda Rapid. Presented at EuroCarBody 2012, October 16-18, Bad Nauheim, Germany (2012)
14. G. Tandon, I. Viaux, Lightweight door ring concepts using hot stamped laser welded blanks. Presented at Great Designs in Steel 2014 (2014)
15. R. Kolleck, W. Weiß, P. Mikoleizik, Cooling of tools for hot stamping applications. IDDRG, Graz, Austria **2010**, 111–119 (2010)
16. Ch. Escher, J. Wilzer, Tool steels for hot stamping of high strength automotive body parts. Int. Conf. Stone Concr. Mach. (ICSCM) **3**, 219–228 (2015)
17. H. Steinbeiss, H. So, T. Michelitsch, H. Hoffmann, Method for optimizing the cooling design of hot stamping tools. Prod. Eng. Res. Devel. **1**(2), 149–155 (2007)
18. F.P. Incropera, D.P. DeWitt, *Introduction to Heat Transfer*, 5th edn. (Wiley, New York, 2011)
19. B. Oberpriller, L. Burkhardt, B. Griesbach, Benchmark 3–continuous press hardening, in *Proceedings of the Conference NUMISHEET* (2008)
20. M. Merklein, J. Lechler, T. Stoehr, Investigations on the thermal behavior of ultra high strength boron manganese steels within hot stamping. Int. J. Mater. Form. **2**(1), 259–262 (2009)
21. esi Group. PAM-STAMP 2015.1 User Guide (2015)
22. F. Schieck, C. Hochmuth, S. Polster, A. Mosel, Modern tool design for component grading incorporating simulation models, efficient tool cooling concepts and tool coating systems. CIRP J. Manuf. Sci. Technol. **4**(2), 189–199 (2011). Energy-Efficient Product and Process Innovations in Production Engineering
23. R. Rahn, I. Schruff, Modern tool steels – a prerequisite for successful hot-stamping of steel sheets, in *Proceedings of New Developments in Sheet Metal Forming Conference, Stuttgart, Germany* (2016), pp. 289–301
24. Woo-Seung Lim, Hong-Seok Choi, Seok-young Ahn, Byung-Min Kim, Cooling channel design of hot stamping tools for uniform high-strength components in hot stamping process. Int. J. Adv. Manuf. Technol. **70**(5), 1189–1203 (2014). Feb
25. D. Jeanjean, Tools and dies specifications for hot forming technologies, in *Presented at Seminar Dedicated to New Hot Forming Technologies, Loire-Etude, St. Chamond, France* (2015)
26. R. Kolleck, S. Pfanner, E.P. Warnke, R. Ganter, New concept for tempering sheet metal forming tools, in *Chemnitz Car Body Colloquium*. Verl. Wiss. Scripten (2005)

27. Hongsheng Liu, Chengxi Lei, Zhongwen Xing, Cooling system of hot stamping of quenchable steel br1500hs: optimization and manufacturing methods. Int. J. Adv. Manuf. Technol. **69**(1), 211–223 (2013). Oct
28. E. Billur, Chapter 16: Tool Materials, Treatments and Coatings, in ed. by T. Altan, A.E. Tekkaya *Sheet Metal Forming - Processes and Applications* (ASM International, 2012), pp. 317–338
29. Y. Nicolas, Hot stamping: a new hot forming technology. *ThyssenKrupp techforum (English ed.)*, (JUILL) (2005)
30. KIND & CO., Edelstahlwerk, KG. Special hot work tool steel CR7V. Product Datasheet (2013)
31. Böhler Uddeholm. H13 tool steel. Product Datasheet (2013)
32. Böhler, W360 isobloc ®. Product Datasheet (2013)
33. Uddeholm. Dievar ®. Product Datasheet (2015)
34. Dörrenberg Edelstahl. Cp2m ®. Product Datasheet (2015)
35. S.A Rovalma, Company web page (2018). Accessed 21 March 2018
36. Höganäs, Glidcop ®dispersion strengthened copper. Product Datasheet (2013)
37. ASTM. Standard terminology relating to wear and erosion. *G40*, 2005
38. N.H. Kim, K.Y. Kwon, C.G. Kang, The effect of cooling rate on mechanical properties in hot press forming of Al-Si coated 22MnB5 sheet and its theoretical temperature prediction, in *2nd International Conference on Hot Sheet Metal Forming of High Performance Steel, CHS2, Luleå, Sweden* (2009), pp. 15–17
39. H. Kim, Prediction and elimination of galling in forming galvanized advanced high strength steels (ahss). Ph.D. Dissertation, The Ohio State University, Columbus, OH, USA (2008)
40. G. Adam Roberts, R. Kennedy, G. Krauss, *Tool Steels* (ASM international, 1998)
41. American Society of Metals. *ASM handbook of "Heat Treating, 3rd printing"*, vol. 04 (ASM International, 1995)
42. O. Salas, J. Oseguera, N. García, U. Figueroa, Nitriding of an h13 die steel in a dual plasma reactor. J. Mater. Eng. Perform. **10**(6), 649–655 (2001). Dec
43. M. Larsson, Why surface coat moulds and dies? in *Recent Advances in Manufacture & Use of Tools & Dies and Stamping of Steel Sheets* (2004), pp. 41–52
44. D.M. Mattox, *Handbook of Physical Vapor Deposition (PVD) Processing* (William Andrew, 2010)
45. S. Mozgovoy, J. Hardell, B. Prakash, High temperature friction and wear studies on tool coatings under press hardening contact conditions, in *International Tribology Conference: 15/09/2015-20/09/2015* (2015)
46. A. Reiter, Pvd coatings for hot metal sheet forming operations, in *Proceedings 2nd Erlanger Workshop Warmblechumformung, Geiger, M* (2007), pp. 103–110
47. ionbond. Company web page (2018). Accessed 21 March 2018
48. T.-G. Lee, Pvd coating technology for press hardening. Presented at Daego Mechatronics & Materials Institute, Korea, October 8th (2008)
49. S.A. Rovalma, Tool steels for hot forming dies (2010)
50. Hans Qvarnström, Technical note: A mathematical formula for transformation between the steel hardness scales of rockwell c and vickers. J. Heat. Treat. **7**(1), 65–67 (1989). Mar
51. A. Reiter, Innovative pvd-beschichtungen für formgebende und schneidende werkzeuge. Presented at 4. Internationales Fachseminar für Schnitt- und Stanzwerkzeughersteller, March 19th (2015)
52. M. Suehiro, J. Maki, K. Kusumi, M. Ohgami, T. Miyakoshi, Properties of aluminized steels for hot-forming, in *SAE Technical Paper*. SAE International (2003)
53. G. Deinzer, A. Stich, K. Lamprecht, G. Schmid, M. Rauscher, M. Merklein, J. Lechler, Presshärten von tailor welded blanks: Werkstoffauswahl, eigenschaften und verbindungstechnik, in *3. Erlanger Workshop Warmblechumformung* (2008), pp. 1–21
54. T. Nishibata, N. Kojima, Effect of quenching rate on hardness and microstructure of hot-stamped steel. Tetsu-to-Hagane **96**(6), 378–385 (2010)
55. K. Hidaka, Y. Takemoto, T. Senuma, Microstructural evolution of carbon steels in hot stamping processes. ISIJ Int. **52**(4), 688–696 (2012)

56. Y. Ishimori, T. Shima, H. Fukuchi, Patent application, JP-A-2007-75834, 2007. JP-A-2007-75834
57. N. Nomura, H. Fukuchi, A. Seto, Effect of high cooling rate on shape accuracy of hot stamped parts, in *5th International Conference on Hot Sheet Metal Forming of High Performance Steel, CHS2, Toronto, ON, Canada* (2015), pp. 549–557
58. T. Senuma, Y. Takemoto, Present status and future perspective of hot stamping technology. J. Jpn Soc. Technol. Plast. **51**(592), 410–415 (2010)
59. T. Senuma, H. Magome, A. Tanabe, Y. Takemoto, New hot stamping technology characterized by its high productivity, in *2nd International Conference on Hot Sheet Metal Forming of High Performance Steel, CHS2, Luleå, Sweden* (2009), pp. 221–228
60. E. Ota, Y. Yogo, T. Iwata, N. Iwata, K. Ishida, K. Takeda, Formability improvement technique for heated sheet metal forming by partial cooling, in *Metal Forming 2014*, vol. 622 of *Key Engineering Materials* (Trans Tech Publications, 2014), pp. 279–283
61. E. Ota, Y. Yogo, N. lwata, Deep drawing technique with temperature distribution control for hot stamping process, in *5th International Conference on Hot Sheet Metal Forming of High Performance Steel, CHS2,Toronto, ON, Canada*(2015), pp. 549–557
62. T. Kurz, G. Luckeneder, T. Manzenreiter, H. Schwinghammer, A. Sommer, Zinc coated press-hardening steel-challenges and solution. in *5th International Conference on Hot Sheet Metal Forming of High Performance Steel, CHS2, Toronto, ON, Canada* (2015), pp. 345–354
63. T. Nishibata, The effect of alloying element on properties of TS 1.8 GPa grade hot-stamped parts. *CAMP-ISIJ*, **21**, 597–598 (2008)
64. M. Nagumo, T. Yagi, H. Saitoh, Deformation-induced defects controlling fracture toughness of steel revealed by tritium desorption behaviors. Acta Mater. **48**(4), 943–951 (2000)
65. H. Fuchigami, H. Minami, M. Nagumo, Effect of grain size on the susceptibility of martensitic steel to hydrogen-related failure. Philos. Mag. Lett. **86**(1), 21–29 (2006)
66. S. Yamasaki, T. Takahashi, Evaluation method of delayed fracture property of high strength steels. Tetsu-to-Hagane **83**(7), 454–459 (1997)
67. M. Matsumoto, Y. Takemoto, T. Senuma, Influence of microstructures on hydrogen embrittlement susceptibility of hot stamped ultrahigh strength components, in *5th International Conference on Hot Sheet Metal Forming of High Performance Steel, CHS2, Toronto, ON, Canada* (2015), pp. 55–64
68. A. Tokizawa, K. Yamamoto, Y. Takemoto, T. Senuma, Development of 2000 MPa class hot stamped steel components with good toughness and high resistance against delayed fracture, in *4th International Conference on Hot Sheet Metal Forming of High Performance Steel, CHS2, Luleå, Sweden* (2013), pp. 9–12
69. S. Tateyama, R. Ishio, K. Hayashi, T. Sue, Y. Takemoto, T. Senuma, Microstructures and mechanical properties of V and/or Nb bearing ultrahigh strength hot stamped steel components. Tetsu-to-Hagane **100**(9), 1114–1122 (2014)
70. K. Yamamoto, K. Hidaka, K. Morioka, T. Sue, Y. Takemoto, T. Senuma, Microstructural control for improving productivity and mechanical properties of hot-stamped products. J. Jpn Soc. Technol. Plast. **54**(625), 137–142 (2013)

Chapter 7
Post-Forming Operations

Eren Billur and Felix Quasniczka

Abstract Once an automotive part is formed and quenched, it may be required to trimmed/pierced, shot blasted (depending on the coating) and then welded to subassemblies and assemblies. It is essential to understand all these steps of manufacturing. After each and every step, quality control—both online and offline—has to be done. This chapter discusses the so-called "Post-Forming Operations".

7.1 Typical Process Chain

Hot-stamping process starts with a coil of sheet steel and ends with the final component or the subassembly. The first process in the chain is decoiling and blanking. The blanks are stacked and moved to the furnace loading area. Another material handling unit takes one batch at a time—which may be up to four blanks per batch—and places them into a furnace. The furnace heats the blanks over their austenitizing temperature. The blanks are then transferred quickly to a press where forming and quenching are done consecutively. The parts are moved out of the press and typically laser trimming/piercing is the last process before welding the component to a subassembly. A typical process chain is shown in Fig. 7.1 [1].

A summary of process chain depending on different blank coatings and process types are shown in Fig. 7.2.

This chapter discusses only the post-forming operations.

E. Billur (✉)
Billur Makine Ltd., Ankara, Turkey
e-mail: eren@billur.com.tr

E. Billur
Atılım University, Ankara, Turkey

F. Quasniczka
Associated Spring, 44330 Plymouth Oaks Blvd, Plymouth, MI 48170, USA
e-mail: FQuasniczka@asbg.com

E. Billur (ed.), *Hot Stamping of Ultra High-Strength Steels*,
https://doi.org/10.1007/978-3-319-98870-2_7

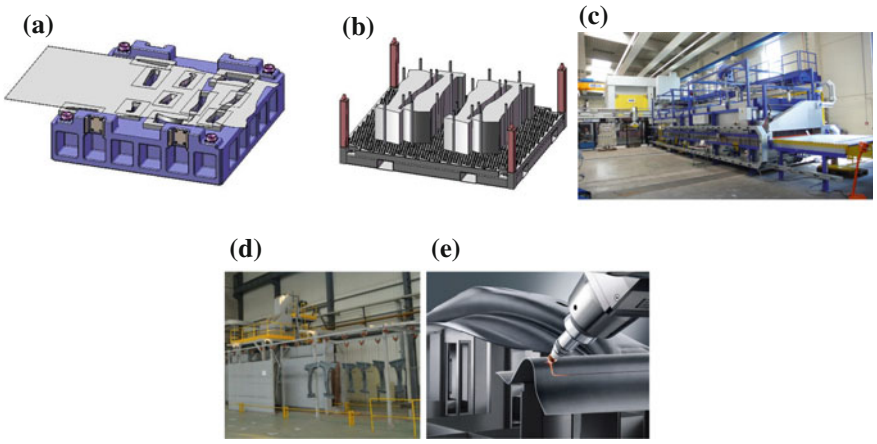

Fig. 7.1 Typical process chain for a hot-stamped component: **a** blanking, **b** material handling, **c** heating, forming and quenching, **d** surface conditioning, **e** trimming/piercing [1–4] (The last two are not mandatory, and depending on the process they may not be required)

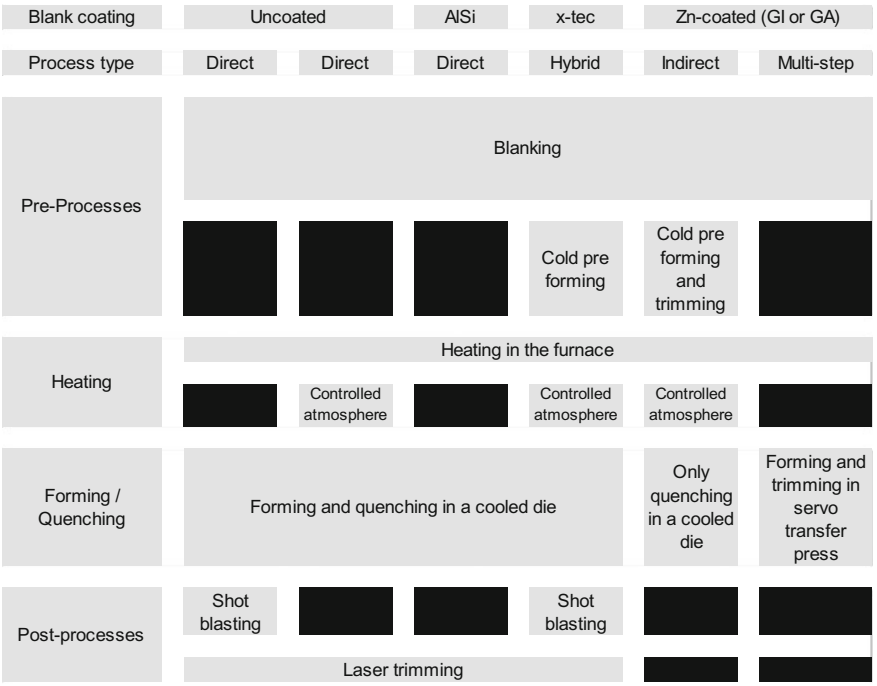

Fig. 7.2 Summary of the processs chains with respect to blank coating and process types (re-created after [5, 6])

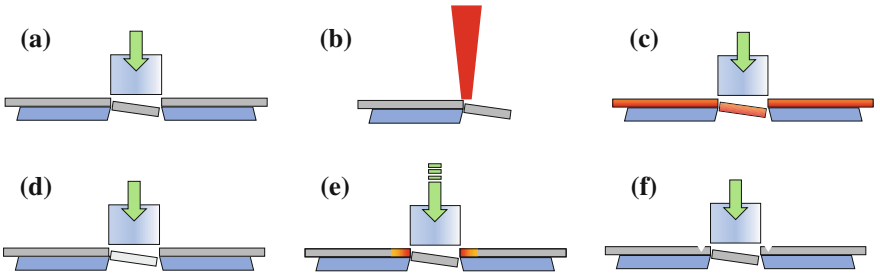

Fig. 7.3 Cutting (trimming, piercing) methods for hot stamped components: **a** hard cutting, **b** laser cutting, **c** hot cutting, **d** cutting of soft zones, **e** adiabatic cutting, **f** cutting with notches [re-created after [7–10]]

7.2 Trimming and Piercing

After hot stamping, the parts may be required to cut. If a hole or shape is cut inside the blank, this is called "piercing". If the periphery of the part is cut, this is called "trimming". In indirect and multi-step hot-stamping processes, post-form trim/pierce are not required. Thus, trimming and piercing are part of direct hot stamping process chain (typically applies to AlSi-coated or uncoated blanks).

Since hot-formed parts have a tensile strength of 1500 MPa (~220 ksi), press forces and tool stresses are extremely high in conventional hard cutting. Thus, several trimming/piercing methods are developed for hot stamping, as shown in Fig. 7.3.

7.2.1 Hard Cutting

Due to very high tensile strength, press forces, and tool stresses are extremely high, in the order of a few hundred tons and 2700 MPa, respectively; if hard trimming would be used (Fig. 7.3a) [11]. Faster wear of the trimming dies and high maintenance cost of the trimming press are still a problem [12].

Laumann [11] studied the effect of hardness on the failure of trimming dies. As seen in Fig. 7.4a, uncoated tool steels would wear out if they were not hardened. Toughness of most tool steels would be reduced as their hardness is increased. Thus, a harder tool steel which would have more wear resistance would now fail by chipping and fracture (Fig. 7.4a). These results show, if hard trimming/piercing would be done, special powder metallurgy tool steels and/or advanced tool coatings would be required [11, 13]. According to a steelmaker, one of the most common tool steels AISI D2 (also known as 1.2379) would fail almost immediately in trimming of 1.6 mm thick, hardened 22MnB5 [14].

Several tool steels and treatments (i.e., nitriding, coating, etc.) are proposed to improve the tool life of hard cutting. One study showed that in piercing holes in a B-pillar, AlCrN PVD (Physical Vapor Deposition) coating would improve the tool

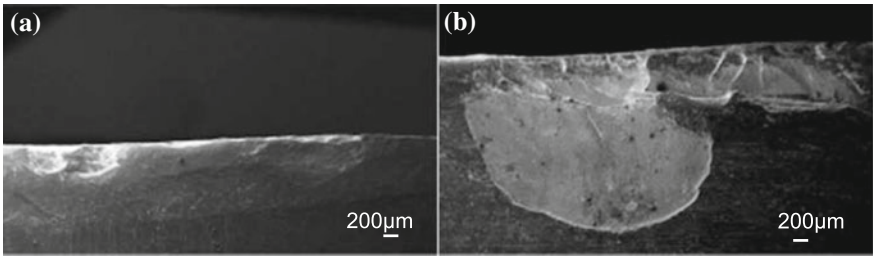

Fig. 7.4 Damage in the cutting edge after 5000 trimmings: **a** areas with low hardness (∼59 *HRC*) wears out, **b** whereas high hardness (∼63 *HRC*) areas failed by chipping/fracture [re-created after [11]]

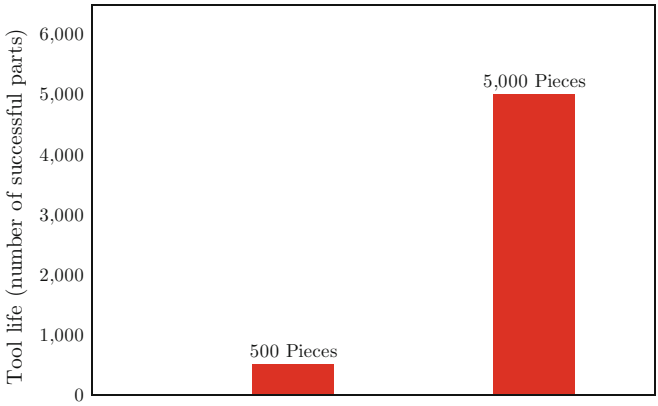

Tool Material	1.3394	1.3394
Tool Coating	PVD TiN	PVD AlCrN
Blank Thickness	n/a	n/a
Blank Coating	AlSi	AlSi

Fig. 7.5 Tool life of TiN-and AlCrN-coated dies, for piercing AlSi-coated 22MnB5 [re-created after [13]]

lifetime by tenfold, Fig. 7.5. Although the overall tool life was still low (5, 000 pieces); both tool wear and burr formations were reduced [13] (Fig. 7.6).

As early as 2002, Industeel developed a new tool steel in X110 CrMoV8 family, trademarked as Tenasteel ® [15]. In a study in 2011, Tenasteel was used to trim hardened 22MnB5 B-pillars, the tool life was found to be in the order of ∼80,000 for 1.6 mm thick material, and dropped to ∼40,000 for 1.8 mm thick material. The same study also confirmed that the typical tool steel D2 (1.2379) could not trim 1.6 mm thick blanks [14]. Another study in 2015 showed that trimming life could be improved with hard coatings [16]. It has to be noted that for a typical hot stamping line, daily production could be calculated as the working hours divided by cycle time

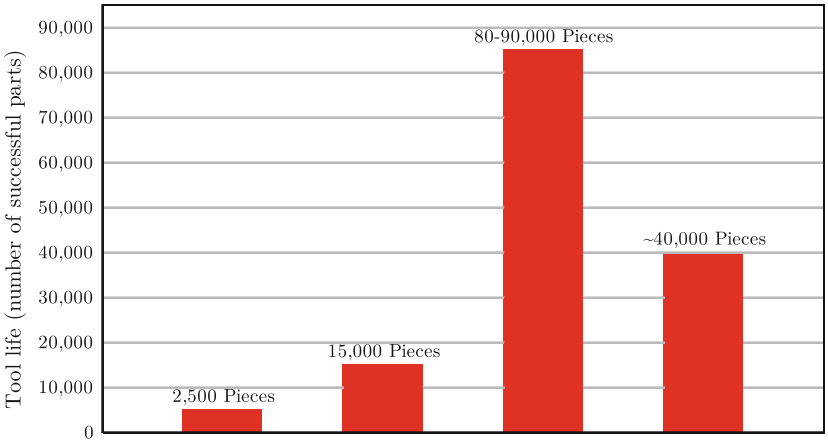

Tool Material	P/M Steel	P/M Steel	Tenasteel	Tenasteel
Tool Coating	Uncoated	BN Coated	Uncoated	BN Coated
Blank Thickness	2.2 mm	2.2 mm	1.6 mm	1.8 mm
Blank Coating	AlSi	AlSi	AlSi	AlSi

Fig. 7.6 Trimming tool lives under different conditions (re-created after [14, 16])

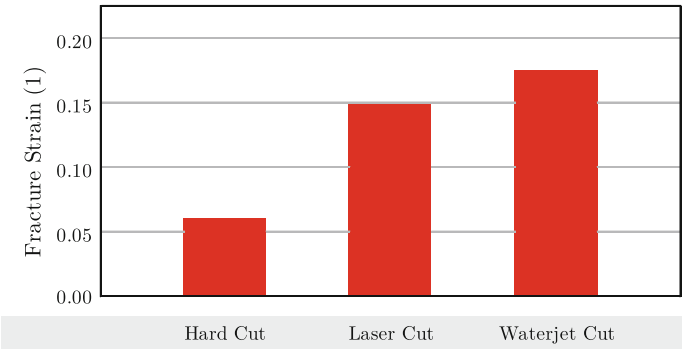

Fig. 7.7 Fracture strain of 22MnB5 after hardening and cutting, measured by DIC method (re-created after [18])

and overall equipment efficiency (OEE). In a 3-shifts plant, 6,000 parts could be manufactured in 20 s cycle time and 70% OEE.

Hard cutting creates burrs, shear zone, and a fracture zone which may have micro-cracks and other irregularities [17]. These irregularities reduce the fracture strain, which would affect the crashworthiness of a component, as seen in Fig. 7.7. In this study, tensile specimens were produced with different cutting methods and the fracture strains were measured via Digital Image Correlation methods [18]. Another study in Spain has shown that the cut edge quality had a direct effect on the fatigue strength as well, Fig. 7.8 [19].

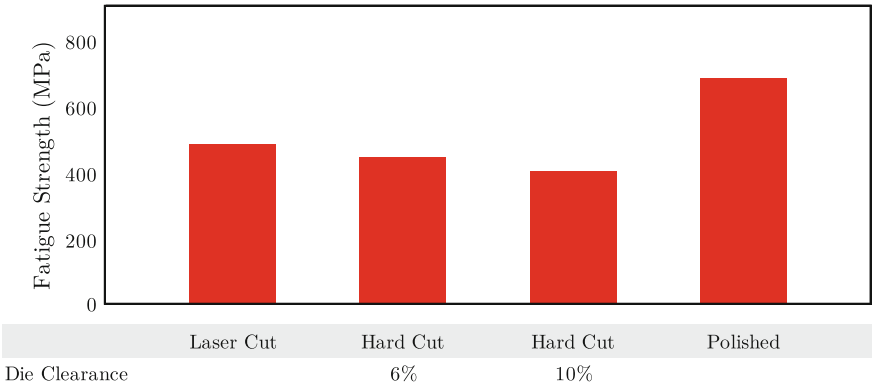

Fig. 7.8 Fatigue Strength after hardening and cutting (re-created after [19])

Several modifications to hard cutting are also proposed, these are discussed in Sect. 7.2.3.

7.2.2 Laser Cutting

Currently, laser cutting is the most commonly used method for cutting purposes. The advantage of using the laser is, that there is no limitation on the shape of the parts to be trimmed. The disadvantages are relatively long cycle times and high capital investment and maintenance cost [19, 20]. However, as explained in the previous section, laser cut parts may have higher fatigue strength and failure strains. The latter one is a significant contributor to the crashworthiness [18, 19].

In principle, when laser is absorbed by a surface, the surface is heated by radiation. When excessive heat is focused on a very small area (i.e., high power density), laser can be used for cutting purposes. Depending on the material type and thickness, cutting could be achieved by evaporation or melting. In the case of hot stamped steel, laser melts the material in the kerf (the width of the cutting groove). Molten steel is removed by reactive gas [21].

Laser cutting can be easily automated. Laser cutters have been long available for fabrication of 2D blanks [21]. Laser blanking (i.e., preparing the initial blanks for hot-stamping process, see Fig. 7.1a) is also proposed and used for small batch production; a hot stamper would use laser cutting to trim/pierce the hot-formed part [20, 22]. Thus, for hot-stamping industry, laser cutters are either 5-axis machines or robotic [2]. Typical five-axis machines have rotary tables with two-parts fixtures. While one fixture is rotated inside the laser cutting machine, an operator can unload the trimmed part from the previous cycle and load the untrimmed part for the next cycle [23]. The time for rotation could be in the order of 2–2.5 s, whereas the dead time between two cycles is as low as 5 s [7].

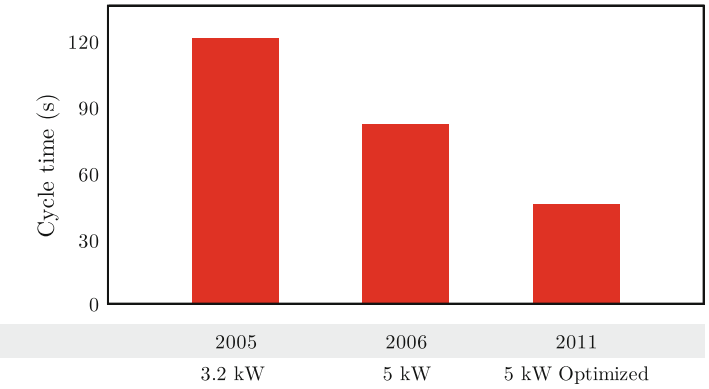

Fig. 7.9 Cycle time improvement in laser cutting of a B-pillar, cutting length is 6.3 m, (re-created after [24])

Fig. 7.10 Approximate cost breakdown of the most common process: direct hot stamping of AlSi-coated 22MnB5 followed by laser trimming (re-created after [22])

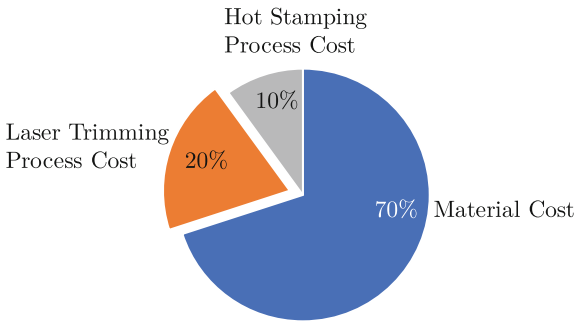

When Volkswagen started with Passat production in 2005, the part required a total of 6.3 m (∼20.7 ft) cutting length: periphery trimming and 22 piercings. At that time, a 3.2 kW, five-axis laser machine was used for the job, and the total cycle time was 120 s. Through several optimizations, the cycle time is reduced to ∼45 s levels in the next few years, Fig. 7.9. Now with the very low cycle times, an operator may not be fast enough to unload/load parts. Thus robotic loaders/unloaders are becoming more common [24]. One has to notice that nowadays 45 s cycle times are standard for laser cutting, however, the hot-stamping press cycle is around 15 s, and in one cycle two or four parts are typically hot stamped. Thus, per each hot-stamping press, three to six laser cutters may be required [23, 25].

Laser cutting can achieve ±0.5 mm tolerances in hot-stamped automotive components [26]. For the areas with larger acceptable tolerances, "Piercing on the fly" can be used. In this mode, the laser cutter head does not move to the precise piercing height. In this case a significant improvement in cycle time can be achieved in the expense of tolerance (±2.5 mm) [7, 24].

As a rule of thumb, the cost of direct hot stamping followed by laser cutting can be calculated as shown in Fig. 7.10.

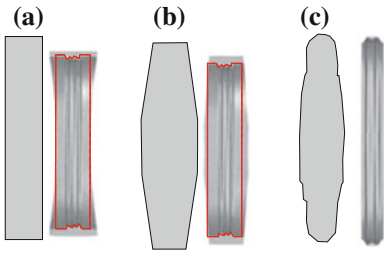

Fig. 7.11 Initial blank shape and final part geometry. Red line shows the areas to be laser trimmed: **a** Iteration 1 starts with a rectangular blank, **b** iteration 2, and **c** final iteration where no laser trimming is required (re-created after [28])

Since laser trimming is still a big part of the cost pie, several methods are developed to reduce—if not totally replace—the need for laser trimming. Alternative trimming methods are explained in the next section.

7.2.3 Alternative Cutting Methods

7.2.3.1 Blank Development

Blank development is designing the initial blank geometry such that no trimming would be necessary after forming/drawing operations, as shown in Fig. 7.11. The method is typically applicable for areas with ±2...3 mm tolerances. In automotive applications several areas could accommodate such large tolerances, including (1) overlapping flanges for spot welding and (2) holes used for e-coat drainage, weld electrode access, or cables [22, 27].

The achievable tolerance level depends on (1) positioning of the blank on the hot-forming die and (2) geometry requirement in the final part. It is essential to locate the blank through two locating holes in the blank [22, 26]. Currently, commercially available simulation software can handle the blank shape optimization through an iterative calculation [29, 30]. A study in 2015 has proven that through simulation the maximum deviation between the desired final part geometry and the hot-stamped part was in the order of 1.21...1.67 mm depending on the edge geometry [26]. Blank development together with nesting optimization could reduce the trimming cost and material cost together (see Fig. 7.10).

7.2.3.2 Hot Cutting

In (in-die) hot cutting process, the trimming/piercing operations are done at the same die set that hot stamps the part. According to Koroschetz et al., there are two different die designs for hot cutting [26]:

1. Hot cutting before forming, using cutting blades,
2. Hot cutting after forming is completed. This one requires actuators.

Hot cutting is limited to areas where the cutting plane is close to 90°. For this reason, not all trimmings and piercings may be suitable for hot cutting process [31]. Although using cams for side piercings have been tried, typically hot cutting is limited ±10° angle from the bolster plane [32, 33].

The first method has a simpler die design, but the flanges may draw-in and/or shrink (due to temperature and also microstructural changes). Thus, the tolerances in the flange geometry depends very much on the process and the die design [26].

Since 2011, Honda is using hot cutting in series production. The cutting is done, however, after the part forming is completed, before the quenching. Thus, the material would be softer to cut, causing much less die stress and press force [34].

One of the most major problems in hot cutting after forming - especially in piercing—is the shrinkage of the blank. As the blank is simultaneously being cooled at a rate over 27 °C/s (49 °F/s) while cutting is performed, the blank would shrink in size. Considering the clearances are 5...15% of the material thickness, the punch must be moved out very quickly once the piercing is completed. For this reason, very fast hydraulic actuators are advised [34–36].

Hot cutting could reduce the cost of the total process by reducing the cycle time, work-in progress and capital investment. Although the main reason for in-die hot cutting was to reduce a secondary step, either it be a laser trim or hard trim process; there are more advantages of hot cutting. Matsuno et al. found that around the hot sheared edge, finer grains of ferrite are formed and thus delayed fracture is prevented [37]. According to a recent study, the optimum process parameters are cutting around ~550 °C (1020 °F) and with 5% clearance [36].

Because of the limitation of cutting angle and the requirement of expensive actuators, hot trimming is typically used in conjunction with other methods. This is explained in detail in Sect. 7.2.3.7.

7.2.3.3 Hot "Half" Cutting

A modification to hot cutting is, hot "half" cutting, in which the process is not completed and the slug is not removed from the blank. Although the word "Half" may suggest that 50% of the thickness is sheared, it may be possible to shear between 10 and 70% of the thickness [37]. The engineers who had developed this technology claims that the technique is a practical solution to difficulty of slug (scrap) removal in the hot cutting process. The slugs are later sheared by hard cutting, as shown in Fig. 7.12 [33, 38, 39].

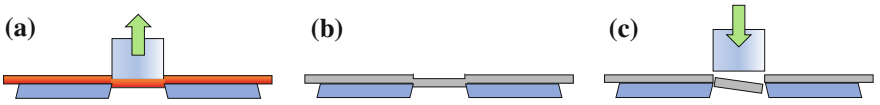

Fig. 7.12 Schematic of hot half cutting: **a** the cutting is done in hot condition but interrupted before the slug is separated, **b** once the part is cooled, **c** it is then hard cut (re-created after [38])

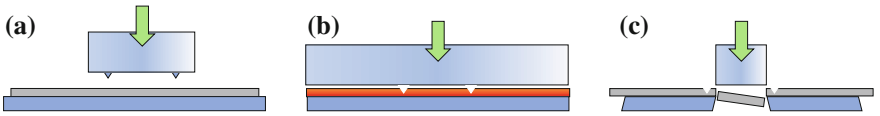

Fig. 7.13 Schematic of cutting with notch: **a** the notch is formed before the **b** hot-stamping process. **c** The blank is then hard cut (re-created after [10])

It was also shown that by hot "half" cutting, the cutting forces in the final hard cutting Fig. 7.12c can be reduced by almost 50%, whereas the energy requirement was reduced by over 80% [38].

7.2.3.4 Cutting with Notch

Another method proposed to reduce the cutting forces and sheared edge damage, is cutting with notch. In this method, a preforming is done to form notch along the cutting line, while the blank is still in as-delivered condition (in Ferritic-Pearlitic phase). The blank is then hot stamped and quenched. The process, depending on the notch direction (upside or downside) can be used to generate burr-free edge and/or to reduce the cutting forces in hard cutting [10] (Fig. 7.13).

7.2.3.5 Cutting Soft Zones

Please see Sect. 8.4.3.

7.2.3.6 Adiabatic Cutting

A typical hard cutting press would typically operate around 25...100 mm/s (1...4 in/s). The plastic deformation in the shear zone generates some heat. When cutting is done with at very high press speeds, over 3 m/s (120 in/s), the heat produced would not have time to dissipate. Thus, temperature increases very rapidly in a very narrow shear band (~100 μm ~4000 μin thickness) for a very short time (less than 100 μs), as shown in Fig. 7.3e. With increased temperature, the material softens, much faster than it strain hardens [25, 40–42].

By using adiabatic cutting, it is possible to get [43, 44]:

1. Almost no burr and very smooth cut edge,
2. Uniform hardness distribution throughout the edge,
3. Very low cycle times, high productivity if the process could be automated,
4. Can be used both for piercing and trimming,
5. No lubricants are required and tool wear is reduced.

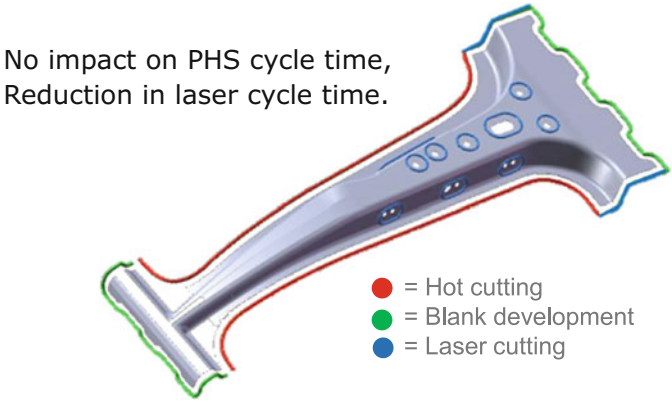

Fig. 7.14 Combining different trimming techniques would reduce the laser cutting length (and thus the laser cycle time), without affecting PHS cycle time (re-created after [44])

Presses that are capable of adiabatic cutting are already commercially available. However, the technique is still not in mass production.

7.2.3.7 Combination of Different Cutting Methods

As discussed in earlier sections, each and every cutting methods has its own advantages and limitations. Even in a single component, it is possible that several holes or outlines could not be hot trimmed (due to geometric limitations). For assembly reasons, some dimensions may have tighter tolerances than others. Thus, it may not be feasible to avoid laser cutting or use only one alternative cutting method.

As discussed in laser trimming section, a typical B-pillar may require as long as 6 m (20 ft) of trimming and piercing. Depending on the thickness of the part and the geometry, trimming of 6 m (20 ft) would typically around 45 s. However, by combining different cutting methods, it may be possible to reduce the laser cut length; and thus, the cycle time in laser cutting. An example B-pillar is shown in Fig. 7.14 [24, 44].

7.3 Surface Conditioning

Uncoated and Zn-coated blanks may have a thin oxide layer, even if protective atmosphere were used in the furnace, Fig. 7.15b. This layer may have iron oxides in the uncoated blanks, and zinc oxide in Zn-coated blanks. These oxides must be removed before welding and painting, Fig. 7.15c. To achieve this, sandblasting, shot blasting or dry-ice (CO_2) blasting is typically used [45–47]. According to a recent

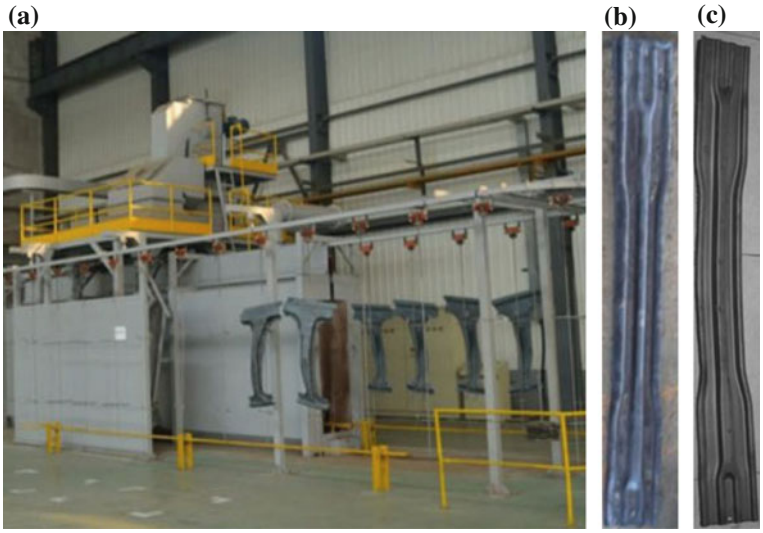

Fig. 7.15 **a** A shot blasting line for hot stamping, **b** an uncoated door beam with scale, **c** the same door beam after shot blasting [4]

study, uncoated and Zn-coated blanks are approximately 22% of the market (uncoated ∼15%, Zn-coated ∼7%) [48].

In shot blasting, small diameter steel balls (0.05...0.3 mm, 2...12 μin) are blown by compressed air. In sandblasting on the other hand, corundum or similar materials are used. Pressure levels are typically around 4–20 bars (∼60...300 psi) [49–51]. The impact from the blasting removes the brittle oxide layer. The process may also introduce some compressive stress. Shot blasting may cause deformation on the thin sheets, and thus may be detrimental to tolerances [46, 52]. A typical sandblasting line is shown in Fig. 7.15a.

After the scale is removed bare steel would be exposed. To prevent oxidation, oiling or coating may be applied [52].

7.4 Quality Control

In conventional cold stamping, the manufacturer receives material and forms the part into the desired geometric shape specified from the customer. The quality department for a cold-stamp operation monitors dimensional results to ensure that part geometry stays within specification set forth by the customer drawing. Quality also ensures that parts do not have any material defects due to bad forming conditions. Splits, excessive thinning, and burrs on trim edges are some of the most common defects that are inherent in the forming process as the production tool wears.

It is important to remember that the hot-stamping process creates both, the geometric part shape and the final material properties. Due to this, manufacturers require additional quality controls which monitor all of the specifications for cold stamping as well as material properties of the final product. The quality department for hot-stamping manufacturers are usually split into two distinct groups, where one is in charge of ensuring parts meet dimensional specifications, and the other is in charge of ensuring that part material properties meet specifications.

This section will be exploring how manufacturers can control dimensional quality throughout the entire hot-stamping process (stamping and post-processing), and how manufacturers can monitor the final material properties of their products.

The mainstream manufacturing process for hot-stamping is usually comprised of the below manufacturing steps. It is important to understand how all of these manufacturing process can impact the final product, and how to monitor and control quality throughout all processes:

- Blanking—cutting a shape from the raw material, which prepares the blank for the heating and stamping process
- Preforming (only in the indirect hot-stamping process)—this is a cold-stamping process which creates part of the geometric shape before the heat-treat, and hot-stamp process.
- Hot-Stamping—the process of heat treating the blank while simultaneously stamping it, creating part form and material characteristics
- Post-Processing—due to the hardness of the material, the part needs to go through post-processing to add any features which need to be held to tight dimensional tolerances
  - Laser Cutting—this is the most common post-processing manufacturing method.
  - Cold Piercing /Trimming—this is another option of adding tight tolerance features but is less popular.

7.4.1 Blanking Quality

Blanking sets the dimensions of any features of the part that is used to locate the hot steel in the hot-stamping die. The blank dimensions need to be precise enough to not interfere with features in the hot-stamp die (such as peripheral guides, etc.). Any hole features placed in the blank and carried through to final product are also set during blanking. The two biggest quality concerns in blanking are (1) Wear in cutting tools (creating excessive burrs in blanks). Keeping the cutting tools and punches sharp and maintained will ensure that the blanks do not form excessive burrs that can cause hinders in the hot-stamping process. It will also ensure that any holes carrying through to the hot-stamp tool and final part will be kept to the correct size (as pins wear, the hole diameter in the metal shrinks). (2) Inconsistent pitch from the raw material feed. Keeping the pitch consistent will ensure that blank fits between peripheral guides, and that hole dimensions are always in the same relative

position to each other as well as trim lines. The final blank shape can be controlled by building a simple jig capturing blank trim. This ensures that there is consistent pitch during the blank stamping process, and that the blank is ok to progress to the next manufacturing process.

7.4.2 Preforming Quality

Preforming is a cold-stamping process and therefore requires all normal quality procedures one would have in a cold-stamp process. With this process, we also need to consider both, the metallurgical component of this operation as well as the dimensional process.

Metallurgical: The most common quality issue one has to control in preforming are surface quality conditions in the steel substrate and in coatings. As with the steel, the part suppliers also produce the final properties of coatings. Different coatings on the steel display various behaviors during the preforming and heating processes. It is important that the preforming process does not remove any coating during the cold-stamping process. Cracks, flaking, and other surface conditions can negatively affect the behavior of coatings on steel before the heat treating and hot-stamping processes. These conditions are unique to part geometry and coating type, and need to be evaluated before production. Surface defects of the steel substrate during preforming can negatively affect metallurgical results of the final hot-stamp product as well, and need to be monitored visually throughout production.

Dimensional: Dimensional properties of the preformed part need to match the predicted shape before moving on to the next operation. The cold-stamp operation usually sets most of the part geometry before moving to hot-stamping for final material properties. It is recommended to have checking fixtures and regular quality control of part dimensions before moving forward to the hot-stamping operation.

7.4.3 Hot-Forming Quality

As mentioned before, the hot-stamping operation is responsible for both, the final form geometry of the part, and the final material properties of the steel substrates and its' coating.

Dimensional: The hot-stamping die is responsible for all of the final form dimensions. Normally, none of the form is influenced by any of the post-processing manufacturing steps. Since the final locating features of the part are created in a later manufacturing operation, it can be difficult to check the dimensional quality of the part's form geometry. To check form in a repeatable manner before final locating features, manufacturers either build a simple holding fixture, or scan parts to final part geometry.

Holding fixtures use a combination of rough locating holes and form to locate the part in a positive manner. Since hole-geometry distorts during hot forming, any holes not pierced during hot forming cannot be used as final locating features. This means that the rough locator holes used for holding or "in-process"? fixtures usually get removed during the laser process as they are no use to the customer. This also means that it is difficult to check parts after hot-stamping due to not having final locating features in the parts.

Scanning equipment can also be used to check part geometry off the hot-stamping die. There are different type of scanners, but in general, the scanning equipment is able to pickup all form geometry points. The operator can then fit the actual scanned results to the theoretical CAD model to understand if any form geometry is off location.

It is important for manufacturers to come up with a part check strategy after hot-stamping, as the part's final geometric form is set in the hot-stamp die.

Metallurgical: Since final material properties are created during the hot-stamping operation, it is important to keep tight quality control on material properties for all parts produced. Every hot-stamp die has a unique operating recipe associated with it which ensures that desired dimensional properties and material properties are achieved. This recipe is determined with much testing before production start, and needs to be set-up with a big enough operating window for production equipment to keep up with the required processing times.

Hot-stamping equipment has many redundant systems measuring all applicable process parameters throughout the production process. Due to these, it is assumed that the production environment is stable and that all part processed meet the processing parameters set forth in the die operating recipe. Due to the critical nature of these parts, manufacturers due to random sampling of parts to ensure that everything produced meets material specifications. A sampling schedule needs to be set-up unique to each manufacturer to ensure that all production shifts have adequate amount of testing. At a minimum parts shall be tested close to the beginning of run to ensure that tooling was set-up correctly, in the middle of the run to ensure that nothing has changed, and at the end of run for verification. Testing frequencies and sample sizes need to take production run sizes, die cavities, and number of ovens into account when being created. It is important to collect parts form all production streams (such as different die cavities of same part, different ovens or oven cavities, etc.) oversampling lifetime. For example, one should never just test parts out of the same oven and die cavities if there are more than one.

All sample parts need to have a full metallurgical evaluation before shipments are released to the customer. To ensure that properties are achieved throughout the entire part, samples are tested at both micro and macro levels. Common tests that are evaluated at the manufacturers are:

- Hardness → Macro and Micro Level
- Tensile Test → Yield Strength, Ultimate Strength, and Elongation
- Microstructure → Check to see if basic martensite microstructure is achieved
- Coating Evaluation → check to see if coating is intact, and if it is properly alloyed.

Table 7.1 Common joining method for hot-stamped steel to other parent metals (re-created after [53–55])

Parent metal	Most common method	Alternative methods
Cold-formed sheet steel	RSW	Arc Welding
Hot-formed sheet steel	RSW	Arc Welding
Aluminum sheet	Resistance Element Welding + adhesive bonding	Element Arc Welding
		Friction Element Welding
		Hemming
		Special riveting in soft zone
Aluminum Profile	Screwing with pre-punched holes + adhesive bonding	Resistance Element Welding + adhesive bonding

7.5 Welding and Assembly

A typical car body consists of 250...400 steel sheets joined together. In the recent years, die-cast, extruded or sheet aluminum are also increasingly used. The main joining method of automotive industry is "Resistance Spot Welding" (RSW). In the last decade, brazing, adhesive bonding, mechanical joinings (clinching, flow drill screws, rivets, etc.,) and resistance element welding are getting more popular with multi-material-mix car bodies which contain steel and aluminum components joined together [53].

Table 7.1 shows the most common welding methods to weld hot-stamped steel to other metals.

7.5.1 Resistance Spot Welding

In resistance spot welding, two or three similar materials (i.e., steel to steel) can be welded using two electrodes. As shown in Fig. 7.16, a typical cycle has four stages and three variables: (1) clamping force (F), (2) current (I), and (3) cycle times (t) [56].

The typical RSW process window is shown in Fig. 7.17a. The minimum welding current (I_{min}) is typically the defined by the weld nugget diameter being around $4\sqrt{t}$ or by a defined minimum shear strength of the weld, Fig. 7.17b. The maximum current (I_{max}) is decided by the expulsion. Expulsion can be defined as a spot welding defect, in which, the molten metal is ejected from the parent metals. The range between the minimum and maximum current is called as "welding current range", and for automotive applications, it is advised to be equal to or over 2 kA [49, 52, 58, 59].

Due to high carbon equivalence of 22MnB5, the current range is typically low. To improve current range, two-pulse (also known as Waveform control) welding can be

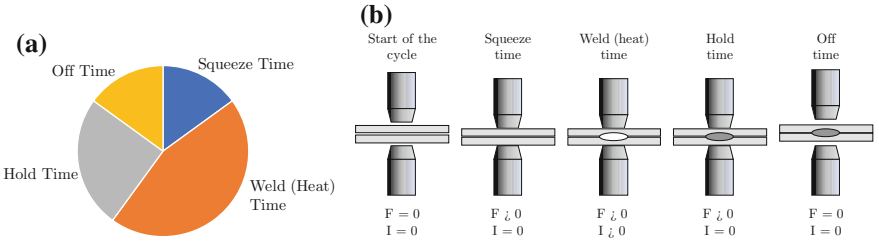

Fig. 7.16 Resistance spot welding: **a** approximate cycle times, **b** electrodes in each cycle (re-created after [57])

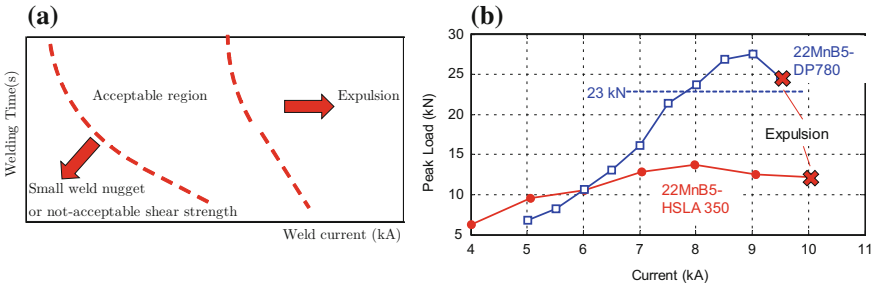

Fig. 7.17 **a** Resistance spot weld parameters and acceptable region (re-created after [59]), **b** peak load the weld can carry is a function of weld current (re-created after [60, 61])

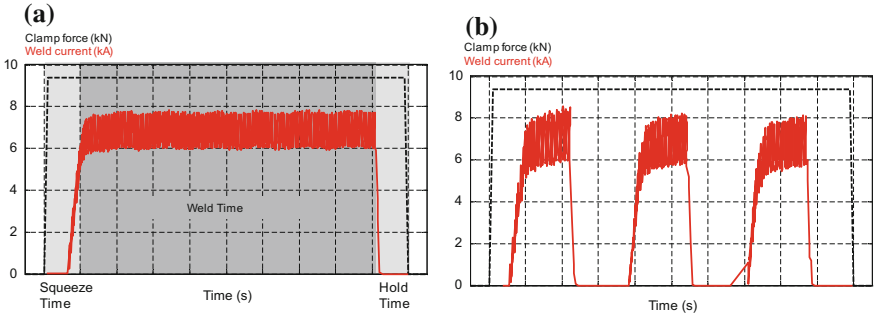

Fig. 7.18 Current and clamp force versus time graphs of (1) single-pulse weld cycle, (2) waveform control with three pulses (re-created after [59])

used. In this method, the clamp force is not removed while the current is turned on and off. Figure 7.18a shows a single-pulse weld cycle, and b shows a three-pulses weld cycle [47, 59].

In resistance welding of hot-stamped steels, (1) coating thickness (especially interdiffusion layer), (2) existence of surface oxides, and (3) final hardness are three important factors. The first two items would change the resistance of the stack, whereas the final hardness is important as it is a result of the microstructure [47, 52].

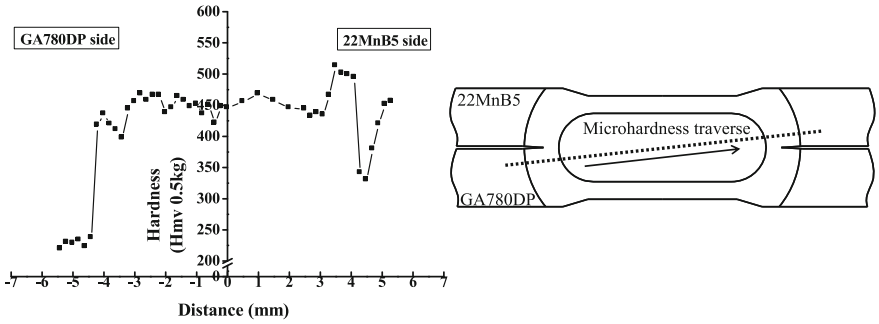

Fig. 7.19 Hardness distribution in a spot weld between AlSi coated 22MnB5 and DP780 GA [60]

A study with tailored tempered Zn-coated blanks showed that with a two-pulse method, a weld current range of 1.7 kA could be found for samples that are annealed at between 650...910 °C (1200...1670 °F). Spot welding was applied after dry-ice blasting. The weld strength was measured right after welding and also after a 10 weeks of VDA 621-425 corrosion test—to simulate lifetime of a vehicle. Results have shown that in the tailored areas (i.e., not heated over 910 °C (1670 °F)) had 12...25% higher weld strength after VDA test [47].

When hot-stamped steel is welded to cold-formed automotive steel, there would be a heat affected, softened zone. Still, since most automotive steels are much softer than this zone. In a study by Choi et al., AlSi coated 22MnB5 was spot welded to DP 780 GA. The weld's strength (i.e., peak load) versus weld current can be seen in Fig. 7.17b. The hardness distribution in the weld is shown in Fig. 7.19 [60] (Fig. 7.20).

When 22MnB5 is welded to another 22MnB5 steel, the weakest point (i.e., the lowest hardness value) in the assembly becomes the heat- affected zone (HAZ). A study in Sweden showed that when 22MnB5 is spot welded to another 22MnB5, the base materials would have almost constant $500HV$ hardness, whereas in the weld zone the hardness may be as low as $350HV$. When such a welded assembly is tensile tested, it would always fail at the weld zone [62]. Another study has shown that spot welds are acting as "metallurgical notches", an analogy to holes and pierces acting as "geometric notches". A hot-stamped steel bumper beam with no holes and welds would absorb more energy without fracture whereas when a spot weld or a hole is introduced a sudden failure would be observed and the energy absorption capacity is significantly reduced, Fig. 7.21 [63].

7.5.2 Arc Welding

As seen in Table 7.1, the second most common method to weld hot-stamped steel to another steel is "arc welding". In automotive industry, arc welding is used in blind

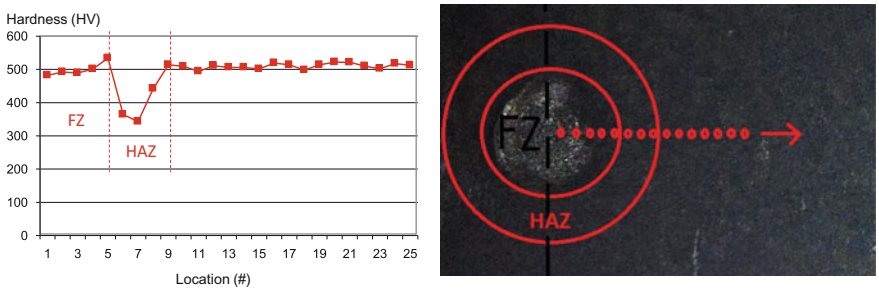

Fig. 7.20 HAZ softening when 22MnB5 is spot welded to 22MnB5 [62]

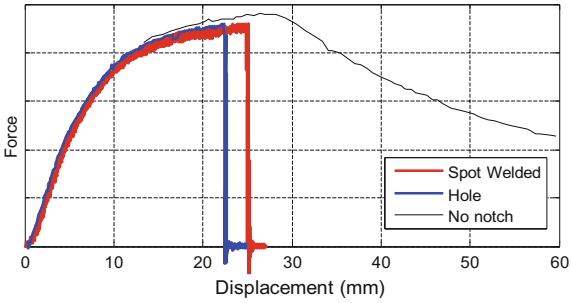

Fig. 7.21 Notches reduce the energy absorption of hot-stamped parts and cause sudden failure. A spot weld would act as a "metallurgical notch" [63]

areas (i.e., accessible only from one side). In this method, electric current is used to melt a consumable electrode [53, 64].

In arc welding of hot-stamped steel to common automotive steels, it was found that there would be a softened area in the heat affected zone (HAZ). As shown in Fig. 7.22a and b, when AlSi- coated 22MnB5 is arc welded to uncoated DP 600 or DP 780, the softest (weakest) point is still in the DP steel. Thus, both in fatigue and static tests, the assembly mostly fails from the soft steel [65, 66].

7.5.3 Other Joining Methods

Recently multi-material mix vehicles are getting more and more common. In these vehicles, not only steel, but also aluminum, carbon fiber, magnesium, and polymers may be used in the car body. It has to be noted that vehicles with aluminum bumpers, doors and closures cannot be classified as multi-material mix, as these components are assembled with bolts (also known as bolt-on components) and are not welded or mechanically joined.

As listed in Table 7.1, for aluminum to hot-stamped steel joinings, resistance element welding is one of the most studied methods and also in mass production for joining aluminum and steel (not necessarily hot stamped) [67, 68].

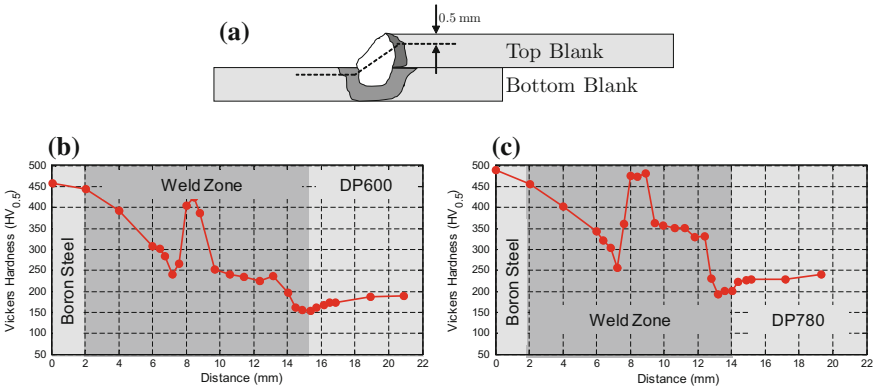

Fig. 7.22 **a** Schematic view of an arc welded lap joint; hardness profile over the dashed line in: **b** DP600-22MnB5, **c** DP780-22MnB5 welds (re-created after [65, 66])

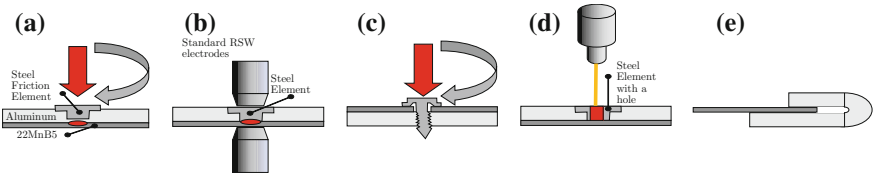

Fig. 7.23 Schematic views of alternative joining methods for hot-stamped steel and aluminum joints: **a** friction element welding, **b** resistance element welding, **c** flow drill screw, **d** element arc welding, **e** hemming (re-created after [55, 67, 70])

One of the earliest vehicles that had both hot-stamped components and aluminum structure was 3rd generation Audi A8 (SOP 2010). In this vehicle 92% of the body-in-white was aluminum, but the B-pillar reinforcement was hot-stamped steel. The hot-stamped reinforcement was spot welded to an HSLA 340 support plate. This plate which had pre-punched holes was later "flow drill screw" ed to the body side panel which was a 6000 series Aluminum (i.e., AlMgSi alloy) [69]. Since then several new methods have been proposed, as seen in Fig. 7.23.

Resistance element welding has been studied by researchers to join 22MnB5 to 6000 series aluminum [71, 72], and steel–polymer–steel sandwich material [56]. Element materials are steel, so that the spot welding is done between two "similar" materials. Several studies have shown elements made of S235 (Mild Steel), S355 (HSLA steel) and 20MnB4 can be welded to 22MnB5 steel [56, 71, 73].

Friction Element Welding is one of the proposed joining methods for hot-stamped steels and aluminum. Audi has been studying the technology since 2012 (if not earlier) [72]. In this method, a high strength steel (e.g., 23MnB4) element is pressed over the soft material (in most cases aluminum) and rotated. The friction creates a hole and generates heat and plasticity in the soft material. By the frictional heat, the steel element is then welded to the base steel (22MnB5), Fig. 7.23a [73]. The system does

not require a precut holes, as opposed to resistance element welding. According to [72], friction element welds may carry over 2.5 times more load, compared to resistance element welded assembly. Thus, with increased load capacity per joint, less number of joints may be feasible. On the negative side, the method requires two side accessibility and leaves 2...3 mm elevation on the application side [72]. The process is already in mass production at Audi with 2nd generation Q7 (SOP 2015) and 4th generation A8 (SOP 2017). The technique is used to join hot-stamped steel to aluminum sheets and castings [54, 55]. Due to heat generated, hot-stamped steel is tempered around the element. A study has found that hardness may drop from $\sim$500 HV to $\sim$300 HV in the heat affected zone [72].

Flow drill screws can be used to join ultra-high strength steels (up to 1000 MPa ($145ksi$) tensile strength) to aluminum extrusions and castings. In this method, a high strength screw is used to penetrate and thread the materials to be joined, Fig. 7.23c. While threading, fastening is also done [74]. However, as of today, the hardness of screws are not enough to penetrate hot-stamped steel [75, 76]. When flow drill screws are used with steels over 700 MPa tensile strength, a pre-pierced hole may be required [68].

A relatively recent solution to join hot-stamped steel to is called "Element arc welding". As seen in Fig. 7.23d, aluminum is first pierced and a steel element with a hole is placed. The element is arc welded to base metal (could be any high strength steel, including hot-stamped steel). The process does not require two-sided accessibility and can be applied both to profiles and sheets. The researchers have shown that 22MnB5 can be welded to 6000 series aluminum with a very high shear strength [70].

References

1. E. Billur, H. Porzner, D. Lorenz, M. Holeček, M. Vrojlik, M. Hoss, B. Damenha, J. Friberg, C. Koroschetz, M. Skrikerud, From concept to virtual reality: Virtual hot forming engineering, in *5th International Conference on Hot Sheet Metal Forming of High Performance Steel, CHS2, Toronto, ON, Canada* (2015), pp. 463–470
2. J. Karlsson, Press requirements. Presented at AP&T Press Hardening, Next Step Seminar, Novi, MI, September 15th (2010)
3. F. Geyer, Strong metal, light cutting. *The Fabricator* (2013), pp. 64–65
4. P. Hu, L. Ying, B. He, *Hot Stamping Technology and the Main Equipment* (Springer, Singapore, 2017), pp. 19–44
5. J. Aspacher, Press hardening - "dead end" or "take off", in *Presented at 25th European Car Body Conference, March 13-14, Bad Nauheim, Germany* (2007)
6. P. Belanger, New Zn multistep hot stamping innovation. Presented at Great Designs in Steel 2017 (2017)
7. S. Kulp, Laser applications in manufacturing high strength body parts, in *Presented at European Automotive Laser Applications (EALA) 2014, February 11-12, Bad Nauheim, Germany* (2014)
8. J. Banik, Hot forming state-of-the-art and trends. Presented at Insight Edition Conference, September 20–21, Gothenburg, Sweden (2011)
9. D. Landgrebe, M. Putz, F. Schieck, A. Sterzing, A. Rennau, Towards efficient, interconnected and flexible value chains – examples and innovations from research on production technologies,

in *Proceedings of 5th International Conference on Accuracy in Forming Technology (ICAFT 2015)* (2015), pp. 61–78
10. M. Feistle, M. Krinninger, R. Golle, W. Volk, Notch shear cutting of press hardened steels, in *Sheet Metal 2015*, vol. 639 of *Key Engineering Materials* (Trans Tech Publications, 2015), pp. 477–484
11. I. Laumann, T. Picas, M. Grané, D. Casellas, M.D. Riera, I. Valls, Hard cutting of tailored hardened 22MnB5, in *IDDRG, Graz, Austria (2010)* (2010), pp. 355–362
12. R. Kolleck, W. Weiß, P. Mikoleizik, Cooling of tools for hot stamping applications, in *IDDRG, Graz, Austria (2010)* (2010), pp. 111–119
13. J. Livezey, High performance coatings for stamping & forming, in *Seminar in the Ohio State University, Columbus, OH* (2010)
14. D. Viale, R. Bhatnagar, G. Baron, P. Jousserand, M. Gomez, Optimization of stamping tools to process very high strength steels; comparison of cold work tool steels. Presented at Great Designs in Steel, Livonia, MI, May 18th (2011)
15. D. Viale, J. Béguinot, F. Chenou, G. Baron, Optimizing microstructure for high toughness cold-work tool steels, in *Proceedings of the 6th International Tooling Conference* (2002), pp. 299–318
16. I.O. Yilmaz, B. Kaftanoglu, T. Hacaloglu, M. Kilickan, Integration of press hardening with cold trimming, in *Proceedings of 5th International Conference on Accuracy in Forming Technology (ICAFT 2015)* (2015), pp. 349–356
17. K. Nothhaft, J. Suh, M. Golle, I. Picas, D. Casellas, W. Volk, Shear cutting of press hardened steel: influence of punch chamfer on process forces, tool stresses and sheared edge qualities. Prod. Eng. Res. Devel. **6**(4), 413–420 (2012)
18. J. Dykeman, Advanced high strength steel - recent progress, ongoing challenges, and future opportunities, in *International Symposium on New Developments in Advanced High-Strength Sheet Steels* (AIST, 2013), pp. 15–28
19. I. Picas, R. Munoz, A. Lara, R. Hernández, D. Casellas, Effect of the cutting process in the mechanical and fatigue properties of press hardened 22MnB5 steel, in *3rd International Conference on Hot Sheet Metal Forming of High Performance Steel, CHS2, Kassel, Germany* (2011), pp. 85–92
20. M. Fritz, Process optimization of laser cutting and in the heating process, in *3rd International Conference on Hot Sheet Metal Forming of High Performance Steel, CHS2, Kassel, Germany* (2011), pp. 239–245
21. N.B. Dahotre, S. Harimkar, *Laser fabrication and machining of materials* (Springer Science & Business Media, 2008)
22. J. Aspacher, D. Haller, Hot stamping part design and feasibility study with respect to functionality and optimization of production cost. Presented at Forming in Car Body Engineering 2014, September 24-25th, Bad Nauheim, Germany (2014)
23. F. Rima, Hot forming pressroom. Presented at AP&T Press Hardening, Next Step Seminar, September 15, Novi, MI, (2010)
24. Michael Fritz, Ralf Kohllöffel, Laser cutting of press-hardened vehicle body parts. ATZproduktion worldwide **5**(2), 18–23 (2012). Jun
25. F. Schieck, High speed impact cutting (HSIC) for PHS components – challenges and potentials, in *6th PHS Suppliers Forum, Caryville, TN, USA* (2017), pp. 272–283
26. C. Koroschetz, M. Skrikerud, R. Kristensson, L.-O. Jonsson, D. Lorenz, H. Porzner, M. Hoss, Cost effective trimming in hot stamping through the combination of accurate blank development, hot and laser cutting, in *5th International Conference on Hot Sheet Metal Forming of High Performance Steel, CHS2, Toronto, ON, Canada* (2015), pp. 617–628
27. N.K. Akafuah, S. Poozesh, A. Salaimeh, G. Patrick, K. Lawler, K. Saito, Evolution of the automotive body coating process—a review. Coatings **6**(2), 24 (2016)
28. C. Koroschetz, M. Skrikerud, Mit hilfe von warmbeschnitt und plattengeometrie-optimierung zum effizienten warmformteil. Presented at Forum Stanztechnik 2014, November 11-12, Bochum, Germany (2014)
29. esi Group. PAM-STAMP 2015.1 User Guide (2015)

30. AutoForm Engineering. AutoForm-Trim plus. *Product catalogue* (2017)
31. B. Osburg, G. Lengfeld, O. Straube, Innovation and globalization as a factor of success for global hotstamping growth, in *New Developments in Sheet Metal Forming Conference,Stuttgart, Germany* (2012), pp. 79–92
32. M. Alsmann, M. Goede, S. Kulp, M. Lalla, J. Patak, F. Russ, Hot Forming - State of the ARt and Future Reuqirements at Volkswagen. Presented at Materials in Car Body Engineering 2014, May 13-14, Bad Nauheim, Germany (2014)
33. Hong-Seok Choi, Jun-Ho Shin, Jin-Gyu Han, Pan-Ki Seo, Byung-Min Kim, Dae-Cheol Ko, The effect of inclined angle and positioning on the sheared edge in mechanical trimming using hot half-trimming of 22mnb5. Adv. Mater. Process. Technol. **2**(2), 245–251 (2016)
34. K. Teshima, Challenges of high-efficiency hot forming processes at Honda. Presented at Forming in Car Body Engineering 2012, September 26-27, Bad Nauheim, Germany (2012)
35. K. Mori, P.F. Bariani, B.A. Behrens, A. Brosius, S. Bruschi, T. Maeno, M. Merklein, J. Yanagimoto, Hot stamping of ultra-high strength steel parts, in *CIRP Annals - Manufacturing Technology* (2017)
36. D. Kim, Y.-J. Jeon, H. Seok Choi, J. Kang, Y.-D. Kim, Y. Moo Heo, J. Deok Kim, S.-T. Won, An investigation of the trimming of boron nitride steel (22mnb5) during the die-quenching process. *Procedia Engineering* **207**, 1540–1545 (2017). International Conference on the Technology of Plasticity, ICTP 2017, 17-22 September 2017, Cambridge, United Kingdom
37. Takashi Matsuno, Yoshihito Sekito, Kaoru Kawasaki, Microstructure characterization of fine grains near hot-sheared surface formed during hot-stamping process. J. Mater. Process. Technol. **229**, 570–581 (2016)
38. Hong-Seok Choi, Byung-Min Kim, Dong-Hwan Kim, Dae-Cheol Ko, Application of mechanical trimming to hot stamped 22mnb5 parts for energy saving. Int. J. Precis. Eng. Manuf. **15**(6), 1087–1093 (2014). Jun
39. K. ichiro Mori, T. Maeno, T. Suganami, M. Sakagami, Hot semi-punching of quenchable steel sheet. Proc. Eng. **81**, 1762–1767 (2014). 11th International Conference on Technology of Plasticity, ICTP 2014, 19-24 October 2014, Nagoya Congress Center, Nagoya, Japan
40. D. Landgrebe, J. Schönherr, N. Pierschel, S. Polster, A. Mosel, F. Schieck, New approaches for improved efficiency and flexibility in process chains of press hardening, in *ASME 2015 International Mechanical Engineering Congress and Exposition* (American Society of Mechanical Engineers, 2015), pp. V02AT02A033–V02AT02A033
41. S. Subramonian, Chapter 1: Blanking, in ed. by T. Altan, A.E. Tekkaya *Sheet Metal Forming - Processes and Applications* (ASM International, 2012), pp. 1–18
42. T. Childs, *Adiabatic Shearing in Metal Machining* (Springer, Berlin, 2014), pp. 27–33
43. D. Landgrebe, T. Barthel, F. Schieck, Trimming of flat and tubular components by high speed impact cutting (hsic), in *ASME 2017 International Mechanical Engineering Congress and Exposition* (American Society of Mechanical Engineers, 2017), pp. V002T02A066–V002T02A066
44. M. Skrikerud, Next generation of compact hot forming lines for optimised throughput with different materials. Presented at Materials in Car Body Engineering 2013, May 7-8, Bad Nauheim, Germany (2013)
45. W. Fristad, New coil-applied coating for press-hardening steel. Proc. Galvatech **2015**, 892–898 (2015)
46. J Wilsius, P Hein, R Kefferstein, Status and future trends of hot stamping of usibor 1500 p. Geiger, M.; Merklein, M.(Edtr.): Tagungsband zum, **1**, 83–101 (2006)
47. Thomas Manzenreiter, Martin Rosner, Thomas Kurz, Gerald Brugger, Reiner Kelsch, Dieter Hartmann, Andreas Sommer, Challenges and advantages in usage of zinc-coated, press-hardened components with tailored properties. BHM Berg- und Hüttenmännische Monatshefte **157**(3), 97–101 (2012). Mar
48. I.M. Gonzalez, O. Straube, Development of zinc coated parts for hotstamping, in *Proceedings of New Developments in Sheet Metal Forming Conference,Stuttgart, Germany* (2016), pp. 265–276

49. S. Hamamoto, H. Omori, T. Asai, N. Mizuta, N. Jimbo, T. Yamano, Steel sheets for highly productive hot stamping. Kobelco Technol. Rev. **35**, 39–44 (2017)
50. I. Garcia, Weight savings and crash resistance in door constructions through hot stamping of door outer panels. Presented at Doors and Closures in Car Body Engineering 2011, November 16-17, Bad Nauheim, Germany (2011)
51. D. Landgrebe, A. Albert, A. Paul, B. Domes, M. Prohl, 20 years of hydroforming experience at the fraunhofer iwu – innovative process variants, in *Proceedings of New Developments in Sheet Metal Forming Conference,Stuttgart, Germany* (2016), pp. 403–423
52. D.W. Fan, B.C. De Cooman, State of the knowledge on coating systems for hot stamped parts. Steel Res. Int. **83**(5), 412–433 (2012)
53. Jens Meschke, Jörn Tölle, Lutz Berger, Multi-material concept for a battery electric vehicle. ATZ worldwide **119**(11), 48–53 (2017)
54. T. Hämmerle, D. Hußmann, The new Audi A8. Presented at EuroCarBody 2017, October 17-19, Bad Neuheim, Germany (2017)
55. T. Hambrech, The new Audi Q7. Presented at EuroCarBody 2015, October 20-22, Bad Nauheim, Germany (2015)
56. N. Holtschke, K. Nagel, Short-term resistance spot welding in connection with high-dynamic actuators. Presented at Joining in Car Body Engineering, April 5, Bad Nauheim, Germany (2017)
57. Miller Electric Manufacturing Company. *Handbook of Resistance Spot Welding* (2012)
58. H. Zhang, J. Senkara, *Resistance Welding: Fundamentals and Applications* (CRC press, 2011)
59. I. Sung Hwang, M. Jin Kang, D. Cheol Kim, Expulsion reduction in resistance spot welding by controlling of welding current waveform. Proc. Eng. **10**, 2775–2781 (2011). 11th International Conference on the Mechanical Behavior of Materials (ICM11)
60. H.S. Choi, G.H. Park, W.S. Lim, B. Kim, Evaluation of weldability for resistance spot welded single-lap joint between ga780dp and hot-stamped 22mnb5 steel sheets. J. Mech. Sci. Technol. **25**(6), 1543 (2011)
61. Xuebo Liang, Xinjian Yuan, Haodong Wang, Xiuyang Li, Ci Li, Xueyu Pan, Microstructure, mechanical properties and failure mechanisms of resistance spot welding joints between ultra high strength steel 22mnb5 and galvanized steel hsla350. Int. J. Precis. Eng. Manuf. **17**(12), 1659–1664 (2016). Dec
62. O. Hedegärd, M. Åslund, Tempering of hot-formed steel using induction heating. Master's thesis at LTU Lulea Technic University (2011)
63. H. Lanzerath, Simulation: Enabler for the efficient design of lightweight boron intensive body structures. Presented at Insight Edition Conference, September 20-21, Gothenburg, Sweden (2011)
64. L. Morello, L.R. Rossini, G. Pia, A. Tonoli, *The Automotive Body: Volume I: Components Design*. Mechanical Engineering Series (Springer, Netherlands, 2011)
65. R. Koganti, S. Angotti, A. Joaquin, C. Jiang, Effect of materials stack-ups on fatigue performance of dp780 and aluminized coated boron steel gmaw lap joint, in *SAE Technical Paper*. SAE International, (2007)
66. R. Koganti, S. Angotti, A. Joaquin, C. Jiang, C. Karas, Effect of materials stack-ups and microhardness distribution on fatigue performance of dp600 and boron steel gmaw lap joint, in *SAE Technical Paper*. SAE International (2007)
67. H. Kurz, M. Goede, Requirements of sustainable automobile production for future material devlopments. Presented at Insight Edition Conference, December 10-11, Solihull, UK (2014)
68. G. Müllers, Achieving car body lightweight today and tomorrow - weight reduction as a result of substitution and combination. Presented at Strategies in Car Body Engineering 2015, March 17-18, Bad Nauheim, Germany (2015)
69. *The Art of Progress: Audi - The New A8* (2010)
70. R. Suzuki, K. Makii, New dissimilar metal spot joining process for aluminum and high-tensile-strengtrh & ceq. steel based on the advantage of arc welding. Presented at Joining in Car Body Engineering, April 5, Bad Nauheim, Germany (2017)

71. Zhanxiang Ling, Yang Li, Zhen Luo, Yueqiao Feng, Zhengmin Wang, Resistance element welding of 6061 aluminum alloy to uncoated 22mnmob boron steel. Mater. Manuf. Processes **31**(16), 2174–2180 (2016)
72. U. Alber, Friction element welding - innovations for hybrid body parts. Presented at Joining in Car Body Engineering, April 19, Bad Nauheim, Germany (2012)
73. G. Meschut, O. Hahn, Joining technologies for multi-material design - a key to efficient future mobility. Presented at Materials in Car Body Engineering 2012, May 11, Bad Nauheim, Germany (2012)
74. S. Kurtenbach, X. Fang, T. Schlichting, A. Breidenbach, H. Dalhoff, M. Töller, Expansion of the applications from flow drill screwing by developing new high-strength elements. Presented at Automotive Engineering Congress, June 4, Nürnberg, Germany (2013)
75. J. Hover, Challenges of joining a boron-steel intensive body structure. Presented at Insight Edition Conference, September 20-21, Gothenburg, Sweden (2011)
76. S. Sinzel, N. Hornbostel, Expansion of the applications from flow drill screwing by developing new high-strength elements. Presented at Joining in Car Body Engineering, April 5, Bad Nauheim, Germany (2017)

Chapter 8
Tailored Properties

Eren Billur and Vladimir Bošković

Abstract Depending on the performance expectations or to facilitate trimming, improve weldability, a single component may be required to have different local properties. The so-called tailored parts can be produced by incoming tailored blanks. It is also possible to have a standard blank, and can be processed in a hot stamping line to have tailored properties. The aim of this chapter is to give a better understanding to the reader about hot stamped parts having tailored properties in body-in-white applications.

8.1 The Need for Tailored Parts

For automotive applications, the main objectives of the hot stamped components are improving crashworthiness and saving weight at the same time. Therefore, the real performance of these parts should be analyzed in crash conditions (i.e., high-strain impact events) [1, 2].

Generally, ultra high strength (more than 1400 MPa or 200 ksi) is achievable with hot stamping. However, this high strength causes several problems, especially in the automotive applications:

1. The elongation usually is reduced as the strength improves, which results in reduction of the energy absorption,
2. Welding of high strength steels to mild steels creates a heat affected zone, and
3. Required loads for both trimming and piercing processes is high due to the high strength.

E. Billur
Billur Makine Ltd., Ankara, Turkey
e-mail: eren@billur.com.tr

E. Billur
Atılım University, Ankara, Turkey

V. Bošković (✉)
Technische Universität Graz, Inffeldgasse 11/1, A 8010, Graz, Austria
e-mail: vladimir.boskovic@tugraz.at

E. Billur (ed.), *Hot Stamping of Ultra High-Strength Steels*,
https://doi.org/10.1007/978-3-319-98870-2_8

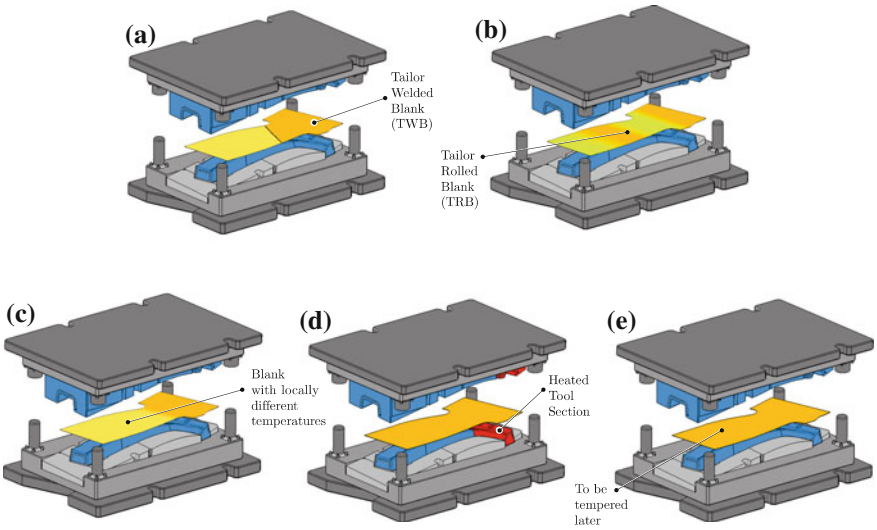

Fig. 8.1 Methods for hot stamping of the parts with tailored properties

To solve these problems, hot stamping parts can be tailored, such that some areas can be fully hardened (martensite), while other areas can remain soft (ferrite+pearlite or bainite). Depending on the role of the structural part (carrying either bending or axial crash load), the best position for the local regions with lower strength and higher ductility can be designed [2–4].

There are four main ways to obtain parts with tailored properties in hot stamping process, Fig. 8.1:

1. The incoming blank can be tailored, as in the case of Tailor Welded Blanks (TWBs), Tailor Rolled Blanks (TRBs), and patchwork blanks,
2. Pre hot stamping process (controlling the blank temperature during heating or the blank cooling rate during transfer),
3. During hot stamping process (controlling the quenching rate),
4. Post hot stamping process (by partially tempering the fully hardened part).

The next sections will discuss these methods.

8.2 Tailored Blanks

Tailored blanks have been commonly used in the automotive industry to reduce the components weight, simply by eliminating the need for reinforcement and/or reducing the blank thickness in low-load areas. Common applications of the tailored blanks are given in Fig. 8.2 [5].

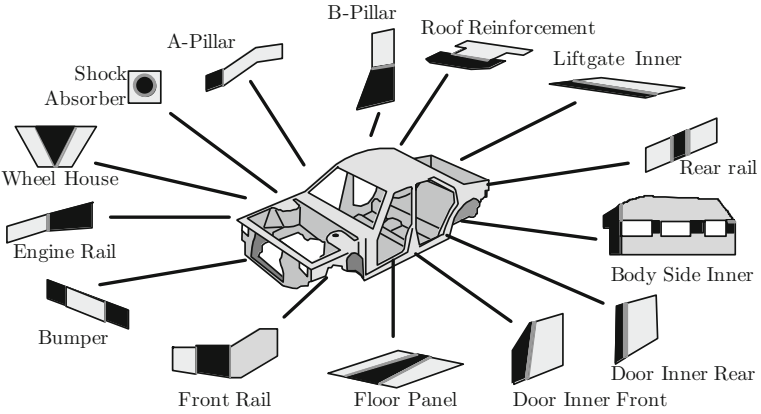

Fig. 8.2 Typical applications of tailored blanks in automobiles [5]

These components either require:

1 A heavy load carrying in some portions, as in the case of a door inner where the areas close to the hinges have to carry more load or
2 An energy absorbing area such as the B-pillar, in which the bottom part should have higher energy absorption capacity and in the upper part high intrusion resistance is required.

The history of tailored parts, (in this particular case Tailor Welded Blanks, TWBs), in the automotive industry began in 1985 at Thyssen Stahl AG, Germany. This development was necessary for the floor pan of the Audi 100, which was upgraded to a fully galvanized body to offer 10 years anti-corrosion warranty [6]. At that time, there were no galvanizing lines to supply the strip at required width. Thus, Thyssen Stahl AG came up with the idea of producing two individual blanks of same dimensions, thickness and coating; and then laser weld them to required dimensions [7]. Recently, a similar study was done at Fraunhofer IWU for magnesium sheets, where the required dimensions were obtained by welded sheets [8].

Tailored blanks have long been used in the automotive industry in cold stamping. Nevertheless, the use of Tailor Welded Blanks (TWBs) and Tailor Rolled Blanks (TRBs) in hot stamping is a more recent technology.

In the next three subsections, details of TWBs, TRBs, and patchwork blanks are given, specifically for hot stamping purposes.

8.2.1 Tailor Welded Blanks

In the case of crash-relevant assemblies, a tailored blank enables a targeted energy absorption in the event of a side or frontal impact while protecting the passenger compartment. For example, with a side rail, a thinner and/or softer sheet may be

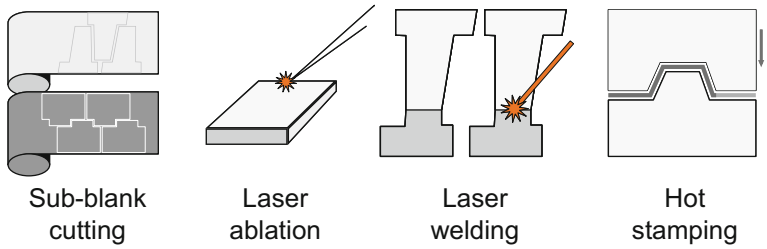

Fig. 8.3 Tailor welded blanks (TWB) may better utilize material and save cost (re-created after [12, 13])

used to absorb the energy; while a thicker and/or stronger sheet at the rear of the component prevents it from entering the passenger compartment [9–11].

Tailor welded blanks (TWBs) are made by butt welding between two or more sheet blanks, and may have:

1. Different thicknesses: where the load carried in the part is not constant, lower guage materials can be used to save weight.
2. Different alloys: where energy absorption and intrusion resistance is required within same part (such as a B-pillar in a vehicle).
3. A combination of (1) and (2).

TWBs help weight reduction and they may also reduce cost by:

1. Reducing the number of parts (i.e., reinforcements) in the subassembly,
2. Reducing the number of required tools,
3. Better utilizing of material by reducing scrap, as seen in Fig. 8.3.

Previous generation Audi A4/A5 (SOP 2007) was a good example for hot stamped TWBs. Tailored blanks were supplied by ThyssenKrupp Tailored Blanks. For rear rail and B-pillar, in which energy absorption was required in some portions, 22MnB5 was welded to HSLA with the same thickness. For tunnel reinforcement, the material was 22MnB5 everywhere, but the thickness was reduced in some areas to save weight, Fig. 8.4 [14].

When two 22MnB5 with different thicknesses are welded to form a TWB (Fig. 8.4a), the properties of weld seam are crucial. Since both base metals have very high strength after hot stamping (in the order of 1500 MPa (215 ksi) UTS), the weld seam also has to have a similar strength. In other words, the weld seam should not be the weakest point of the assembly. Several researchers have shown that a hardness drop occurs in the weld seam area if the contact between the blank and dies cannot be sustained. In this particular case, the location of the weld seam in the tailored blank must match to the step in the die, i.e., Δx in Fig. 8.5 should be as closed as possible to zero. Any misalignment over 4 mm in Δx ($\sim 5/32$”) may lower the hardness around the weld zone to approximately 300 HV. For comparison, the base metal is around 500 HV in the areas contacting the upper and lower dies. [9, 10, 15–17].

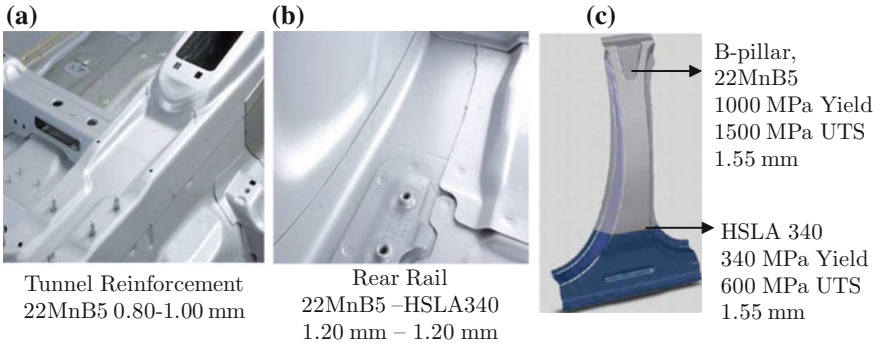

Fig. 8.4 Hot stamped TWB use in Audi A5 (SOP 2007) (re-created after [14])

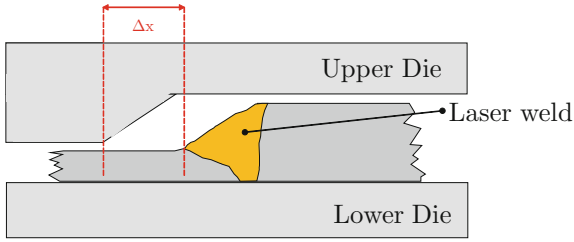

Fig. 8.5 Alignment of the blank in the dies (re-created after [17])

When 22MnB5 is welded to a low-strength high-ductility steel such as HSLA 340 or materials explained in Sect. 4.3 in Chap. 4, the main goal is to improve the energy absorbing of the component. A typical example for such a TWB is B-pillar (see Fig. 8.4c). The ductile bottom part should absorb the crash energy during a side impact, at the same time the upper part must be strong enough to prevent penetration to the passenger compartment. Hardness distribution of such a tailor welded B-pillar before and after hot stamping process is given in Fig. 8.6 [10, 11, 18].

While designing such a B-pillar. It is important to have a material that can undergo the same process window with 22MnB5. So that, furnace temperature, heating time and cooling rate does not need to be adjusted. HSLA 340 and materials listed in Sect. 4.3 can be used without additional effort. Different properties can be reliably achieved by hot stamping process and the transition zone can be as narrow as the width of the weld seam, 1...2 mm (0.04...0.08") [19].

As discussed in Chap. 4, hot stamping blanks could be uncoated, AlSi coated, or Zn coated. For sheets with AlSi coating, an additional ablation process is done before welding to remove the coating (Fig. 8.3). If AlSi coated is not removed, aluminum would dissolve in weld seam and create an intermetallic precipitation, Fig. 8.7. This would weaken the weldment [9, 11, 15, 20, 21].

Before welding the sub-blanks, the coating (typically AlSi) has to be removed on both sides so that the weld area is free from aluminum [22]. The width of ablation

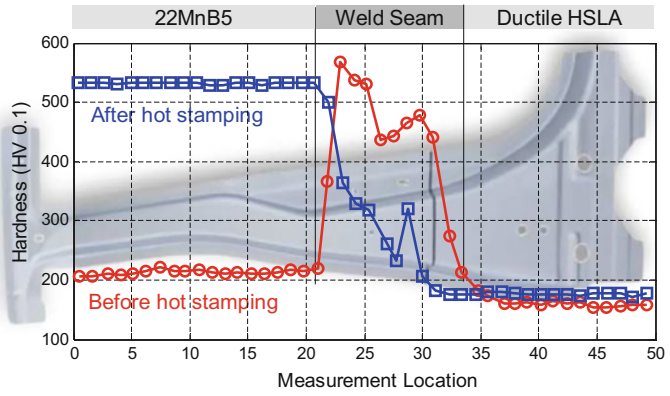

Fig. 8.6 Hardness measurements of a tailor welded B-pillar, before and after hot stamping (re-created after [10, 17])

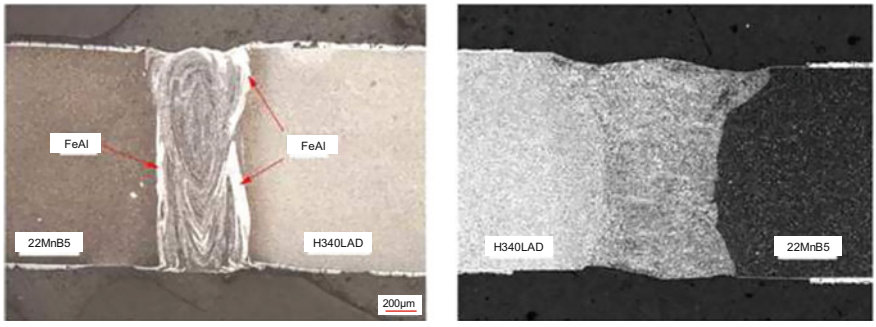

Fig. 8.7 Comparison of direct welded (left) and laser ablated and then welded blanks (right)

is selected such that even with a very wide weld, the weld pool would be safe. The typical process is "laser ablation", as shown in Fig. 8.8 [23].

There are two similar but distinct methods of ablation, developed at approximately same times, one by ArcelorMittal and one by ThyssenKrupp [9, 24]. The "partial ablation" process is protected by ArcelorMittal patent. In this process, the AlSi layer is removed from the blank while the intermetallic layer remains, Fig. 8.9a. According to several studies, the remaining layer would provide protection against corrosion and decarburization of the steel substrate. In "complete ablation" method, both the AlSi coating and the intermetallic layer are removed, Fig. 8.9b. The ablation depth can be adjusted by adjusting laser energy [22, 24–26].

Another possible ablation method is thermal ablation by induction. In this case, only the near-surface areas of the steel substrate are heated via a high-frequency electromagnetic field, thereby heating the surface coating and ultimately driving away the coating by means of Lorentz forces produced by the electromagnetic field [27]. Experimental studies have shown that only "partial ablation" is possible with

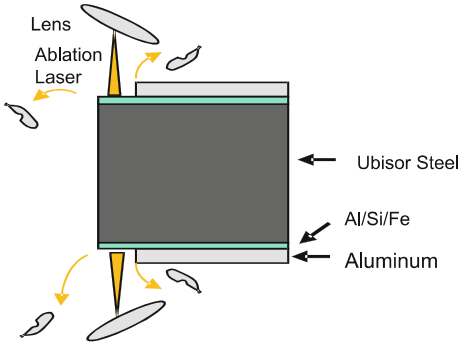

Fig. 8.8 Laser ablation is used to remove the coating around the weld zones [23]

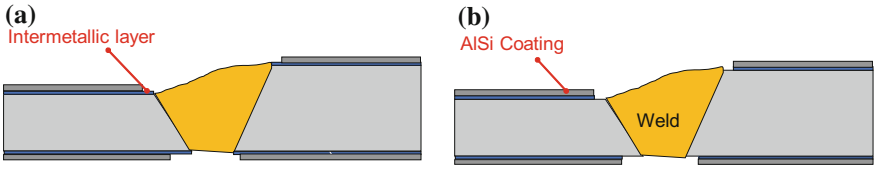

Fig. 8.9 Schematic diagrams for: **a** partial ablation, **b** complete ablation (re-created after [26])

induction method. Since the intermetallic layer cannot be removed, and this layer would even grow by the thermal influence.

Zn coated blanks may not require an additional ablation process before laser welding process [28].

According to a study, for energy absorption in a B-pillar, the best method may be TWB's. The study showed that hot stamped 22MnB5 would absorb 1, 800 J energy (Fig. 8.10a) in a component level testing. On the other hand, a multi-strength (i.e., tailor hot stamped with soft zones) hot stamped B-pillar can absorb 2,300 J of energy (as shown in Fig. 8.10c). The base portion of this B-pillar has a lower tensile strength (about 600 MPa) than the upper portion (about 1500 MPa). This is achieved by using a differential heating temperature (for further information about this technique please see Sect. 8.3.1). The tests showed, however, that the highest energy absorption could be achieved with a Tailor Welded Blank (TWB), where the base material is 340 MPa (Yield Stress) grade HSLA. In this case, the total energy absorbed was 3, 300 J (Fig. 8.10b) [29]. This is very similar to what Audi was using in the previous generation A4 (SOP 2008) [30].

One of the earliest studies with DUCTIBOR 500 tailor welded blanks was a rear rail part, laser welded to USIBOR 1500 (22MnB5), Fig. 8.11. In this particular example, the reference part had a monolithic thickness of 2.0 mm, but failed due to plastic collapse. The proposed part saves 4.1 kg (9.0 lbs.) per vehicle, while having equivalent crash performance [31, 32].

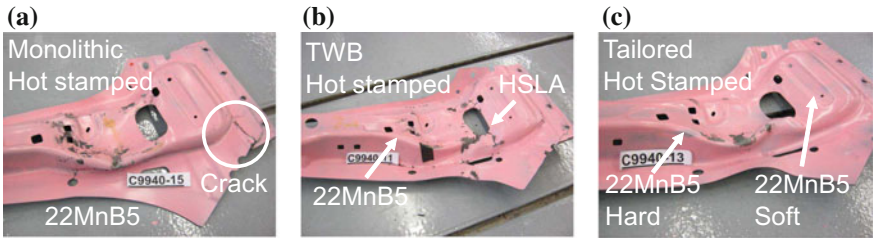

Fig. 8.10 Component level testing of several B-pillars: **a** Monolithic (single piece) hot stamped, **b** Tailor Welded Blank (TWB) with an HSLA 340 and **c** tailor tempered (with soft zones) (re-created after [29])

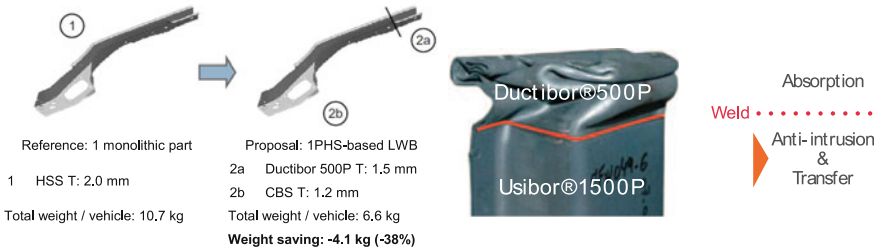

Fig. 8.11 Proposed use of tailor welded DUCTIBOR and USIBOR [31, 32]

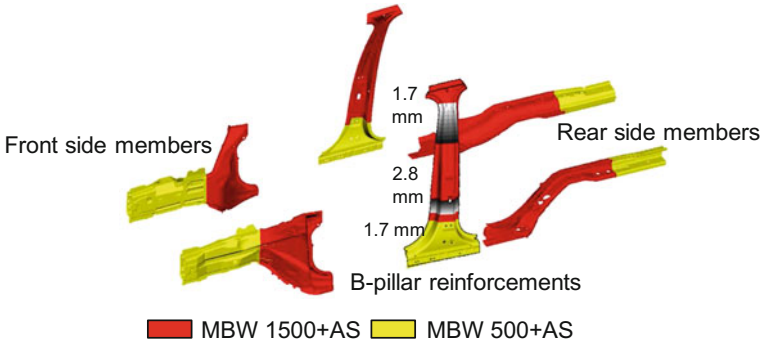

Fig. 8.12 Hot stamped tailor welded blanks in 2014 Volvo XC90 (re-created after [33, 34])

Tailor welded blanks with "high elongation hot stamping steels" are increasingly used in the last years. One such example is second- generation Volvo XC90. As seen in Fig. 8.12, the car has a total of six TWB components, made by joining AlSi-coated MBW500 and MBW1500 steels. This vehicle's B-pillars are also tailor rolled (see Sect. 8.2.2) [33, 34].

Utilizing large hot stamped TWB components such as door rings was planned since 2010. ArcelorMittal had shown its S-in-Motion concept car in EuroCarBody 2010, and introduced the idea of door ring similar to the one as shown in Fig. 8.13a

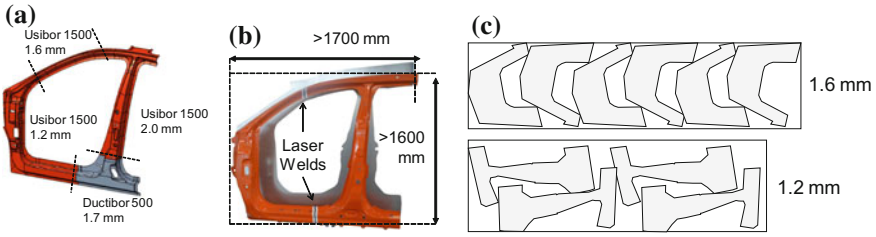

Fig. 8.13 Door rings: **a** the first four sub-blanks concept was introduced in 2010 (re-created after [35]), **b** door ring of Acura MDX with two sub-blanks, and **c** the nesting optimization for two sub-blanks door ring (re-created after [23, 40])

[35]. Since then, many Tier 1's and equipment suppliers have prepared their production to handle larger components, like door rings and even body sides for trucks and SUV's. For example, press makers started offering much larger bolster area (press bed dimensions) to accommodate larger dies for such panels. Similarly larger laser trimming machines have been built and offered to accommodate these types of components [36, 37].

In May 2013, Honda rolled out its Acura MDX model with a hot stamped door ring for the first time in automotive industry. In this vehicle, blanks with two different thicknesses (1.2 and 1.6 mm) were welded and hot formed to a final shape as seen in Fig. 8.13b. By sub-blank nesting optimization, the material utilization was improved from 53–63% (Fig. 8.13c). This design has improved the crash energy management, by eliminating spot welds between components and having an uninterrupted load path. It also saved about 3.1 kg (6.8 lbs.) per vehicle [23]. In July 2014, Acura TLX was rolled out, which also had hot stamped door ring. However, in Acura TLX, the door ring was not a TWB, but a single piece with 1.4 mm uniform thickness. This design saved 4.1 kg (9 lbs.) per vehicle compared to the predecessor model [38, 39].

In 2014, ArcelorMittal introduced S-in motion pickup truck. In this study, inner and outer reinforcements were designed with laser welded Usibor 1500 steel and were compared to cold stamped steel versions. Figure 8.14 shows the inner reinforcements. The hot stamped TWB design had saved 6.60 kg (14.6 lbs.) per vehicle, compared to cold stamped multi-part design [35].

In the same vehicle, the outer body side reinforcement was also designed with several different TWB options. Figure 8.15 shows only three of these designs. The cold-formed solution weighed 17.3 kg, whereas 3 sub-blank version was 15.9 kg. The 5 sub-blank weighed 15.6 kg. Material utilization in the cold-formed version was 56%, which was improved to 62% in three sub-blanks version and to 70% in five sub-blanks version [35]. In 2017, the new Chrysler Pacifica was introduced, which had a five-pieces TWB door ring and a two-pieces TWB B-pillar reinforcement. This design had saved 8.6 kg (19 lbs.) per vehicle [41, 42].

In 2018, Acura RDX became the first car to have hot stamped inner and outer door rings. In this design, both rings involve the side sill as well. By using two hot stamped rings, it was possible to further downgage both layers and save more weight. Another

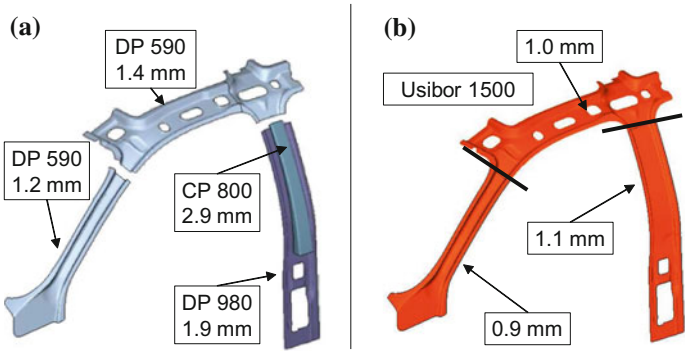

Fig. 8.14 "T-bone", inner reinforcement design: **a** cold stamped and spot welded four pieces, **b** tailor welded (laser welded) blank for hot stamping (re-created after [35])

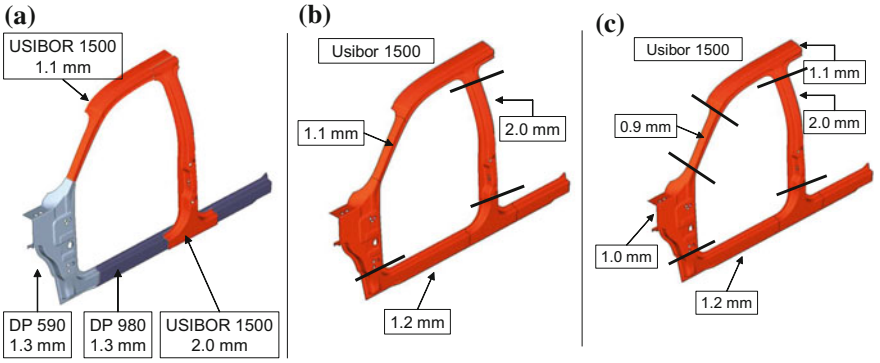

Fig. 8.15 Body side reinforcement concepts: **a** cold-formed four pieces, **b** two sub-blanks TWB, **c** five sub-blanks TWB (re-created after [35])

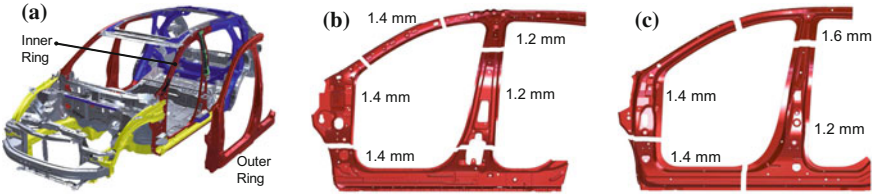

Fig. 8.16 Acura RDX: **a** schematic of inner and outer door rings, **b** sub-blanks of inner door ring, **c** sub-blanks of outer door ring (re-created after [43])

advantage was material utilization, as the inner ring was a TWB of five sub-blanks and the outer was of 4, as seen in Fig. 8.16 [43].

Recently, studies have been shown that in these TWB designs, 1500 MPa tensile strength steel can be replaced with 1900–2000 MPa tensile strength steel; 450–500 MPa tensile strength steel can be replaced with 1000–1200 MPa tensile

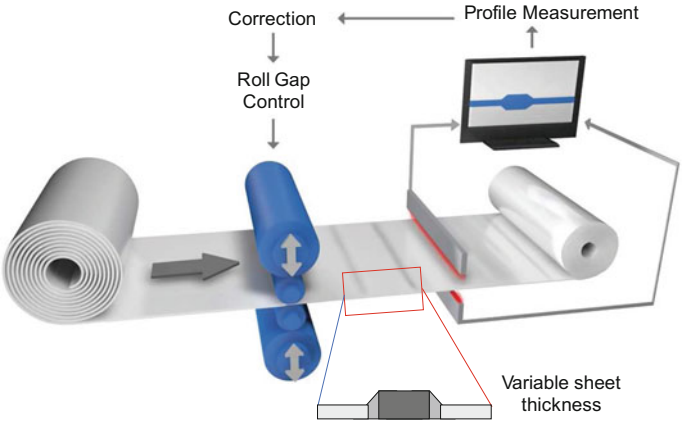

Fig. 8.17 Process principle of tailor rolling (courtesy of Mubea TRB GmbH)

strength steel to further downgage the steels [22]. It was estimated an additional 10% weight savings could be realized by this replacement [44].

8.2.2 Tailor Rolled Blanks

Tailor Rolled Blanks (TRB®) are produced by a strip rolling process known as "flexible" rolling. In tailor rolling process, the roll gap (so, the blank thickness) is adjustable during production, Fig. 8.17. Thus, a single blank with variable local thicknesses can be obtained. TRBs can be an alternative to Tailor Welded Blanks with different thicknesses. In contrast to a tailor welded blank, the thickness transition does not occur abruptly, but continuously over an adjustable length [45, 46]. The achievable transition slope is a function of the rolling speed. Today, the most economic transition slope is stated with 1:100, which means 1 mm thickness difference over a length of 100 mm [47].

Car body components using tailor rolled blanks have been used in mass production since 2001 and have been used in over 150 different applications by today. Tailor rolled blanks have been used in hot stamping industry since 2006. In only one decade, more than 50 million parts were hot stamped using tailor rolled blanks. By using tailor rolled blank, it is possible to optimize in terms of functional improvement (typically improvement of stiffness) and part integration (or eliminating the need for reinforcements). Some of the hot stamped TRB applications are listed in Table 8.1 [48–50].

According to a study in 2010, tailor rolled blanks is one of the most promising methods to save weight, while maintaining the crashworthiness, Fig. 8.18 [50]. Since 2011, Ford is using tailor rolled blanks in Focus and since 2013 in Kuga/Escape. In Focus, tailor rolled blanks saved about 1.4 kg/vehicle, compared to the B-pillar of sim-

Table 8.1 Hot stamped TRB applications in various vehicles (this may not be the full list)

SOP	Make/Model	Hot Stamped TRB Application	Reference
2006	BMW X5	B-Pillar, five levels: 1.2–2.2 mm, saved 4 kg (9 lbs.).	[51]
2006	Dodge Caliber	B-Pillar, four levels: 1.0–1.9 mm	[50]
2006	Jeep Patriot and Compass	B-Pillar, four levels: 1.09–1.95 mm	[50]
2007	Mercedes C-Class	Rear bumper, three levels, saved 2 kg (4.5 lbs.)	[52]
2008	BMW X6	B-Pillar, four levels: 1.2–2.2 mm, saved 4 kg (9 lbs.)	[53]
2010	Volvo S60	Cantrail, saved 3 kg (6.6 lbs.).	[54]
2011	Audi A6	Heelpiece four levels: 1.0–1.75 mm.	[55]
2011	Ford Focus	B-Pillar, eight levels: 1.35–2.7 mm, saved 1.4 kg (3 lbs.), Fig. 8.19	[56]
2012	Audi A3 (and most MQB Platform vehicles)	Heel piece, seven levels: 0.95–1.7 mm, saved 1.1 kg (2.5 lbs.).	[57, 58]
2012	BMW 3 series	B-Pillar, three levels: 2.4–2.9 mm, saved 1.3 kg (3 lbs.).	[59]
2012	VW Golf	B-Pillar, three levels: saved 4 kg (9 lbs.).	[60]
2013	Ford Escape / Kuga	B-pillar, seven levels: 1.55–2.7 mm, saved 1.2 kg (3 lbs.)	[61]
2014	Peugeot 308	Two parts, saved 1.6 kg	[62]
2014	Renault Twingo	B-Pillar, saved 1 kg	[63]
2014	Volvo XC90	B-pillar, three levels: 1.7–2.8 mm, Fig. 8.12	[33]
2015	BMW 7	B-pillar, 6 levels: 1.3–2.2 mm, saved 2.8 kg (6 lbs.), hybrid CFRP, Fig. 8.20	[64]
2017	Honda Accord	Roof bow, three levels: 1.0–1.6 mm	[65]
2017	Subaru Impreza (US)	B pillar, eight levels: 1.4–2.75 mm	[66]
2018	Audi A8	B-pillar, four levels: 1.5–2.0 mm; front cross member, three levels: 1.3–1.8 mm	[67]

ilar sized C-Max (see Fig. 8.19). In Kuga/Escape, this number is around 1.2 kg/vehicle [56, 61].

Mubea has developed the tailor rolled B-pillar, which can reduce the need for a patch-reinforcement, as seen in Fig. 8.20. One problem with such a B-pillar was spot welding. In a B-pillar assembly, the B-pillar and the closing plate should be welded to the body side panel, which is typically 0.6–0.7 mm thick mild steel. In such a condition, there would be three layers to be welded. When the thickest portion of the blank has to be welded, the thickness ratio would be so high that high-quality spot welding may not be possible [59, 66]. For this reason, Mubea developed a flange

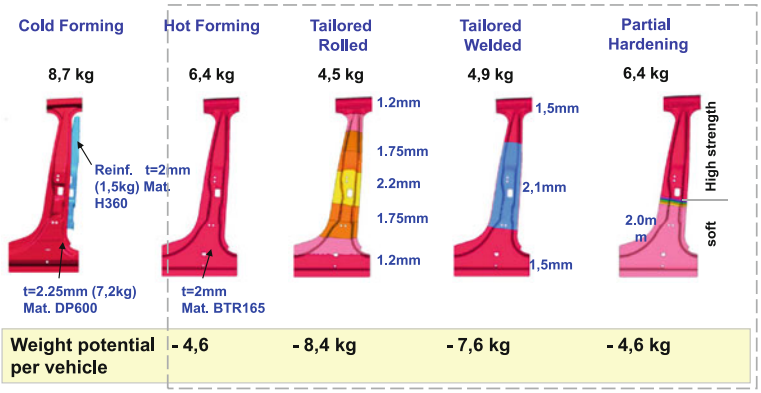

Fig. 8.18 Different strategies to save weight with hot stamping [50]

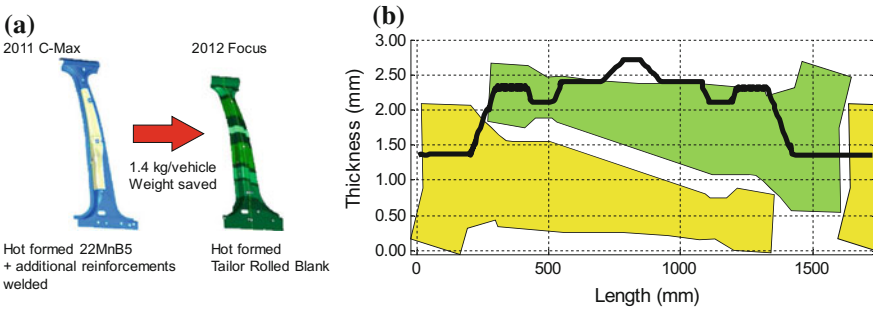

Fig. 8.19 Tailor Rolled B-pillar of Ford Focus: **a** compared to Ford C-Max, TRB saved 1.4 kg/vehicle (re-created after [68]), **b** nested blank layout in tailor rolled coil (re-created after [56])

Fig. 8.20 Development of tailor rolled B-pillars (courtesy of Mubea TRB GmbH)

technology. In this method, the B-pillar's flanges are trimmed. The part is laser welded to the closing plate, and the closing plate itself is spot welded to the body side panel. By removing some of the flanges, further weight savings can be realized [69]. Lastly, a tailor rolled hot stamped B-pillar with carbon fiber-reinforced polymer patch was developed as early as 2013 [70]. A very similar design (hot stamped TRB and a carbon fiber patch) has been in production at BMW 7 series, commercially known as carbon core [64].

In tailored rolling, the coating thickness cannot be uniform, as the coating is also being squeezed [71].

A relatively new technique to produce blanks with tailored thicknesses can be named as tailor forged blanks. Although not in mass production, at lab scale it was shown that a blank could be forged to be thinner in the areas of interest [71].

8.2.3 Patchwork Blanks

Patchwork blanks are similar to tailor welded blanks (TWBs). However, in a patchwork blank, the sub-blanks are not laser butt welded, instead, they are overlapped and resistance spot welded. As the blank is heated over its austenitizing temperature, so does the spot welds. Thus the welds are also austenitized and quenched. This increases the strength of the weld (Fig. 8.21a), and can reduce the risk of ruptures at weld spots (compared to cold stamping). With strong welds, the number of spot welds can be reduced, resulting in cost savings [50, 72, 73].

Hot stamped patchwork blanks were first used in 2007 Volvo V70's B-Pillars [75]. In this vehicle (and its derivative XC70), the B-pillar was made of two uncoated sub-blanks, the main sub-blank being 2.0 mm thick and the patch was 1.4 mm thick. The sub-blanks were joined with 46 spot welds. [76]. Patchwork hot stamped blanks are also used in (1) 2007 Fiat 500 B-pillar (2 mm main blank + 1 mm patch) [77], (2) 2011 Ford Explorer's B-pillar (1.3 mm main blank + 1.3 mm patch) [78], (3) A-pillar of 2014 Subaru WRX [74], (4) rear rail of 2014 Fiat 500X (1.5 mm main blank + 1.5 mm patch, TWB with 1.6 mm ductile boron steel) [79]. A similar rear rail is also used in Fiat Egea/Tipo and is shown in Fig. 8.21c (courtesy of FCA Turkey).

There are two potential problems with patchwork blanks: (1) corrosion and (2) weld quality after stamping. Air or moisture may be trapped between the spot welded blanks and may start corroding both of the blanks from the interior areas, i.e., crevice corrosion [80, 81]. AlSi-coated steels could be a solution for this problem [50].

Weld quality has to be investigated under two conditions: before and after hot stamping process. Before hot stamping, the quality control is relatively straightforward: (1) positions of each spot welds, (2) weld nugget diameter, and (3) presence of spatters. However, after hot stamping, it is important to make sure that the spot welds are not: (1) deformed and (2) at the edge of the patch. To avoid such problems, finite element simulations are typically used to design the patch geometry and weld spot locations. In some cases, additional spot welds may be applied after hot stamping [76, 82]. A recent study has found both numerically and experimentally, that by

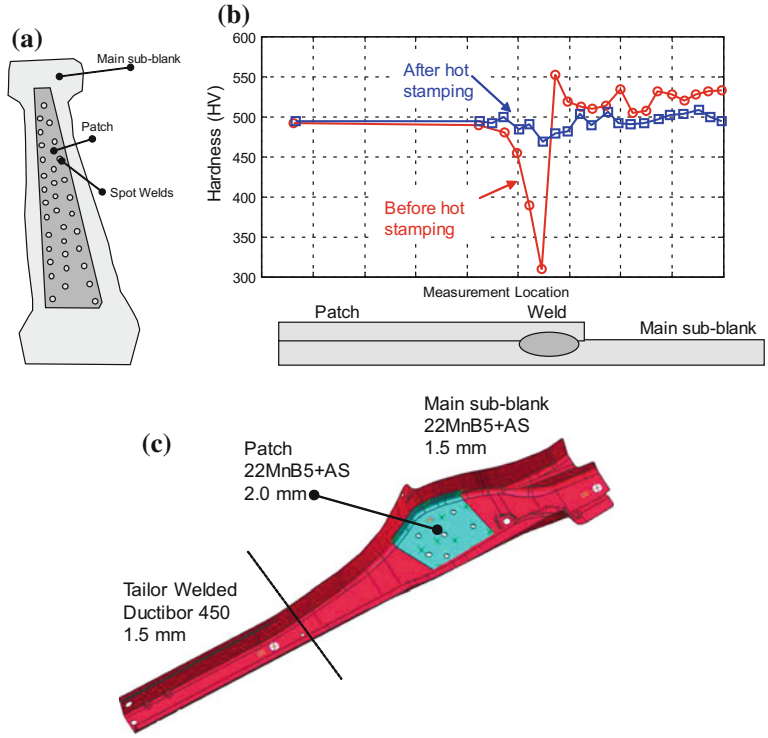

Fig. 8.21 Patchwork blanks: **a** schematic view of a B-pillar, **b** hardness profile aronud a spot weld, before and after hot stamping (re-created after [74]), **c** rear rail of Fiat Egea/Tipo (courtesy of FCA Turkey)

only four spot welds, it was still possible to have approximately 88% of the peak force and 82% of the energy absorption [83]. Another relatively recent improvement in patchwork blanks is to use remote laser spot welding, instead of resistance spot welding [84]. A patch welded B-pillar assembly with approximately 50 spot welds can be welded in approximately 23 s, with 2.8 kW laser source [85].

8.3 Tailoring Final Properties

This section explains how uniform blank (having the same thickness and material composition) can get tailored properties at the end of hot stamping process. The main idea behind tailoring final properties is to have approximately 100% martensite in the "hard zones", and much less martensite in the "soft zones". According to the authors, the possibility of "manipulating" the properties of the material can be done at three different stages:

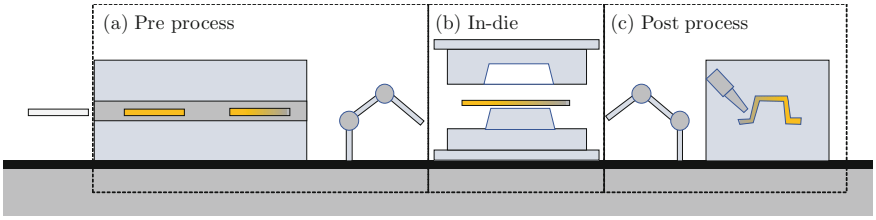

Fig. 8.22 Process types to obtain tailoring final properties

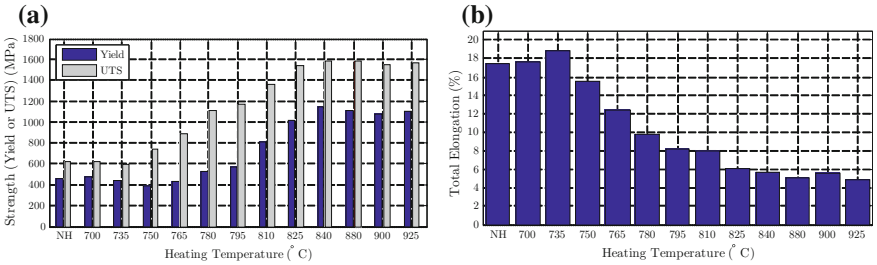

Fig. 8.23 Change of final properties of hot stamped blanks, with changing heating temperature (re-created after [86])

1. Pre process,
2. In-die process, and
3. Post process, as shown in Fig. 8.22.

8.3.1 Tailored Heating (Pre Process)

If a portion of the hot stamping blank is not austenitized, even though it is quenched very fast, the portion will not transform to martensite. Mechanical characteristics of a part after hot stamping depends on the heating temperature. To have a fully austenitized state, the blank has to be heated to or over approximately 880 °C (1620 °F). If the part is quenched from this temperature, 22MnB5 steel would have over 1,000 MPa yield, 1,500 MPa tensile strength (145 and 220 ksi, respectively); but approximately 5% total elongation. In contrast, if the blank is heated below austenitization temperature, for example, to 780 °C (1440 °F), the total elongation would be around 10%. A summary of mechanical properties of a part after quenching from several heating temperatures is given in Fig. 8.23 [86].

To achieve partial austenitization, local temperature of the blank must be controlled during heating. Producing tailored part by partial austenitization method saves energy, since less heat energy is applied to the material. There are mainly two methods to control blank temperature during heating in a roller hearth furnace:

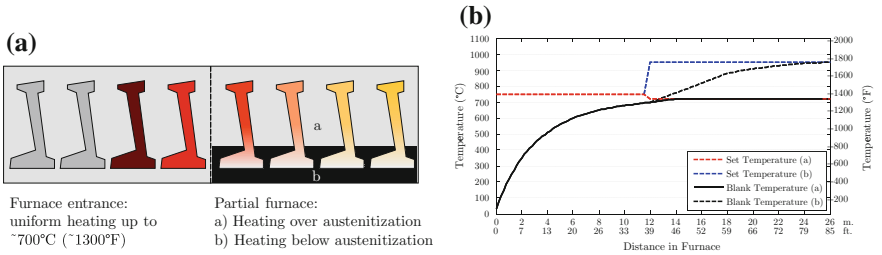

Fig. 8.24 A divided oven: **a** may have more than one heating zones, where **b** temperature can be controlled independently (re-created after [90])

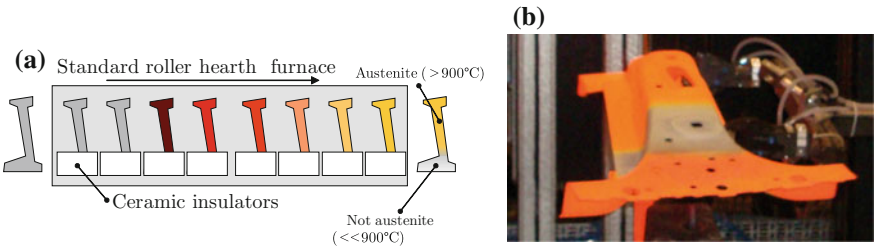

Fig. 8.25 Using a ceramic insulator, it is possible to control austenitization in the areas of interest (re-created after [73, 88])

1. By utilizing divided furnaces, typically used by Benteler [50, 87] as shown in Fig. 8.24,
2. By using insulator blocks to reduce the radiation heating in the areas of interest, used by BMW and Magna [73, 88], Fig. 8.25. Currently components with this method are used in BMW 6 and 4 series Gran Coupe (SOPs 2012 and 2014, respectively) and BMW 3 Gran Tourer (SOP 2013) [89].

In this technique, the method selected by the hot stampers is not dependent on the feasibility, but the patents. Heinemann et al., analyzed three relevant patents for "tailored heating" techniques [91]. A summary is given in Table 8.2.

Fernandez et al., listed the advantages and disadvantages of tailored heating as [95]:

Advantages:

1. Simple technique,
2. Size of soft zones can be adjusted.

Disadvantages:

1. Large transition zone (25–50 mm),
2. Large spread of material properties,
3. Non-flexible (in the case of divided furnace).

Table 8.2 Some patents about partial austenitization [91]

Applicant, Year and Patent number	Summary	Disadvantage	Reference
Benteler, 2000, DE20014361U1	Defines target strength properties of a B-pillar	Only a brief description, cannot be applied	[92]
BMW, 2009, DE102009023195A1	Two-sided covering of a preformed blank	Limited to indirect process, large isolation areas	[93]
Voestalpine Automotive, 2010, WO2010109012A1	Using cooled steel heat absorber in the furnace	High additional cost of cooling the extra mass	[94]

In addition to these, there could be formability issues in the soft zones, which is colder and in a less ductile state.

Behrens and Hübner [96] showed a new way of tailored heating using conduction. As discussed in Sect. 5.1.4, it is not possible to homogeneously heat up the nonuniform cross section parts using only one couple of electrodes, Fig. 8.26. To solve this problem, a set of electrode couples and welding tongues are used in tandem as shown in Fig. 8.27. In this method, E1, E2, E7, and E8 are electrodes, and the rest are welding tongues. Voltage in Transformers 1, 2, and 3 are controlled independently and thus, can achieve a temperature distribution of uniform or tailored heating as shown in Fig. 8.28. The authors also claimed that a conduction heated boron steel has slightly better elongation properties. Tensile test showed that a conduction heated blank had 7.6% total elongation compared to 6.5% total elongation with furnace heated blank [96].

8.3.2 Tailored Cooling (In-Die Process)

In the previous subsection, the part was not fully austenitized. In tailored cooling, the whole blank is austenitized; hard zones are quenched at a high cooling rate (over 27 °C/s (49 °F/s)) and soft zones are quenched at a lower cooling rate. This can be achieved by four methods [3, 81, 97]:

1. Using a heated die segments, Fig. 8.29
2. Adjusting tool contact surfaces (i.e., no contact),
3. Using tool materials with different thermal conductivities,
4. Precooling some portion of the blank after fully austenitizing.

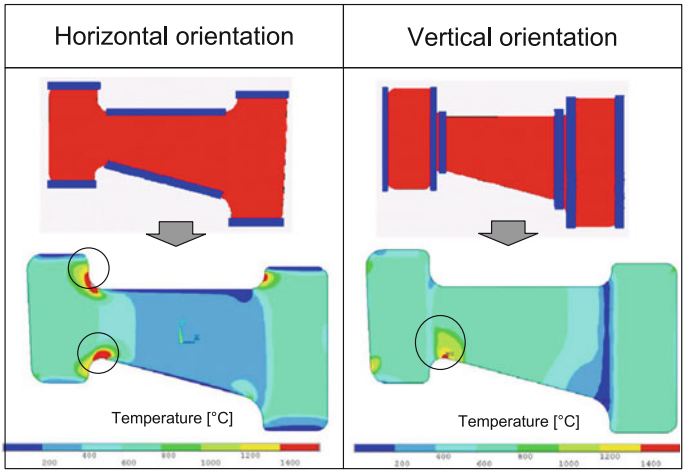

Fig. 8.26 A B-pillar blank cannot be homogenously heated using three electrode couples [96]

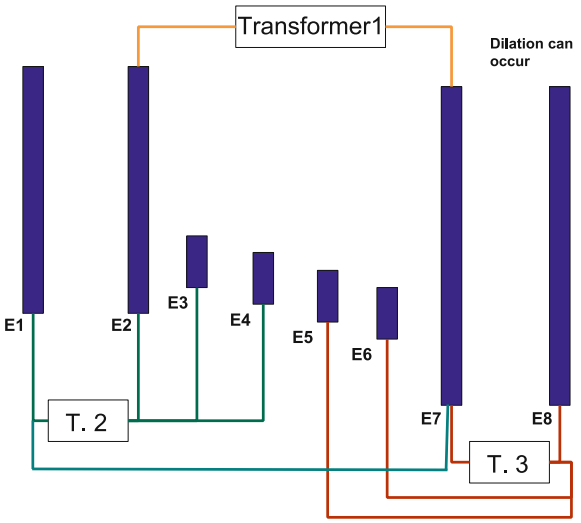

Fig. 8.27 Transformer circuits and electrode/welding tongue assembly [96]

8.3.2.1 Heated Die Segments

The cooling rate of the blank determines the martensite fraction. The cooling rate is a function of the contact pressure and the temperature gradient (ΔT). If a segment of the die is heated (or in sometimes is not cooled efficiently and forms a hot spot), sections of the part in contact with this area would not have the critical cooling rate.

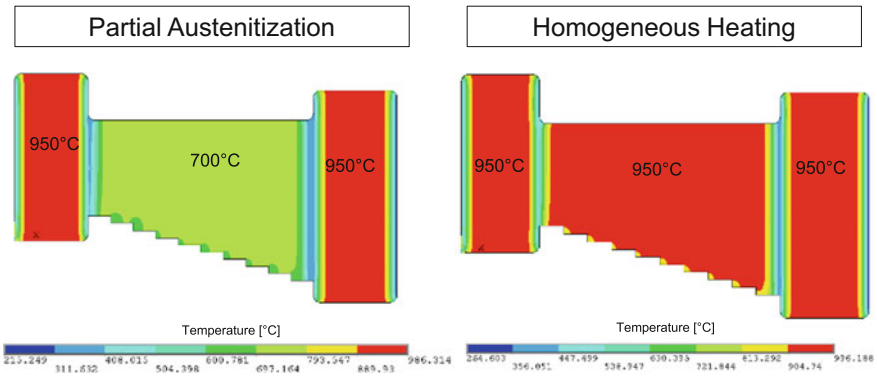

Fig. 8.28 Using the method above, it is possible to control the heating and achieve tailored/partial austenitization [96]

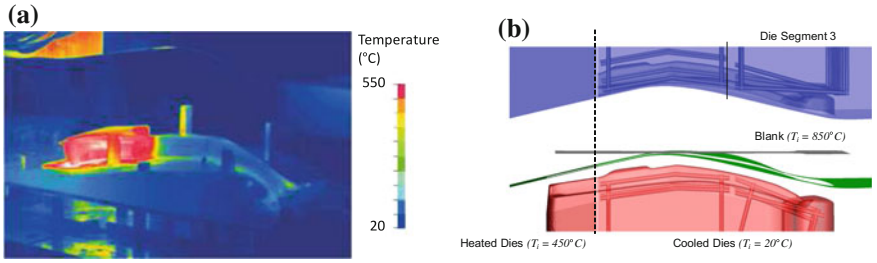

Fig. 8.29 Heated die segments for tailored cooling: **a** thermal camera image of a real die (re-created after [98]), **b** simulation mesh showing the segments and cooling channels [99]

This method has been in mass production for many vehicles now, including but not limited to the 1st generation Audi Q5 [100], 1st generation VW Tiguan [72]. These two were the first vehicles to have such components [101]. In addition to these cars, 2011 Audi A6 [55], 2016 Honda Civic [102], 2016 Ford Fiesta [103], 2016 Audi Q7 [104], 2017 Honda Accord [65], and 2018 Audi A8 [67] are well known to have soft zones, produced by heated die segments. Honda rear rails are shown in detail in Sect. 8.4.1.

Typically, heated segments could be between 300–550 °C (570–1020 °F) [105]. A tool segment of over 400 °C (750 °F) would avoid martensitic transformation to start if kept at the die for a long time. Due to productivity concerns, blanks are not left in the press for longer than 15 s. In this case, the part would be taken out of the press and "air cooling" would start. In this phase, some martensite may form [99, 105].

By heated tool segments, very narrow (5–25 mm wide) transition zone can be achieved. The system is flexible, by heating segments in the flange or any area of interest, complicated parts can be produced with relatively little spread of material properties. However, the die design must compensate for thermal expansion and

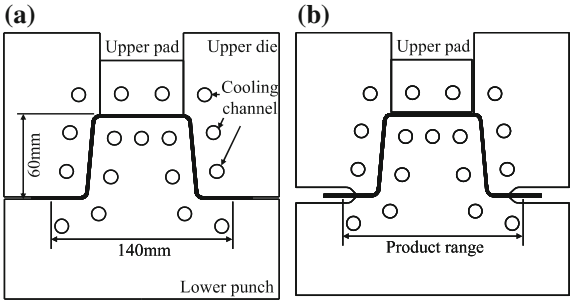

Fig. 8.30 **a** Conventional hot stamping tool yielding monolithic (uniform) properties, **b** soft flanges by adjusting tool contact areas [110]

contraction, which may be costly to maintain in mass production conditions. Due to these facts, late changes and modifications may be expensive [95, 101, 102, 105–107].

8.3.2.2 Adjusting Tool Contact Surface

In this method, an air gap is created between the blank and tool in purpose. As, the thermal contact conductance (h_c) (Sect. 10.2.4) between the blank and the die is a function of pressure and gap (see Fig. 10.10 in Chap. 10), an air gap would significantly reduce the cooling rate. The final properties of the soft zone is a function of distance between the blank and the tool, dimensions of the groove, initial heating temperature and blank thickness. The method is also known as "die-relief" method [81, 99, 108, 109].

The method has two important advantages: (1) a very narrow transition zone (in the order of 12–15 mm width) is achievable and (2) it can be easily implemented to already formed "indirect hot stamped" components as well [95, 111].

8.3.2.3 Die Segments with Different Thermal Properties

The tool's thermal conductivity also has an effect on the cooling rate. Typically, high thermal conductivity tool steels are used for hot stamping. Theoretically, an insert with low thermal conductivity would also reduce the cooling rate.

Kolleck and Veit had used ceramic inlays in the die, as shown in Fig. 8.31. The first few parts had relative uniform 500 HV hardness. However, after a few cycles, the ceramic insert's temperature increased over 200 °C (400 °F) while the steel tools were still at around 60 °C (140 °F) . The areas contacting this portion was approximately 200 HV, as seen in Fig. 8.31c [112].

The method may not be feasible for mass production, as the first few parts are not in the same strength/elongation level until a "steady-state" is achieved. In real

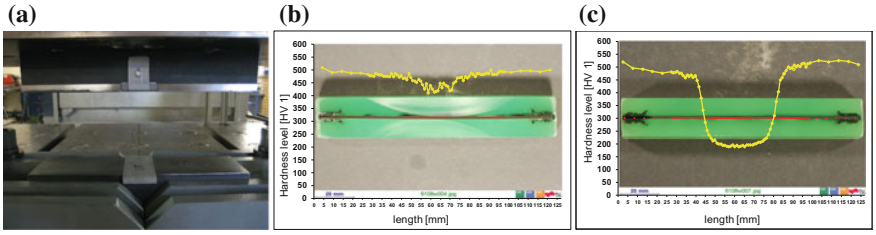

Fig. 8.31 **a** Test tool with inserts from ceramic, **b** hardness distribution of the first part after quenching, **c** after a few cycles [112]

production conditions, the production may require to be halted for any maintenance or safety reason. As an advantage for the process, it can also be applied to indirect formed parts.

8.3.2.4 Precooling Before Stamping

Tailored properties can also be achieved by fully austenitizing a blank but then letting some areas to cool. Note that, Fig. 8.24a differs from Fig. 8.32a. In the former, the soft zones are never austenitized, in the latter the whole part is austenitized first.

The technique has been mass produced since 2013, in Ford Escape/Kuga. The rear rail of this vehicle is produced by this method. The soft zone had 400 MPa yield, 550 MPa tensile strength and over 20% total elongation (approximately 60 and 80 ksi respectively), see Fig. 8.36 [61]. The method may cause large transition zones in the order of 50–150 mm width [113].

Benteler has been developing a new modular furnace design that can accommodate this process [87]. Schwartz has developed a "thermal printer", which can precool the areas of interest, as shown in Fig. 8.33 [113].

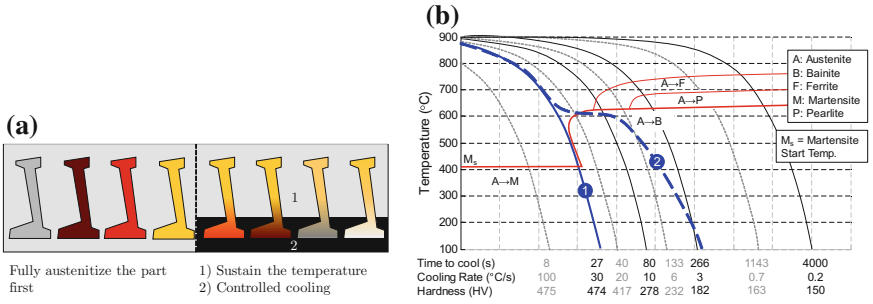

Fig. 8.32 **a** Schematic view of precooling, **b** a sample microstructure evolution

Fig. 8.33 A blank out of thermal printer [113]

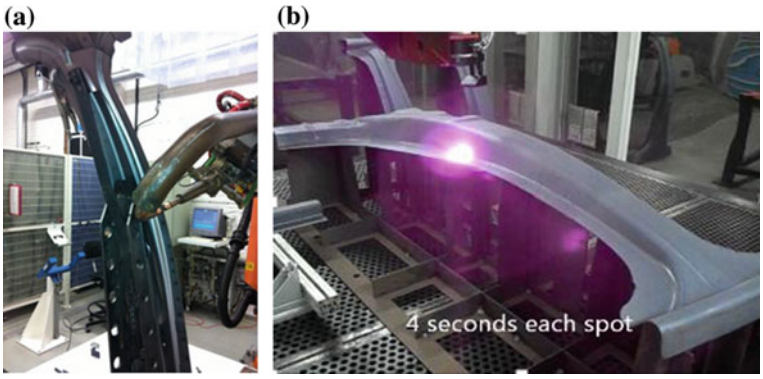

Fig. 8.34 Post process annealing can be done by: **a** induction [2] or **b** laser [101]

8.3.3 Post Process Annealing

The last method for obtaining tailored properties is to temper the soft zones, after the part is fully hardened in a conventional hot stamping line. This can be done by induction or laser, Fig. 8.34. A study of induction tempering will be explained in detail in Sect. 8.4.2 [2].

Currently, BMW 3 series (SOP 2012) and X5 (SOP 2013) have induction annealed B-pillar flanges in mass production. The estimated volume of these cars are approximately 350, 000 and 160, 000 vehicles/year, respectively [59, 89]. Gestamp, a Tier 1 hot stamping supplier is also working on laser tempering in prototype scale. It is expected that Gestamp will put this technique in mass production [101, 114].

The method is relatively simple and flexible to implement, however may cause geometric instability and spread of material properties [95, 106].

8.4 Uses of Tailored Properties

Parts with tailored properties may be employed to improve the energy absorption performance, weld quality or to facilitate trimming/piercing. Next subsections will investigate how these goals are achieved.

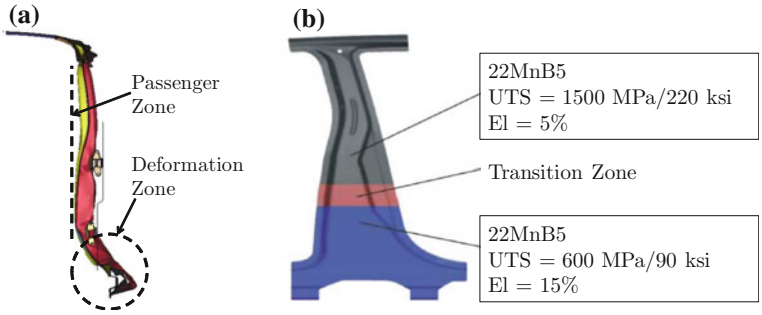

Fig. 8.35 **a** Side view of a B-pillar after crash [115], **b** tailored properties for high elongation and energy absorption in deformation zone and intrusion resistance in passenger zone [3]

8.4.1 Tailored Properties for Improved Energy Absorption

As shown in Fig. 8.35, in the case of a side impact, the B-pillar should not intrude into passenger zone. To achieve this and yet to still absorb the energy of the impact, the upper portion of the B-pillar should resist to intrusion while the bottom portion most deform to absorb the energy [115].

VW group's solution to this problem in a chronological order was as follows: (1) the 2006 VW Passat had a fully hardened B-pillar outer and a tailor welded HSS inner reinforcement, (2) the 2008 Audi A4/A5 had a conventional HSS B-pillar inner reinforcement and a tailor welded hot stamped outer (see Fig. 8.4c), (3) the 2008 VW Tiguan/Audi Q5 had a conventional HSS inner and a tailored (partly hardened) hot stamped outer. Since 2008, several VW Group models also have tailored B-pillar reinforcement, including but not limited to: 2012 Audi A6 [55], both 2010 and 2018 Audi A8 [67, 116], 2017 Audi Q7 [104].

Tailored B-pillars can be found also in 2014 Mercedes C-Class [117], 2016 BMW X1 (F48) and 5 Series (G30) [89], 2017 Ford Fiesta [103], and 2018 Honda Accord [65].

Similar approach is also required in the front and rear rails. The outer portions of these components must absorb the crash energy, while at a certain point the deformation should be stopped. 2008 Audi Q5 was one of the first vehicles to have tailored rear rails [100]. In 2013, Ford Escape / Kuga had tailored rear rails as well, Fig. 8.36 [61].

In 2015, Honda and Gestamp together co-developed a new rear rail design. As shown in Fig. 8.37, the rear rail assembly (composed of a 1.1 mm hot stamped rail and a 0.8 mm hot stamped cap) would deform and crush as planned by the designers [118]. The design has been already implemented in 2016 Honda Civic [102] and 2017 Honda Accord [65] and replaces a four-piece assembly which would be at around 25% heavier [118]. The design eliminated the patches, and thus may save the initial cost of building four different dies and spot welding all these components. Gestamp has also shown the feasibility studies of such designed front rails [101]. Currently, front rails produced by hot stamping are tailor welded blanks, where the energy absorbing areas are stamped from more ductile steel grades [119].

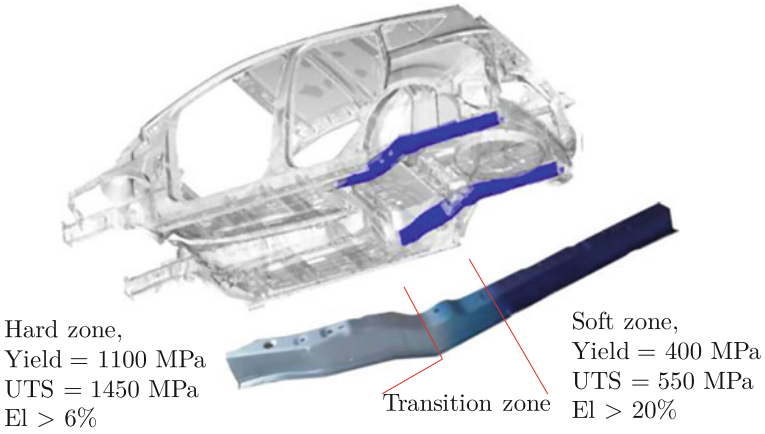

Fig. 8.36 Rear rails of Ford Escape / Kuga (re-created after [61])

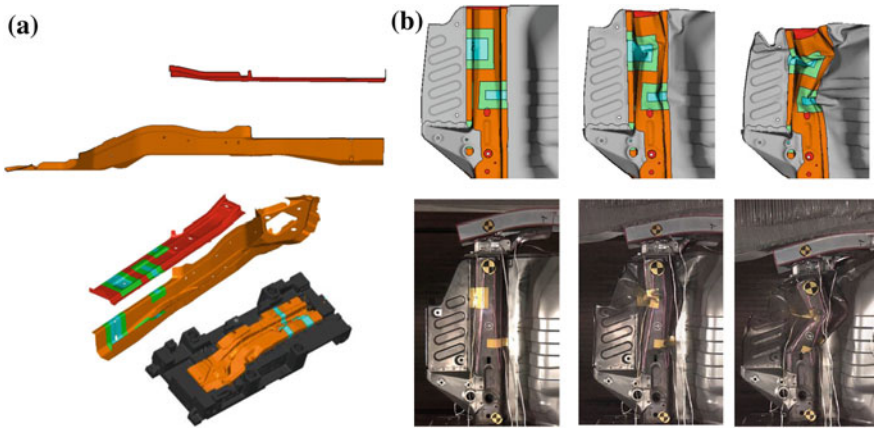

Fig. 8.37 Three-point bend rear rail assembly: **a** the rear rail and the cap geometry, and the die that hot stamps the rail, **b** tempered soft zones are used for deformation control and energy absorbing [118])

8.4.2 Reduction of Metallurgical Notch Sensitivity

After hot stamping, 22MnB5 steel would have a martensitic microstructure and hardness in the order of 470–500 HV [120, 121]. These parts are often welded to: (1) other reinforcement pieces and/or (2) the body assembly. In the event of a crash, the energy absorbed and intrusion resistance are both affected by sheet strength.

Several studies have shown that when fully hardened 22MnB5 is spot welded to another sheet, the heat affected zone may be as soft as 280–350 HV, Fig. 8.38. In the event of a crash, deformation concentrates around the weld zones, initiate the cracks and therefore the overall strength of the structure is reduced. Several studies have

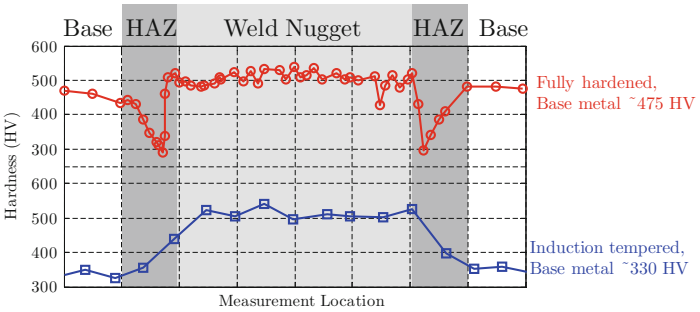

Fig. 8.38 Hardness measurement across a spot weld: (top) spot welding after hot stamping, (bottom) spot welding after tempering (re-created after [2, 122])

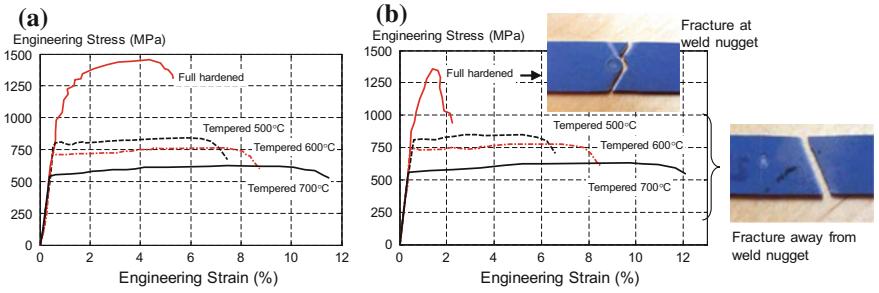

Fig. 8.39 Engineering strain–stress diagrams for: **a** tensile specimens as hardened/tempered, **b** hardened/tempered then spot welded. Note that, fully hardened samples always fail around the weld nugget, tempered specimens fail away from the weld nugget (re-created after [2])

proven that softening the weld flanges to around 300–350 HV range reduces the risk of crack initiation at the weld nugget. As a result, the total assembly may absorb more energy [2, 72, 106, 122].

When a fully hardened 22MnB5 steel is subjected to tensile test, typically over 950 MPa yield, around 1400–1500 MPa tensile strength and over 5% total elongation is expected, Fig. 8.39a. When a spot weld is introduced to a tensile specimen, the strength level drops to 1300 MPa level and the total elongation would be around 1.5–2%. The early fracture is observed, because deformation localizes in the heat affected zone around 1100 MPa stress, and around 1300 MPa fracture is observed always around the weld nugget, Fig. 8.39. It is also important to notice that spot welding did not change the UTS and elongation values of the tempered specimens [2, 122].

In a study in Sweden, hot stamped B-pillar reinforcements were drop tower tested with and without flange tempering before spot welding. When the flanges were at fully hardened condition, cracks always initiate at the spot welds, Fig. 8.40a. The study concluded that if the flanges were tempered before spot welding, approximately 30% more energy could be absorbed [2].

Fig. 8.40 Three-point drop test results at same energy level: **a** fully hardened B-pillar, spot welded along the flanges, **b** B-pillar with tempered and spot welded flanges [2]

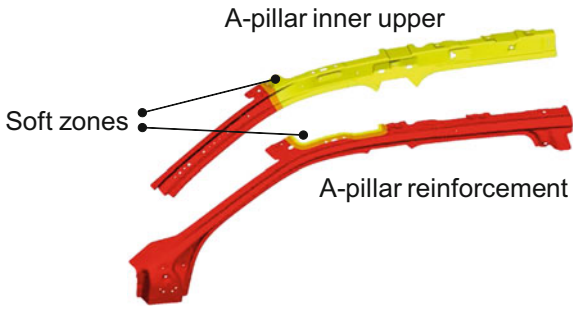

Fig. 8.41 A-pillar assembly of Volvo XC90 where soft zones are used to improve the weld quality (re-created after [33, 34])

Soft zones are used in weld areas to increase the welding quality in automotive industry. A study by BMW has shown that when the upper flange of the B-pillar is softened, the performance in a pole test is improved significantly [89]. As discussed earlier, since 2012, at least two different BMW models (F30 3-series and F15 X5) have soft flanges in their B-pillars for welding purposes [59, 89]. Volvo has shown that the spot weld strength would be increased by 30% if the weld was applied after tempering. If the tempering is done after welding, peel load would be increased by almost 60% [123]. Since 2010, most Volvo models have a soft zone in the A-pillar for welding quality improvement (including S60, V40, XC90, and S90) [33, 106, 123, 124]. XC90's A-pillar assembly is shown in Fig. 8.41. The soft zone width of the A-pillar reinforcement is as narrow as 16 mm, whereas the transition zone is 30 mm wid [101].

In Audi Q7 and Bentley Bentayga, B-pillar has soft flanges and lower piece—the latter is only for energy absorption. In both vehicles, the body outer side panel is aluminum, and B-pillar is not spot welded. The soft flanges are used for riveting [101, 104, 125].

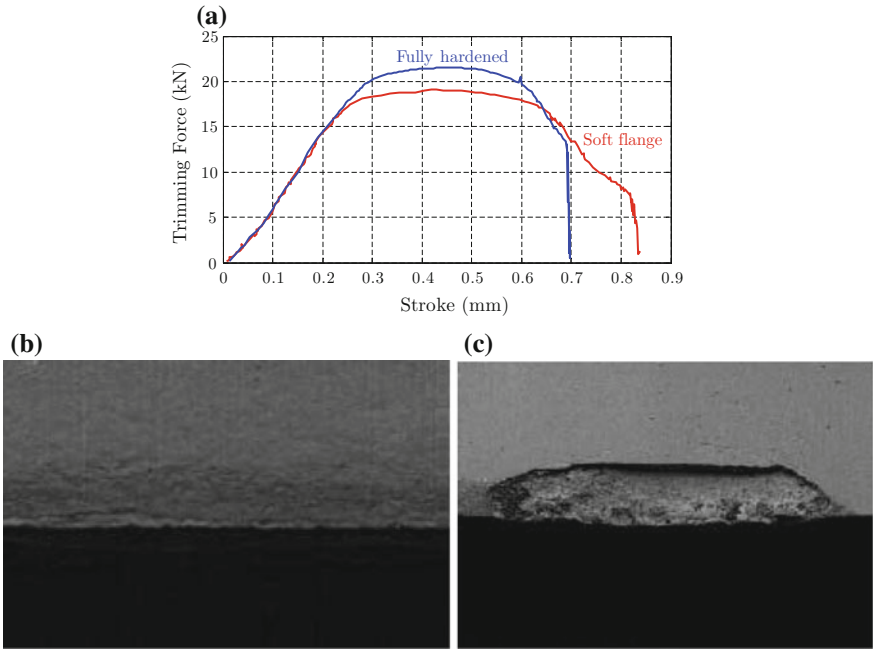

Fig. 8.42 Soft flange trimming versus full hard trimming: **a** punch force–stroke comparison, trimming edge tool after **b** 50 soft flange trimming, **c** 25 full hard trimming (re-created after [110])

8.4.3 Tailored Properties to Facilitate Trimming and Piercing

As discussed in Sect. 7.2 in Chap. 7, trimming and piercing of hot stamped parts are challenging due to their very high hardness. Currently, using soft zones for trimming and piercing purposes is still in R&D phase. A numerical study showed that during trimming of 1.9 mm thick hardened 22MnB5 steel, the die stresses were in the order of 2,900 MPa (420 ksi). When the flanges were softened using less conductive tool steels, the die stresses were reduced to 1,700 MPa (245 ksi) [126].

In another study, researchers used die relief method to obtain soft flanges, Fig. 8.30. CPM-M4 tools with TiCN coating were used to trim a 15 mm long blank. Although, the trimming force was only reduced by approximately 18%, the tool surfaces were worn/damaged much less with the soft zone trimming. Trimming forces and the die surface SEM images after 50 trimmings are shown in Fig. 8.42 [110].

References

1. C. Chen, M. Dingman, Improving phs performance through orientation of the blank rolling direction. in *Presented at Great Designs in Steel*, MI, 17th May 2009
2. O. Hedegärd, M. Åslund, Tempering of hot-formed steel using induction heating. Master's Thesis, Chalmers University of Technology, Sweden, 2011
3. H. Karbasian, A.E. Tekkaya, A review on hot stamping. J. Mater. Process. Technol. **210**(15), 2103–2118 (2010)
4. A. Abdollahpoor, X. Chen, M.P. Pereira, N. Xiao, B.F. Rolfe, The crash behaviour of hot stamped components–the effect of tailoring conditions, in *5th International Conference on Hot Sheet Metal Forming of High Performance Steel* (CHS2, Canada, 2015), pp. 591–599
5. N.P. Lutsey, Review of technical literature and trends related to automobile mass-reduction technology. *Institute of Transportation Studies* (2010)
6. J.E. Sacco, Blanks create opportunity to expand steel potential. Am. Metal Mark. (USA) **107**(8), 00 (1999)
7. A. Mertens, *Tailored Blanks: Stahlprodukte für den Fahrzeug-Leichtbau* (Verlag Moderne Industrie, 2003)
8. F. Schieck, Temperature and strain rate related forming technologies for improved forming limits, in *Presented at Advanced Forming Methods and Materials in the Automotive Industry* (Shanghai, China, 2014)
9. R. Stopp, L. Schaller, K. Lamprecht, E. Keupp, G. Deinzer, Warmblechumformen in der automobil-serienfertigung – status, trends, potenziale, in *2. Erlanger Workshop Warmblechumformung*, ed. by M. Geiger, M. Merklein (Meisenbach, Bamberg, 2007)
10. R. Kolleck, V. Boskovic, R. Vollmer, Angepasste bauteileigenschaften durch den einsatz von tailor welded blanks im presshärten, in *10. Erlanger Workshop Warmblechumformung*, ed. by M. Merklein (Meisenbach, Bamberg, 2015)
11. F.-J. Lenze, J. Bian, S. Sikora, Einsatz pressgehärteter stähle im karosseriebau: Stand und trends der entwicklung, in *2. Erlanger Workshop Warmblechumformung*, ed. by M. Geiger, M. Merklein (Meisenbach, Bamberg, 2007)
12. P. Brettnacher, Innovative integration concept for a hot-stamped door ring using tailored welded blanks. in *Presented at Insight Edition Conference*, Sweden, 20–21 September 2011
13. ArcelorMittal. Tailored blanks. Product Catalogue (2013)
14. E. Hilfrich, D. Seidner, Crash safety with high strength steels. in *Presented at International Automotive Congress*, China, 30 October2008
15. G. Deinzer, A. Stich, K. Lamprecht, G. Schmid, M. Rauscher, M. Merklein, J. Lechler, Presshärten von tailor welded blanks: Werkstoffauswahl, eigenschaften und verbindungstechnik, in *3. Erlanger Workshop Warmblechumformung* (2008), pp. 1–21
16. W. Eberlein, Vergleich verschiedener stahl- und designkonzepte für verstärkung b-säule, in *Tagungsband zum 4*, Erlanger Workshop Warmblechumformung, ed. by Marion Merklein (Meisenbach, Bamberg, 2009), pp. 173–184
17. A. Breuer, Optimizing parameters for hotformed tailored-blank applications. in *Presented at Great Designs in Steel 2015*, USA, 13 May 2015
18. P.S. Feuser, Ein Ansatz, zur Herstellung von pressgehärteten Karosseriekomponenten mit maßgeschneiderten mechanischen Eigenschaften: Temperierte Umformwerkzeuge, Prozessfenster, Prozesssimulation und funktionale Untersuchung: Zugl.: Erlangen-Nürnberg, Univ., Diss., *volume 226 of Bericht aus dem Lehrstuhl für Fertigungstechnologie* (Meisenbach, Bamberg, 2012), p. 2012
19. ThyssenKrupp Steel Europe. *Warmumformung im Automobilbau*. Die Bibliothek der Technik (2012)
20. C. Kim, M.J. Kang, Y.D. Park, Laser welding of al-si coated hot stamping steel, in *11th International Conference on the Mechanical Behavior of Materials (ICM11)* (Procedia Engineering, 2011), pp. 2226–2231

21. L.E.E. Jung-Han, K.I.M. Jong-Do, O.H. Jin-Seok, P.A.R.K. Seo-Jeong, Effect of al coating conditions on laser weldability of al coated steel sheet. Trans. Nonferrous Metals Soc. China **19**(4), 946–951 (2009)
22. D. Wenk, Global capability: Hot stamping. in *Presented at Global Automotive Lightweight Materials Asia 2014*, China, 26–27 March 2014
23. R.Z. Mallen, J. Riggsby, Development of a global first suv body construction. in *Presented at Great Designs in Steel*, MI, 1st May 2013
24. L. Cretteur, R. Vierstraete, Q. Yin, W. Ehling, A. Pic, Development of a laser decoating process for fully functional al si coated press hardened steel laser welded blank solutions, in *Proceedings of the 5th International WLT-Conference: Lasers in Manufacturing* (Munich, Germany, 2009), pp. 15–18
25. J.-F. Canourgues, Aurelien Pic, Pascal Verrier, Rene Vierstraete, Wolfram Ehling, and Bernd Thommes. Plate, 24 December 2013. US Patent 8,614,008
26. G. Tandon, S. Gaied, F. Schmit, I. Viaux, New developments in laser welded blanks using alsi coated boron steel. in *Presented at Great Designs in Steel 2017* (2017)
27. M. Koch, et al., Method for joining coated steel substrates. *German Patent, DE102008006624B4* (2012)
28. T. Manzenreiter, M. Rosner, T. Kurz, G. Brugger, R. Kelsch, D. Hartmann, A. Sommer, Challenges and advantages in usage of zinc-coated, press-hardened components with tailored properties. BHM Berg- und Hüttenmännische Monatshefte **157**(3), 97–101 (2012)
29. G. Kim, Posco's strategy for steel in car body lightweight design. in *Presented at Insight Edition Conference, September 18-19, Neckarsulm* (Germany, 2012)
30. M. Medricky, R. Struck, C. Sunderkötter, D. Lorenz, P. Olle, B.A. Behrens, Thermo-mechanical coupled simulation of hot forming processes considering die cooling. in *Presented at LS-DYNA Update Forum*, Germany, 12 November 2009
31. D.D. Múnera, A. Pic, D. Abou-Khalil, F. Shmit, F. Pinard, Innovative press hardened steel based laser welded blanks solutions for weight savings and crash safety improvements. SAE Int. J. Mater. Manf. **1**, 472–479 (2008)
32. A. Pic, F. Pinard, *Usibor ®and ductibor ®: a "hot" combination for safer and lighter cars*, pp. 12–13 (ArcelorMittal Update, 2009)
33. H. Ljungqvist, K. Amundsson, O. Lindblad, The all-new Volvo XC90 car body, in *Presented at EuroCarBody 2014* (Bad Nauheim, Germany, 2014), pp. 21–23
34. H. Lindberg, Advanced high strength steel technologies in the 2016 volvo xc90, in *Presented at Great Designs in Steel 2016* (Livonia, USA, 2016)
35. G. Tandon, I. Viaux, Lightweight door ring concepts using hot stamped laser welded blanks, in *Presented at Great Designs in Steel 2014* (2014)
36. H. Siebels, New press design for high volume production of hot-formed titanium parts, in *Presented at Seminar Dedicated to New Hot Forming Technologies* (St. Chamond, France, 2015)
37. F. Geyer, 5 axis laser cutting of hot formed steel, in *Presented at Great Designs in Steel 2015* (Livonia, USA, 2015)
38. A. Madsen, 2015 acura TLX body structure review, in *Presented at Great Designs in Steel 2015* (USA, 2015)
39. Honda North America. Private communication (2015)
40. Altair Engineering. Industry first hot stamped door ring. Altair Enlighten Award Nominee (2013)
41. ArcelorMittal. Jet set. *Automotive Manufacturing Solutions*, pp. 40–41 (2017)
42. J. Tibbenham, J. Truskin, Advanced high-strength steel technologies in the 2017 chrysler pacifica, *Presented at Great Designs in Steel 2017* (2017)
43. J. Riggsby, 2019 acura rdx world's first inner & outer door ring system, in *Presented at Great Designs in Steel 2018* (2018), p. 2018
44. L. Dormegny, New generation press-hardened steel solutions: Further mass reduction and safety increase, in *Presented at Materials in Car Body Engineering 2018* (Germany, 2018)

45. Henning Wallentowitz, Stefan Gies, Strukturentwurf von Kraftfahrzeugen: Aerodynamik, Design & Package, Plattformen und Module, Betriebsfestigkeit Crashsicherheit; Vorlesungsumdruck Strukturentwurf von Kraftfahrzeugen (Ika, 2008)
46. J. Brecht, B. Göddek, Warmgeformte tailor rolled products maßgeschneiderte leichtbaulösungen für die fahrzeugstruktur, in *Tagungsband zum 9 Erlanger Workshop Warmblechumformung*, ed. by M. Merklein (Meisenbach, Bamberg, 2014)
47. Gerhard Hirt, Cornel Abratis, Jochen Ames, Alexander Meyer, Manufacturing of sheet metal parts from tailor rolled blanks. J. Technol. Plast. **30**(1/2), 1 (2005)
48. M. Rehse, Flexible rolling of tailor rolled blanks, in *Presented at Great Designs in Steel*, Livonia, 8 March 2006
49. Mubea Tailor Rolled Blanks GmbH. Private communication (2015)
50. T. Ausmann, Hot stamping technologies, tailor rolled blanks, in *Presented at AP&T Press Hardening*, Next step seminar (MI, 2010), p. 2010
51. M. Pfestorf, The mixed material concept of the new BMW X5, in *Presented at Great Designs in Steel 2007*, USA, 7 March 2007
52. G. Ast, M. Oberle, The new c-class, in *Presented at EuroCarBody 2007* (Germany, 2007)
53. M. Pfestorf, D. Copeland, Technological innovations in body in white manufacturing of the BMW X6, in *Presented at Great Designs in Steel*, MI, 9 April 2008
54. M. Bergwall, S. Dahlström, O. Lindblad, The new volvo s60 car body, in *Presented at EuroCarBody 2010*, Germany, 18–20 October 2011
55. B. Mleksuch, H. Elsäßer, M. Schrimm, K.-G. Michel, The new audi a6, in *Presented at EuroCarBody 2011*, Germany, 18–20 October 2011
56. R. Quick, O. Träbing, The new ford focus, in *Presented at EuroCarBody 2011*, Germany, 18–20 October 2011
57. C. Bielz, S. Heis, The new audi a3, in *Presented at EuroCarBody 2012*, Germany, 16–18 October 2012
58. P. Šimon, N. Jiří, Škoda kodiaq, in *Presented at EuroCarBody 2016*, Germany, 17–20 October 2016
59. M. Becker, P. Kühnel, The body of the new BMW 3 series, in *Presented at EuroCarBody 2012*, Germany, 16–18 October 2012
60. S. Birch, Golf closes the gasoline/diesel gap, loses mass, and gains premiumness. Automot. Eng. Int. **3**(9), 10–15 (2012)
61. S. Morgans, 2013 Ford Escape, in *Presented at Great Designs in Steel*, MI, 1st May 2013
62. C. Patois, M. Barbier, Body-in-white of the new peugeot 308, in *Presented at EuroCarBody 2014 - 16th Global Car Body Benchmarking Conference* (Germany, 2014)
63. H. Gaumont, P. Jauvion, Twingo 3, in *Presented at EuroCarBody 2014*, Germany, 21–23 October 2014
64. M. Ahlers, K. Sammer, New BMW 7 Series. Carbon Core, in *Presented at EuroCarBody 2015*, Germany, 20-22 October 2015
65. T. Marukawa, Y. Shoji, M. Nakamura, Accord, in *Presented at EuroCarBody 2017*, Germany, 17–19 October 2017
66. T. Ayabe, A. Nakashima, T. Ueda, Subaru impreza, in *Presented at EuroCarBody 2017*, Germany, 17-19 October 2017
67. T. Hämmerle, D. Hußmann, The new Audi A8, in *Presented at EuroCarBody 2017*, Germany, 17–19 October 2017
68. F. Pohl, J. Hover, Challenges and opportunities for lightweight designs in volume production, in *Presented at Insight Edition Conference*, Germany, 18–19 September 2012
69. M. Zoernack, Material related design with tailor rolled products, in *Presented at Great Designs in Steel 2016*, USA, 16 May 2016
70. J. Brecht, B. Göddek, Warmgeformte tailor rolled products - funktionsoptimaler leichtbau für die fahrzeugkarosserie, in *Tagungsband zum 8 Erlanger Workshop Warmblechumformung*, ed. by Marion Merklein (Meisenbach, Bamberg, 2013)
71. Liyana Tajul, Tomoyoshi Maeno, Takaya Kinoshita, Ken-ichiro Mori, Successive forging of tailored blank having thickness distribution for hot stamping. Int. J. Adv. Manuf. Technol. **89**(9), 3731–3739 (2017). Apr

72. D. Berglund, Hot stamping of ultra high strength steels - possibilities and challenges, in *Presented at Insight Edition Conference*, Sweden, 20–21 September 2011
73. M. Neyer, End user insights and outlook, in *Presented at AP&T Press Hardening*, Next step seminar (MI, 2011)
74. K. Uejima, C. Beku, T. Onoe, The 2015 WRX STI, in *Presented at EuroCarBody 2014*, Germany, 21-23 October 2014
75. P. Nyström, M. Fermer, The new volvo V70 and XC70 car body, in *Presented at EuroCarBody 2007*, Germany, 16-18 October 2007
76. Johnny K. Larsson, Joel Lundgren, Einar Asbjörnsson, Håkan Andersson, Extensive introduction of ultra high strength steels sets new standards for welding in the body shop. Weld. World **53**(5), 4–14 (2009)
77. A. Torelli, M. Tagliani, The new fiat 500 car body, in *Presented at EuroCarBody 2007*, Germany, 16–18 October 2007
78. S. Morgans, 2011 Ford Explorer, in *Presented at Great Designs in Steel*, MI, 18th May 2011
79. F. D'Aiuto, M.M. Tedesco, Development of new structural components with innovative materials and technological solutions. in *Presented at Materials in Car Body Engineering 2015*, Germany, 22–23 April 2015
80. ArcelorMittal. Tailored blanks - value proposal (2009)
81. M. Merklein, M. Wieland, M. Lechner, S. Bruschi, A. Ghiotti, Hot stamping of boron steel sheets with tailored properties: a review. J. Mater. Process. Technol. **228**, 11–24 (2016). Hot Stamping
82. Chengxi Lei, Zhongwen Xing, Xu Weili, Zhenjun Hong, Debin Shan, Hot stamping of patchwork blanks: modelling and experimental investigation. Int. J. Adv. Manuf. Technol. **92**(5), 2609–2617 (2017). Sep
83. C.C.K. Huang, S.W. Wang, P.K. Lee, T.R. Chen, H.Y. Liou, P.K. Cheng, Y.T. Chen, The effect of welding spot arrangement on the energy absorption of hot-stamped patchwork b-pillar. in *6th International Conference on Hot Sheet Metal Forming of High Performance Steel, CHS2* (USA, 2017), pp. 573–580
84. B. Gerhards, O. Engels, U. Reisgen, S. Olschok, Laser beam welding of press hardened ultrahigh strength 22mnb5 steel, lasers in manufacturing 2015-lim 2015 und world of photonics congress. in *International Congress Center Munich*, vol. 22 (Germany, 2015)
85. J.K. Larsson, Laser welding of press-hardened components. in *Presented at European Automotive Laser Applications (EALA) 2014*, Germany, 11–12 February 2014
86. M. Glatzer, T. Stöhr, M. Merklein, S. Sikora, K. Lamprecht, G. Deinzer, Einfluss unterschiedlicher wärmebehandlungsrouten auf die robustheit der mechanischen eigenschaften des stahls 22mnb5, in *Tagungsband zum 4 Erlanger Workshop Warmblechumformung*, ed. by Marion Merklein (Meisenbach, Bamberg, 2009)
87. B. Dvorak, J.J. Tawk, T. Vit, Advanced design of continuous furnace for hot stamping line. in *Advanced High Strength Steel and Press Hardening: Proceedings of the 2nd International Conference (ICHSU2015)*, pp. 611–619 (World Scientific, 2016)
88. P. Süß, M. Pfestorf, Press hardening at BMW. in *Presented at Insight Edition Conference*, Sweden 20–21 September 2011
89. C. Rauber, Press hardened steel - applications and future requirements at BMW. in *Presented at Materials in Car Body Engineering 2015*, Germany 22–23 April 2015
90. R. Hund, M. Braun, Continuous improvement of hot forming technology. in *3rd International Conference on Hot Sheet Metal Forming of High Performance Steel, CHS2*, pp. 189–200 (Germany, 2011)
91. S. Heinemann, K.-U. Haars, M. Kotzian, T. Vietor, Gezielte eigenschaftseinstellung von hochfesten stählen, mittels partieller austenitisierung, für den einsatz in der großserie, in *Tagungsband zum 7 Erlanger Workshop Warmblechumformung*, ed. by Marion Merklein (Meisenbach, Bamberg, 2012)
92. L. Gehringhoff, H.-J. Knaup, B-column for motor vehicle, February 25 2003. US Patent 6,524,404

93. E. Frank, B. Woelfer, B. Glueck, Herstellung eines partiell pressgehärteten blechbauteils. Patent Application, DE102009023195A1 (2009)
94. A. Sommer, D.Hartmann, T. Haegele, Method for producing partially hardened steel components. Patent Application, WO2010109012A1 (2010)
95. B. Fernandez, J. Zarate, I. Garcia, S. Varela, Tailor strategies in press hardening. in *3rd International Conference on Hot Sheet Metal Forming of High Performance Steel, CHS2*, pp 437–446 (Germany, 2011)
96. B.A. Behrens, S. Hübner, Conductive heating in press-hardening process. in *Presented at Doors and Closures in Car Body Engineering 2011*, Germany, 16–17 November 2011
97. Ralf Kolleck and Robert Veit. Tools and technologies for hot forming with local adjustment of part properties. in *THERMEC 2009 of Materials Science Forum*, vol. 638, pp. 3919–3924 (Trans Tech Publications, 2010)
98. A. Breidenbach, R. Dams, T. Gerber, S. Reiter, S. Sikora, O. Straube, *Sechs wege zur optimal b-säule (six ways to optimize b-pillar - in german)* (ATZ Online, 2009), pp. 126–133
99. E. Billur, C. Wang, C. Bloor, M. Holecek, H. Porzner, T. Altan, Advancements in tailored hot stamping simulations: Cooling channel and distortion analyses. AIP Conf. Proc. **1567**(1), 1079–1084 (2013)
100. M. Hahn, T. Rebele, R. Weiss, The new audi q5 car body. in *Presented at EuroCarBody 2008*, Germany, 21–23 October 2008
101. P. Belanger, Steel innovations in hot stamping. in *Great Designs in Steel 2016* (2016)
102. S. Crichley, T.J. Palesano, New global model introduction: the all-new 2016 honda civic. in *Presented at Great Designs in Steel 2016*, USA, 16 May 2016
103. L. Reifenstein, F. Timm, F. Pohl, All New Ford Fiesta. in *Presented at EuroCarBody 2017*, Germany, 17–19 October 2017
104. T. Hambrech, The new Audi Q7. in *Presented at EuroCarBody 2015*, Germany, 20–22 October 2015
105. P. Feuser, T. Schweiker, M. Merklein, Partially hot-formed parts from 22mnb5–process window, material characteristics and component test results. in *10th International Conference on Technology of Plasticity*, pp. 408–413 (Aachen, Germany, 2011)
106. C. Wästlund, Tailored properties for press-hardened body parts. in *Presented at Insight Edition Conference*, Sweden, 20–21 September 2011
107. R. George, Hot forming of boron steels with tailored mechanical properties, experiments and numerical simulations (2011)
108. K. Mori, P.F. Bariani, B.A. Behrens, A. rosius, S. Bruschi, T. Maeno, M. Merklein, J. Yanagimoto, Hot stamping of ultra-high strength steel parts. in *CIRP Annals - Manufacturing Technology* (2017)
109. esi Group. PAM-STAMP 2015.1 User Guide (2015)
110. H.S. Choi, W.S. Lim, P.K. Seo, C.G. Kang, B.M. Kim, Local softening method for reducing trimming load and improving tool wear resistance in cutting of a hot stamped component. in *Steel Research Int. Special Edition*, pp. 419–422 (2011)
111. K. Mori, Y. Okuda, Tailor die quenching in hot stamping for producing ultra-high strength steel formed parts having strength distribution. CIRP Ann. **59**(1), 291–294 (2010)
112. R. Kolleck, W. Weiß, P. Mikoleizik, Cooling of tools for hot stamping applications. in *IDDRG, Graz, Austria (2010)*, pp. 111–119 (2010)
113. H. Lehmann, New developments in furnaces for press-hardening. in *5th International Conference on Hot Sheet Metal Forming of High Performance Steel, CHS2*, pp. 331–341 (Canada, 2015)
114. M. Garcia, Remote laser welding. in *Presented at European Automotive Laser Applications (EALA) 2013*, Germany, 19–20 February 2013
115. B. Macek, Optimization side crash performance using a hot-stamped b-pillar. in *Presented at Great Designs in Steel Seminar* (2006)
116. A. Fidorra, J. Baur, The art of progress: Audi - the new a8. in *Presented at EuroCarBody 2010*, Germany, 18–20 October 2010

117. P. Wilhelmy, C. Finkeldey, A. Grossmann, Mercedes-benz c-class. in *Presented at EuroCar-Body 2014 - 16th Global Car Body Benchmarking Conference* (Germany, 2014)
118. B. Klein, S. Crichley, K. Khang, Hot stamp rear frame optimization. in *Presented at Great Designs in Steel 2015*, USA, 13 May 2015
119. B. Fossati, A. Machado-Baglietto, M. Cappelaere, Hot stamping industrialization at Renault. in *Presented at Forming in Car Body Engineering 2014*, Germany, 24–25 September 2014
120. P. Åkerström, Modeling and simulation of hot stamping. Ph.D. thesis, Luleå University of Technology, Sweden, 2006
121. H.-H. Bok, M.-G. Lee, E.J. Pavlina, F. Barlat, H.-D. Kim, Comparative study of the prediction of microstructure and mechanical properties for a hot-stamped b-pillar reinforcing part. Int. J. Mech. Sci. **53**(9), 744–752 (2011)
122. S. Burget, S. Sommer, Characterization and modeling of fracture behavior of spot welded joints in hot-stamped ultra-high strength steels. in *Published at 11th LS-DYNA Forum* (Germany, 2012)
123. M. Fermer, Designing body structure for real life safety. in *Presented at Insight Edition Conference*, Germany, 18–19 September 2012
124. S. Nedic, A. D'Elia, N. Palmquist, The all new volvo V90 car body. in *Presented at EuroCar-Body 2016*, Germany, 17–20 October 2016
125. M. Page, A. Feaver, B. Mooiman, Bentley bentayga. in *Presented at EuroCarBody 2016*, Germany, 17–20 October 2016
126. I. Laumann, T. Picas, M. Grané, D. Casellas, M.D. Riera, I. Valls, Hard cutting of tailored hardened 22MnB5. in *IDDRG, Graz, Austria (2010)*, pp. 355–362 (2010)

Chapter 9
Hot Tube Forming

Eren Billur and Frank Schieck

Abstract Tube forming is used to manufacture hollow geometries, otherwise would be stamped and welded. Automotive components could be produced by simply bending and preforming of tubular blanks; or by tube hydroforming (THF). Until recently, THF was limited to aluminum alloys and steels up to 1000 MPa tensile strength. Nowadays, hot tube hydroforming and tube bending & quenching processes are used in automotive industry to produce complex parts over 1500 MPa tensile strength.
In this chapter, tubular parts are discussed which are produced by using Mn-B alloyed steels. There are currently three different technologies which can deliver formed and hardened tubular parts:

(1) in the so-called **3DQ** process the tubes are only bent or twisted and heat treated [1] (Sect. 9.1)
(2) in the **hot tube forming** the tube may be filled with gas or granular medium to avoid collapsing but the forming is done by an external die set. Pressure may be generated inside the tube, but is not controlled and is the result of volume reduction [2, 3] (Sect. 9.2), and
(3) **hot hydroforming** where the forming is done by the pressure generated by the fluid or granular medium inside the tube [2] (Sect. 9.3).

Tubular parts are favored as they can further save weight and packaging by eliminating the need of flanges for spot welding, as shown in Fig. 9.1. This is especially useful in areas like A-pillars as a thinner pillar would improve the driver's vision

E. Billur (✉)
Billur Makine Ltd., Ankara, Turkey
e-mail: eren@billur.com.tr

E. Billur
Atılım University, Ankara, Turkey

F. Schieck
Fraunhofer IWU, Chemnitz, Germany
e-mail: Frank.Schieck@iwu.fraunhofer.de

E. Billur (ed.), *Hot Stamping of Ultra High-Strength Steels*,
https://doi.org/10.1007/978-3-319-98870-2_9

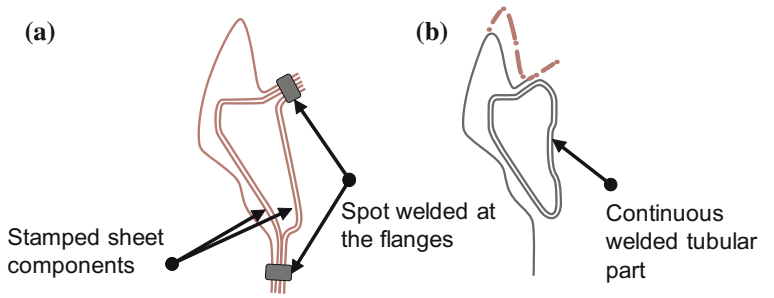

Fig. 9.1 Comparison of A-pillar cross sections of **a** stamped and welded sheets, **b** tubular parts (recreated after [5])

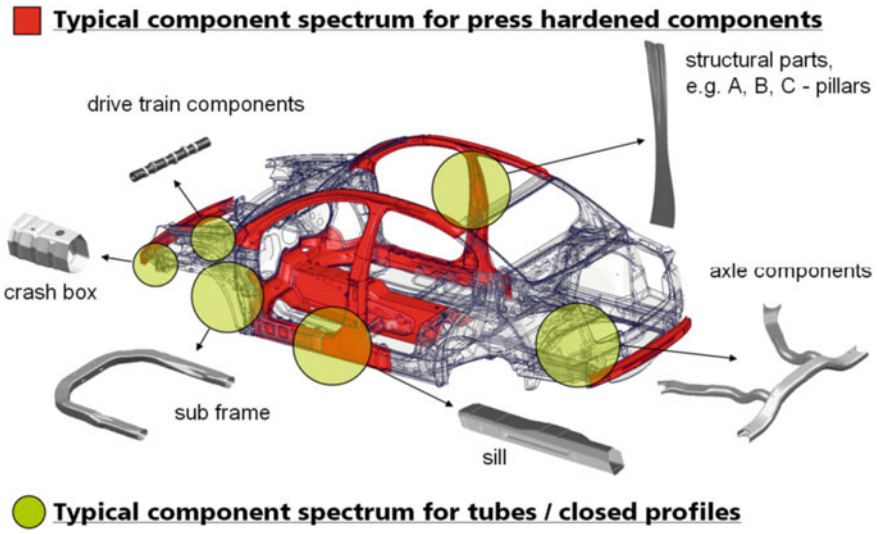

Fig. 9.2 Possible applications areas for hot formed tubes [7]

[4, 5]. Elimination of spot welded flanges are also beneficial in axial crush components such as crashboxes [6]. Figure 9.2 shows the automotive parts that are typically press hardened and those which could be replaced by a tubular product [7].

9.1 3DQ

3DQ is an abbreviation which stands for "Three-Dimensional Hot Bending and Direct Quenching" [1]. In 3DQ process a tubular profile with constant cross section is quickly heated using induction heaters. By using movable roller dies the part is bent. As the material is fed, water is sprayed on the induction heated portion of the

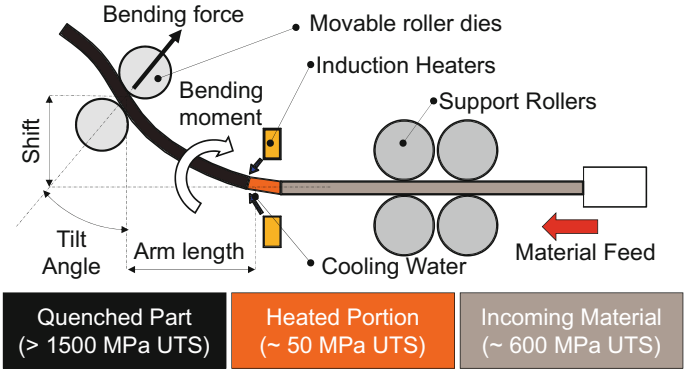

Fig. 9.3 Schematic of 3DQ system (recreated after [8–10])

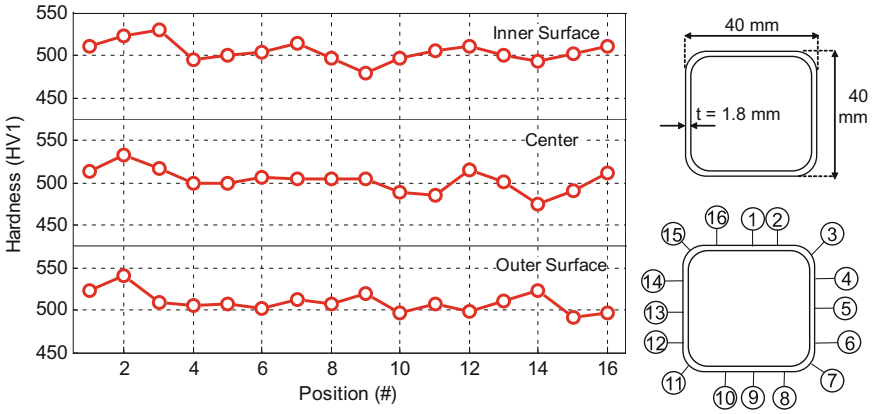

Fig. 9.4 Hardness distribution of a part produced by 3DQ process (recreated after [10])

tube to quench and harden it. The schematic of the process and the material strength through the process is illustrated in Fig. 9.3. It is also possible to replace the movable roller dies with an industrial robot to bend and twist the tubular part [1, 8–10].

By using this technology, Vickers hardness in the order of 500–550 HV is achievable. More importantly, throughout the cross section the hardness variation could be kept within ±10%, as shown in Fig. 9.4.

It is also possible to generate tailored properties by using on/off control on the induction heater. Figure 9.5 shows the hardness distribution of a part with tailored quenching. In applications like crashboxes, this can bring an additional 20-40% more energy absorbing capacity, as shown in Fig. 9.6 [10].

According to Hamasaki and Yumoto [11], the technology was already in mass production for door beams and seat reinforcement parts in early 2016. Mazda has shown that the ISOFIX connection in the rear seats of an MPV model was produced by this method, as shown in Fig. 9.7a [12]. In 2015, Honda has patented a very similar

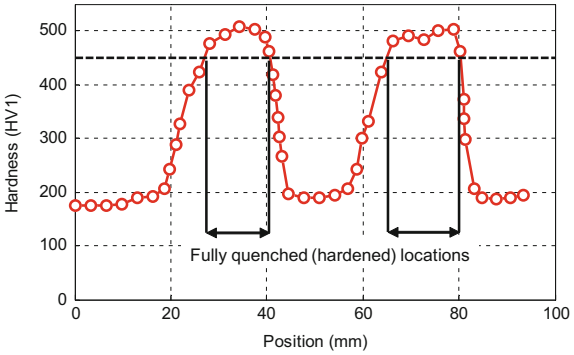

Fig. 9.5 Hardness distribution of a part produced by 3DQ process (recreated after [10])

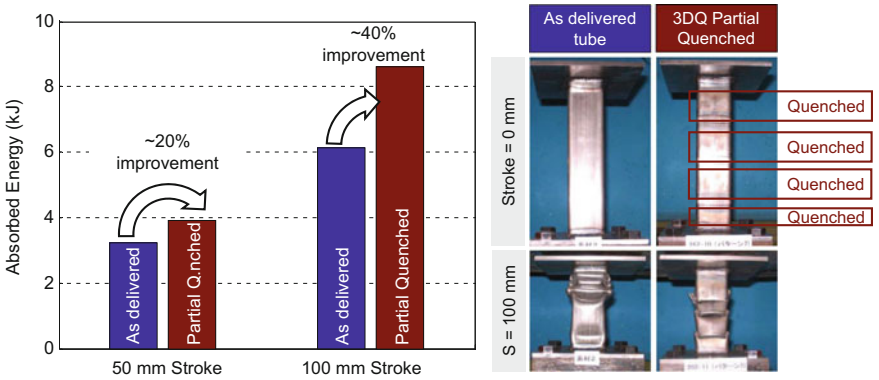

Fig. 9.6 Crush performance of a tailor quenched part (recreated after [10])

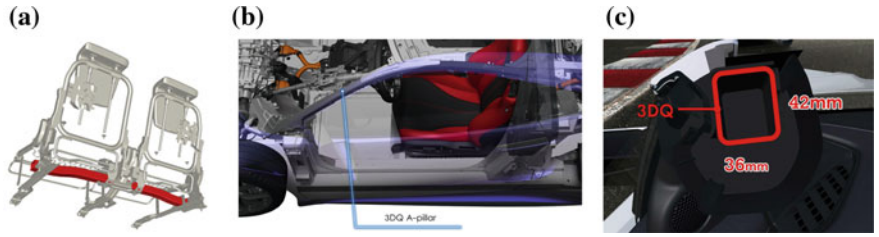

Fig. 9.7 Industrial applications of 3DQ process: **a** seat reinforcement of Mazda 5/Premacy (SOP 2013) [12], **b**, **c** A-pillar of Acura/Honda NSX (SOP 2016) [16]

process for front rail production [13]. Later in 2016, Honda started production of the sports car NSX (known as Acura NSX in some markets) [14]. This vehicle's A-pillars were produced by 3DQ process, as shown in Fig. 9.7b, c [15].

9.2 Hot Tube Forming

In 3DQ process, the part is bent and/or twisted but the cross sectional geometry is kept constant. In many applications, however, change in cross section may be required or preferred for further light-weighting and/or packaging purposes. One such part, for example, is the rear suspension torsion beam, Fig. 9.8c [3, 17].

In this process, the forming is done by solid punch and dies, as shown in Fig. 9.8. Although some internal pressure (up to 4 MPa) may be present at the beginning of the process, pressure increases as a result of reduction in internal volume, not by pumping. The pressure values are much lower compared to hot tube hydroforming process. As hot forming process requires the tube heated over 900 °C, liquid medium cannot be used for building up pressure. Since water would boil and oil may catch fire at this temperature level, either gas or granular medium (such as ceramic beads, quartz sand, etc.) are filled inside the tube [2, 3, 18].

The process could be direct or indirect. In the direct process [19]:

(1) Tube is heated (by induction , conduction [3, 18, 19], but also could be in furnace [20])
(2) Pressurizing the tube, typically up to 4 MPa to avoid the collapse of the tube [3, 19, 21]
(3) Forming process by using solid punch and die. During forming, the internal pressure may increase as high as 4–8 times of the initial pressure-depending on the volume reduction and temperature [3, 21]
(4) Tube quenching, could be done by water cooled dies [19] or spraying air or water–air directly in or over the tube [3, 20].

In the indirect hot tube forming, the deformation is done in cold condition. Formed tubes are later heated and quenched [22, 23]

With this process, the final parts were measured to have tensile strength over 1500 MPa in most cases when quenching is done over the critical cooling rate (27 °C/s).

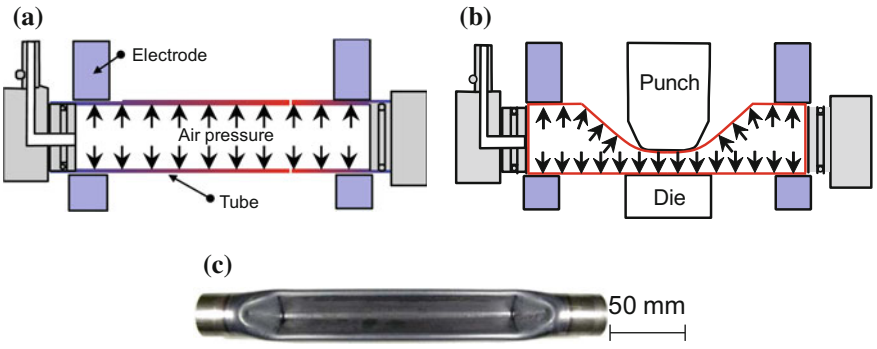

Fig. 9.8 Direct hot tube forming of a hollow torsion beam: **a** initial stage, **b** pressure builds up as forming is completed, **c** an experimental torsion beam (recreated after [3, 18])

However, if spray cooling is not employed properly, the strength may be lower than 1000 MPa [3, 19, 20].

Hot tube forming has been applied to body components, such as: A-pillar reinforcements, side door beams, bumper beams, sill reinforcements; and chassis components, such as subframe and torsion (twist) beams.

Tubular A-pillar reinforcements have been used in a number of convertible vehicles, including but not limited to Peugeot 307 CC (SOP 2003) [24], smart roadster (SOP 2003) [25], 1st generation MINI Cabrio (SOP 2004) [26], MINI Roaster (SOP 2012) [27]. In another convertible car VW Eos, A-pillar was made of hot stamped sheet, but tubular parts were used between the B-pillars and in the door beams [28].

Fifth-generation Ford Mustang (SOP 2005) had front and rear bumper beams made by "Form-Fixture Hardening". In this technology, roll formed profiles were cut to length, heated over austenitization temperature and press formed. During press forming not only a sweep radius may be given, but also the profile may be formed. Such parts were also used in other vehicles [29, 30].

Porsche used hot formed tubes in their vehicles as well. In the first generation Porsche Cayenne (SOP 2002), the rocker reinforcement was made of BTR 155 (similar to 22MnB5 but with higher Mn content) and had 1200 MPa yield strength and 1600 MPa tensile strength [31, 32]. Tubular components were also used in 911 Carrera (SOP 2012) in a Z-shaped geometry which consists of three tubes that are MAG welded [33].

In a 2009 study, the best rear axle in 13 B-segment vehicles was found to have 22MnB5 torsion beam [34]. Conventionally, these beams are cold formed and later quenched (similar to indirect hot stamping) [23, 35]. A tempering process may also be required to ensure the fatigue life [36].

Benteler developed a special air hardening steel BAS100 for subframe application in the W204 Mercedes C-class (SOP 2007). The design included 4 tubular parts, the thinnest had a wall thickness of 1.3 mm; the thickest was 1.65 mm. The design shown in Fig. 9.9b replaced an aluminum cast design and saved an additional 2 kg (~4.5 lbs) [31, 37].

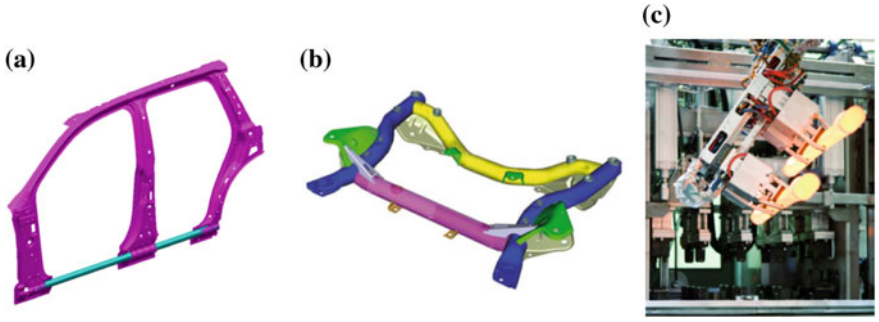

Fig. 9.9 Hot tube forming examples: **a** rocker reinforcement of Porsche Cayenne (SOP 2002), **b** front subframe of Mercedes C-class (SOP 2007) [31]; **c** indirect hot forming of torsion beams [22]

9.3 Hot Tube Hydroforming

In hot tube hydroforming, the tube is heated first and placed onto a die set. The ends of the tube are sealed and pressurized gas or granular medium is forced inside the tubular blank. The forming forces are applied by the high pressure built inside the tube [2]. It is also possible to feed material as in the case of cold tube hydroforming. After the deformation, the part could be quenched with water [38, 39] or by the tool active surface of the cavity. In this case, a water cooling channel system inside the die inserts are typically required [40].

The tubes could be heated by induction [41], conduction (Joule heating by electric resistance) [42] or in a furnace [20, 41]. In most academic studies, manual handling or robotic system is used to place the tubes in the dies [20, 41]. Figure 9.10 shows the experimental setup at Fraunhofer IWU, where induction heating and robotic material handling were employed [41].

In the so-called "Form Blow Hardening" process, roll formed profiles or U-O-formed tubes are heated and formed with air pressure. However, the quenching is done by using water [30]. This technique has been studied by several researchers [30, 38, 39], using different materials, as tabulated in Table 9.1.

In 2011, SEAT published a study on form blow hardening process. In this study, they replaced the A-pillar, cantrail and roof rail assembly of SEAT León (Mk2, SOP 2005) with a form blow hardened part, as shown in Fig. 9.11. The results were summarized as [43]:

1. 7.9 kg(17.4 lbs) weight reduction per car,
2. Material utilization was increased from 40 to 95%,
3. Number of components in the assembly on one side of the car was reduced from 5 to 2, and the roof rail could be eliminated, see Fig. 9.11.

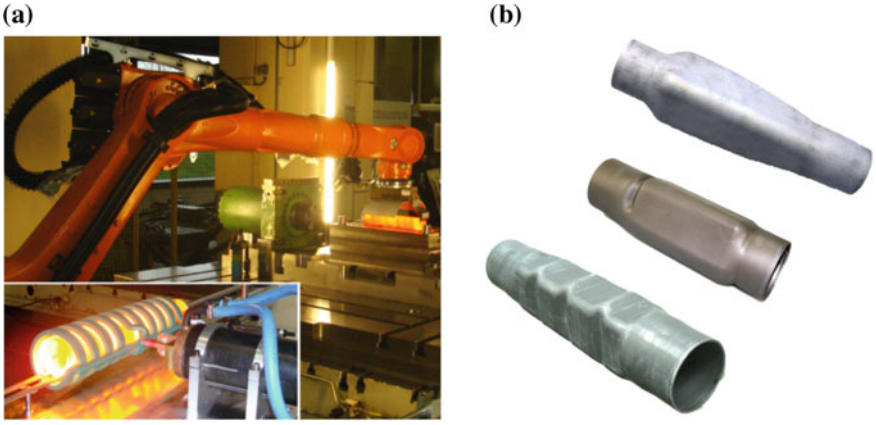

Fig. 9.10 Hot hydroforming studies at Fraunhofer IWU: **a** induction heating and the robotic material handling system, **b** sample parts produced, including a crashbox (recreated after [41])

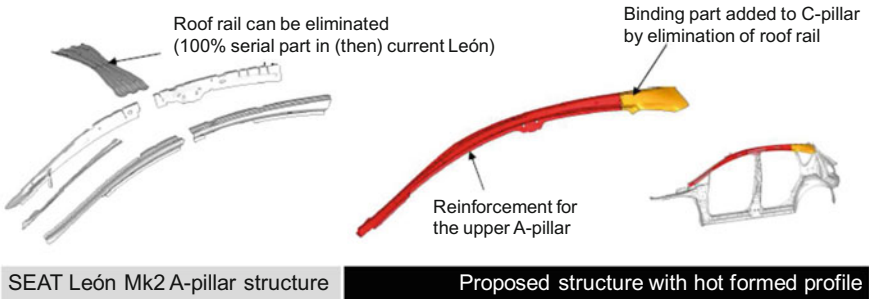

Fig. 9.11 Comparison of components in production versus proposed hot forming: A total of five stampings were replaced by one hydroform and one stamping. The roof rail could be eliminated (recreated after [43])

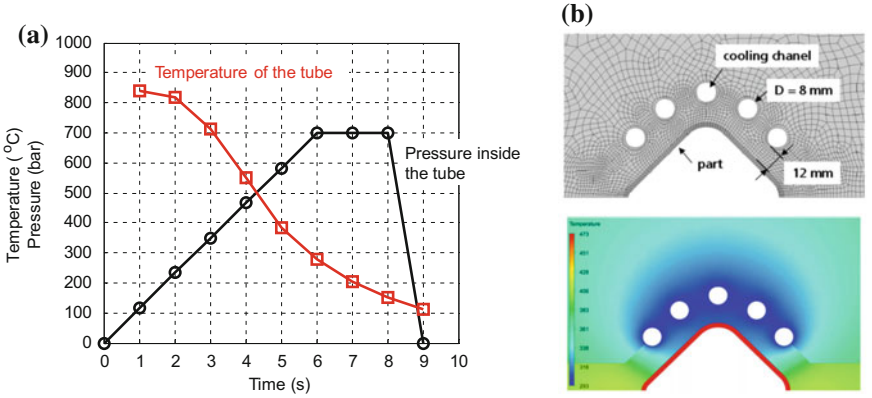

Fig. 9.12 Forming and quenching with air: **a** change of pressure in the tube and temperature of the tube, **b** simulation of heat transfer to the dies and cooling channels (recreated after [41])

Landgrebe and Schieck have developed a hot hydroforming setup in which both forming and quenching are done by compressed air. As shown in Fig. 9.12a, the internal pressure could be increased to 70 MPa (700 bars). The tools are cooled with internal cooling channels Fig. 9.12b. The parts produced with this technique were measured to have hardness values between 460 and 530 HV [44]. Crashbox and camshafts are among the parts produced.

Table 9.1 shows the strength values from several hot hydroforming studies using various tube materials.

Chen et al. used granular medium to hot form T-shapes. In this study, the tubes were heated in a furnace and manually transferred to the die. After the granular medium was filled, a punch was forced to compress the granular medium. As the volume was decreased, the pressure inside the tube was increased to 100 MPa. As the internal pressure increases, the tube loses its heat to granular medium and the tool surface. By optimizing corresponding to a cooling rate up to 50 °C/s [45].

Table 9.1 Summary of hot formed tube studies

Material	Yield Stress (MPa)	UTS (MPa)	Reference
22MnB5	1050–1200	1400–1550	[38]
27MnB5	1150–1350	1500–1700	[38]
30MnB5	1200–1400	1550–1750	[38]
22MnB5	1050–1300	1450–1750	[39]
22MnB5	n/a	1430–1620	[41]
LH800	n/a	∼1150	[41]
MW1000L	n/a	∼1900	[41]
34MnB5	n/a	∼2000	[41]
42SiCr	n/a	∼2300	[46]

References

1. A. Tomizawa, N. Shimada, H. Matsuda, H. Mori, Development of three-dimentional hot bending and direct quench (3dq) mass processing technology, in *Proceedings of International Conference "Hydroforming of Sheets, Tubes and Profiles"* (2012), pp. 127–138
2. H. Chen, S. Hess, J. Haeberle, S. Pitikaris, P. Born, A. Güner, M. Sperl, A.E. Tekkaya, Enhanced granular medium-based tube and hollow profile press hardening. CIRP Ann. - Manufact. Technol. **65**(1), 273–276 (2016)
3. T. Maeno, K. Mori, K. Adachi, Gas forming of ultra-high strength steel hollow part using air filled into sealed tube and resistance heating. J. Mater. Process. Technol. **214**(1), 97–105 (2014)
4. S. Nedic, H. Ljungquist, E. Hollander, The new volvo xc60 car body, in *Presented at EuroCar-Body 2008, October 21–23, Bad Nauheim, Germany* (2008)
5. Springer Fachmedien Wiesbaden. Schlanke a-säule: Bessere sicht, weniger gewicht. ATZExtra (2014)
6. The New Volvo V70 and XC70 Car Body (2007)
7. R. Neugebauer, F. Schieck, S. Polster, A. Mosel, A. Rautenstrauch, J. Schönherr, N. Pierschel, Press hardening - an innovative and challenging technology. Arch. Civil Mech. Eng. **12**(2), 113–118 (2012)
8. H. Kubota, A. Tomizawa, K. Yamamoto, N. Okada, Development of finite element analysis method for three-dimensional hot bending and direct quench (3dq) process. AIP Conf. Proc. **1532**(1), 568–573 (2013)
9. N. Shimada, A. Tomizawa, H. Kubota, H. Mori, M. Hara, S. Kuwayama, Development of three-dimensional hot bending and direct quench technology, in *Procedia Engineering*, vol. 81 (2014), pp. 2267 – 2272. *11th International Conference on Technology of Plasticity, ICTP 2014, 19–24 October 2014, Nagoya Congress Center, Nagoya, Japan*
10. K. Uematsu, N. Shimada, A. Tomizawa, H. Mori, Development of three-dimensional hot bending and direct quench using robot, in *2015 International Conference on Intelligent Informatics and Biomedical Sciences (ICIIBMS)* (2015), pp. 165–171
11. Y. Hamasaki, A. Yumoto, Automotive solution (2): equipment development of 3-dimensional hot bending and direct quenching (3dq). Nippon Steel Sumitomo Metal Tech. Rep. **112**, 74–80 (2016)
12. Mazda, *Mazda Adopts the World's First 3-dimensional Hot Bent Hardened Square Tube (Translated from Japanese)* (2013)
13. Y. Ohta, Structure for front side frames of automobile, December 15 2015. US Patent 9,211,913
14. B. Snavely, Honda rolls out first acura nsx supercar in ohio factory, in *USA Today* (2016)
15. Acura NSX (2016)

16. Honda, 2017 Acura Nsx Press Kit - Space Frame and Body Panels (2016)
17. W.W. Zhang, C. Han, S.J. Yuan, Optimization of pre-form shapes by response surface methodology for hydro-forming of 780 mpa torsion beam. Int. J. Adv. Manufact. Technol. **85**(5), 1227–1237 (2016)
18. K. Mori, *Smart Hot Stamping for Ultra-high Strength Steel Parts* (Springer, Berlin, 2015), pp. 403–408
19. V. Leire, P. Inaki, H. Izuru, Z. Jose Ignacio, M. Anegla, S. Jose Juan, P. Uwe, Gas forming of boron steel tubes at low pressure-applasting. Steel Res. Int. **81**(9), 552–555 (2010)
20. B. A. Behrens, S. Hübner, S. Schrödter, J. Uhe, Conductive heating opens up various new opportunitites in hot stamping, in *Proceedings of 5th International Conference on Accuracy in Forming Technology (ICAFT 2015)* (2015), pp. 157–174
21. M. Ishikuza, N. Ueno, M. Saika, T. Komatsu, *Molding Device and Molding Method* (2017)
22. W. Linnig, A. Zuber, A. Frehn, G. Leontaris, W. Christophliemke, The twist beam rear axle design, materials, processes and concepts. ATZ Worldwide eMag. Ed. **111**(2), 10–17 (2009)
23. A. Frehn, T. Säuberlich, Tubular steel components for light weight axle designs, in *Proceedings of the 3rd International Conference on Steels in Cars and Trucks (SCT2011)* (2011), pp. 10–19
24. P. Perrot, R. Vincenti, C. Feuvrier, The peugeot 307 cc body. Proc. EuroCarBody **2003**, 172–237 (2003)
25. P. Sebastian, M. Pickenhahn, The new smart-roadster car body. Proc. EuroCarBody **2003**, 172–237 (2003)
26. F. Brunies, E. Heinl, Body concept of the new mini cabrio. Proc. EuroCarBody **2004**, 272–294 (2004)
27. C. Rauber, Press hardened steel - applications and future requirements at BMW, in *Materials in Car Body Engineering 2015* (2015)
28. *The EOS - More than an Automotive Structure: A Masterpiece on Body-Design* (2006)
29. A. Gier, Hot forming and hardening of rollformed sections, *Aluminum and Steel Forming, Automotive Engineering* (2005), pp. 172–237
30. H. Lanzerath, M. Tuerk, Lightweight potential of ultra high strength steel tubular body structures. SAE Int. J. Mater. Manf. **8**, 813–822, 04 (2015)
31. U. Diekmann, T. Säuberlich, A. Frehn, Luftvergütende hochfeste stähle für mehr crashsicherheit. ATZ - Automobiltechnische Zeitschrift **109**(12), 1128–1135 (2007)
32. R. Mušálek, P. Haušild, J. Siegl, J. Bensch, J. Sláma, Mechanical properties and fracture behavior of high-strength steels. Strength Mater. **40**(1), 142–145 (2008)
33. Dr. Ing. h. c. F. Porsche AG Presse-Datenbank. http://presse.porsche.de
34. S. Lepre, G. Desvignes, Advanced high strength steels and tubular multiwall technology in a twist axle application, in *Presented at Great Designs in Steel, Livonia, MI, May 17th* (2009)
35. O.S. Seo, S.J. Yoon, C.H. Suh, H.Y. Kim, Numerical modeling of hot press forming process of boron steel tube. AIP Conf. Proc. **1252**(1), 1216–1222 (2010)
36. Y. Cho, S. Park, Application of ahss for light weight automotive body and chassis parts, in *Materials in Car Body Engineering 2009* (2009)
37. L. Hein, K. Weise, Lightweight chassis cradles, in *Presented at Great Designs in Steel, Livonia, MI, April 9th* (2008)
38. O. Vestermark, Nodes for hardened boron profile. Master Thesis, Luleå University of Technology (2008)
39. A. Gutermuth, Form blow hardening, in *Presented at Forming in Car Body Engineering 2011, September 27th, Bad Nauheim, Germany* (2011)
40. R. Neugebauer, A. Göschel, A. Sterzing, F. Schieck, Gas forming with integrated heat treatment for high performance steel-a solution approach for press hardened tubes and profiles, in *2nd International Conference on Hot Sheet Metal Forming of High-Performance Steel, Verlag Wissenschaftliche Scripten, Luleå, Auerbach* (2009), pp. 181–188
41. R. Neugebauer, M. Werner, A. Paul, F. Schieck, Media based press hardening of tubes—opportunities and challenges, in *Proceedings of the 5th International Conference on Tube Hydroforming. Kenichi Manabe:[S. n.]* (2011), pp. 100–107

42. G.N. Chu, Y.L. Lin, M.Q. Ding, Hot hydroforming of 22mnb5 tube by resistance heating. JOM **68**(7), 1983–1989 (2016)
43. V. Oliveras Mérida, X. A. Ripoll, M. Ferstl, A. Zahinos Ruiz, V. Clua, Applying new blow-forming processes to obtain new structural components for automotiva industry: a-pillar, in *Selected proceedings from the 15th International Congress on Project Engineering* (2011), pp. 211–222
44. D. Landgrebe, F. Schieck, Hot gas forming for advanced tubular automobile components: opportunities and challenges, in *ASME 2015 International Manufacturing Science and Engineering Conference* (American Society of Mechanical Engineers, 2015), pp. V001T02A087–V001T02A087
45. H. Chen, A. Güner, N. Ben Khalifa, A.E. Tekkaya, Granular media-based tube press hardening. J. Mater. Process. Technol. **228**, 145–159 (2016). (Hot Stamping)
46. M. Bohuslav, J. Hana, V. Ivan, K. Petr, M. Uwe, Flexibility, productivity, and innovation power - core competencies of a tier 1 supplier, in *Neue innovative Konzepte für die Innenhochdruckumformung* (2014), pp. 107–114

Chapter 10
Computer Modeling of Hot Stamping

Harald Porzner and Eren Billur

Abstract Tool design based on computer models is nothing new for stamping industry. Although mostly the same software packages are used for cold and hot stamping simulations, simulation of hot stamping differs significantly; as it is not only a mechanical simulation. Hot stamping is a multiphysics problem with heat transfer, metallurgical transformations and even fluid dynamics in the cooling channels.

10.1 FE Modeling of Hot Stamping Process

Simulation of a typical cold forming operation requires one flow stress curve, anisotropy coefficients (r_0, r_{45} and r_{90}), friction parameters and a yield criterion and its variables (Hill 48, Barlat 90, etc.). However, a hot stamping process requires more input parameters than regular cold forming operations since there are: (1) mechanic, (2) thermic, (3) metallurgic, and (4) fluid mechanic fields involved in the process and all these are interrelated as illustrated in Fig. 10.1 [1, 2].

Simulation of hot forming process can be divided into at least four stages, as shown in Fig. 10.2. When tailored parts are simulated, there may be six stages. In each stage, different physics are involved. The gravity stage is modeled as implicit and includes only the mechanical field. Holding and forming stages include both mechanical and thermal fields. Forming has to be completed with a blank that is still at the austenite phase and no phase transformation is desired. The quenching stage involves thermal and metallurgical fields. If tailored quenching is modeled, the part would be moved out of the press, while the soft zone is still over the martensite start (M_s) temperature. Thus, the part may distort. In commercially available software packages, this can be

H. Porzner
ESI North America, Farmington Hills, MI, USA
e-mail: harald.porzner@esi-group.com

E. Billur (✉)
Billur Makine Ltd., Ankara, Turkey
e-mail: eren@billur.com.tr

E. Billur
Atılım University, Ankara, Turkey

E. Billur (ed.), *Hot Stamping of Ultra High-Strength Steels*,
https://doi.org/10.1007/978-3-319-98870-2_10

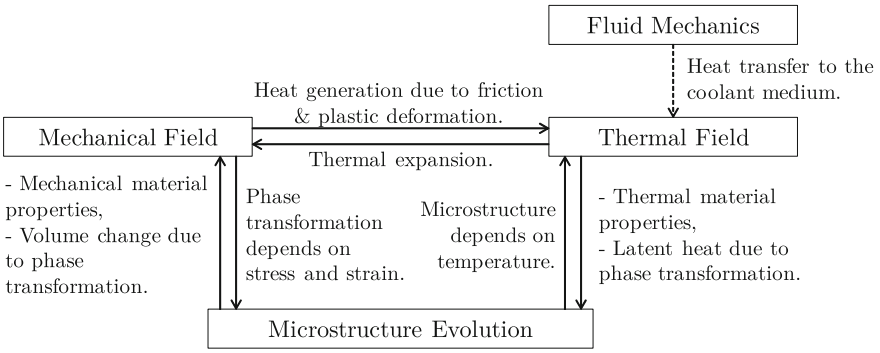

Fig. 10.1 Multiphysics problem of hot forming [1, 2]

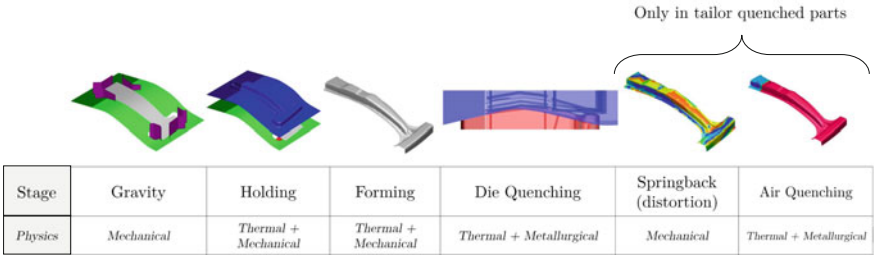

Fig. 10.2 Stages of a hot forming simulation and physics involved in each stage (recreated after [4])

handled with Springback models. Also, to have the final hardness distribution an additional "air quenching" may be required [3, 4].

Fluid mechanics is not included in quick simulations, to avoid costly couplings. For forming stage, the die faces can be modeled using shell elements. However, if cooling channels are to be modeled, solid elements are required. Weigert et al., from Volkswagen stated that a cooling simulation using solid elements and including cooling channels can eliminate the need for prototype dies in mass production [5].

10.2 Inputs to Simulation

10.2.1 Properties of the Blank

To be able to model the forming stage, the blank material's flow stress is required at high temperatures (up to 800 °C, ~1500 °F). As seen in Fig. 10.3a–c, at high temperatures (i.e., >550 °C, >1000 °F) the strain rate has significant effect on the flow stress. As temperature decreases, flow stress increases. Notably, at 300 °C (572 °F),

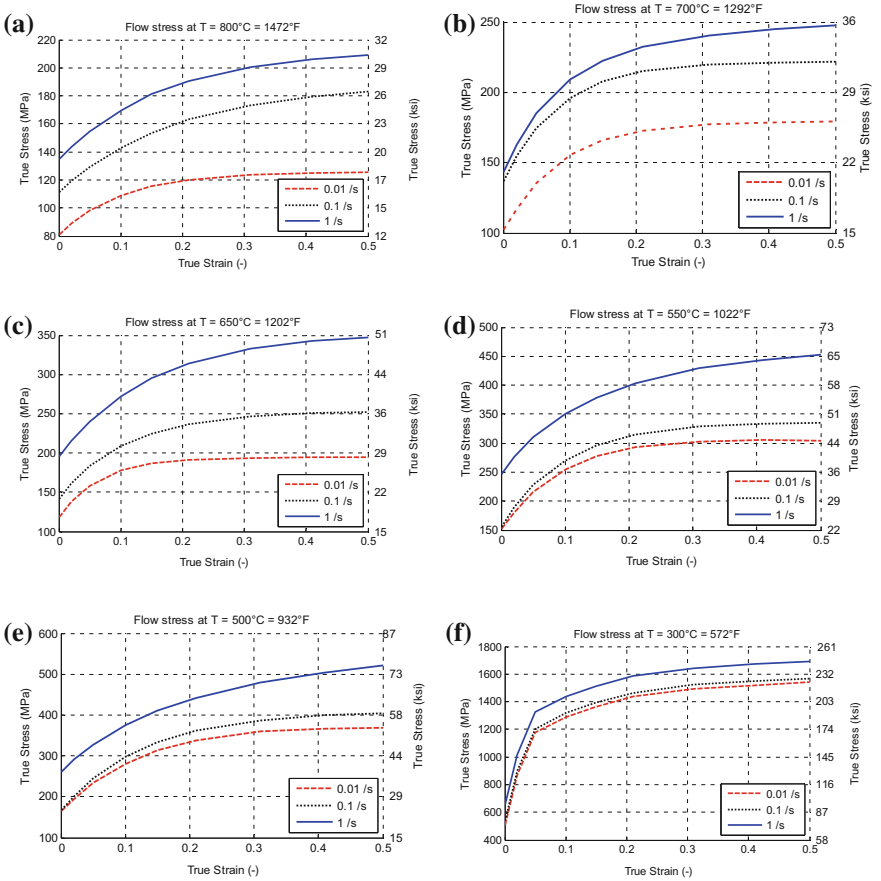

Fig. 10.3 Flow stress at 300–800 °C (570–1470 °F) at three strain rates [7]

martensite transformation is almost completed [6], and the flow stress goes over 1500 MPa (>220 ksi), as seen in Fig. 10.3f. For best results, the flow stress should be a function of strain, strain rate, temperature and microstructure.

Other than the flow stress, the elastic properties of the blanks have to be entered. The elastic modulus as a function of temperature is given in Fig. 10.4.

Thermal properties are essential to be able to calculate the instantaneous temperature in the stamping and quenching stages. The properties included in the simulation are as follows:

(1) Heat Capacity (C): energy required to heat or cool unit mass of blank by 1°, units are: kJ/kg·°C and $BTU/lb\cdot$°F, in several FE codes, heat capacity can be entered as a function of temperature and phase. For 22MnB5, the values are given in Fig. 10.5a.

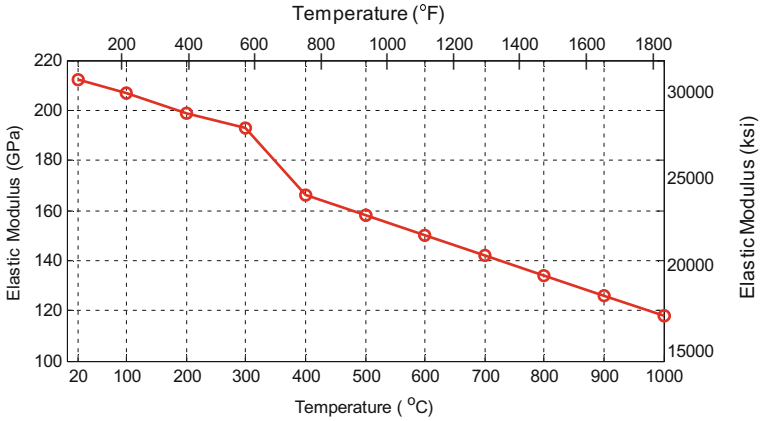

Fig. 10.4 Elastic modulus as a function of temperature (created using the data from [8])

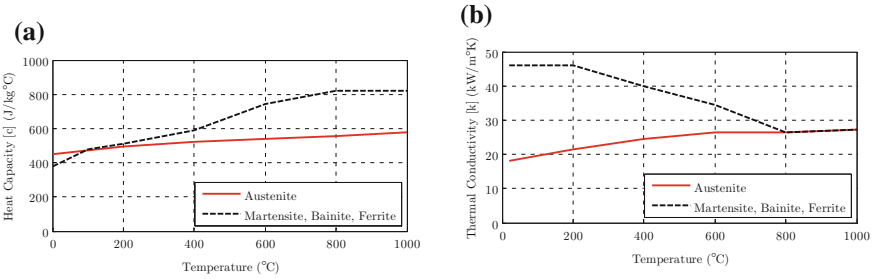

Fig. 10.5 **a** Heat capacity and **b** thermal conductivity of 22MnB5 as a function of temperature and phase. If available, also enthalpy could be used to model the latent heat of phase transformations [7]

(2) Coefficient of thermal expansion (CTE, α): change in dimension by temperature, and units are $1/\,^{\circ}\mathrm{C}$ or $1/\,^{\circ}\mathrm{F}$. CTE for 22MnB5 can be approximated as:

$$\alpha = 1.3x10^{-5}\frac{1}{^{\circ}\mathrm{C}} \approx 0.7x10^{-5}\frac{1}{^{\circ}\mathrm{F}} \tag{10.1}$$

(3) Thermal conductivity (k): can be expressed as a function of phase and temperature, as shown in Fig. 10.5b.

An important aspect in hot stamping are the phase transformations. In contrary to cold forming processes, press hardening of steel is a heat treatment process. Stampers also need to simulate heat treatment, including phase transformations. Initially, the blank is heated to over its austenitizing temperature and soaked for some time. In the simulation, it is convenient to start with the assumption that 100% of the microstructure is austenite. PAM-STAMP is using a Johnson–Mehl–Avrami equation

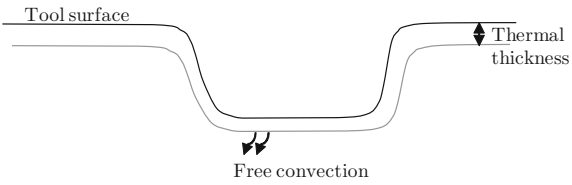

Fig. 10.6 Concept of thermal thickness [7]

to calculate the austenite decomposition during quenching. The values are already in the material library for USIBOR 1500 material [7].

10.2.2 Properties of the Tools

In order to calculate the heat loss of the blank and the heating of the tools, the tools have to be modeled as thermally conductive. Since a heat capacity is required to achieve this, the tools must have mass, which only solid elements would have. If shell elements are to be used, an artificial "thermal thickness" can be added as shown in Fig. 10.6. It is assumed that below the thermal thickness, there would be a free convection with air that emulates the thermal conductivity of the real tool mass. This way, the tools had a realistic heat capacitance and conductance which allows non-isothermal simulations. The best option is to use solid elements, as explained in Sect. 10.3.4.

To be able to calculate the local tool temperature variation in time, a thermal thickness of 6 mm can be applied [7]. The initial temperature of the tools can be assumed to be uniform and 75 °C for mass production conditions, if a cyclic cooling simulation cannot be done [9]. Thermal conductivity (k) and specific heat values (C) can be entered as constant. For H13 tool steel, these values would be [7]:

$$k = 31\frac{W}{m^2 \cdot {}^\circ\mathrm{C}} = 17.9\frac{BTU}{\mathrm{ft} \cdot \mathrm{h} \cdot {}^\circ\mathrm{F}} \tag{10.2}$$

$$C = 650\frac{J}{kg{}^\circ\mathrm{C}} \cong 0.16\frac{\mathrm{BTU}}{lb{}^\circ\mathrm{F}} \tag{10.3}$$

10.2.3 Friction

Friction is one of the most influential input to the simulations. For cold forming simulations, until recently a "constant friction coefficient" was entered. In reality, however, friction is a function of [10]:

1. Pressure level,

2. Relative sliding velocity,
3. Interface temperature,
4. Surface roughness of tool and the blank coating,

In the last few years, several metal-forming software allowed to enter friction as a function of sliding velocity and pressure [7]. More recently, a new tribology analysis plug-in is added to FE software for cold stamping purposes which can calculate "local friction coefficient" based on surface roughness and lubricity [11].

In hot stamping, presence and type of the blank coating, tool material and coating, interface temperature and contact pressure are known to have effect on friction coefficient [12–18]. A recent study have shown that the most effective variable changing AlSi coated blank's friction coefficient was temperature [19]. Two independent studies have shown that in hot stamping, sliding velocity does not affect friction significantly [15, 20].

It is also possible to use a temperature dependent friction coefficient with the new FE software. In this case, friction coefficients can be input as shown in Fig. 10.7 for AlSi coated blanks.

Zn-based coatings typically would have lower friction coefficient, compared to AlSi coated and uncoated blanks. Figure 10.8 summarizes different studies of friction coefficient determination of Zn-based coated blanks [15, 21–25], and Fig. 10.9 of uncoated blanks [25–27].

Although not common in the industry, hot forging lubricants [16] or dry-film lubricants such as graphite [14] or MoS_2 [20] can be applied on the dies. Friction coefficient as low as 0.15 have been reported with lubrication [16].

10.2.4 Thermal Contact Conductance

Heat extracted from the blank can be calculated using the "thermal contact conductance" , time elapsed (t), surface area in contact (A), and the temperature gradient (ΔT). It is known that the thermal contact conductance is a function of gap between

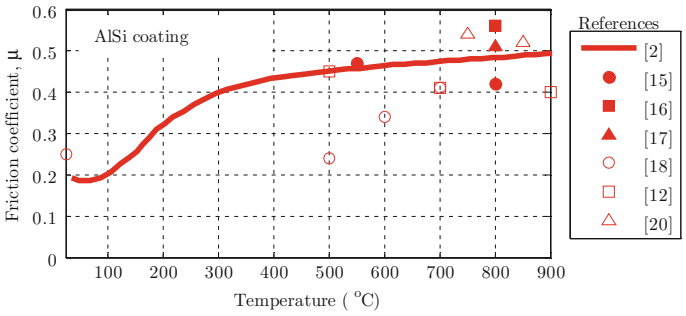

Fig. 10.7 Friction coefficients for AlSi coated blanks at elevated temperatures

the blank and tool, if they are not in contact; a function of interface pressure if they are in contact. The coefficient increases with the increasing pressure, until the pressure exceeds a threshold value [28].

Through several papers in literature, including [6, 9, 29–31], for Al/Si coated 22MnB5 material the thermal contact conductance can be used as in Fig. 10.10. Merklein et al., found that the threshold value is 30 MPa (4.4 ksi), after which the thermal contact conductance does not increase anymore [30].

10.3 Stages of a Simulation

10.3.1 Gravity

In this stage, the lower die set (i.e., the punch and the blank holder) were fixed and the blank is subject to an implicit gravity field ($9.81\,\mathrm{m/s^2} \approx 32.2\,\mathrm{ft/s^2}$). During this stage, guide pins may be used to ensure the blank sits in its position. Due to the very short time, heat transfer is not included in this stage. However, the elastic properties

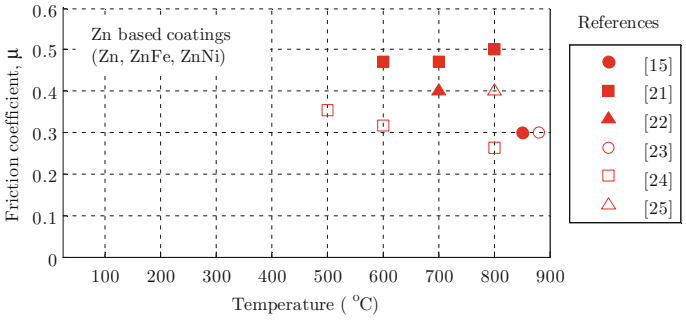

Fig. 10.8 Friction coefficients for Zn-based coated blanks at elevated temperatures

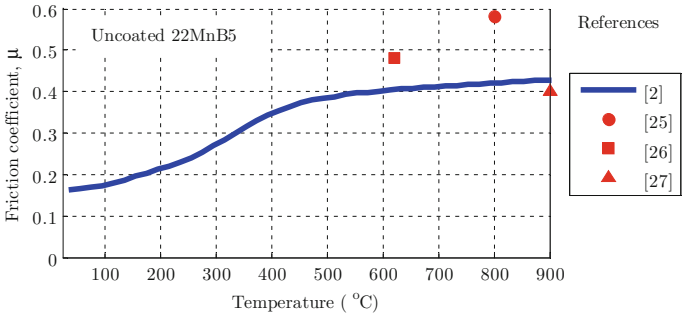

Fig. 10.9 Friction coefficients for uncoated blanks at elevated temperatures

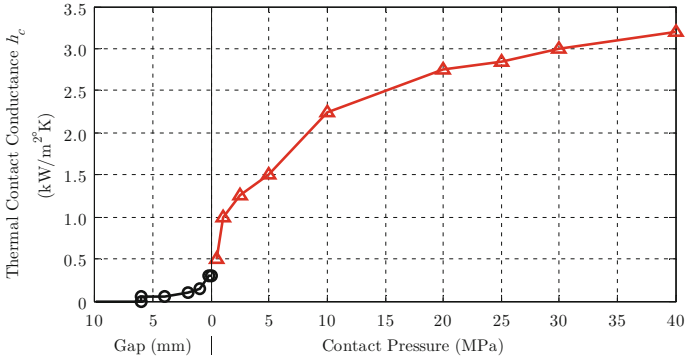

Fig. 10.10 Thermal contact conductance input to simulation, as a function of pressure and gap. (created using the data from [7, 9, 30])

of the blank depend on blank temperature (i.e., the Elastic Modulus may be in the range of 120–140 GPa ≈17,500–20,000 ksi).

10.3.2 Holding

After the implicit gravity stage, a holding stage is modeled. Here, the upper die set is moved down with the press speed and the lower die set (blank holder, punch, etc.) are fixed in all directions. The stage ends when the reaction force on the blank holder force exceeds the predefined value. To calculate the heat loss properly, it is advised to keep the blank on the lower die set for the same duration as in real life.

10.3.3 Forming

This is the stage where all the deformation is given to the part. In this stage, all secondary activators (like blank holder, pad, etc.) are force controlled, but the upper die set is controlled by kinematics. The stage ends when the force on the upper die exceeds a predefined force or the stroke of the press slide is completed.

10.3.4 Quenching

During quenching stage, the dies are clamped with the given force. Heat transfer and phase transformations take place in this stage. This stage can be modeled as “thermal only”, meaning there may be no mechanical calculations. In quenching stage, the

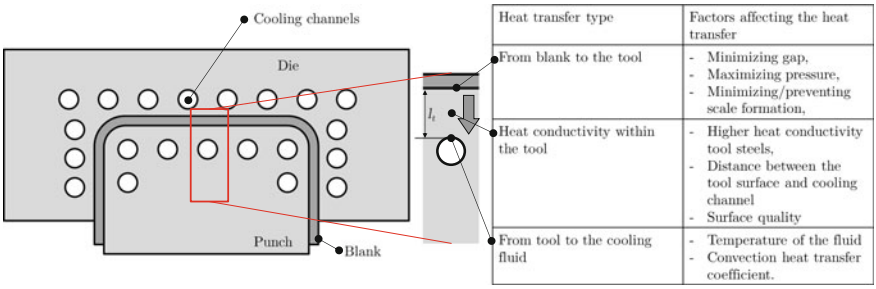

Fig. 10.11 Different modes of heat transfer to be calculated (recreated after [3, 33])

pressure distribution is typically assumed to be constant over time and is transferred from the end of forming stage. Metallurgical calculations are also activated, so the final distribution of martensite can be checked.

Quenching simulations can be done by three different assumptions, with increasing complexity:

1. Using shell dies and assumed constant temperature allover the die components and through time (isothermal),
2. Using shell dies and thermal thickness—an assumed thermal thickness, Fig. 10.6, for heat capacity (non-isothermal)
3. Using solid dies and cooling channels.

In the quenching simulation, three different heat transfer conditions have to be addressed [3, 7], as shown in Fig. 10.11:

1. The heat transfer between blank and can be now modeled as a function of pressure and gap (see Fig. 10.10).
2. The heat conductivity within the tool is modeled by the solid dies and the correct value of the heat conductivity of the tool steel (Eq. 10.2).
3. Heat transfer from die to coolant can be modeled by using CFD analysis, by which, the pressure drop and temperature rise of the cooling fluid can also be modeled. However, this would be very CPU-intensive [32]. To simulate the effectiveness of the cooling channels, "turbulent flow in a circular tube" assumption can be used .

In this assumption, the flow is assumed to be in steady-state, turbulent and at an average temperature of incoming and outgoing cooling fluid ($T_{Av} = (T_{in} + T_{out})/2$). With all these assumptions, one constant heat convection coefficient can be calculated as [3, 34]:

$$h_c = 0.023 \left(\frac{\mu C_p}{k}\right)^{0.8} \left(\frac{v_m \rho}{\mu}\right)^{0.33} \frac{(k)}{d} \tag{10.4}$$

At the end of quenching stage, the cooling rate for each element could be calculated. Based on Johnson–Mehl–Avrami equation, the phase fractions can be estimated. Using phase fractions, hardness can be estimated by following empirical formulas [35]:

$$HV = 188.5(X_f + X_p) + 283.8X_b + 514.4X_m \tag{10.5}$$

where X is the phase fraction; subscript $_f$ stands for ferrite, $_p$ pealite, $_b$ bainite and $_m$ martensite. Once the Vickers Hardness is calculated, yield and tensile strength values can be estimated [36, 37]:

$$YS \simeq 2.167HV - 55.73 \tag{10.6}$$

$$UTS \simeq 3.0412HV - 76.116 \tag{10.7}$$

Most FE software capable of hot stamping simulations have these calculations already implemented in.

10.3.5 Air Quenching

In tailor quenched parts, the final properties (e.g., Vickers hardness and ultimate tensile strength) of the soft zones are of interest, for which the final phase fractions are required. Phase transformations could only be completed if the blank is cooled under martensite finish temperature (M_f) which is for 22MnB5 about 280 °C (~540 °F). When heated die segments are used for tailored quenching, temperature in the soft zone may be well over martensite start M_s (approximately 425 °C, 800 °F) [3].

Thus, to be able to predict the final hardness of the part, an additional "air quenching" stage is added for tailored quenched parts. The duration of this stage (in terms of analysis time) should be decided by the austenite phase fraction. Once most of the austenite is transformed to other phases, the stage could be stopped. For example, Fig. 10.12 shows the change of the maximum austenite percentage with time. As seen, at the beginning of the air quenching stage ($t = 0$), the austenite fraction (at the local maxima) is 100%. After 80 s, it goes below 0.5%. For this particular case, the air quenching time can be selected as 80 s [3, 4].

10.3.6 Distortion

Springback is elastic recovery of the material after the load is removed [38]. Hot stamping is favored in forming ultra high strength steels because springback is minimized. Therefore, typically keeping the parts within the tolerances is easier with hot stamping. However, if the cooling is not uniform, then thermal distortion may occur. Distortion is defined as the shape change caused by [39] the following:

(1) Stresses caused by thermal expansion,
(2) Stresses caused by volume changes due to phase changes.

In tailored quenched parts, a nonuniform cooling is introduced intentionally. Typically, the final phase changes in the soft zones take place after the part is taken out of the press, where the blank is not clamped. In addition, hard zones are transformed to martensite (which is bct, body-centered tetragonal) and the soft zones are transformed mostly to bainite (a combination of Ferrite (bcc – body-centered cubic) and Cementite (complex orthorhombic)), which creates a change in densities [40]. To calculate distortion, dilatation data from austenite to martensite and austenite to bainite are required.

At the end of air quenching stage, during which the blank was not locked, part distorts. It could also move and/or rotate. To be able to quantify the distortion, a new stage of "distortion" is added and two separate "final part" meshes are imported from air quenching stage: at $t = 0$ s and $t = 80$ s. Then, using "Best Fitting"? transformation, the two parts are moved and rotated to the same location. Then, "Distance between objects" can show the distortion in air quenching stage, Fig. 10.13.

The model described can be further improved by: (1) adding a springback stage between die quenching and air quenching, and (2) modeling the blank as a tailor-welded blank. The first improvement can add the effects of plastic deformation to

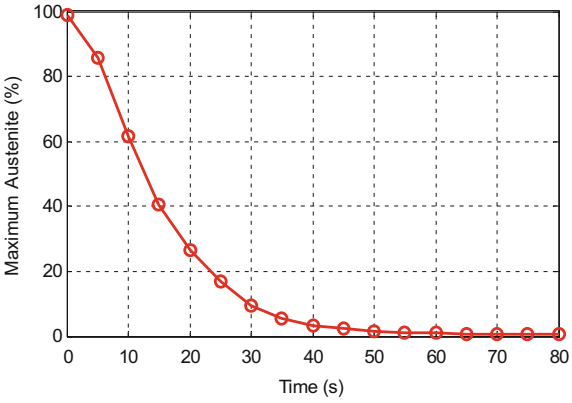

Fig. 10.12 Change of maximum austenite fraction with time in air quenching stage [3]

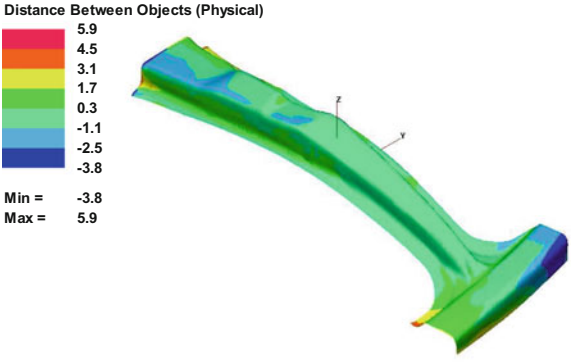

Fig. 10.13 A preliminary distortion simulation after tailored quenching (part with soft zone) [3]

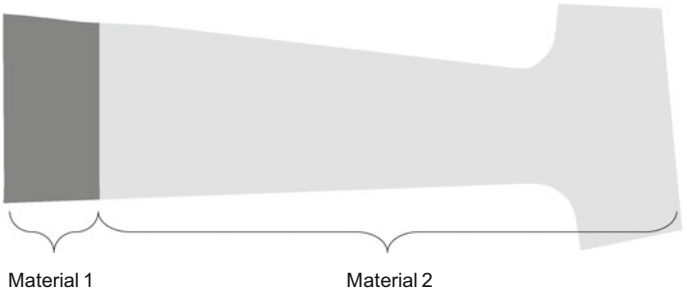

Fig. 10.14 Blank can be modeled as tailor-welded blank to have two different material properties for further improved distortion model [4]

distortion. The second improvement allowed that the yield stress (which in turn affects the distortion) to be modeled more realistically in the soft zone. In reality, the yield stress is much lower in the soft zone. Thus, the internal stresses could yield the blank earlier in the soft zone, compared to hard zone. In this new model, the whole blank has same material properties (austenite) in the beginning. However, below martensite start temperature ($M_s = 280\,°C = 540\,°F$), Material 1 will have flow stress for bainite microstructure, whereas Material 2 will have flow stress for martensite, Fig. 10.14 [4].

10.4 Case Studies

10.4.1 Numisheet 2008 B-pillar

In 2008, at the 7th International Conference and Workshop on Numerical Simulation of 3D Sheet Metal Forming Processes (NUMISHEET 2008), Audi has shared the die design of a B-pillar reinforcement for benchmarking purposes. This was one of the earliest and still one of the most detailed problem description for anyone who wants to start learning simulation of hot stamping [9]. However, the model lacks the cooling channels, as at that time no simulation software could handle cooling channel simulation. The part had no cracks, but a local neck. After the conference, thickness distribution of several sections was also shared. One can easily check his/her simulation model with this benchmark data [8, 41].

In this case study, no tailored properties were used. The blank was 1.95 mm thick. In the first stage, gravity, only the blank and the lower die set (i.e., punch, blankholder and guiding pins) is modeled. Dies were assumed to be 75 °C (167 °F) at the beginning. A non-isothermal model is used with shell die elements and 6 mm thermal thickness (see Fig. 10.6). An implicit gravity simulation is done and the blank sagged onto lower die set, within the guide pins, as shown in Fig. 10.15.

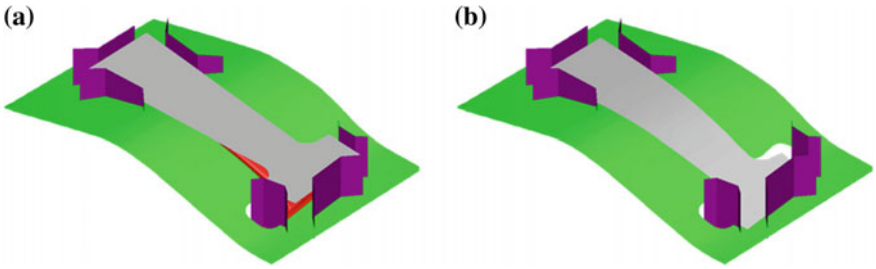

Fig. 10.15 Gravity stage: **a** initial setup, **b** end of stage with sagged blank [3]

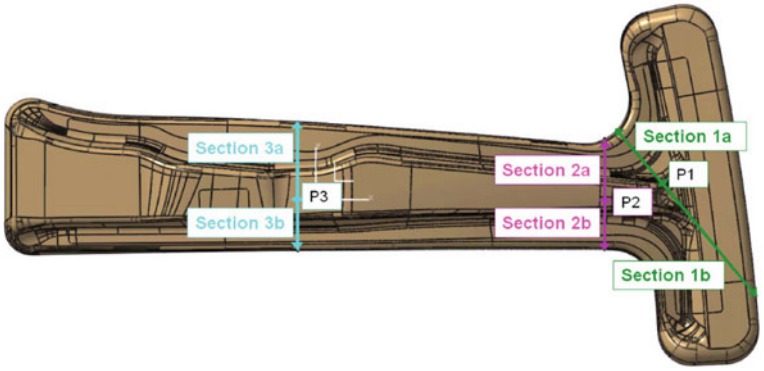

Fig. 10.16 Reference sections for thickness measurements [9]

In this model, blankholder force was not applied, as there was a constant gap between the upper die and the blankholder ($t + 0.4\,\text{mm} = 2.35\,\text{mm} \approx 0.1$"). For CPU time optimization, holding stage was not modeled. In forming stage, the upper die was moved down with an imposed displacement. This is the most realistic way of simulating the reality, as Audi has measured press slide location (i.e., stroke) at given time increments and shared this data with the benchmark. The stage was controlled by time and ends at 1.61 s, corresponding to 320 mm stroke.

At the end of forming stage, the temperature on the blank was found to be 671−850 °C (1240−1560 °F). Thus, it was ensured that the forming stage was completed with 100% Austenite phase. The benchmark committee has selected three sections (Fig. 10.16) and gave the thickness measurements in these [9].

Figure 10.17 shows the worst and best-predicted sections. As seen, in the best-predicted section, predicted thickness points were very close to the center of the error bars.

In this particular part, existence of a local neck was known. To evaluate a possible neck, Forming Limit Diagrams (FLDs) are generally used. However, in hot stamping there are many variables that can affect necking, such as the local temperature gradient, strain rate and microstructure. To be able to predict crack and/or neck by

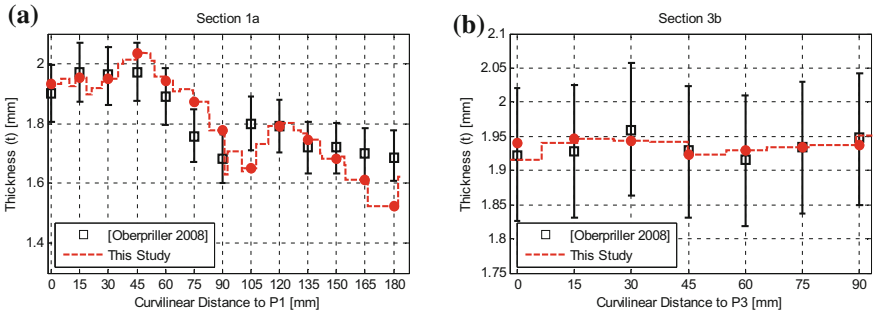

Fig. 10.17 Comparison of thickness predictions with benchmark measurements: **a** the worst predicted section, **b** the best predicted section (measurements from [9])

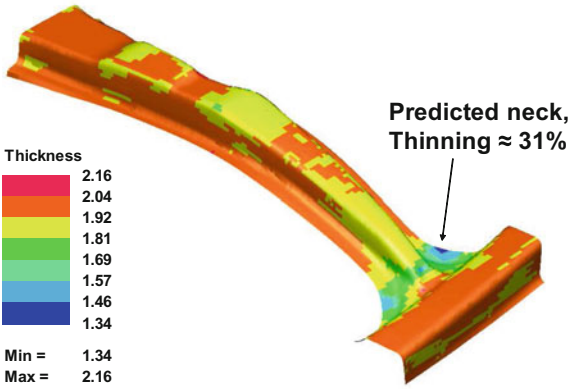

Fig. 10.18 Thickness distribution and predicted neck in the B-pillar [3]

using FLD, a number of FLDs would be required for given temperature and strain rate conditions. Thus, FLDs may not be useful [3].

As a very simple method, thinning could be used. According to one study, 30% thinning is the threshold for local necking in hot stamping [42]. In this case study, a point was found to be 1.34 mm thick, corresponding to 31.3% thinning, Fig. 10.18. However, a better way of deciding necking in simulation is to find "characteristic point" at which the strain rate vs. time changes significantly [43]. When such an analysis is done, it would be seen that the part starts local necking in a particular element at approximately 1.2 s after forming stage.

In this case study, the overall thickness distribution was found to be between 1.34–2.16 mm. This was similar to Shapiro's simulation, which has shown the thickness to be around 1.43–2.19 mm [8].

During quenching stage, the dies were fixed in their positions and heat transfer takes place between the blank and the shell dies without cooling channels. This stage takes 20 s. During this stage, phase transformations occur. Figure 10.19 shows how the martensite formation takes place with time. By this type of analysis, it is also possible to determine the necessary quenching time (if the simulation really emu-

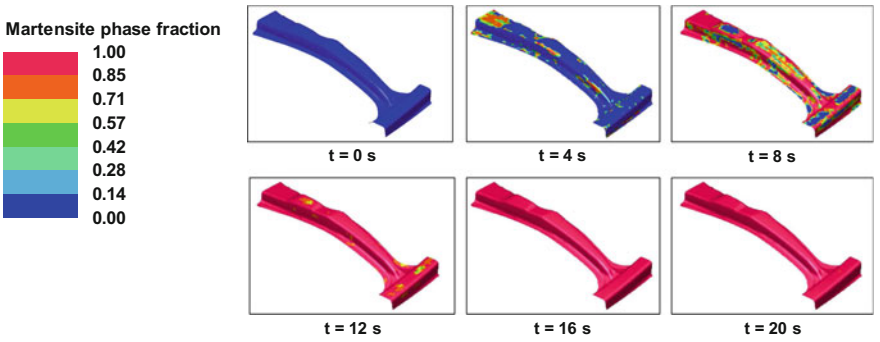

Fig. 10.19 Evolution of martensite transformation [3]

lates the steady-state conditions) to get 100% martensitic structure. In this particular case study, 16 s quenching seems to be sufficient. After 20 s, the Vickers hardness distribution was calculated to be between 487 and 514 [3].

10.4.2 Cyclic Cooling in a Tailored Part

In this case study, as published at [4], dies and process parameters for a tailored B-pillar was investigated. The "soft zone" was created by tailored quenching/controlled cooling. The process parameters such as: (1) blankholder force application, (2) cooling channel design (locations, diameters and numbers of channels), and 3) time for quenching can be optimized by using simulation. In addition, the final properties such as: (1) Vickers hardness, (2) yield and tensile strength and (3) distortion can be predicted.

The B-pillar model was modified from Numisheet geometry. Dies were modified to have two zones, where the lower end of the blank would be in contact with hot dies (Fig. 10.20). The cooled portion was divided into two segments and the cooling channels were designed for "gun drilling" process. The blank thickness was assumed to be 1.2 mm.

The overall process was divided into 6 stages: (1) Gravity, (2) Holding, (3) Forming, (4) Quenching, (5) Springback, and (6) Air Quenching. In this particular case study, simulation of the first three stages (gravity, holding, and forming) can be used to predict potential failures (cracks, wrinkles) in the hot formed part.

If a one-piece blankholder has to be used, this part would crack at the top and would have wrinkles in the bottom, as seen in Fig. 10.21. Since the dies are already segmented, the blankholder can also be segmented. With local adjustment of the blankholder force a part without any defects can be produced [4]. All these trials can be done easily on computer simulation, which may have cost time and money in the shop floor.

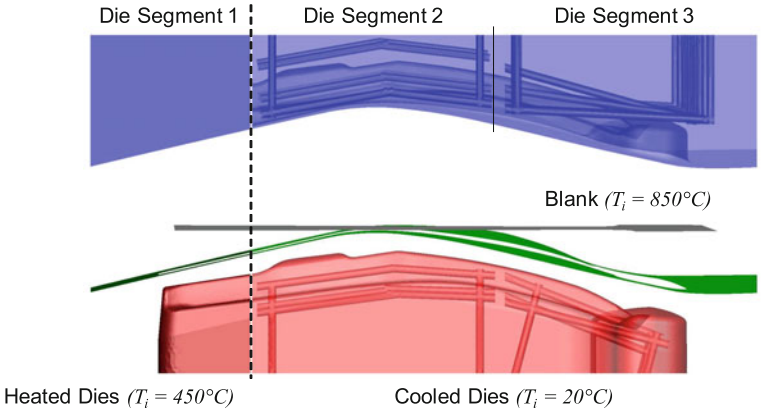

Fig. 10.20 Evolution of martensite transformation [4]

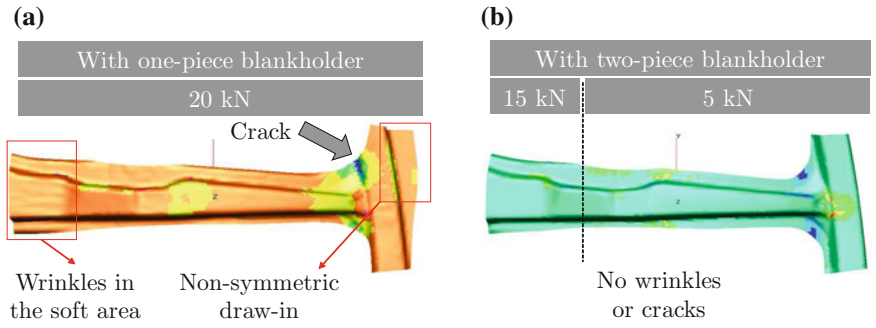

Fig. 10.21 **a** Part would have many defects with one-piece blankholder, **b** a two-piece blankholder with optimized holding forces can solve these defects [4]

Once the part is successfully formed it is quenched (held between cooler die halves) to obtain the final microstructure, hardness, and strength. In this stage, the die halves are pressed with a constant force—which could be limited by the available press. Computer simulation could be used to design quenching stage process parameters, such as: (1) duration of quenching stage (see Fig. 10.19), (2) number, diameter and location of cooling channels, and (3) number, power and location of heating cartridges (in case of tailored parts).

To ensure the cooling channels are designed properly for a robust production, "a cyclic quenching simulation" is required. In these simulations, solid dies with cooling channels are used. The dies are assumed to be 20 and 450 °C at the beginning of the first part, and the evolution of temperature can then be traced. The cyclic simulation is run for 10 cycles of (1) 10 s die quenching followed by, (2) 6 s transfer time. During all these 16 s coolant is assumed to flow in the cooling channels. Figure 10.22a shows the temperature evolution in one of the die segments. Figure 10.22b shows a sample part.

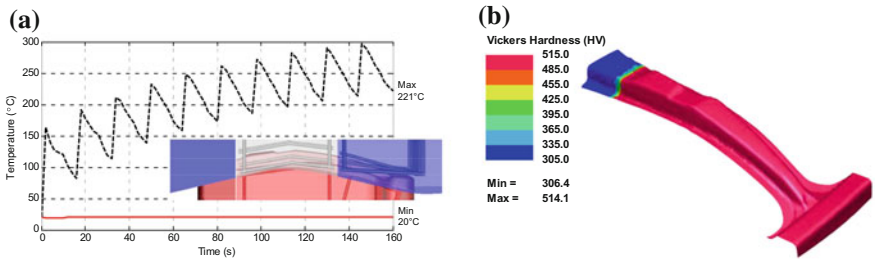

Fig. 10.22 **a** Temperature evolution in upper die middle segment, **b** final hardness of the part [4]

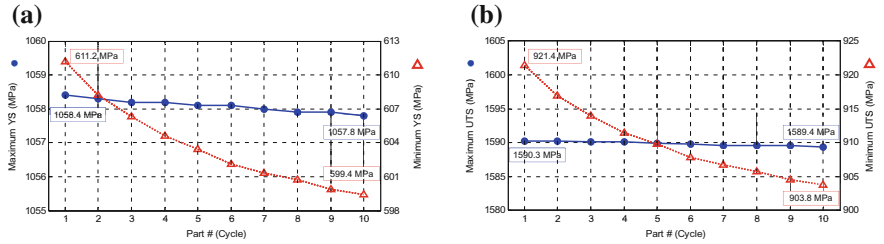

Fig. 10.23 **a** Temperature evolution in upper die middle segment, **b** final hardness of the part [4]

The highest temperature in the cooled segments was observed in the upper die middle segment. The temperature was found to be over 200 °C, but as can be seen from Fig. 10.23, final part properties were not affected with this hot spots. For more robust production, it is always possible to increase (1) the number of cooling channels (which is additional machining) or (2) the flow rate per cooling channel.

10.5 Recent Improvements in Simulation Technology

With the advanced simulation techniques, it is now possible to simulate TWB's, TRB's and patchwork blanks. It is possible to have a blank with local different properties, this can be thickness, material grade or temperature. Figure 10.24 shows an example B-pillar geometry with two patches. It is also possible to optimize the spot weld locations.

As discussed in Sect. 7.2.3.1, if the blank contour could be optimized such that no post-forming trimming would be required, significant cost savings could be realized. This can be achieved by computer simulation, although it may be CPU-time intensive. Typically, blank development is used in the areas where the geometric tolerances are $\pm 2 \ldots 3$ mm [44–46]. With the new software, the algorithm to generate the developed blank is as follows (see Fig. 10.25).

Another recent development is virtual die spotting. Die spotting is manually grinding the tools, to make sure the contact is evenly distributed. Depending on the com-

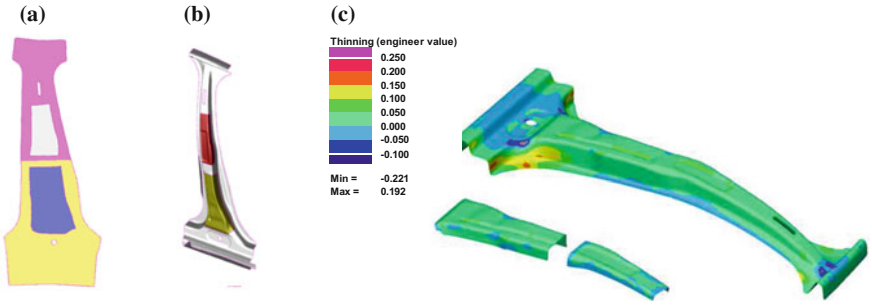

Fig. 10.24 Patchwork blank: **a** initial blank, **b** final geometry, **c** thinning distribution in the main blank and the patch sub-blanks

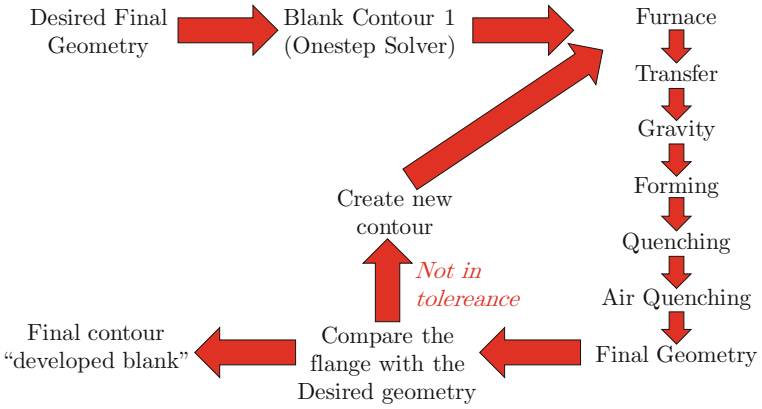

Fig. 10.25 Blank developing algorithm (recreated after [44])

plexity of the tool and experience of the die spotter, the process may take days to weeks [47]. Die spotting is more critical in hot stamping, as gap between the dies and the part can result in a soft zone. Due to thinning and thickening of the blank, elastic deflections of the dies and the press; a die that is perfectly machined and assembled to CAD design would not perform well.

Currently virtual die spotting can be done at two stages:

1. modifying the thermal contact conductance, such that even some gaps are treated as contact. This would be a quick solution to see if the part is feasible or not.
2. modifying the tool surfaces (punch, die, pad, blankholder, etc.) to accomodate for the thinning. This is an iterative method and each time die geometries are modified, it is advised to run a full simulation to see the final results.

References

1. P. Åkerstrüm, Modeling and simulation of hot stamping. Ph.D thesis, Luleå University of Technology, Luleå, Sweden (2006)
2. H. Porzner, *Virtual Prototyping: Hot Forming Engineering with Virtual Manufacturing*. Presented at AP&T Press Hardening, Next Step Seminar, September 19th, Dearborn (2012)
3. E. Billur, Fundamentals and applications of hot stamping technology for producing crash-relevant automotive parts. Ph.D Dissertation, The Ohio State University, Columbus (2013)
4. E. Billur, C. Wang, C. Bloor, M. Holecek, H. Porzner, T. Altan, Advancements in tailored hot stamping simulations: cooling channel and distortion analyses. AIP Conf. Proc. **1567**(1), 1079–1084 (2013)
5. P. Weigert, Challenges in mass production of press hardened components focusing co2 reduction, *Insight Edition Conference* (2011)
6. H. Karbasian, A.E. Tekkaya, A review on hot stamping. J. Mater. Process. Technol. **210**(15), 2103–2118 (2010)
7. ESI Group, PAM-STAMP 2015.1 User Guide (2015)
8. A. Shapiro, Finite element modeling of hot stamping. Steel Res. Int. **80**(9), 658–664 (2009)
9. B. Oberpriller, L. Burkhardt, B. Griesbach, Benchmark 3–continuous press hardening, in *Proceedings of the Conference NUMISHEET* (2008), pp. 115–124
10. K. Roll, Simulation of sheet metal forming–necessary developments in the future, in *International Conference NUMISHEET* (2008), pp. 3–11
11. J. Pilthammar, M. Sigvant, S. Kao-Walter, Including die and press deformations in sheet metal forming simulations. J. Phys.: Conf. Ser. **734**(3), 032036 (2016)
12. C. Dessain, P.H. Hein, J. Wilsius, L. Penazzi, C. Boher, J. Weikert, Experimental investigation of friction and wear in hot stamping of usibor 1500p, in *1st International Conference on Hot Sheet Metal Forming of High Performance Steel, CHS2, Kassel, Germany* (2008), pp. 217–227
13. A. Yanagida, A. Azushima, Evaluation of coefficients of friction in hot stamping by hot flat drawing test. CIRP Ann. - Manufact. Technol. **58**(1), 247–250 (2009)
14. A. Azushima, K. Uda, A. Yanagida, Friction behavior of aluminum-coated 22MnB5 in hot stamping under dry and lubricated conditions. J. Mater. Process. Technol. **212**(5), 1014–1021 (2012)
15. M. Vilaseca, J. Pujante, D. Casellas, C. Dessain, A. Blaise, M. Bachmann, M. Alsmann, A. Hamasaiid, M. Grausem, K. Eriksson, D. Berglund, A. Ademaj, U. Weidig, K. Steinhoff, J. Hardell, G. Lindkvist, S. Mozgovoy, H. Åhlin, B. Prakash, M. Oldenburg, *Wear Measurement Methodology and Test Facility to Increase the Efficiency of Hot Stamping for High Performance Component Production (TESTTOOL). EUR (Luxembourg. Online)* (Publications Office, 2014)
16. K. Uda, A. Azushima, A. Yanagida, Development of new lubricants for hot stamping of al-coated 22mnb5 steel. J. Mater. Process. Technol. **228**, 112–116 (2016). (Hot Stamping)
17. A. Ghiotti, F. Sgarabotto, S. Bruschi, A novel approach to wear testing in hot stamping of high strength boron steel sheets. Wear, **302**(1), 1319–1326 (2013). (Wear of Materials 2013)
18. X. Tian, Y. Zhang, J. Li, Investigation on tribological behavior of advanced high strength steels: influence of hot stamping process parameters. Tribol. Lett. **45**(3), 489–495 (2012)
19. J. Venema, J. Hazrati, D. Matthews, T. Van Den Boogaard, An insight in friction and wear mechanisms during hot stamping, in *Key Engineering Materials*, vol. 767 (Trans Tech Publications, 2018), pp. 131–138
20. M. Yanhong, B. Wang, M. Huang, J. Zhou, X. Li, Investigation on tribological characteristics of boron steel 22mnb5-tool steel h13 tribopair at high temperature. Proc. Inst. Mech. Eng. Part J: J. Eng. Tribol. **231**(2), 165–175 (2017)
21. A. Ghiotti, S. Bruschi, F. Medea, Comparison of tribological and wear performances of alsi and zn coatings in hot stamping of boron steel sheets. Wear **332–333**, 810–821 (2015). (20th International Conference on Wear of Materials)
22. K Isaksson, M Jönsson, D Berglund, The direct press hardening process for zn-coated ultra-high strength steels, in *Advanced High Strength Steel and Press Hardening: Proceedings of the 2nd International Conference (ICHSU2015)* (World Scientific, Singapore, 2016), pp. 556–563

23. J. Kondratiuk, P. Kuhn, Tribological investigation on friction and wear behaviour of coatings for hot sheet metal forming. Wear **270**(11–12), 839–849 (2011)
24. A. Ghiotti, S. Bruschi, F. Sgarabotto, P.F. Bariani, Tribological performances of zn-based coating in direct hot stamping. Tribol. Int. **78**, 142–151 (2014)
25. H. Fujimoto, M. Nakata, M. Uchihara, K. Imai, N. Kojima, Y. Kaseda, Formability and weldability of zn coated steel sheet for hot-stamping. Trans. Soc. Autom. Eng. Jpn **47**(4) (2016)
26. R. Neugebauer, F. Schieck, S. Polster, A. Mosel, A. Rautenstrauch, J. Schönherr, N. Pierschel, Press hardening - an innovative and challenging technology. Arch. Civil Mech. Eng. **12**(2), 113–118 (2012)
27. R. Kelsch, A. Sommer, H. Schwinghammer, K. Radlmayr, T. Kurz, G. Luckeneder, J. Faderl, Hot forming of zinc coated press hardening steel. characterisation of forming behaviour and new process routes for mass production, in *6th International Conference on Hot Sheet Metal Forming of High Performance Steel, CHS2, Atlanta, GA, USA* (2017), pp. 337–344
28. T. Altan, G. Ngaile, G. Shen, *Cold and Hot Forging: Fundamentals and Applications* (ASM International, Materials Park, 2005)
29. M. Merklein, J. Lechler, T. Stoehr, Characterization of tribological and thermal properties of metallic coatings for hot stamping boron manganese steels, in *Proceedings of the Seventh International Conference on Coatings in Manufacturing Engineering* (Citeseer, 2008), pp. 219–228
30. M. Merklein, J. Lechler, T. Stoehr, Investigations on the thermal behavior of ultra high strength boron manganese steels within hot stamping. Int. J. Mater. Form. **2**(1), 259–262 (2009)
31. P. Salomonsson, M. Oldenburg, Investigation of heat transfer in the press hardening process, in *2nd International Conference on Hot Sheet Metal Forming of High Performance Steel, CHS2, Luleå, Sweden* (Wissenschaftliche Scripten, 2009; Godkänd; 2009; 20090622 (ysko)), pp. 239–246
32. M. Kintsch, S. Szabo, R. Schneider, W. Rimkus, An analysis of the hot-forming process with thermal and ICFD simulations, in *Presented at European LS-DYNA Conference*, *9–11 May, Salzburg, Austria* (2017)
33. H. Steinbeiss, H. So, T. Michelitsch, H. Hoffmann, Method for optimizing the cooling design of hot stamping tools. Product. Eng. **1**(2), 149–155 (2007)
34. F.P. Incropera, D.P. DeWitt, *Introduction to Heat Transfer*, 5th edn. (Wiley, New York, 2011)
35. H.-H. Bok, M.-G. Lee, E.J. Pavlina, F. Barlat, H.-D. Kim, Comparative study of the prediction of microstructure and mechanical properties for a hot-stamped b-pillar reinforcing part. Int. J. Mech. Sci. **53**(9), 744–752 (2011)
36. J. Min, J. Lin, Y. Min, Effect of thermo-mechanical process on the microstructure and secondary-deformation behavior of 22mnb5 steels. J. Mater. Process. Technol. **213**(6), 818–825 (2013)
37. A. Bardelcik, M.J. Worswick, S. Winkler, M.A. Wells, A strain rate sensitive constitutive model for quenched boron steel with tailored properties. Int. J. Impact Eng. **50**, 49–62 (2012)
38. N.K. Sever, Investigation of lubrication and springback in forming of draw quality and advanced high strength steels. Ph.D thesis, The Ohio State University (2012)
39. G.E. Totten, *Steel Heat Treatment: Metallurgy and Technologies* (CRC Press, New York, 2006)
40. American Society of Metals, *ASM handbook of "Heat Treating, 3rd Printing"*, vol. 04 (ASM International, 1995)
41. B. Ghoo, Y. Umezu, Y. Watanabe, N. Ma, R. Averill, An optimization study of hot stamping operation. AIP Conf. Proc. **1252**(1), 537–544 (2010)
42. H.S. Choi, B.M. Kim, K.J. Nam, S.Y. Ha, S.H. Cha, C.G. Kang, Development of hot stamped center pillar using form die with channel type indirect blank holder. Int. J. Autom. Technol. **12**(6), 887–894 (2011)
43. D. Banabic, *Formability of Sheet Metals* (Springer, Berlin, 2010), pp. 141–211
44. C. Koroschetz, M. Skrikerud, R. Kristensson, L.-O. Jonsson, D. Lorenz, H. Porzner, M. Hoss, Cost effective trimming in hot stamping through the combination of accurate blank development, hot and laser cutting, in *5th International Conference on Hot Sheet Metal Forming of High Performance Steel, CHS2, Toronto, ON, Canada* (2015), pp. 617–628

45. J. Aspacher, D. Haller, Hot stamping part design and feasibility study with respect to functionality and optimization of production cost, in *Presented at Forming in Car Body Engineering 2014, September 24–25th, Bad Nauheim, Germany* (2014)
46. N.K. Akafuah, S. Poozesh, A. Salaimeh, G. Patrick, K. Lawler, K. Saito, Evolution of the automotive body coating process—a review. Coatings **6**(2), 24 (2016)
47. A. Hedrick, Dievestigation: diemaking from concept to reality, in *The Fabricator* (2010)

Chapter 11
Economics of Hot Stamping

Eren Billur, Rick Teague and Barış Çetin

Abstract Hot stamping industry includes several businesses, including, steel makers, die makers, equipment suppliers, Tier suppliers, and automotive OEM's. The industry is composed of more than 100 companies and exceeds USD 6 Billion of annual revenue. This chapter reviews the industry and gives a future outlook from automotive and defense industries. Please note that this chapter is derived from publicly available data, and includes co-authors' personal opinions as well.

11.1 The Hot Stamping Industry

In this section, the vertical market of automotive hot stamped components is investigated. The industry can be divided into at least five different layers as follows:

1. Steel makers and service centers,
2. Die makers, (which will not be discussed in this chapter),
3. Equipment suppliers (furnace, press, automation),
4. Tier suppliers (Tier 1–2 suppliers, typically for automotive industry),
5. OEM's (vehicle makers)

E. Billur (✉)
Billur Makine Ltd., Ankara, Turkey
e-mail: eren@billur.com.tr

E. Billur
Atılım University, Ankara, Turkey

R. Teague
Telos Global, 1880 Hwy 116, Caryville, TN 37714, USA
e-mail: rteague@telosphs.com

B. Çetin
FNSS Defense Systems Co. Inc., R&D Center, Gölbaşi, Ankara, Turkey
e-mail: cetin.baris@fnss.com.tr

E. Billur (ed.), *Hot Stamping of Ultra High-Strength Steels*,
https://doi.org/10.1007/978-3-319-98870-2_11

11.1.1 Steel Makers and Service Centers

Steel makers have been discussed in Chap. 4. Currently, most of the coated steels are supplied by ArcelorMittal. ThyssenKrupp and Posco are also supplying AlSi coated steels. In China, several domestic steel makers can also sell their coated steels [1–3]. Uncoated 22MnB5 can be supplied by many steel makers, but is not favored by the industry due to its scaling and decarburization problems [4, 5]. Zn-coated blanks (predominantly) by voestalpine and others are estimated to be 5% of the total market [6].

In 2009, there were five plants producing AlSi coated 22MnB5. Out of these, three of them belonged to ArcelorMittal, and others were by ThyssenKrupp and Nippon Steel. The total production in that year was around 220,000 metric tons [1]. At that time, the prediction for 2013 was roughly 700,000 metric tons. However, in 2013, a total of 850,000 metric tons of AlSi coated steel was produced at 9 locations. In 2014, it was estimated that the demand would be 3 million metric tons by 2020 [7]. By 2017, the demand has already surpassed 2.5 million metric tons and a total of 10 lines are already in production [8] (Fig. 11.1).

With the patents' expiration and many new developments in the steel making and coatings technologies, hot stamping steel market may have higher growth rate in the next years.

For the steel maker, producing 22MnB5 may be easier than that of producing other AHSS grades such as DP or Q&P. In the case of DP and Q&P steels, the steel mill is responsible from the chemistry, heat treatment and the coil's mechanical properties (yield, UTS, elongation, etc.). In hot stamping grades, the steel mill is only responsible for the chemistry. The final properties are given at the hot stamping company.

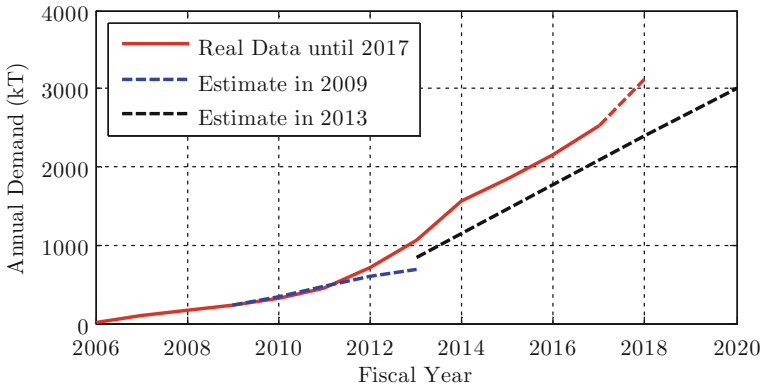

Fig. 11.1 Hot stamping steel demand has surpassed the previous estimates and is already over 2.5 million tons per year [1, 7, 8]

Once the steel coils are produced, they are typically sent to "steel service centers". Here, slitting and/or shearing can be done. For tailor welded blanks, blanking/ablation/welding and for tailor rolled blanks the flexible rolling are done at steel service centers. Tailor welded blanks are mostly done by ArcelorMittal Tailored Blanks [7] or Wisco Tailor Welded Blanks (previously known as TWB Company or ThyssenKrupp Tailor Welded Blanks) [9]. Tailor welded hot stamping blanks demand was approximately 8,400,000 blanks per year in 2015. Two-thirds of this demand was supplied by Wisco tailored blanks who owns 47 laser welding lines around the globe (not necessarily all can supply hot form blanks) [9]. ArcelorMittal Tailored Blanks had three laser welding lines dedicated to hot forming in 2013; with an annual capacity of over 3,000,000 blanks per year [7].

Tailor rolled blanks (TRB) are supplied by the German company Mubea. An estimated 6,000,000 hot stamped TRB components have been produced per year in the last few years.

11.1.2 Equipment Suppliers

As explained in Chap. 5, a typical hot stamping line consists of a furnace/heating system, a press and material handling system.

As for the furnace suppliers, there are AP&T, Benteler, Ebner, Eisenmann and Schwartz[1] [4, 10–13]. Out of these, Schwartz have delivered at least 280 furnaces for hot stamping industry, having over 60% of the market share [14].

AP&T has already delivered over 50 multi-chamber-furnaces [15] (see Sect. 5.1.3) since developing them in 2013 [16]. Benteler is one of the largest tier 1 suppliers in hot stamping area. They have developed a modular furnace system since 2016 [10]. Ebner, a 70 year old heat treatment furnace maker based in Austria, started producing furnaces for hot stamping in 2010. In its first year of introduction, two furnaces were sold [17]. Eisenmann has been in the furnace business since 1951. High-temperature applications started in 1980s. In 2011, Eisenmann acquired Ruhstrat who was one of the first PHS furnace makers. Since 2016, Eisenmann is also supplying furnaces for hot stamping industry.

For hot stamping, hydraulic presses are the conventional forming machines. Recently, servo-mechanical presses are also used. Schuler was one of the first major press makers to produce hydraulic presses for hot stamping. In 1990, Schuler supplied its first hot stamping press [18]. In 2018, Schuler has already delivered a total of 100 hot stamping presses [19].[2]

Press maker Loire Gestamp (formerly known as Loire SAFE) delivered their first hydraulic hot stamping press in 1998. By 2011, they have already sold over 30 lines [20]. Although they claim to have supplied over 30% of the hot stamping presses worldwide [21] according to the company's press releases. We found in our own

[1] Suppliers are listed alphabetically.

[2] Major press makers are listed in chronological order of supplying their first hot stamping press.

database, that Loire has supplied at least 60 presses in hot stamping worldwide until 2017.

Swedish maker AP&T supplied its first hydraulic hot stamping press in 2001. By 2013, they have already supplied over 70 hot stamping lines [4]. Today, the number of AP&T hot stamping presses have surpassed 90 [22].

In addition to these press makers, Amino (Japanese, servo-mechanical), Fagor (Spanish, both hydraulic and servo-mechanical), Hyundai WIA (South Korean, hydraulic) Macrodyne (Canadian, hydraulic) and Neff (German, hydraulic) have also supplied significant numbers of presses to hot stamping industry [23–27].

11.2 Hot Stamping Lines

As of 2017, there were already more than 400 hot stamping lines around the world. The database study shown here has been started in Center for Precision Forming, at The Ohio State University in 2012. Data before 2012 has been derived from the literature. Figure 11.2 shows the number of lines from 2011 to 2017.

It was also interesting to see how the trend of the number of parts produced per year and installed hot stamping lines match. As seen in Fig. 11.3, an average hot stamping line can make slightly over 1 million parts per year.

Out of 403 lines in the database, 312 of them were operated by Tier 1 and 2 suppliers. Another 49 lines were operated by the OEM's. There are approximately 15 lines that could not be classified. Rest of the lines are operated by steel makers or equipment suppliers. The database was last updated in March 2017.

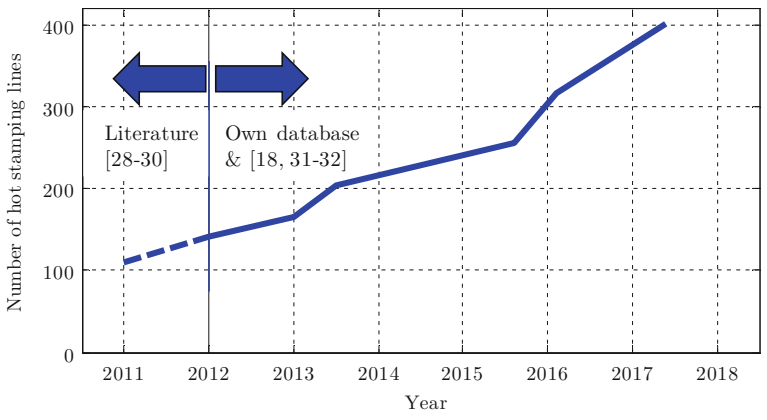

Fig. 11.2 Number of hot stamping lines have almost quadrupled since 2011 and surpassed 400 in 2017 (own database, with data from [18, 28–32])

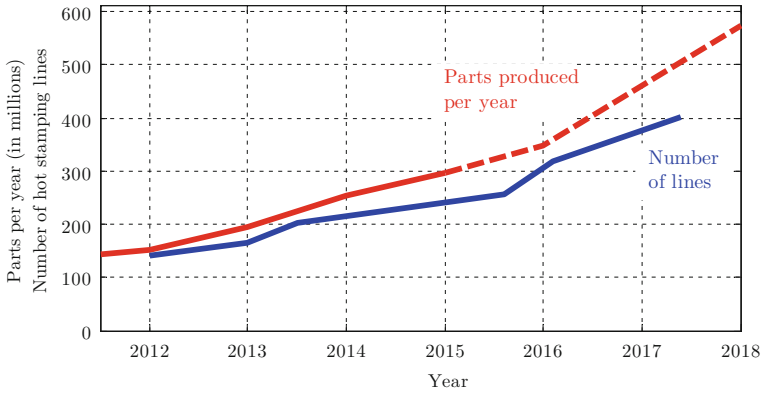

Fig. 11.3 An average hot stamping line produces 1 million parts per year (annual part production data is from [33])

11.2.1 Tier Suppliers

As discussed in detail in Chap. 3, the industry has started in late 1970s early 80s in Sweden. In 1982, Plannja AB was the first Tier 1 Supplier to have a hot stamping line. In 1990s, there were only two Tier 1 suppliers: Benteler and SSAB HardTech (new name of Plannja AB) [28, 34].

In 2000s, Sofedit, Gestamp, and Magna Cosma started hot stamping. Later in this decade, Sofedit was acquired by ThyssenKrupp; and SSAB HardTech by Gestamp [35–37].

By 2017, there were approximately 60 tier suppliers, operating approximately 75% of the hot stamping lines. Out of all tier suppliers, the most lines are at Gestamp, Benteler, and Magna. The big three have operations all around the world and accounted for more than half of all the lines operated by tier suppliers. There are also many tier suppliers in Asia, who have been investing heavily in hot stamping, in the last couple of years.

11.2.1.1 Gestamp

Gestamp had only one hot stamping line at Griwe, Germany when they acquired SSAB HardTech in 2004, which had 15 lines at that time [35, 37]. By 2010, Gestamp had 23 lines and in 2011 they acquired ThyssenKrupp Metalforming (previously Sofedit) and gained access to another five lines. Currently, Gestamp has 84 lines around the world (including but not limited to USA, Germany, France, Turkey, Korea, and China). Gestamp's evolution in number of lines is shown in Fig. 11.4.

Until 2018, Gestamp only utilized direct hot stamping but uses both coated and uncoated materials. Beginning this year, they are expected to start Zn-coated multi-step hot stamping. Gestamp produces tailored parts as well, for example to VW, Audi

and Honda with two or three different zones. The method at Gestamp is to heat the dies so that the quenching rate is controlled [6, 38–40].

11.2.1.2 Benteler

Benteler has been in hot stamping business since 1991. By the end of 2011, Benteler already had 42 lines around the world and another four were under construction [41, 42]. In 2014, Benteler already had 60 lines [28], as shown in Fig. 11.4.

11.2.2 Vehicle Manufacturers (OEM's)

11.2.2.1 Volkswagen

The first OEM to invest in an in-house hot stamping line was Volkswagen. The decision was made in August 2003 and only in 11 months, the first line was installed. In July 2004, Kassel plant had its first line. By the end of August 2004, VW had a total of six hot stamping lines. Initially, the production started for the then new VW Passat (SOP 2005) [35, 45]. Until 2008, the lines have been used to produce parts for Tiguan, Eos, Passat CC, Scirocco and Audi A4 & A5 [46]. The lines were used for direct, indirect and hybrid hot forming in the beginning [47]. VW is using direct process as much as possible since 2010 [48].

VW group have been using hot stamped products in their vehicles since 1994. The first applications were limited to door beams and bumper beams [28]. In 2003, VW Golf V had four hot stamped parts: A and B-pillar reinforcements on both sides,

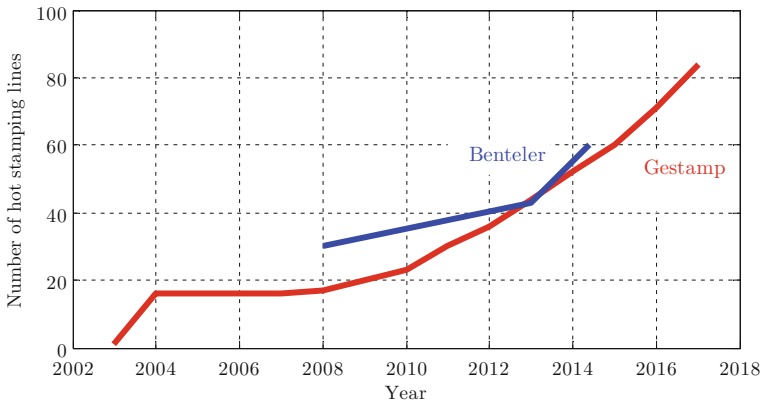

Fig. 11.4 Number of hot stamping lines of the large Tier 1 suppliers (data from [28, 35, 37, 42–44])

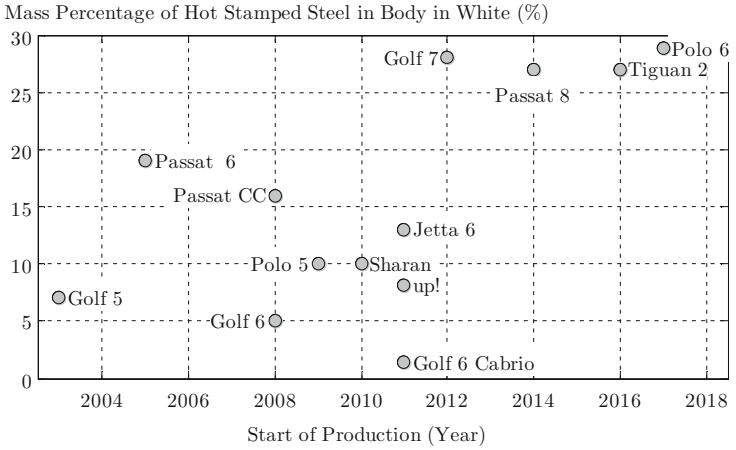

Fig. 11.5 Mass percentage of hot stamped steel in body-in-white of several Volkswagen models since 2003 (data from [48, 49, 51–57])

which accounted for ∼7% of the body-in-white by mass [45, 49]. In 2005, the new Passat had 15 hot stamped components, approximately 19% of the body-in-white mass. Nine of these components were hot stamped—for the first time in automotive industry—in-house. The rest were purchased from tier 1 suppliers [45]. According to an article at the Automotive Engineering International, in 2009, 100% of the bumper beams of Volkswagen branded cars were hot stamped [50]. This information is not valid in 2018, as the new Touareg (SOP 2018) has extruded aluminum bumper beams [51].

The use of hot stamped steels have surpassed 25% limit since 2012 in the new MQB platform. As seen in Fig. 11.5.

As of 2017, Volkswagen has a total of 14 hot stamping lines, 12 in Kassel plant and 2 in Wolfsburg [51].

11.2.2.2 Fiat

The second in-house hot stamper has been Fiat Group, in Italy. Since September 2008, Cassino plant in Italy is hot stamping USIBOR 1500 for several Fiat Group vehicles. The whole line, including blanking and trimming lines were supplied by AP&T. There are a total of five hot stamping lines. Trimming is done by hard cutting (two lines) and laser cutting (eight lines) [58, 59].

Fiat group owns a number of automotive brands including Fiat, Lancia, Alfa Romeo, Maserati, Ferrari, and acquired the Chrysler Group in 2014 to form FCA. Chrysler group included Chrysler, Dodge, Jeep, and Ram. Figure 11.6 shows use of hot stamped components in some of Fiat Group vehicles. In 2018, the new RAM 1500 is introduced. The truck has very limited hot stamped steel in its chassis, but

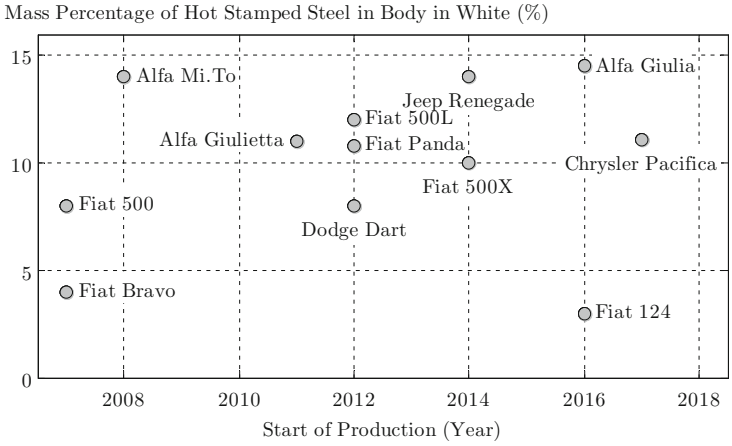

Fig. 11.6 Mass percentage of hot stamped steel in body-in-white of several Volkswagen models since 2003 (data from [58, 59, 61, 63–67])

the cab has over 30% hot stamped steel, including a door ring [60]. 2017 Chrysler Pacifica also has a five sub-blank TWB door ring [61] Group company Alfa Romeo uses warm formed 6000 series Aluminum in its 4C model [62]. The production may be handled at the same line that produces hot stamped parts.

11.2.2.3 BMW

BMW started using hot stamped boron steels, initially in their 3 series convertible A-pillar in 2000 (Fig. 3.9). Since then the application has increased, but was limited only to B-pillars in most vehicles. The 2005 3 Series (E90), for example, had only its B-pillars hot stamped. By 2008, BMW X5 and X6 SUV's had their B-pillars hot stamped using tailor rolled blanks [68, 69].

BMW group vehicles have increased dramatically with the introduction of new 7-series in 2008. The vehicle had approximately 60 kg hot stamped boron steel and this car was the first application of zinc-coated boron steels. 16% of Body-in-white in BMW 7 series is composed of hot stamped boron steels [70].

With 5 series GT (SOP 2009), BMW started in-house hot stamping in its Dingolfing plant. The plant has two identical lines, with a Dieffenbacher hydraulic press, Fig. 11.7. The technology was developed together with voestalpine. The blank material used is 22MnB5 with ~15 μm thick Zn coating. Blanks were cold formed and trimmed first, later they are austenitized and hardened (indirect hot stamping process). This method eliminates the need of laser cutting [71, 72]. Uncoated and Zn-coated parts of BMW 5 GT is shown in Fig. 11.8.

As of 2014, all BMW models have at least their A-pillars (for convertibles) or B-pillars (for all others) hot stamped. Beginning with E-segment (i.e., 5, 6, and 7

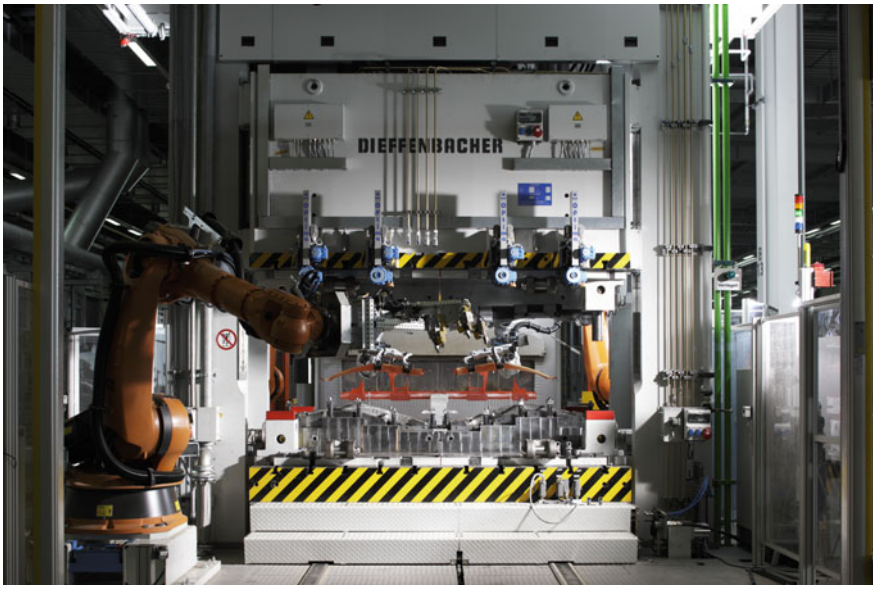

Fig. 11.7 One of BMW's hot stamping lines in Dingolfing [71]

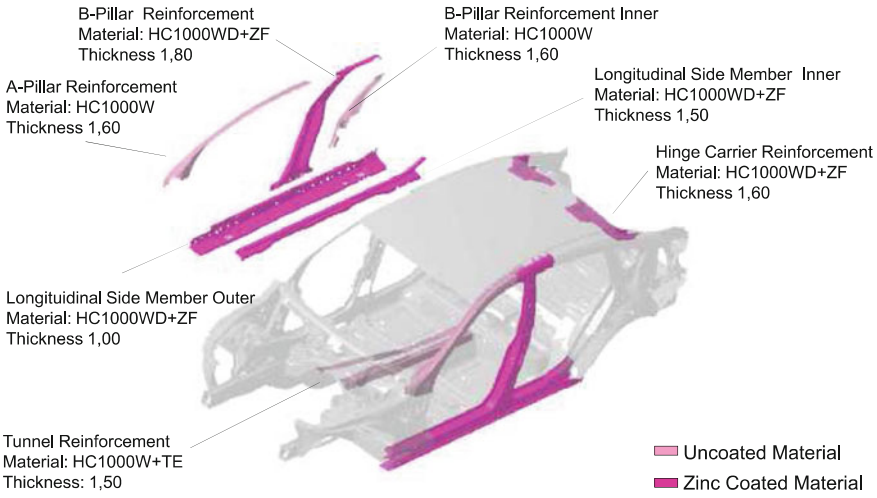

Fig. 11.8 Use of boron steels in BMW 5 GT (SOP 2009). (ZF stands for Zn-Fe based coating) [73]

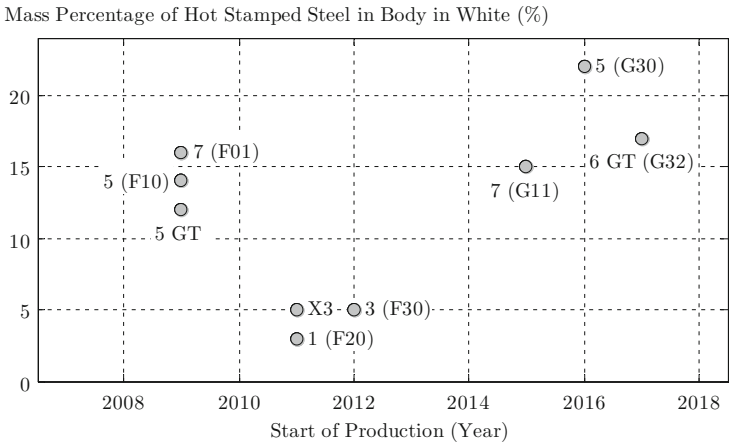

Fig. 11.9 Mass percentage of hot stamped steel in body-in-white of several BMW models since 2009 (data from [70, 73–79])

series), over 15% hot stamped steel is common. The new BMW 5 series (G30, SOP 2016) has 22% of its body hot stamped [74, 75] (Fig. 11.9).

11.2.2.4 Audi

Audi has 2 hot stamping lines in Ingolstadt plant since 2009. The lines have gas-fired roller hearth furnaces, each measuring 23 m long and 600 ton hydraulic presses for forming [80].

In 2013, Audi added a new plant in Münchmünster where two more hot stamping lines are installed. These lines however, have multi-chamber type furnaces [81]. Each line has 24 chambers furnace. The fully automated line has five laser units after the press, inline and automated. The production can be changed from one part to another in around 15 min [82]. To sum up, as of 2018, Audi has four in-house lines.

As seen in Fig. 11.10, most Audi vehicles have >10% of their body-in-white hot stamped. The only exclusion was the old A8, which was an Aluminum intensive vehicle. In the previous generation Audi A8, all body-in-white and hang-on parts were made of Aluminum. Only its B-pillars, which accounted for ~8% of the body mass, were hot stamped [85]. The new Audi A3 (SOP 2012) has approximately 26% of its body-in-white consist of hot stamped steel, which was a record breaker in 2012 [87].

Contrary to the Al-intensive earlier versions, the new Audi A8 (SOP 2017) is literally a "multi-material-mix" body. As seen in Fig. 11.11.

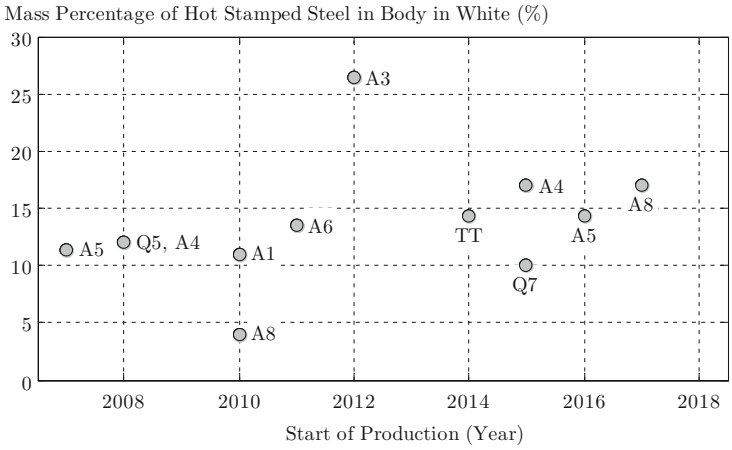

Fig. 11.10 Mass percentage of hot stamped steel in body-in-white of several Audi models since 2007 (data from [80, 83–91])

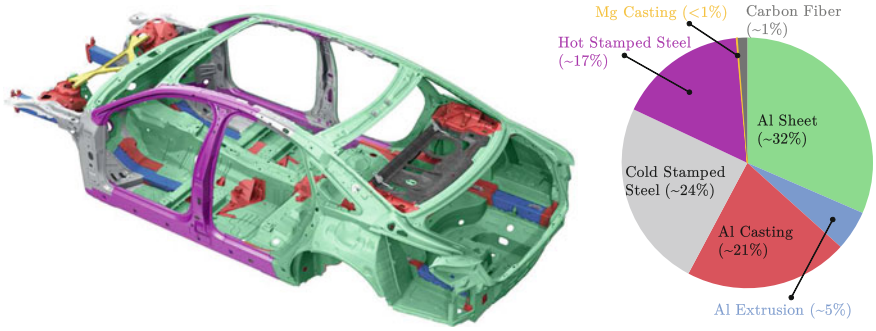

Fig. 11.11 Multi-material mix of Audi A8 (SOP 2017) (image from [80], infograph recreated after [88])

11.2.2.5 Seat

Seat has three hot stamping lines in Barcelona, with roller hearth furnaces [81]. Most Seat models are sharing the same MQB platform and somewhat shared upperbodies. Thus, the usage of hot stamped steels in Seat Mii could be similar to VW up!, new Ibiza to Polo 6, and Leon Mk3 to Golf 7, in Fig. 11.5.

11.2.2.6 Proton

In 2012, the Malaysian car manufacturer, also owner of the better known Lotus brand, Proton invested in an in-house hot stamping line. The line was located at Miyazu (a subsidiary of Proton) in Tanjung Malim, Malaysia. Line was bought from Schuler

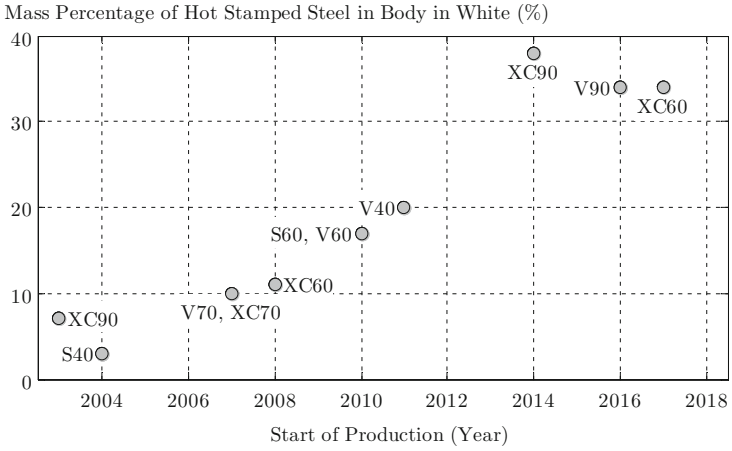

Fig. 11.12 Mass percentage of hot stamped steel in body-in-white of several Audi models since 2007 (data from [80, 83–91])

and currently stamps parts for New Proton Prevé [92]. According to Proton's website in August 2012, none of the previous models had hot stamped steel parts [93]. With this line, Proton became the 6th OEM to have an in-house hot stamping line, 1st in the ASEAN region [94].

Since 2012, Prevé (SOP 2012), Suprima S (SOP 2013), Iriz (SOP 2014) and Persona (SOP 2016) vehicles are fitted with 8 to 19 hot stamped components [94, 95].

11.2.2.7 Volvo

Volvo has been long using hot stamped components, but started in-house hot stamping only in 2014. They have two AP&T lines in Olöfstrom, Sweden. Each line consists of a 1200 ton hydraulic press and 21 chambers multi-chamber furnaces. Cycle time is around 12 s [96]. As explained in earlier sections Volvo uses tailor welded, tailor rolled, patchwork and tailor tempered blanks. Some of these are also stamped in-house, although some of them are done at tier suppliers [96, 97].

As seen in Fig. 11.12, Volvo cars introduced after 2010 had already over 15% of the body-in-white hot stamped. 2012 Volvo V40 was the first vehicle to have over 20% [98, 99]. Since 2014, most of the new products based on Scalable Platform Architecture (SPA) have over 30% of their body-in-white mass composed of hot stamped steels. This is currently the highest usage of hot stamped steels. However, it is important to note that about 5–6% this mass is energy absorbing hot-formed steels, as described in Sect. 4.3 in Chap. 4. [96, 100, 101].

11.2.2.8 Honda

Honda started using hot stamped components in 2007. The first hot stamped part was fuel tank, a relatively deep drawn part—typically not included in body-in-white mass calculations. The part was co-developed with Benteler. 1.6 mm thick AlSi coated blanks were deep drawn in a direct process, to 133 mm depth (5.2") [102, 103].

Since then several parts in body-in-white have also been used [103]. For example, 2012 Honda Civic had hot stamped B-pillar upper, roof rail and rocker reinforcement which accounted for 6.3% of the body mass [104]. In 2013 Honda Fit (also known as Honda Jazz), only B-pillar reinforcement was hot stamped, corresponding to 1.5% of the body mass [105].

In May 2013, Honda rolled out the Acura MDX, the first car to have a hot stamped door ring. This design had a two sub-blank TWB [103]. This was followed with the single blank door ring in Acura TLX (SOP 2014) [106]. Currently the latest generations Civic and Accord have 14–15% respectively [40, 107]. The new Acura RDX has the first inner and outer door rings, as explained in Chap. 8. This vehicle also has 15% of its body mass hot stamped [108].

Honda has at least one in-house hot stamping line, since 2012, in Japan. The line supplies N-Box with B-pillars. The line uses a short time diffusion process, and thus can employ a shorter roller hearth furnace. Direct water cooling and in-die hot cutting are also used to reduce the costs of hot stamping. It was claimed that with this line, the cost of hot stamped B-pillar was equal to cold stamped DP980 [109].

11.2.2.9 Renault

Renault currently has two hot stamping lines, one in Valladolid, Spain; and one in Douai, France. As of 2014, Renault required 47 different hot stamped parts for all its products. These two lines were supplying 17 of them. The average cycle time was 18 s. In their first year, the lines were planned to hot stamp around 10,000 tons of steel. It was expected that in 2018, the lines would be hot stamping 60,000 tons per year [110].

Figure 11.13 shows the number of hot stamped parts used in Renault cars, based on the year they were introduced. Currently, Renault is producing TWB's with ductile steels in these lines [110].

11.3 Feasibility of Hot Stamping

Methodology of hot stamping is a simple process that has developed a global reputation of being somewhat complicated. There are three basic reasons this reputation exists. First, there is a general lack of know-how. Many hot stamping factories are being operated by staff that have little to no experience in the actual process method-

ology necessary to meet the quality and delivery requirements mandated for hot stamping. The positive is that hot stamping has grown at such a rapid pace over the last decade; however, the challenges are a result of the evidence indicating hot stamping has grown faster than the expertise needed to support this growth.

Second, the objective to increase profits and improve equipment efficiency is a priority to everyone involved in hot stamping— from the manufacturer producing series production to the end user purchasing the stampings. This is obviously smart business if the proper strategies are implemented, but unfortunately for so many companies this is not the case. The objective to increase throughout has caused many to abandon a proven process methodology, thus resulting in unplanned costs generated from serious production downtime due to equipment failures and high maintenance costs.

Third, the investment cost is, in most cases, the decision-maker for starting or expanding most businesses. Hot stamping has a high investment cost attached to it, primarily because of the special manufacturing equipment required as well as the buildings and utility infrastructures needed to run the process effectively. With any production the objective is to be the most efficient with the least amount of cost possible; to achieve this goal the latter has become the drive—efficiency with low-cost investment. As with achieving the proper mechanical and geometrical requirements, there must be strict and uncompromised processes in place. The same is true when selecting the right equipment, the proper manufacturing space, and the resources to support these processes. There are so many examples of Hot Stamp Lines and manufacturing facilities around the world that were not designed properly from the outset, resulting in poor performance and poor ROI to the investor.

In summary, the feasibility of hot stamping is dependent upon the strict discipline to not compromise. The know-how, the process methodology, and the design and integration of the manufacturing equipment and manufacturing footprint have strict

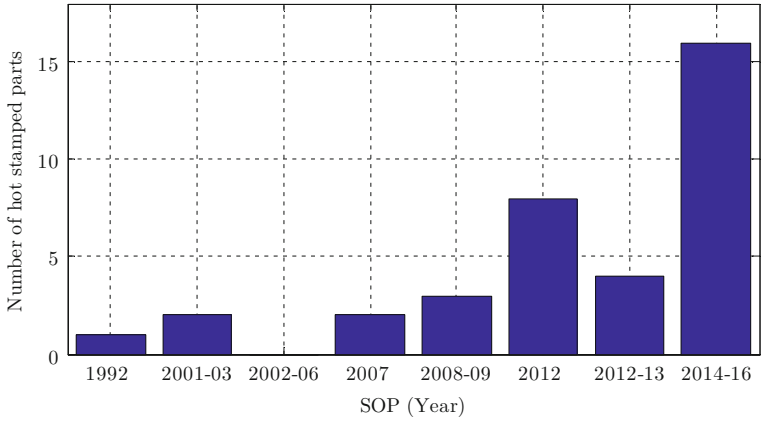

Fig. 11.13 Number of hot stamped components in Renault vehicles (data from [110])

requirements. These must be followed to meet the proven requirements needed to be both successful and profitable.

11.4 Future Outlook on Hot Stamping Business

As of today, majority of hot stamped components are used in automotive industry. However, several studies have been implemented to hot form armor steels or to use hot stamping steels in thick grades in defense industry [111, 112]. Previous generation Audi A8L Security was a special armored version for civilian use. This vehicle had "hot-formed armor steel" to achieve VR7 ballistic class [113], and was another example showing hot stamped steels could be used for armoring / defense applications.

11.4.1 Automotive Industry

The future of hot stamping appears to be strong, a prediction that can be based on both facts and assumptions. First, the most current platforms being released for quote as well as the preproduction prototyping activity show not only hot stamp components designed in body-in-white, but also an increase in the number of components. The OEM engineers responsible for the structural design are showing a trend with components such as door rings, which in past designs were associated with only one OEM.

Another important fact is the overall lack of competition in hot stamping. Steel producers have been attempting for the last decade to provide a high-strength product that can be manufactured in conventional stamping press lines. To date, nothing has been produced that provides the same results without the high cost associated with quality issues such as the unpredictability of spring-back and expensive manufacturing equipment including press systems and dies. In addition, the excessive maintenance costs related to each of the aforementioned processes have resulted in negative impacts to the profit and loss of many companies.

In conclusion, the assumptions show that there will be continued strong growth in auto sales, specifically in the China and NAFTA regions, as well as the reports indicating a steady growth in the EV market in the same regions show an increasing need for hot stamp components, indicating a strong future for the process.

11.4.2 Defense Industry

In defense industry, especially in production of armored combat vehicles, advanced and ultrahigh-strength steels are widely used. These high-strength steels could be

used for both manufacturing of structural parts and protection plates. In armored combat vehicles, TCMP (Thermomechanical Rolling Processed) and QT (Quenched & Tempered) steels are widely used. TMCP plates and tubes are produced in accordance with EN 10149 and EN10025-4, whereas QT steels are with EN 10025-6 standard [114]. Armor steels could be classified as a specific area in the QT family. There are several steelmakers which produces this specific class of steels, i.e., armor steels, with various mechanical properties. In a general manner, it could be stated that an armor steel has approximately a yield strength of 1250 MPa and an ultimate tensile strength (UTS) of 1700 MPa [115]. With today's technology, it is now possible to obtain this UTS level of armor steels with hot stamping method (UTS $\sim$ 1, 800 MPa, 260 ksi).

As a common challenge in automotive and defense industries, it is relatively a difficult task to form these high-strength steels such as S960QL, S900MC, DP1180 and similar, in armor combat vehicle production. Furthermore, Gas Metal Arc Welding (GMAW) is a commonly used joining technique in the defense industry. In order to weld high carbon steels like armor plates with GMAW technique, there should be some extra operations to be processed. It is almost a compulsory task to apply pre-heating to those steels before welding operation, with the aim of preventing the cold cracks. Cold cracks are typical defects of welded joints of pearlitic and martensitic steels [116]. It is also stated in the literature that post-weld heat treatment (PWHT) operation improves the mechanical properties of the final part in welding of armor steels [117]. While improving the weld quality, these operations create a post-tempering effect, which softens the steel. Pre-heating and post-heating treatments commonly influences an area larger than the Heat Affected Zone (HAZ) created during welding operation. As a result, the large-scale degradation of the microstructure, i.e., mechanical properties with the effect of pre-heating and post-weld heat treatment and the difficulties in forming and could be eliminated by application of hot stamping technique in defense industry. By means of the hot stamping technique and high ductility of 22MnB5 at austenization temperature, some welding operations might be eliminated in body design. Furthermore, this technique would absolutely decrease the tonnage values needed in forming operations and also the raw material cost. There is a reasonable amount of price difference between a standard hot stamping steel and an armor steel. The price of an armor steels may easily reach up to two times that of conventional mild steel.

On the other hand, the application of hot stamping in production of armored combat vehicles may have a disadvantage of resulting in higher distortions compared to conventional cold forming. However, there are some recent approaches in improvement of distortion like pre-stress engineering, dynamic clamping or optimization of quenching process by simulation software. It is thought that with the help of these new techniques if distortion problem can be decreased to a reasonable amount, hot stamping application may have a remarkable potential in defense industry as well.

References

1. T. Vietoris, Hot stamping with USIBOR1500®. Presented at AP&T Press Hardening, Next Step Seminar, Novi, MI (2010). Accessed 15 Sept 2010
2. Posco, Automotive steel data book (2016)
3. E. Hilfrich, D. Seidner, Crash safety with high strength steels. Presented at International Automotive Congress, Oct. 30, Shengyang, China (2008)
4. M. Skrikerud, Next generation of compact hot forming lines for optimised throughput with different materials. Presented at Materials in Car Body Engineering 2013, May 7–8, Bad Nauheim, Germany (2013)
5. S. Sepeur, The company Nano-X GmbH: Products for the automotive industry. Presentation at Deutsche Börse, July 10th, Frankfurt, Germany (2006)
6. B. Osburg, G. Lengfeld, O. Straube, Innovation and globalization as a factor of success for global hotstamping growth, in *New Developments in Sheet Metal Forming Conference, Stuttgart, Germany* (2012), pp. 79–92
7. W. Ehling, F. Schmit, Innovations in laser welding for press hardened steels. Presented at Materials in Car Body Engineering 2014, May 13–14, Bad Nauheim, Germany (2014)
8. L. Dormegny, Efficient lightweighting with new press hardenable steels. AMS Webinar (2017)
9. A. Breuer, Optimizing parameters for hotformed tailored-blank applications. Presented at Great Designs in Steel 2015, May 13, Livonia, MI, USA (2015)
10. B. Dvorak, J.J. Tawk, T. Vit, Advanced design of continuous furnace for hot stamping line, in *Advanced High Strength Steel and Press Hardening: Proceedings OF THE 2ND International Conference (ICHSU2015)* (World Scientific, 2016), pp. 611–619
11. A. Oppermann, Press hardening furnaces with integrated flexible tailored tempering. Presented at Great Designs in Steel 2018 (2018)
12. A. Weiland, Press hardening of steel: a holistic approach, in *Proceedings of Metal Forming Technology Day (MEFTECH 2017), May 12th, Bursa, Turkey* (2017), pp. 50–68
13. H. Lehmann, New developments in furnaces for press-hardening, in *5th International Conference on Hot Sheet Metal Forming of High Performance Steel, CHS2, Toronto, ON, Canada* (2015), pp. 331–341
14. Schwartz GmbH, Company web page. (2018), https://schwartz-wba.com/products/heat-treatment-systems-for-press-hardening/?lang=en. Accessed June 10 2018
15. AP&T. Ap&t launching new generation of multi-layer furnace for press hardening. Press Release (2016)
16. AP&T, Next-gen furnace for press hardening. Metal Forming Magazine (2016), p. 14
17. F.J. Ebner, Hotphase - press hardening automotive solutions by EBNER, in *3rd International Conference on Hot Sheet Metal Forming of High Performance Steel, CHS2, Kassel, Germany* (2011), pp. 247–253
18. J. Aspacher, D. Haller, Hot stamping part design and feasibility study with respect to functionality and optimization of production cost. Presented at Forming in Car Body Engineering 2014, September 24-25th, Bad Nauheim, Germany (2014)
19. Schuler Group. 100th hot stamping line sold. Press Release (2018). Accessed 13 Feb 2018
20. J.M. Berasategi, C. Garbalena, B. Irazu, G. Gonzalez, Past and future for taylor-made hot stamping lines, in *3rd International Conference on Hot Sheet Metal Forming of High Performance Steel, CHS2, Kassel, Germany* (2011), pp. 255–261
21. Loire Gestamp, Company profile. 24th International Sheet Metal Working Technology Exhibition 25 - 29 October 2016 - Hanover, Germany (2016)
22. AP&T Group. Company web page (2018), https://www.aptgroup.com/solutions/automotive/press-hardening. Accessed 10 June 2018
23. T. Maki, M. Amino, K. Hirano, H. Murai, Mechanical link servo press for hotforming, in *5th International Conference on Hot Sheet Metal Forming of High Performance Steel, CHS2, Toronto, ON, Canada* (2015), pp. 179–187
24. A. Ormaetxea, G. Ibañez, Servomechanical press makes foray into hot stamping. Stamp. J. (2015), pp. 18–21

25. Hyundai WIA, Company web page (2018), http://en.hyundai-wia.com/business/machinery_press03.asp. Accessed 10 June 2018
26. Macrodyne Technologies Inc. Company web page (2018), http://www.macrodynepress.com/hydraulic-presses/hot-stamping-presses/. Accessed 10 June 2018
27. H. Kömpf, NEFF - Hot Forming. Presented at Automotive Engineering Expo, June 4–6, Nürnberg, Germany (2013)
28. R. Lapsien, Hot forming at benteler - current applications and trends for the future. Presented at Materials in Car Body Engineering 2014, May 13–14, Bad Nauheim, Germany (2014)
29. R. Hund, M. Braun, Continuous improvement of hot forming technology, in *3rd International Conference on Hot Sheet Metal Forming of High Performance Steel, CHS2, Kassel, Germany* (2011), pp. 189–200
30. P. Belanger, *The future for press hardening in the automotive industry*. Presented at AP&T Press Hardening, Next Step Seminar, Novi, MI, October (2011), p. 2011
31. H. Siebels, New press design for high volume production of hot-formed titanium parts. Presented at Seminar Dedicated to New Hot Forming Technologies, Loire-Etude, St. Chamond, France (2015)
32. E.J. Watkins, Hot stamping market, materials, coatings, and developments. Presented at Schuler Hot Stamping Workshop, May 14, Dearborn, MI, USA (2013)
33. M. Oldenburg, Simulation methods for press hardening applications. Tutorial presented at 5th International. Conference on Hot Sheet Metal Forming of High Performance Steel, CHS2, June 2nd, Toronto, ON, Canada (2015)
34. P. Fahlblöm, Analys för val av emballagesystem: en studie gjord för att underlätta valet av emballagesystem. Master's Thesis, Luleå University of Technology, Sweden (1997)
35. M. Kahl, Some like it hot. Automot. Manuf. Solut. 49–52 (2004)
36. U. Ekström. Gestamp acquires ssab hardtech. Presented at Press Release by SSAB Public Affairs (2004). Accessed 12 Nov 2004
37. Gestamp Corporacion, Cold forming & UHSS for lightweight steel applications. Presented at Uddeholm Automotive Tooling Seminar, February 5, Sunne, Sweden (2004)
38. D. Berglund, Hot stamping of ultra high strength steels - possibilities and challenges. Presented at Insight Edition Conference, September 20-21, Gothenburg, Sweden (2011)
39. P. Belanger, New Zn multistep hot stamping innovation. Presented at Great Designs in Steel 2017 (2017)
40. S. Crichley, T.J. Palesano, New Global Model Introduction: The All-New 2016 Honda Civic. Presented at Great Designs in Steel 2016, May 16, Livonia, MI, USA (2016)
41. T. Ausmann, *Hot stamping technologies, tailor rolled blanks*. Presented at AP&T Press Hardening, Next Step Seminar, Novi, MI, September (2010)
42. A. Kröning, Lightweight solutions for body applications. Presented at Insight Edition Conference, September 20–21, Gothenburg, Sweden (2011)
43. Gestamp, Annual report (2016)
44. L. Hein, K. Weise, Lightweight chassis cradles. Presented at Great Designs in Steel, Livonia, MI (2008). Accessed 9 April 2008
45. B. Kögel, "weltmeister im formhaerten" (world champion in form hardening - in german). Blech-Sonderdruck, Issue 5, NC Verlag (2006)
46. I. Schnaitmann, Volkswagen orders Schuler laser cutting lines (2008)
47. P. Weigert, Challenges in mass production of press hardened components focusing CO2 reduction, in *Insight Edition Conference* (2011)
48. M. Norden, T. Woelke, The new volkswagen sharan - size and responsibility. Presented at EuroCarBody 2010, October 18–20, Bad Neuheim, Germany (2010)
49. D. Havrilla, Laser welding of AHSS. Presented at Great Designs in Steel, Livonia, MI (2007). Accessed 7 Mar 2007
50. L. Brooke, H. Evans, Lighten up! Automot. Eng. Int. 16–22 (2009)
51. Volkswagen Media Services, http://www.volkswagen-media-services.com
52. H. Michalzik, H. Cordes, The passat CC. Presented at EuroCarBody 2008, October 21–23, Bad Nauheim, Germany (2008)

53. D. Holzkamp, Recent developments on UHSS welding and its simulation for prevention of heat distortion. Presented at Insight Edition Conference, September 20–21, Gothenburg, Sweden (2011)
54. F. Wegert, A. Wanning, The best place on earth - the new VW golf cabriolet. Presented at EuroCarBody 2011, October 18, Bad Neuheim, Germany (2011)
55. P. Dahlke, *Flexibility, productivity, and innovation power - core competencies of a tier 1 supplier*, in New Developments in Sheet Metal Forming, Stuttgart, Germany (2012), pp. 21–39
56. P. Šimon, N. Jiří, Škoda kodiaq. Presented at EuroCarBody 2016, October 17–20, Bad Nauheim, Germany (2016)
57. K. Heuer, C. Schwering, Polo 6th Generation. Presented at EuroCarBody 2017, October 17–19, Bad Neuheim, Germany (2017)
58. F. Rima, Hot forming pressroom. Presented at AP&T Press Hardening, Next Step Seminar, September 15, Novi, MI (2010)
59. G. Lucia, Recent developments in fiat on hot forming processes and related simulation methodologies, in *Insight Edition Conference* (2011)
60. D. Reed, P. Belanger, Hot Stamped Steel One-Piece Door Ring, in the All-New 2019 Ram 1500. Presented at Great Designs in Steel (2018)
61. J. Tibbenham, J. Truskin, Advanced High-Strength Steel Technologies, in the, Chrysler Pacifica. Presented at Great Designs in Steel 2017 (2017)
62. M. Consalvo, F. Ferrero, M. Passariello, Alfa Romeo 4C. Presented at EuroCarBody 2013, September 25–26, Bad Nauheim, Germany (2013)
63. J. P. McGuire. Advanced high strength steel stamping technologies. Presented at Great Designs in Steel, Livonia, MI (2012). Accessed 16 May 2012
64. F. Manfredi, M. Verzilli, T. Meoli, Fiat 500X. Presented at EuroCarBody 2014, October 21–23, Bad Nauheim, Germany (2014)
65. S. Odan, K. Uchibori, N. Goto, Mazda MX-5. Presented at EuroCarBody 2015, October 20–22, Bad Nauheim, Germany (2015)
66. F. D'Aiuto, M.M. Tedesco, Development of new structural components with innovative materials and technological solutions. Presented at Materials in Car Body Engineering 2015, April 22-23, Bad Nauheim, Germany (2015)
67. L. Sciarretta, Alfa romeo giulia. Presented at EuroCarBody 2016, October 17–20, Bad Nauheim, Germany (2016)
68. M. Pfestorf, The mixed material concept of the new BMW X5. Presented at Great Designs in Steel 2007, March 7, Livonia, MI, USA (2007)
69. M. Pfestorf, D. Copeland, Technological innovations in body in white manufacturing of the BMW X6. Presented at Great Designs in Steel, Livonia, MI (2008) 9 April 2008
70. M. Pfestorf, Multimaterial lightweight design for the body in white of the new BMW 7 series (2009)
71. N. Glies, Innovative pressen für die BMW automobile der zukunft. Press Release by BMW (2009). Accessed 2nd July 2009
72. O. Meyer, L. Rosenlehner, The body of the new BMW 5 series sedan. Presented at EuroCarBody 2010, October 18–20, Bad Nauheim, Germany (2010)
73. D. Copeland, M. Pfestorf, The body in white of the new BMW 5 Series Gran Turismo. Presented at Great Designs in Steel, Livonia, MI (2010). Accessed 5 May 2010
74. C. Rauber, Press hardened steel - applications and future requirements at BMW. Presented at Materials in Car Body Engineering 2015, April 22–23, Bad Nauheim, Germany (2015)
75. B. Albinski, An intelligent material mix for future lightweight requirements. Presented at Materials in Car Body Engineering 2017, May 16–18, Bad Nauheim, Germany (2017)
76. H. Stauch, Design in comfort and dynamics: the body of the new BMW X3. Presented at Strategies in Car Body Engineering 2011, March 22–23, Bad Nauheim, Germany (2011)
77. M. Becker, P. Kühnel, The body of the new BMW 3 series. Presented at EuroCarBody 2012, October 16–18, Bad Nauheim, Germany, 2012
78. M. Ahlers, K. Sammer, New BMW 7 Series. Carbon Core. Presented at EuroCarBody 2015, October 20–22, Bad Nauheim, Germany (2015)

79. R. Pilsl, K. Sammer, The BMW 6 Series Gran Tourismo. Presented at EuroCarBody 2017, October 17–19, Bad Neuheim, Germany (2017)
80. Audi Media Services, http://www.audi-mediaservices.com
81. M. Alsmann, M. Goede, S. Kulp, M. Lalla, J. Patak, F. Russ, Hot Forming - State of the ARt and future reuqirements at Volkswagen. Presented at Materials in Car Body Engineering 2014, May 13–14, Bad Nauheim, Germany (2014)
82. R. König, J. Patak, Audi ultra strategy - new production lines for the next generation of high-volume press hardening. Presented at Forming in Car Body Engineering 2014, September 24–25th, Bad Nauheim, Germany (2014)
83. H.D. Wilde, M. Wunsch, Die karosserie des neuen audi a5 coupé. Presented at EuroCarBody 2007, October 16–18, Bad Nauheim, Germany (2007)
84. M. Hahn, T. Rebele, R. Weiss, The new audi q5 car body. Presented at EuroCarBody 2008, October 21–23, Bad Nauheim, Germany (2008)
85. A. Fidorra, J. Baur, The art of progress: audi - the new a8. Presented at EuroCarBody 2010, October 18–20, Bad Neuheim, Germany (2010)
86. B. Mleksuch, H. Elsäßer, M. Schrimm, K.-G. Michel, The new audi A6. Presented at EuroCar-Body 2011, October 18–20, Bad Nauheim, Germany (2011)
87. C. Bielz, S. Heis, The new audi A3. Presented at EuroCarBody 2012, October 16–18, Bad Nauheim, Germany (2012)
88. T. Hämmerle, D. Hußmann, The new Audi A8. Presented at EuroCarBody 2017, October 17–19, Bad Neuheim, Germany (2017)
89. N. Oleff, M. Silbernagl, The new audi A5 - sogehtcoupe. Presented at EuroCarBody 2016, October 17–20, Bad Nauheim, Germany (2016)
90. T. Hambrech, The new Audi Q7. Presented at EuroCarBody 2015, October 20–22, Bad Nauheim, Germany (2015)
91. G. Seehafer, D. Schmid, Audi TT Coupé. Presented at EuroCarBody 2014, October 21–23, Bad Nauheim, Germany (2014)
92. Schuler, Private communication (2013)
93. Proton, Company web page (2012) Accessed 14 Aug 2012
94. Wikipedia, Proton RESS (2018). Accessed 11 June 2018
95. Proton, Proton: Safety is our priority. Presented at ASEAN Automobile Safety Forum 002-2014, December 1–2, Bangkok, Thailand (2014)
96. H. Ljungqvist, K. Amundsson, O. Lindblad, The all-new Volvo XC90 car body. Presented at EuroCarBody 2014, October 21–23, Bad Nauheim, Germany (2014)
97. P. Belanger, Steel innovations in hot stamping. Great Designs in Steel 2016 (2016)
98. E. Billur, Fundamentals and applications of hot stamping technology for producing crash-relevant automotive parts. PhD Dissertation, The Ohio State University, Columbus, OH, USA (2013)
99. R. Mattsson, Volvo car's press hardening strategy. Presented at AP&T Press Hardening, Next Step Seminar, September 19th, Dearborn, MI, USA (2012)
100. S. Nedic, A. D'Elia, N. Palmquist, The all New Volvo V90 Car Body. Presented at EuroCar-Body 2016, October 17–20, Bad Nauheim, Germany (2016)
101. S. Nedic, H. Lindberg, C. De Leij, The all-new XC60 2018 Car Body. Presented at EuroCar-Body 2017, October 17–19, Bad Neuheim, Germany (2017)
102. B. Macek, Developing a deep drawn hot stamped fuel tank guard. Presented at Great Designs in Steel 2007, March 7, Livonia, MI, USA (2007)
103. R. Zum Mallen, J. Riggsby, Development of a global first SUV body construction. Presented at Great Designs in Steel, Livonia, MI (2013). Accessed May 1 2013
104. T. Yamada, S. Imamura, K. Honda, Honda - the new civic. Presented at EuroCarBody 2012, October 16–18, Bad Nauheim, Germany (2012)
105. M. Emura, Y. Ohkawa, K. Hada, Honda fit. Presented at EuroCarBody 2013, September 25–26, Bad Nauheim, Germany (2013)
106. A. Madsen, 2015 Acura TLX body structure review. Presented at Great Designs in Steel 2015, May 13, Livonia, MI, USA (2015)

107. T. Marukawa, Y. Shoji, M. Nakamura, Accord. Presented at EuroCarBody 2017, October 17–19, Bad Neuheim, Germany (2017)
108. J. Riggsby, 2019 acura rdx world's first inner & outer door ring system. Presented at Great Designs in Steel (2018)
109. K. Teshima, Challenges of high-efficiency hot forming processes at Honda. Presented at Forming in Car Body Engineering 2012, September 26–27, Bad Nauheim, Germany (2012)
110. B. Fossati, A. Machado-Baglietto, M. Cappelaere, Hot stamping industrialization at Renault. Presented at Forming in Car Body Engineering 2014, September 24–25, Bad Nauheim, Germany (2014)
111. N. Stefansson, A. Nichols, M. Cleppe, Elevated temperature forming methods for metallic materials (2012)
112. M. Maikranz-Valentin, U. Weidig, U. Schoof, H.-H. Becker, K. Steinhoff, Components with optimised properties due to advanced thermo-mechanical process strategies in hot sheet metal forming. Steel Res. Int. **79**(2), 92–97
113. Audi AG, The audi model range. Press Release over Audi MediaCenter (2017)
114. P. Dainelli, F. Maltrud, Management of welding operations with high strength steels. Soudage et Techniques Connexes **66**(7–8), 33–38 (2012)
115. E. Billur, B. Çetin, M. Gürleyik, New generation advanced high strength steels: developments, trends and constraints. Int. J. Sci. Technol. Res. **2**(1), 50–62 (2016)
116. I.K. Pokhodnya, V.I. Shvachko, Cold cracks in welded joints of structural steels. Mater. Sci. **32**(1), 45–55 (1996). Jan
117. S. Kara, M.H. Korkut, Zırhlı muharebe araçlarında kullanılan zırh plakalarında kaynak sonrası ısıl lemin birleşim mukavemetine etkisinin araştırılması. Savunma Bilimleri Dergisi **11**(2), 159–171 (2012)